HR23B, A BIOMARKER FOR HDAC INHIBITORS

Thesis submitted for the degree of Doctor of Philosophy
Department of Oncology
University of Oxford

By
Omar Ali Khan
Linacre College

Hilary 2013

Declaration

All the work presented in this thesis was carried out wholly by me apart from the immunostaining for HR23B carried out on CTCL specimens from the clinical trial which was performed by Dr. Victoria Wood and statistical analysis on the VICTOR trial data which was performed by Rose Wharton. No part of my thesis has been accepted or is currently being submitted for any other degree or diploma in this university or elsewhere. My research was carried out under the supervision of Professor Nicholas B. La Thangue, Medical Sciences Division, University of Oxford.

Omar Ali Khan

January 2013

Publications during D. Phil.

Fotheringham S, Epping MT, Stimson L, Khan O, Wood V, Pezzella F, Bernards R, La Thangue NB.

Genome-wide loss-of-function screen reveals an important role for the proteasome in HDAC inhibitor-induced apoptosis

Cancer Cell, 2009, 15(1):57-66.

Khan O, Fotheringham S, Wood V, Stimson L, Zhang C, Pezzella F, Duvic M, Kerr D and La Thangue NB.

HR23B is a biomarker for tumor sensitivity to HDAC inhibitor-based therapy

PNAS, 2010, 107(14):6532-7

New M, Olzcha H, Liu G, Khan O, Stimson, L, McGouran J, Kerr D, Coutts A, Kessler B, Middleton M and La Thangue NB.

A regulatory circuit that involves HR23B and HDAC6 governs the biological response to HDAC inhibit

Cell Death Differ., 2013, 10:1306-16.

ACKNOWLEDGEMENTS

I would like to acknowledge and thank Professor Nick La Thangue for supervising me during my studies. I would also like to thank and acknowledge Professor Mark Middleton, my clinical supervisor, for providing support and guidance and in particular, for enabling me to spend valuable time in the laboratory.

I am grateful to the Oxford Biomedical Research Council for providing funding to allow me to undertake this research.

This work would not have been possible without the assistance and helpful provision of resources from my collaborators: Dr. Francesco Pezzella, Professor Kevin Gatter and Dr. Ruth Asher from the department of pathology, University of Oxford. I would also like to thank Rachel Mager from the department of Oncology and Richard Lisle from the Nuffield Department of Clinical Laboratory Sciences for assistance in obtaining tissue microarrays.

I would like to thank Dr. Madeleine Duvic for assistance in immunohistochemistry scoring for CTCL specimens.

I would like to thank Rose Wharton from Centre for Statistics in Medicine, University of Oxford, for statistical analysis on the VICTOR trial patient data.

This study would not have been possible without the great help and friendship from all of my colleagues, past and present, from the Laboratory of Cancer Biology in Oxford. I would particularly like to thank Dr. Victoria Wood and Dr. Susan Fotheringham for helping me to settle in to life in the lab and for their initial assistance with experimental techniques. I would also like to thank Dr. Panos Zalmas, Dr. Lindsay Stimson, Maria New, Dr. Geng Liu, Dr. Simon Carr and Dr. Heidi Olzscha for help with project ideas and techniques and for making my experience in the laboratory environment enjoyable.

I would like to thank Dr. John Waters for his friendship and allowing me to use his home as a study and library when I needed peace and quiet.

I would like to express my sincere thanks to my parents who have provided me with great encouragement and love throughout my life and have contributed so positively to my education from the very beginning. I would also like to thank my twin brother Usman for support and friendship from as early as I can remember.

I was blessed with Aleena, my daughter during the very early days of my research and my son, Samih, arrived in the world on the penultimate day of my lab research. They have been an endless source of joy and fascination for me and their smiles have washed away any tiredness after a long day at work.

Lastly, I would like to express profound thanks to my wife Gohar whose love, tenderness and patience with me has been never-ending and quite extraordinary.

ABBREVIATIONS

17-AAG	17-allylamino-17-demethoxygeldanamycin
Ac	acetylation
ADP	adenine diphosphate
Akt	v-Akt murine thymoma viral oncogene
AMC	amino-coumarin
AML	acute myelocytic leukaemia
AMP	adenosine monophosphate
AMPK	adenosine monophosphate kinase
APL	acute promyelocytic leukaemia
ATG	autophagy-related
ATP	adenine triphosphate
Bcr-Abl	breakpoint cluster region/Abelson murine leukaemia viral oncogene
BRCA1	breast cancer related 1
ºC	degrees centigrade
CCK2	casein threonine kinase 2
CCR	chemokine receptor
CKI	cyclin-dependent kinase inhibitor
CLA	conjugated linoleic acid
CLL	chromic lymphocytic leukaemia
CML	chronic myeloid leukaemia
CO_2	carbon dioxide
CoREST	Co-repressor for element-1-silencing transcription factor complexes
CP	core particle
CQ	chloroquine
CR	complete response
CRC	colorectal cancer
c-Raf	v-raf1 murine leukaemia viral oncogene
CTCL	cutaneous T cell lymphoma
DAB	diaminobenzidine
DAC	deacetylase
2-DE	two-dimensional gel electrophoresis
DFS	disease free survival
DMSO	dimethyl sulfoxide
DNA	deoxyribonucleic acid
ECOG	Eastern Cooperative Group
EDTA	Ethylenediaminetetraacetic acid
EGFR	Epidermal growth factor receptor
EMEA	European Medicines Agency
Erk	Elk-related tyrosine kinase
ERAD	endoplasmic reticulum-associated degradation

FACS	fluorescent activated cell sorting
FCS	foetal calf serum
FDA	Food and Drug Administration
FOXO	forkhead box transcription factor
GFP	green fluorescent protein
GIST	gastrointestinal stromal tumour
H	hour
H_2O_2	hydrogen peroxidase
HAT	histone acetyltransferases
HCC	hepatocellular cancer
HCQ	hydroxychloroquine
HDAC	histone deacetylase
HEK	human embryonic kidney hnRNPI
HEPES	4-(2-hydroxyethyl)-1-piperazineethanesulfonic acid
HER-2	herstatin 2
HL	Hodgkin lymphoma
HIF-1α	hypoxia-inducible factor
HIV	human immunodeficiency virus
HPV	human papillomavirus
HR	homologous recombination
HRP	horseradish peroxidase
HR23A	human Rad 23 A
HR23B	human Rad 23 B
HSF1	heat-shock factor protein 1
hsp70	heat shock protein 70kD
hsp90	heat shock protein 90kD
IgG	immunoglobulin
IHC	immunohistochemistry
KDa	kilodalton
KRAS	Kirsten rat sarcoma viral oncogene homologue 1
LAMP	lysosomes-associated membrane protein
LC3	microtubule-associate light chain 3
LKB1	liver kinase B1
Lys	lysine
mDA	mega dalton
Me	methylation
MEF2	myocyte-enhancer factor 2
MF	mycosis fungoides
MM	multiple myeloma
mM	millimolar

µM	micromolar
µs	microsecond
MPR	misfolded protein response
mTOR	mammalian target of rapamycin
mRNA	messenger ribonucleic acid
MyoD	myogenic differentiation antigen
NAD^+	nicotinamide adenine dinucleotide
NBR1	neighbour of BRCA1 gene 1
NcoR	nuclear receptor corepressor
NER	nucleotide excision repair
NES	nuclear export signal
NF-□B	nuclear factor kappa B
NLS	nuclear localisation signal
nM	nanomolar
NPV	negative predictive value
NSCLC	non small cell lung cancer
ORB	Oxford Radcliffe Biobank
OS	overall survival
PAGE	polyacrylamide gel electrophoresis
PARP	poly-ADP-ribose
PBS	phosphate buffer saline
PI3K	phospoinositide 3 kinase
PD	progressive disease
Ph	phosphorylation
PPV	positive predictive value
PR	partial response
PTCL	peripheral T cell lymphoma
PVDF	polyvinylidene difluoride
%	percentage
Rad	radiation sensitive
Rb	retinoblastoma
ROS	reactive oxygen species
RNA	ribosomal ribonucleic acid
RP	regulatory particle
RR	response rate
RT-PCR	reverse transcription polymerase chain reaction
SAC	spindle assembly checkpoint
SAHA	suberoylanilide hydroxamic acid
SAR	structure activity relationship
SCC	squamous cell carcinoma
SD	stable disease

SDS	sodium doedecyl sulfate
SEM	standard error of the mean
SHP-2	tyrosine phosphatase SHP2
shRNA	small hairpin ribonucleic acid
siRNA	small interfering ribonucleic acid
SIRT1	sirtuin 1
SLS	stone-like structure
SMRT	silencing mediator for retinoid and thyroid hormone receptors
Sp1	transcription factor Sp1
SS	Sézary syndrome
STAT	signal transducer and activator of transcription
TBP2	thioredoxin binding protein 2
TDAC	tubulin deacetylase
Th2	T-helper 2
TMA	tissue microarray
Treg	T regulatory cells
TSA	trichostatin A
TSC	tuberous sclerosis complex
TSS	total staining score
TTP	time to progression
Ub	ubiquitination
UB	ubiquitin binding
UBA	ubiquitin-associated protein
UBL	ubiquitin-like protein
UIM	ubiquitin interacting motif
UPS	ubiquitin proteasome system
UV	ultraviolet
UVRAG	UV radiation resistance associated gene protein
V	volt
VCP	valosin-containing protein
VEGF	vascular endothelial growth factor
VPA	valproic acid
VWA	vonWillebrand factor A
WT	wild-type
XP	Xeroderma pigmentosum
XPC	Xeroderma pigmentosum complementary group C
Zn^{2+}	Zinc

ABSTRACT

As our understanding of cancer biology increases and novel therapies are developed, an increasing number of predictive biomarkers are becoming clinically available. Aberrant acetylation has been strongly linked to tumourigenesis and the modulation of acetylation through targeting histone deacetylase (HDAC) has led to the introduction of many HDAC inhibitors. To date, two have had regulatory approval for the treatment of cutaneous T cell lymphoma (CTCL). Modifications in chromatin control underpin the mechanism of action of HDAC inhibitors. A genome wide loss-of-function screen identified HR23B as a gene that governs sensitivity to HDAC inhibitors. HR23B shuttles ubiquitinated cargo proteins to the proteasome and elevated levels may contribute to cell death mediated by this pathway. It also governs cell sensitivity to drugs that act directly on the proteasome. HDAC inhibitors influence proteasome activity and there may be a synergistic interaction with proteasome inhibitors. HR23B and HDAC6 interact and HDAC6 may be a negative regulator of apoptosis and a positive regulator of autophagy and through its ability to down-regulate HR23B, may impact on the cellular outcome of HDAC inhibitor treatment. Expression of HR23B has been correlated with clinical response to HDAC inhibitors in a retrospective analysis of CTCL patients. The tissue expression of HR23B and the autophagy marker LC3 has been investigated and there may be a reciprocal relationship in their expression in some tumours which may provide prognostic information and patients with low HR23B expression but high levels of autophagy appear to have a particularly poor prognosis. Well designed, biomarker-driven prospective clinical trials are needed to clarify the predictive and prognostic roles of HR23B.

Omar Ali Khan Linacre College Submitted for the degree of D.Phil

Hilary term, 2013

LIST OF FIGURES

1.1.	Chromatin structure regulates transcriptional activity	5
1.2.	Schematic depiction of the different isoforms of HDAC	7
1.3.	Chemical structures of selected HDAC inhibitors from the four different classes of HDAC inhibitors	18
1.4.	The pathways affected by HDAC activity	26
1.5.	Regulation of autophagy	32
1.6.	Autophagy cascade: initiation and elongation	34
1.7.	Autophagy cascade: maturation and lysosomal fusion	35
1.8.	The ubiquitin-proteasome pathway.	47
1.9.	Rad23 and its human homologue HR23B	52
1.10.	Functions of HR23B	54
3.1.	Effect of HDAC inhibitors on apoptosis in tumour cell lines	87
3.2.	Protein expression of PARP and cleaved PARP upon HDAC inhibitor treatment as an indicator of apoptosis	89
3.3.	Comparison of apoptosis induced by SAHA at one concentration across different cell lines	91
3.4.	Effect of other HDAC inhibitors on induction of apoptosis in melanoma cell lines	92
3.5.	Effect of HDAC inhibitors on expression of HR23B	94
3.6.	Effect of bortezomib on expression of HR23B	96
3.7.	Effect of HDAC inhibitors on cellular localisation and expression of HR23B	98
3.8.	Basal levels of HR23B in CTCL and melanoma cell lines	100
3.9.	Effect of depleting HR23B using siRNA in melanoma and CTCL upon HDAC inhibitor-induced apoptosis	102
3.10.	Effect of depleting HR23B using siRNA in U2OS and melanoma cells on HDAC inhibitor-induced apoptosis	104
3.11.	Effect of over-expression of HR23B on HDAC-inhibitor induced apoptosis	106
4.1.	Proteasome activity in CTCL and melanoma cells treated with HDAC inhibitors	111-2
4.2.	Effect of depleting HR23B on proteasome activity in MYLA cells	114-5
4.3.	Effect of depleting HR23B on proteasome activity in A2058 cells	117-8
4.4.	Measuring proteasome function after HDAC inhibitor, proteasome inhibitor or combination treatment using GFPu1 cells and cells transiently transfected with GFPu1	121-2
4.5.	Effects of bortezomib treatment on HR23B expression in A2058 melanoma cells and impact of depletion of HR23B on apoptosis	125
4.6.	Effects of combining SAHA and bortezomib on apoptosis in different	

	cell lines	127-8
4.7.	Effects of combination dosing of SAHA and bortezomib on HR23B, PARP and acetylated histone H3 expression	131
4.8.	Effects of sequential and concurrent combination dosing of SAHA and bortezomib on apoptosis	133
4.9.	Effects of depletion of HR23B on apoptosis induced by SAHA and bortezomib in combination	135
4.10.	Effects of varying levels of HR23B expression on apoptosis induced by SAHA and bortezomib alone and in combination	137
5.1.	Autophagy and HR23B expression in cancer cells treated with HDAC inhibitors	142-3
5.2.	Autophagy and HR23B in cells treated with valproic acid	144
5.3.	HR23B and LC3 expression using immunofluorescence in cells treated with SAHA	146
5.4.	Effects of varying levels of HR23B on autophagy and apoptosis after HDAC inhibitor treatment	148-9
5.5.	Effects of varying levels of HR23B on autophagy after 5-fluorouracil (5-FU) treatment	151
5.6.	Effects of combining SAHA and chloroquine on apoptosis and autophagy	153-4
5.7.	Effects of combining SAHA and chloroquine on apoptosis and autophagy in A2058 cells	156-7
5.8.	Expression of HDAC6, autophagy and apoptosis markers and HR23B expression in cancer cells treated with SAHA	159
5.9.	Effects of manipulating levels of HDAC6 on expression of autophagy markers and apoptosis	162-3
5.10.	Effects of manipulating levels of HDAC6 on expression of autophagy markers and apoptosis as determined by immunofluorescence	165-8
6.1.	HR23B expression in multiple tumour types	175-7
6.2.	Expression of HR23B in cutaneous T cell lymphoma (CTCL)	181
6.3.	Expression of HR23B in non-malignant T cells	182
6.4.	Expression of HR23B in normal colon tissue, primary colon cancer, nodal and liver metastases	184-7
6.5.	HR23B staining scores in normal colon tissue compared to primary colon cancer, nodal metastases and liver metastases (unpaired samples)	189
6.6.	HR23B expression in SAHA-treated CTCL biopsies	196-7
6.7.	HR23B expression in PXD101 and depsipeptide-treated CTCL biopsies	200
7.1.	HR23B and LC3 expression in colorectal cancer	206
7.2.	HR23B and LC3 expression in primary melanoma	208
7.3.	HR23B and LC3 expression in primary melanoma samples from pilot clinical trial	210
7.4.	HR23B and LC3 expression in melanoma samples treated with valproic acid from pilot clinical trial	211
7.5.	HR23B and LC3 expression in melanoma samples treated with	

valproic acid from pilot clinical trial 213
7.6. HR23B and LC3 expression in resected primary melanoma samples and resected metastases post-treatment with valproic acid (VPA) from pilot clinical trial 215
7.7. Examples of HR23B expression in colorectal cancer specimens from patients in VICTOR trial 220-1
7.8. Disease-free and overall survival in patients from VICTOR trial stratified according to HR23B expression 223
7.9. Examples of LC3 expression in colorectal cancer specimens from patients in VICTOR trial 227-8
7.10. Disease-free and overall survival in patients from VICTOR trial stratified according to LC3 expression 230
7.11. Examples of HR23B expression and LC3 expression in the same patients (colorectal cancer patients from the VICTOR trial) 233
7.12. Disease-free and overall survival in patients from VICTOR trial stratified according to HR23B and LC3 expression 236

8.1 A model for the interplay between HR23B and HDAC6 in regulating the cellular response to HDAC inhibitor therapy 257

Appendices

I. siRNA optimisation 274
II. Proteasome assay optimisation 275
III. LC3 antibody optimisation 277
IV. Immunohistochemistry controls 279
V. Inter-observer agreement using the Kappa statistic of immunohistochemistry scoring 281
VI. Effect of depleting HR23B using siRNA in colorectal and melanoma cells upon HDAC inhibitor-induced apoptosis 284

LIST OF TABLES

1.1.	Summary of substrates, associated proteins and functions of class I HDACs	9
1.2.	Summary of substrates, associated proteins and functions of class IIa HDACs	12
1.3.	Summary of substrates, associated proteins and functions of class IIb HDACs	14-15
1.4.	Classification of HDAC inhibitors with potency and clinical status	19-20
1.5.	Predictive biomarkers in clinical use in oncology	59
1.6.	Class I/II and IV HDACs; cancer associations	61
2.1	Details of colorectal tissue microarrays with number of evaluable samples	75
2.2	Semi quantitative IHC staining evaluation of HR23B in CTCL biopsies	80
2.3	IHC scoring system used for HR23B in melanoma, colorectal and multi-tumour TMA	81
6.1.	Summary of HR23B expression in CTCL together with characteristics of neoplastic cells HR23B expression in multiple tumour types	179
6.2.	Summary of phase II clinical trial patients, total staining score, and clinical outcome	191
6.3.	Summary of TSS for pre-treatment expression of HR23B in biopsies from phase II clinical trial	193
6.4.	Summary of TSS for pre-treatment and post treatment expression of HR23B in biopsies from phase II clinical trial	194
6.5.	Summary of TSS in CTCL biopsies taken from patients treated with PXD101 and depsipeptide. HR23B expression in SAHA-treated CTCL biopsies	198
6.6.	Negative predictive value of HR23B in retrospective analysis of SAHA treated CTCL patients	202
7.1.	Baseline patient characteristics of VICTOR trial patients	217
7.2.	Survival characteristics of VICTOR trial patients (HR23B)	219
7.3.	Overall and disease free survival stratified according to HR23B expression in VICTOR trial patients	221
7.4	Results of three separate univariate Cox models estimating effect of HR23B on disease free and overall survival	224
7.5.	Survival characteristics of VICTOR trial patients (LC3)	226
7.6.	Overall and disease free survival stratified according to LC3 expression in VICTOR trial patients	229

7.7 Results of three separate univariate Cox models estimating effect of LC3 on disease free and overall survival 231
7.8. HR23B and LC3 score frequencies in VICTOR trial cohort 232
7.9. Overall and disease free survival stratified according to HR2B and LC3 expression in VICTOR trial patients 235
7.10. Results of three separate univariate Cox models estimating effect of HR23B and LC3 combined on disease free and overall survival 238

TABLE OF CONTENTS

CHAPTER 1

GENERAL INTRODUCTION **1**

1.1.	Epigenetics	2
1.2.	Chromatin adaptations and regulation of transcription	3
1.3.	Histone deacetylases	6
1.3.1.	Introduction.	6
1.3.2.	Class I HDACs	8
1.3.3.	Class IIa HDACs	10
1.3.4.	Class IIb HDACs	13
1.3.5.	Class IV HDAC (HDAC11)	16
1.3.6.	HDAC catalytic activity	16
1.4.	HDAC inhibitors: development and role in cancer therapeutics	17
1.4.1.	HDAC inhibitors	17
1.4.2.	HDAC inhibitors in clinical use	20
1.4.2.1.	Vorinostat	20
1.4.2.2.	Romidepsin	22
1.4.2.3.	Other HDAC inhibitors	23
1.5.	Mechanisms of HDAC inhibitor-induced cell death	25
1.6.	Combining HDAC inhibitors with other chemotherapeutic Agents	27
1.7.	Intracellular clearance mechanisms: autophagy, the ubiquitin proteasome system and the integrated regulation of cell fate	28
1.7.1.	Introduction	28
1.7.2.	Autophagy	30
1.7.3.	Signalling pathways in autophagy	31
1.7.4.	Cellular events and the machinery of autophagy	33
1.7.5.	Physiological functions of autophagy	36
1.7.6.	Autophagy and carcinogenesis	37

1.7.7.	Autophagy as a mechanism of tumour suppression	39
1.7.8.	Measuring autophagy	40
1.7.9.	Autophagy in anti-cancer therapeutics	42
1.7.9.1	Proteasome inhibitors and HDAC inhibitors	42
1.7.9.2	Autophagy inhibitors	43
1.8.	The ubiquitin-proteasome system	43
1.8.1.	Cellular events and the machinery of the UPS	43
1.8.2.	The 26S proteasome	48
1.8.3.	Developing of therapies targeting the UPS	49
1.8.4.	Small molecule inhibitors of proteasome catalytic Activity	49
1.9.	Regulated targeting of proteolytic substrates to the proteasome	51
1.9.1	UBA/UBL domain containing proteins	51
1.9.2	Rad23 in proteasomal degradation	53
1.9.3	Role of Rad23 in protection of ubiquitinated substrate from proteolysis	55
1.9.4	Intramolecular interactions of the UbA and UbL domains and impact on function	56
1.10.	Biomarkers	57
1.10.1.	Types of biomarkers	57
1.10.2.	Prognostic relevance of tissue expression of HDACs	60
1.10.3.	Pharmacodynamic biomarkers	63
1.10.4.	Future clinical development of predictive biomarkers	63
1.11	HR23B, a biomarker for HDAC inhibitors	64
1.11.1.	Introduction	64
1.11.2.	Objectives and achievements	65

CHAPTER 2

MATERIALS AND METHODS **67**

2.1.	Cell culture	68
2.2.	Compounds and drug treatments	68

2.3.	Transfection and siRNA	69
2.4.	Electroporation	69
2.5.	Flow cytometry	70
2.6.	Immunoblotting	71
2.7.	Assay for proteasome activity	71
2.8.	Immunofluorescence.	72
2.9.	Immunohistochemistry	73
2.10.	Tissue sources and histopathology examination	75
2.11.	Patients and methods (pilot trial)	76
2.11.1.	Inclusion and exclusion criteria	76
2.11.2.	Treatment	77
2.11.3.	Study design	78
2.11.4.	Specimen storage	78
2.12	VICTOR trial retrospective analysis: study design	78
2.13	Immunohistochemistry scoring and evaluation	79
2.14	Statistical analysis	82

CHAPTER 3

RESULTS

EFFECT OF HDAC INHIBITOR AND PROTEASOME INHIBITOR TREATMENT ON CTCL, COLORECTAL AND MELANOMA CELL LINES: CELL CYCLE EFFECTS AND EFFECTS ON HR23B EXPRESSION **84**

3.1.	Introduction	85
3.2.	Effects of HDAC inhibitor treatment on apoptosis in tumour cell lines	86

3.3. Effects of HDAC inhibitors on the expression of HR23B 93

3.4. Alteration in pre-treatment HR23B levels impacts on HDAC inhibitor-mediated apoptosis 101

3.5. Conclusion. 107

CHAPTER 4

RESULTS

PROTEASOME ACTIVITY IN CTCL AND MELANOMA CELL LINES TREATED WITH HDAC INHIBITORS 108

4.1. Introduction 109

4.2. HDAC inhibitor treatment causes a decrease in proteasomal activity 109

4.3. A reduction in HR23B protein levels rescues both HDAC inhibitor- and proteasome inhibitor-mediated apoptosis 124

4.4. HDAC inhibitor and proteasome inhibitors synergize at low concentrations to cause similar levels of apoptosis as at higher concentrations of single inhibitor treatment 126

4.5. Conclusion. 138

CHAPTER 5

RESULTS

AUTOPHAGY IN HDAC INHIBITOR TREATED CELLS: INTERPLAY BETWEEN HR23B AND HDAC6 139

5.1. Introduction 140

5.2. HR23B influences autophagy 141

5.3. Effects of inhibiting autophagy on apoptosis 152

5.4. Interplay between HR23B and HDAC6 158

5.5. Conclusion 170

CHAPTER 6

RESULTS

EXPRESSION PATTERNS OF HR23B IN HUMAN TUMOUR TISSUES AND HR23B AS A PREDICTIVE BIOMARKER FOR RESPONSE TO THERAPY IN CTCL 171

6.1. Introduction. 172

6.2. HR23B expression is variable across different tumour types 175

6.3. HR23B expression in CTCL 178

6.4. HR23B expression in normal colon and colon cancer 183

6.5. HR23B expression in CTCL biopsies from a phase II clinical trial with SAHA 190

6.6. Conclusion 202

CHAPTER 7

RESULTS

DETECTION OF HR23B AND LC3 EXPRESSION IN HUMAN TUMOURS AND THEIR PROGNOSTIC ROLE IN COLORECTAL CANCER 203

7.1. Introduction. 204

7.2. HR23B expression and autophagy in human tumours 205

7.3. Autophagy during HDAC inhibitor treatment in patients 209

7.4. Prognostic significance of HR23B and LC3 216

7.4.1. HR23B expression 218
7.4.2. LC3 expression 225
7.4.3. Assessment of HR23B and LC3 expression 232

7.5. Conclusion. 238

CHAPTER 8

DISCUSSION AND FUTURE PERSPECTIVES 240

8.1. Cell lines from different tumour types demonstrate differences in sensitivity to HDAC inhibitors with alterations in HR23B levels having similar effects on induction of apoptosis 241

8.2. Patterns of HR23B expression after HDAC inhibitor treatment 242

8.3. Extrapolating results from the shRNA screen to other cell lines and tumour types 244

8.4. The importance of the ubiquitin-proteasome pathway in the cellular response to HDAC inhibitors 245

8.5. HR23B and resistance to HDAC inhibitor therapy via autophagy 245

8.6. HR23B and HDAC6 247

8.7. Immunohistochemistry and the expression of HR23B 248

8.8. Apoptosis, autophagy and prognosis . 249

8.9. Clinical perspectives 252

8.10. Conclusions 255

REFERENCES 258

APPENDICES **273**

Appendix I siRNA optimisation 274

Appendix II Proteasome assay optimisation 274

Appendix III LC3 antibody optimisation 277

Appendix IV Immunohistochemistry controls 279

Appendix V Inter-observer agreement 281-2

Appendix VI Effect of depleting HR23B using siRNA in colorectal and melanoma cells 284

CHAPTER 1

INTRODUCTION

1. General Introduction

1.1. Epigenetics

Transcriptional control is achieved through transcriptional regulators that bind specific DNA sequences leading to the modification of chromatin structure which consequently controls accessibility of DNA to regulatory factors (Ting et al., 2006). DNA methylation and histone modification are mechanisms that have been implicated in transcriptional regulation and the main factor influencing chromatin structure is the state of amino-acid residues within histone tails which serve as targets for many post-translational modifications (Inche and La Thangue, 2006). Epigenetics refers to the regulation of gene expression via post-translational modification of protein complexes associated with DNA without alterations in the DNA sequence. The post-translational modifications that have been studies the most in this field are acetylation and deacetylation. In normal cells, there is a delicate balance between histone acetylation and deacetylation and aberrant acetylation is associated with carcinogenesis.

Inhibition of histone deacetylase (HDAC) converts chromatin to an open structure and can activate certain genes that inhibit tumour growth (Kouzarides, 2007). Therefore small molecule inhibitors of the HDACs may modulate gene expression resulting in inhibition of tumour growth. These inhibitors could then be used as a potential therapy against particular tumours as they could essentially reactivate protective or necessary genes, which have been silenced by a mutation or a number of mutations within the tumour. Tumour cell proliferation could then be limited resulting in cell cycle arrest, differentiation or apoptosis. If the specific gene expression

profile and effects on cell cycle progression for each individual HDAC inhibitor is known, a personalised approach for each individual tumour type is possible.

1.2. Chromatin adaptations and regulation of transcription

The basic structure of chromatin consists of the nucleosome which comprises a 146 base pair of DNA wrapped around an octamer of core histones (2 H2A-H2B dimers and a H3-H4 tetramer) (Bentley et al., 1984; Luger et al., 1997). Histone H1 does not form part of the octamer but acts as a linker and plays a more regulatory role in the chromatin condensation process. Histone proteins compact massive amounts of genomic DNA into a size and structure that can be easily housed in the eukaryotic nucleus. Post-translational modifications occur at the histone amino terminus which forms a tail and extends from the core. This tail is lysine rich and the majority of modifications occur at these residues. These modifications of the histone tails can impact on the interactions between DNA, histones and the transcriptional machinery to modulate gene transcription. These proteins are post-translationally modified by, amongst others, lysine acetylation and ubiquitination, serine phosphorylation, sumoylation and methylation of lysines and arginines. The arrangement of these modifications on the histone tails is termed the 'histone code' which is read by other proteins recruited to the chromatin which then determine the downstream effect of these modifications (Jenuwein and Allis, 2001).

Acetylation and deacetylation are regulated by two groups of enzymes with opposite activities: histone acetyltransferases (HATs) and HDACs. The former are recruited within a complex to regions in the chromatin containing gene promoters for genes whose activation is required.

These complexes also contain other coactivators required for successful gene transcription. HATs catalyse the transfer of an acetyl group from acetyl-co-A to the ε-amino site of lysine, neutralizing the positive charge on histones and results in relaxation of the interaction between DNA and histones and an open chromatin (Chan et al., 2001). There is greater access to transcription factor complexes that frequently leads to increased DNA transcription (figure 1.1). However microarray analyses have demonstrated that the inhibition of histone deacetylation can cause both up- and down-regulation of gene expression demonstrating the complexity of the regulation of gene expression (Mitsiades et al., 2004a; Peart et al., 2005).

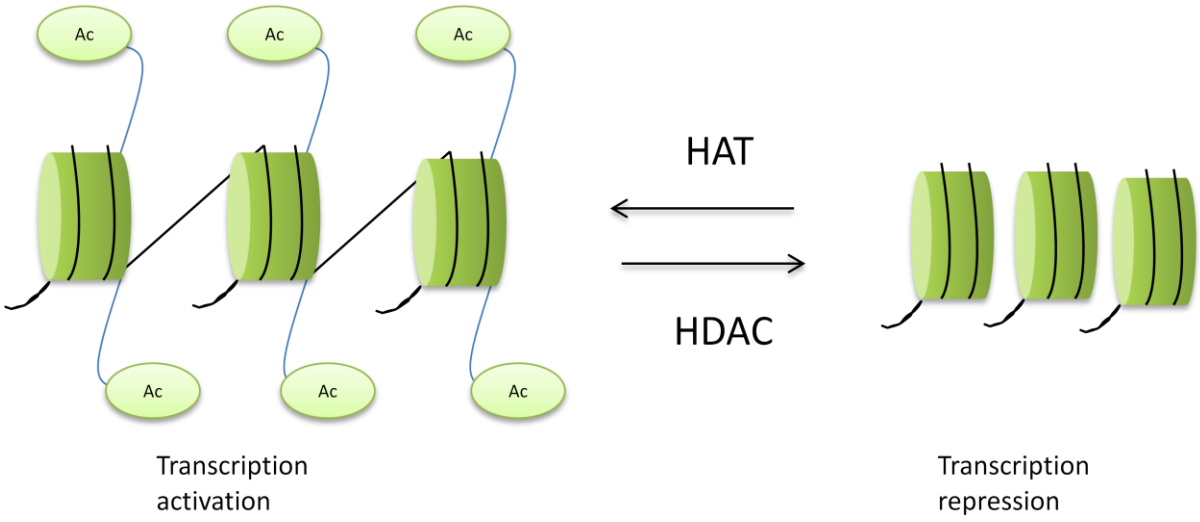


Figure 1.1: Chromatin structure regulates transcriptional activity

Post-translational modifications such as acetylation (Ac) modulate the transcriptional activity of genes. Acetylation of histones by histone acetyltransferases (HATs) adds acetyl groups to histone tails allowing a more open chromatin conformation and increased accessibility to transcription factor complexes, whilst the removal of these bulky acetyl groups by histone deacetylases (HDACs) allows a more compact form of chromatin and leads to transcriptionally inactive chromatin. Other modifications of histone tails include phosphorylation, methylation and ubiquitination.

1.3. Histone deacetylases (HDACs)

1.3.1. Introduction

There are eighteen HDACs which are classified according to functional and phylogenetic criteria based on their homology to yeast proteins (Carey and La Thangue, 2006). They are divided into the classical Zn^{2+}-dependent (class I, IIa, IIb and IV) and Zn^{2+}-independent, nicotinamide adenine dinucleotide (NAD)-dependent (class III) enzymes. These HDACs all contain at least one catalytic domain apart from HDAC6 which has two and many also contain a nuclear localisation sequence (NLS) (figure 1.2) (Marks, 2010a). The class III family of HDACs are called sirtuins and were first identified as homologues of the yeast protein SirT2 (Imai et al., 2000). They differ from class I/II/IV HDACs as they are dependent on the cofactor NAD and are not responsive to any of the small molecule HDAC inhibitors (Imai et al., 2000).

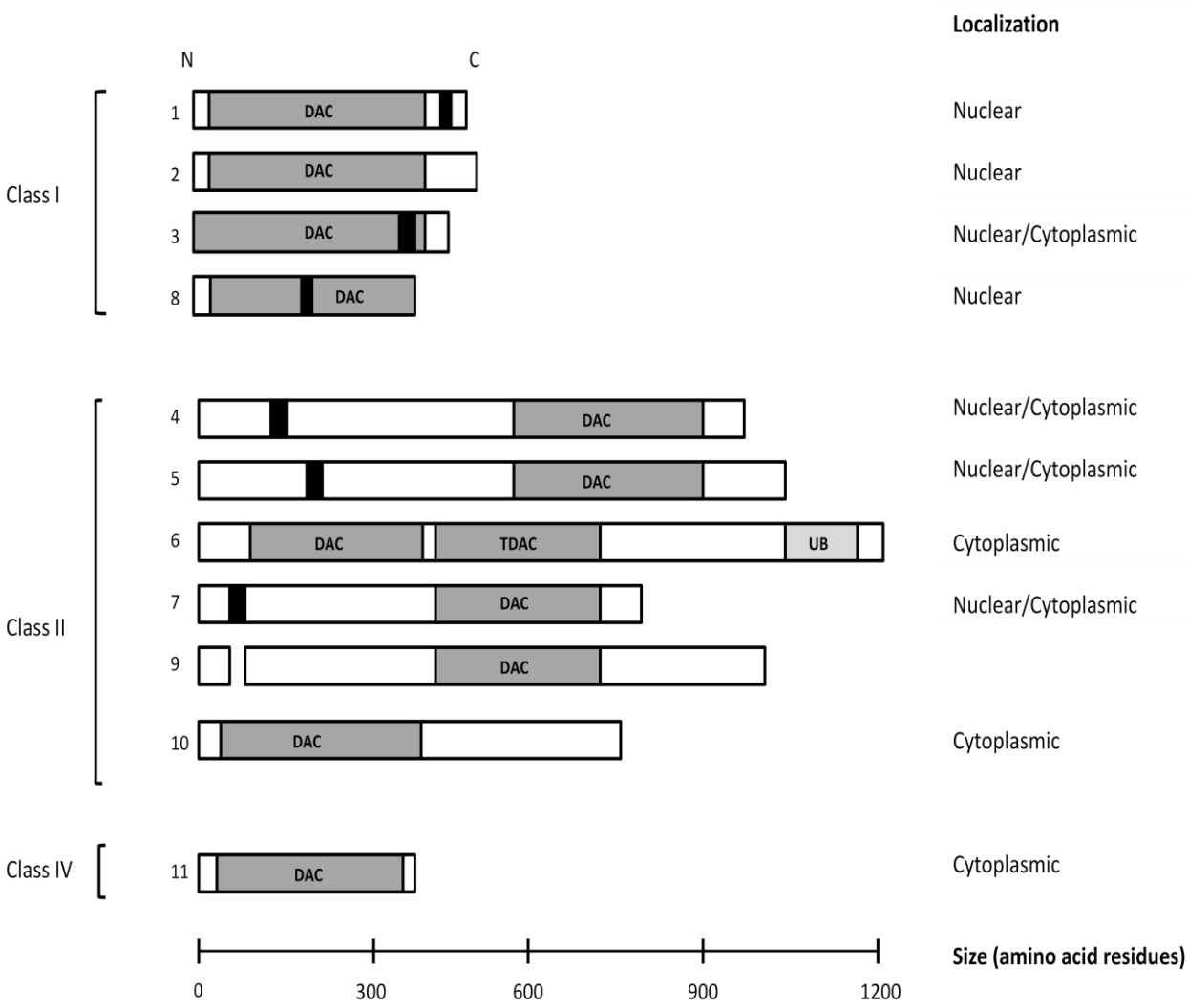


Figure 1.2

Schematic depiction of the different isoforms of HDAC

Bars depict the length of the protein. The Zn^{2+}-dependent catalytic domain of the Class I and II HDACs is shown in dark gray and the ubiquitin-binding domain of HDAC6 is shown in light grey (deacetylase domain, DAC; tubulin deacetylase domain, TDAC; ubiquitin binding, UB). Black depicts a NLS. N, N-terminus, C, C-terminus. Subcellular localization is also indicated.

1.3.2. Class I HDACs

Class I HDACs comprise HDAC 1-3 and 8 and are ubiquitously expressed in all cells and are homologous to the yeast HDAC reduced potassium dependence 3 (Rpd3) (de Ruijter et al., 2003a). Their structure is simpler than class II HDACs comprising an N-terminal deacetylase domain and a relatively short C-terminal tail. Mammalian HDAC1 and HDAC2 are almost identical with similar catalytic domains and are homologous in the C-terminal tail with tandem casein-kinase 2 (CK2) phosphorylation sites (Yang and Seto, 2008). The tail of HDAC1 also contains a sumoylation motif. They are present together in a complex so their individual functions are difficult to determine. They are located in the nucleus and target multiple substrates (Table 1).

HDAC 3 differs from HDACs 1 and 2 in that it has only one CK2 phosphorlation site (Zhang et al., 2005). HDAC3 is the only Class I HDAC that can be found in both the nucleus and the cytoplasm and this shuttling process appears to be an essential feature of its function (Takami and Nakayama, 2000). HDAC8 consists almost entirely of the catalytic domain and instead of CK2 sites; HDAC8 has a conserved motif for protein kinase A phosphorylation and negative regulation of deacetylase activity (Lee et al., 2004). It is located in both the nucleus and cytoplasm.

Table 1.1: Summary of substrates, associated proteins and functions of class I HDACs

CLASS 1 HDACs			
HDAC	Substrates and associated proteins	Putative functions	References
HDAC1 **HDAC2**	Multi-protein repressor complexes: Sin3A, Mi2/NuRD, Co-REST DNA-binding proteins SP1 Rb-1 binding protein Rb P53 Myo D NF- κB	Deletion: neural precursor maturation defects Regulation of cardiac growth, morphogenesis and contractility Increased sensitivity to DNA damage, impaired DSB repair by NHR Suppression of tumour cell apoptosis Regulation of chromatin compaction (HDAC2) Regulation of ROS signalling and apoptosis	(Bhaskara et al., 2008; Marchion et al., 2009; Miller et al., 2010; Montgomery et al., 2007; Witt et al., 2009; Yang and Seto, 2008)
HDAC3	NcoR/SMRT Rb NF-κB HDAC4	Deletion: embryonic lethality Inactivation: interruption of cell cycle progression DNA damage Compromised DNA repair and apoptosis Regulation of mitosis by Aurora B kinase activity	(Bhaskara et al., 2008; Li et al., 2006)
HDAC8	None known	Unknown	

Abbreviations: SP-1, specificity protein 1; Rb, retinoblastoma; NF- κB, nuclear factor kappa B; NcoR/SMRT, nuclear receptor co-repressor-1/silencing mediator for retinoid or thyroid-hormone receptors; Myo-D, myogenic differentiation, ROS, reactive oxygen species

1.3.3. Class IIa HDACs

Class IIa HDACs comprise HDAC4, HDAC5, HDAC7 and HDAC9 and are related to the yeast protein Hda1 (de Ruijter et al., 2003a). Hda1 consists of an N-terminal deacetylase domain and a long C-terminal extension of unknown function. In mammals, only the N-terminal deacetylase domain is shared and there is a long N-terminal extension in class IIa members (HDAC4, 5, 7 and 9). This N-terminal extension contains binding sites for myocyte enhancer factor 2 (MEF2) and 14-3-3 proteins. MEF2 and 14-3-3 proteins are consequently major partners of class IIa HDACs. MEF2 binds to class IIa HDACs and promotes their nuclear localisation and 14-3-3 proteins stimulate their cytoplasmic retention in a phosphorylation dependent manner. The nuclear function of class IIa HDACs is regulated by different signalling pathways through reversible phosphorylation at 14-3-3 binding sites and they act as signal transducers (Yang and Seto, 2008).

The mechanism through which class IIa HDACs repress transcription is yet to be fully elucidated. Intrinsically, class IIa HDACs possess very weak catalytic activity and they recruit class I HDACs through their C-terminal HDAC domain which may account for some of their catalytic activity (Haberland et al., 2009). Class IIa HDACs are also subject to ubiquitination and sumoylation, the former promotes protein degradation but the consequences of the latter are less well understood (Li et al., 2004). Sumoylation may result in formation of a transcriptional repression domain and may increase the transcriptional repression potential of HDAC4 (Kirsh et al., 2002) .

The expression pattern of class IIa HDACs is relatively tissue-restricted compared to other HDACs; HDAC4 is highly expressed in brain and growth plates of the skeleton and HDAC5 and HDAC9 expression is very high in muscle, heart and brain. HDAC7 expression is high in endothelial cells and thymocytes, specifically in T-cell precursors (Verdin et al., 2003).

The catalytic domain of HDAC9 is located in the amino-terminus similar to the Class I HDACs. There are three splice variants known so far, HDAC9a, HDAC9b and HDRP/HDAC9c and the latter has no catalytic domain and is thought to function as a novel co repressor (Zhou et al., 2001). The presence of different splice variants of HDAC9 might represent an example of increasing the specificity of HDAC activity where one isoform is expressed at certain times in specific cell types. Putative functions and associated proteins of class IIa HDACs are summarised in table 1.2.

Table 1.2: Summary of substrates, associated proteins and functions of class IIa HDACs

Class IIa HDACS			
HDACs	Substrates and associated proteins	Putative functions	References
HDAC4	Class I HDACs MEF-2 binding site (HDAC4, isoforms of HDAC9)	Skeleton formation Regulation of neural survival in retina	(Sun et al., 2009; Vega et al., 2004)
HDAC5		Deletion leads to cardiomegaly in mice Myocardial and skeletal muscle development	(Urbich et al., 2009; Zhang et al., 2002a; Zhang et al., 2002b)
HDAC7		Regulation of vascular endothelial development and vascular integrity	(Dequiedt et al., 2003)
HDAC9		Muscle cell differentiation Cardiomyocyte differentiation Regulation of HR (with HDAC10)	(de Ruijter et al., 2003b; Montgomery et al., 2007; Zhang et al., 2002a)

Abbreviations: MEF-2, myocyte enhancer factor 2; HR, homologous recombination

1.3.4 Class IIb HDACs

HDAC6 contains tandem deacetylase domain and a C-terminal zinc finger and is a major cytoplasmic deacetylase (Boyault et al., 2007). The zinc finger can bind ubiquitin. There is also a SE14-repeat domain present in human and other higher mammalian HDAC6. The other class IIb HDAC is HDAC10 which has an N-terminal half that is very similar to the first deacetylase domain of HDAC6 and the C-terminal half is leucine rich (Fischer et al., 2002; Kao et al., 2002). HDAC10 has at least two splice variants and a catalytic domain has been identified in the amino-terminus, and another potential catalytic domain has been identified in the C-terminus. It has been found in complex with most of the other HDACs and is the only HDAC where the recombinant protein shows catalytic activity (Haberland et al., 2009). HDAC10 is similar in structure to HDAC6 but has an extra inactive domain.

HDAC6 contains an additional deacetylase domain which has been shown to function as an α-tubulin deacetylase (Matsuyama et al., 2002). Deacetylation of tubulin destabilizes microtubule assembly. HDAC6 senses misfolded proteins by binding to their ubiquitin residues. The fate of these misfolded proteins is determined by the balance of HDAC6 and valosin-containing protein (VCP) within a multicomponent repressive complex and VCP favours proteasomal degradation (Boyault et al., 2007). HDAC6 acts as a bridge between the dynein motors and the ubiquitination process, directing polyubiquitinated proteins to the aggresome. HDAC6 binding to ubiquitin dissociates heat shock protein 90 (HSP90) and heat shock factor-1 (HSF1) from the complex and this results in induction of the heat shock response (Dai et al., 2007). HDAC6 therefore acts as a

stress sensor promoting accumulation of ubiquitinating proteins when proteasomal function is compromised.

HDAC inhibitors impact on these pathways in a number of different ways. HDAC6 inhibition leads to HSP90 hyperacetylation and there is loss of chaperone function and client proteins important for survival and proliferation such as Akt, Bcr-Abl, c-Raf and ErB2 (Bali et al., 2005; Kovacs et al., 2005). These are more susceptible to poly-ubiquitination and proteasomal degradation. Their loss induces endoplasmic reticulum (ER) stress. HDAC hyperacetylation of tubulin impairs the dynein motor complex required for aggresome formation (Kawaguchi et al., 2003a). Failure of aggresome formation lessens the cell's ability to cope with ER stress and may result in apoptosis.

Table 1.3: Summary of substrates, associated proteins and functions of class IIb HDACs

Class IIb HDACs			
HDAC	Substrates and associated proteins	Putative functions	References
HDAC6	Co-localises with microtubules and dynein motor complexes Cortactin HSP-90	Regulation of cell motility, cell adhesions, chemotaxis and protein transport Modulation of protein folding and maturation Movement of	(Johnston et al., 1998; Kawaguchi et al., 2003a; Kovacs et al., 2005)

		ubiquitinated proteins along microtubules to sites of aggresomes Formation of stress granules Stimulation of heat shock response	
HDAC10	Rb-binding sites	Role in cell cycle progression Modulation of HSP-90 acetylation Effect on proteasomal degradation of VEGF receptors and angiogenesis Regulation of HR (with HDAC9) Regulation of ROS signaling and apoptosis	(Kotian et al., 2011)

Abbreviations: HSP-90, heat shock protein-90; Rb, retinoblastoma, VEGF, vascular endothelial growth factor; HR, homologous recombination; ROS, reactive oxygen species

1.3.5. Class IV HDAC (HDAC11)

HDAC11 is the only member of the Class IV HDACs and little is known of its function. It may have a role in immune system regulation via its involvement in interleukin-10 expression (Lian et al., 2012) and OX40L surface expression in Hodgkin lymphoma (HL) (Buglio et al., 2011).

1.3.6. HDAC catalytic activity

The catalytic domains of HDAC inhibitors consist of a single α/β domain composed of an eight-stranded β –sheet sandwiched over a dozen α-helices (Finnin et al., 1999). The catalytic centre contains a zinc ion chelated by side chains of histidine and aspartate residues. Many HDAC inhibitors exert their inhibitory effect via the Zn^{2+}-dependency of HDAC enzymes. These include trichostatin A (TSA), vorinostat, belinostat, dacinostat, panabinostat and givinostat). They contain a pharmacophore containing a cap, connecting unit, linker and a zinc binding group that chelates the cation in the catalytic domain of the target HDAC.

The cellular functions of HDAC enzymes are diverse and it is unclear which of the two broad groups of HDAC inhibitors (based on specificity) will provide the greatest clinical benefit and optimum toxicity profile. As HDACs have a wide variety of functions the mechanisms of cell death induced by HDAC inhibitors are probably multiple. HDAC activity is not restricted to the control of chromatin; in fact there are numerous other proteins that may be regulated by acetylation all of which impact on their mechanism of action. However, based on DNA microarray studies, only a small percentage of genes (5-10%) are influenced by HDAC inhibition

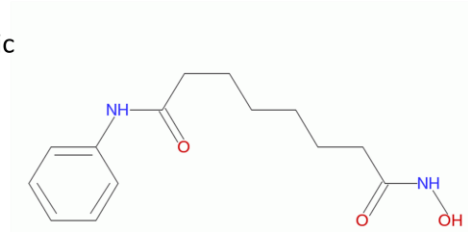
and consequently alternative mechanisms are also likely to contribute to cell death (Glaser et al., 2003; Mitsiades et al., 2004b). The explanation for this may be that other modifications such as methylation are dominant and repress genes more than histone deacetylation. Indeed, there are numerous non-histone targets, including DNA-binding transcription factors, chaperones, nuclear import factors, signalling mediators, tumour suppressors, DNA repair enzymes and cell mobility proteins. Several of these are important in tumour-cell growth and proliferation lending weight to this hypothesis (Khan and La Thangue, 2012a)). Phylogenetically, the three classes of HDAC evolved before histones themselves suggesting that the effects on non-histone substrates may be of equal or even greater importance (Gregoretti et al., 2004).

1.4. HDAC inhibitors: development and role in cancer therapeutics

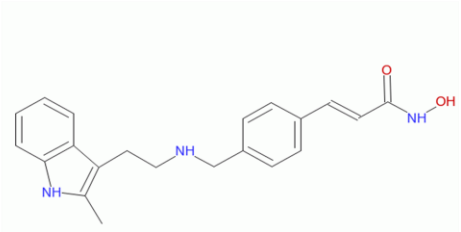
1.4.1. HDAC inhibitors.

The current classification of HDAC inhibitors is based on their chemical structures. Broadly these are subdivided into short chain fatty acids, hydroxamic acids, cyclic tetrapeptides, aliphatic acids and benzamides (figure 1.3, table 1.4) (Marks and Xu, 2009). They may also be classified according to their specificity for HDACs. The pan-deacetylase inhibitors include vorinostat, panabinostat, belinostat, resminostat and TSA. Butyrate and valproate inhibit Class I and IIa HDACs while romidepsin, entinostat and mocetinostat are considered to be class I-specific. Tubacin is HDAC6-specific.

Hydroxamic acids

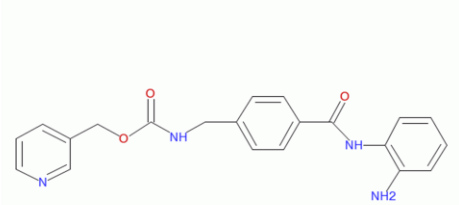


vorinostat

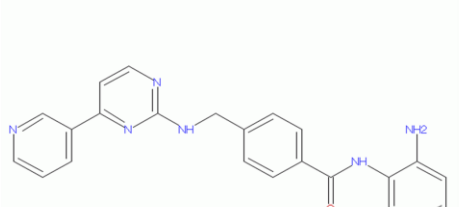


panabinostat

Benzamides

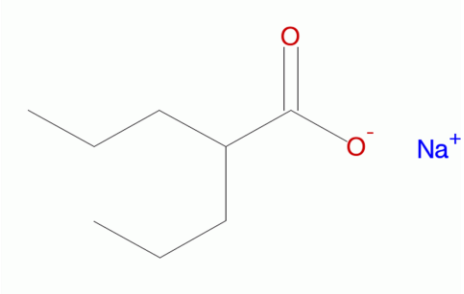


MS-275

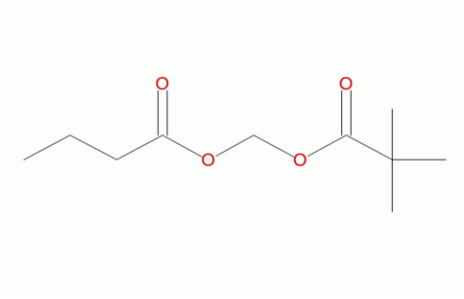


mocetinostat

Aliphatic acids

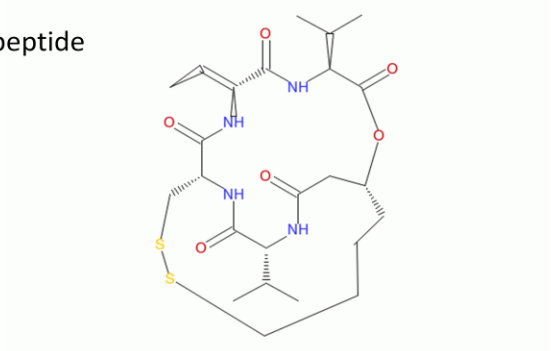


valproic acid



AN-9

Cyclic tetrapeptide



Romidepsin

Figure 1.3: Chemical structures of selected HDAC inhibitors from the four different classes of HDAC inhibitors.

Table 1.4: Classification of HDAC inhibitors with potency and clinical status

Chemistry	Compound	Potency	Clinical status
Hydroxymate	SAHA (Vorinostat)	nM	Approved (CTCL) Phase II, III
	PXD101 (Belinostat)	nM	Phase I, II, III
	LBH589 (Panobinostat)	nM	Phase II, III
	ITF2357 (Givinostat)	nM	Phase I,II
	PCI-24781 (CRA-024781)	nM	Phase I
	JNJ-26481585	µM	Phase I
	4SC-201 (Resminostat)	µM	Phase I, II
Benzamide	MS-275 (Entinostat)	µM	Phase II
	MGCD0103 (Mocetinostat)	µM	Phase II
Cyclic tetrapeptide	Depsipeptide/FK228 (Romidepsin)	nM	Approved (CTCL and PTCL) Phase I, II
Aliphatic acids	Valproic acid	mM	Phase I, II,III

	Butyrate	mM	Phase II
	Pivanex (AN-9)	mM	Phase I,II

Abbreviation: CTCL, cutaneous T-cell lymphoma; PTCL, peripheral T-cell lymphoma

1.4.2. HDAC inhibitors in clinical use

There are many dozens of clinical trials that have been performed with a variety of single agent HDAC inhibitors but only two HDAC inhibitors have received Food and Drug Administration (FDA) and European Medicines Agency (EMA) approval, namely vorinostat and romidepsin (table 1.4, reviewed in (Marks, 2010a; New et al., 2012)).

1.4.2.1. Vorinostat

Two phase II trials of vorinostat resulted in its FDA approval. In one study, 33 patients with either advanced mycosis fungoides (MF) (85% had stage IIB or above) or Sézary syndrome (SS) were recruited. The group had been heavily pre-treated and the majority of patients had received at least one prior chemotherapy regimen. Although there were no complete responses (CR), eight patients had a partial response (PR) and seven of these patients had advanced-stage disease (four of whom had SS; response rate (RR): 24%). The time to progression (TTP) for all patients was 12.1 weeks, but this interval was 30.2 weeks among responders. Almost half the patients with baseline pruritus derived symptomatic relief, and the overall clinical benefit rate was 58%. A proportion of tumours showed a reduction in dermal and epidermal lymphocytes, and a reduction

in microvessel density was seen in all patients. Furthermore, analysis of lesion biopsies in responders showed a shift in localization of phosphorylated signal transducer and activator of transcription 3 (STAT3) from nuclear to cytoplasmic suggesting that vorinostat may inhibit proliferation of CTCL cells by inactivating STAT3.

The second phase II trial involved 74 patients with advanced MF or SS, who were also heavily pre-treated. The objective RR was 29.7% (36.4% in patients with SS). The median TTP was 4.9 months overall, but this end point was not reached at the time of publication for responders; 43.4% of patients had pruritus relief, including patients who did not meet objective response criteria.

These response rates were comparable to response rates seen with other agents used in advanced disease such as bexarotene and denileukin diftitox. Indeed, if clinical benefit from pruritus was also considered, then response rates were considerably higher. Similar response rates were seen in a phase II clinical trial in relapsed non-Hodgkin lymphoma (NHL) and mantle cell lymphoma. Currently, there are over 40 phase I–III trials of vorinostat, alone or in combination with cytotoxic chemotherapeutic agents or newer targeted therapies, in patients with CTCL and other haematological and solid malignancies.

Despite the promising results in CTCL the efficacy of vorinostat in several tumour types including acute myeloid leukaemia, HL, NHL, prostate, thyroid, ovarian, breast, colorectal, non-small cell lung, head and neck and glioblastoma has been moderate at best (Khan and La Thangue, 2012a). After some initial early reports of success in mesothelioma (Zauderer and

Krug, 2012), a recent large phase III trial has shown no survival benefit of vorinostat compared to best supportive care (Krug et al., 2011).

1.4.2.2. Romidepsin

Romidepsin (FK-228, depsipeptide) was isolated from *Chromobacterium violaceum* (WB968) and is the only inhibitor of this class in clinical trials and inhibits HDAC catalytic activity at nanomolar concentrations (Prince and Dickinson, 2012). Romidepsin was approved by the FDA for patients with relapsed/refractory CTCL. Two phase II trials were conducted in a total of 167 patients suffering from relapsed, refractory or advanced CTCL (Whittaker et al., 2010). In both trials the ORR was 34% and the CR was 6% with a median time to response of 2 months and a median duration of response of longer than 12 months. The most commonly reported adverse events included fatigue, nausea, vomiting, anorexia and diarrhoea. Abnormalities on electrocardiograms have been noted in most trials of romidepsin. The clinical relevance of these findings remains under investigation but there may be an association with co-administered anti-emetics.

Romidepsin has also been found to have clinical benefit in the treatment of the rare and difficult to treat peripheral T cell lymphoma (PTCL) (Piekarz et al., 2011). In this phase II trial in patients with refractory PTCL a RR of almost 40% was seen with manageable toxicities. There was limited efficacy seen in a recent phase II trial in multiple myeloma (MM) (Niesvizky et al., 2011). Unfortunately, trials in solid tumours have been disappointing with limited responses seen

in glioblastoma, small cell lung cancer, prostate, colorectal, renal cancer and squamous cell cancers of the head and neck (Khan and La Thangue, 2012a).

1.4.2.3 Other HDAC inhibitors

Belinostat (PXD101) was developed by Topotarget Prolifix and was identified as an inhibitor of HDAC at nanomolar concentrations in various cell lines and was shown to have anti-tumour activity in human tumour xenografts. Belinostat has shown moderate activity in phase II trials in thymoma and thymic carcinoma and some limited responses in myelodysplastic syndrome and hepatocellular carcinoma (Cashen et al., 2012; Giaccone et al., 2011; Yeo et al., 2012). A trial in ovarian cancer has also demonstrated limited efficacy but there were no clinical responses in a phase II trial in pleural mesothelioma (Mackay et al., 2010; Ramalingam et al., 2009). Phase I and II trials of belinostat are ongoing in CTCL as well as in several other tumour types, both of single-agent treatment and as combination regimens with agents including bortezomib, 5-fluorouracil, 5-azacytidine, carboplatin, paclitaxel and isotretinoin.

Other hydroxamic acid inhibitors in clinical development include panabinostat (LBH589) which is more potent than vorinostat *in vitro* and in a trial of 11 patients with CTCL treated with the HDAC inhibitor LBH589, two individuals achieved CR and four attained PR, an overall RR of 60% (Shao et al., 2010). This agent is currently in phase II–III clinical development in patients with CTCL and it has received Orphan Drug Design Designation by the FDA and EMA for the treatment of CTCL. It has also been found to have activity in haematological cancers including MM and HL (Dickinson et al., 2009; Ocio et al., 2010). Panobinostat has not been found to have

efficacy in a recent phase II trial in metastatic renal cancer (Hainsworth et al., 2011). A phase II trial of givinostat in MM has demonstrated only modest clinical benefit (Galli et al., 2010).

A number of benzamide based inhibitors have been developed and these include entinostat (MS-275), which has shown some selectivity for Class I HDACs. It is also a brain region selective inhibitor and has shown efficacy *in vivo* against glioblastoma (Eyupoglu et al., 2006). In phase II trials, entinostat demonstrated a PR in one patient with lymphoma but a phase II trial in melanoma of entinostat showed no clinical responses (Hauschild et al., 2008; Simonini et al., 2006).

The benzamide HDAC inhibitor, mocetinostat, has shown some promise in haematological cancers but trial recruitment was temporarily halted due to potential cardiac complications. However, no association with pericardial effusions was found and trial recruitment resumed. This phase II trial reported encouraging results in a group of heavily pre-treated HL patients (Boumber et al., 2011). MGCD0103 has recently been granted orphan drug designation by the FDA for the treatment of HL.

A pan-HDAC hydroxymate inhibitor, resminostat has recently been shown to have clinical efficacy in the treatment of hepatocellular carcinoma and advanced HL. It has recently received Orphan Drug Designation by the FDA for the treatment of both these malignancies.

1.5. Mechanisms of HDAC inhibitor-induced cell death

HDAC inhibitors mediate cell death through several pathways. These include cell growth arrest, effects on DNA repair and mitosis, induction of apoptosis, anti-angiogenic effects and effects on the misfolded protein response pathway (reviewed in (Khan and La Thangue, 2012a; Marks, 2010a; New et al., 2012)). HDAC inhibitors also induce autophagy although this may be a mechanism of resistance rather than cell death (figure 1.4). Modulation of histone and, more generally, protein acetylation, alters pathways that promote proliferation, angiogenesis, senescence and survival in cancer cells. HDAC inhibitors are known to induce senescence in tumour cells which may be a mechanism of tumour suppression although paradoxically, stromal cell activation by HDAC inhibitors may promote tumour cell survival. Autophagy induction and modulation of the immune system are consequences of HDAC inhibitor therapy and their precise impact on cancer biology remains unclear. There are global effects on gene expression induced by HDAC inhibitors and these may affect as yet undiscovered cellular processes. Successful therapeutic use of HDAC inhibitors may thus depend on subtleties of the cellular milieu, the specific HDACs targeted and the relative dependence of the malignant phenotype on the unique set of pathways influenced by a specific drug.

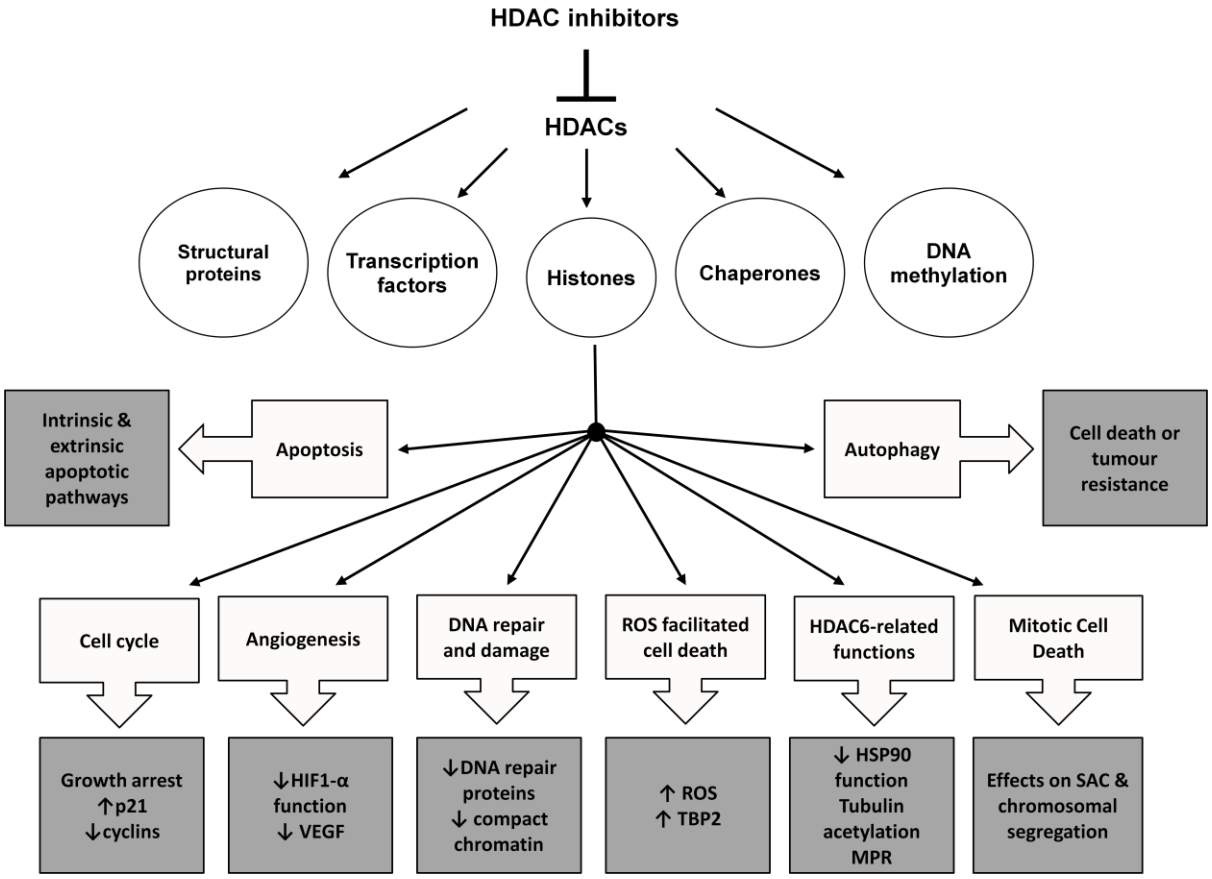


Figure 1.4: The pathways affected by HDAC activity

Acetylation of histone provides an important level of epigenetic control on gene expression through altering chromatin activity. A variety of non-histone proteins are regulated by their acetylation level, including transcription factors, chaperones and structural proteins, which allow HDAC to influence a multiplicity of physiological pathways. The gene silencing activity of DNA methylation also relies on HDAC. Control of the cell cycle, apoptosis, differentiation, angiogenesis and invasion represent some of the most important pathways affected by HDAC. Many of these pathways are abnormal in tumour cells.

Abbreviations: HIF-1α, hypoxia inducible factor-1α; VEGF, vascular endothelial growth factor; ROS, reactive oxygen species; TBP-2, TATA binding protein-2; HSP-90, heat shock protein-90; MPR, misfolded protein response; SAC, spindle assembly checkpoint

1.6. Combining HDAC inhibitors with other chemotherapeutic agents.

Acetylation controls numerous cellular pathways as detailed in previous sections. Improved understanding of these pathways and the mechanisms through which HDAC inhibitors exert their anti-tumour effects has led to development of rational combination drug strategies with other chemotherapeutic agents.

HDAC inhibitors adjust the balance in favour of proapoptotic pathways and they have therefore been tested in solid tumours in the pre-clinical and clinical settings in combination with conventional chemotherapeutic agents such as platinum compounds (Ramalingam et al., 2010), topoisomerase inhibitors (Munster and Daud, 2011), nucleoside analogues (De et al., 2009; Kalac et al., 2011), tyrosine kinase inhibitors (Bruzzese et al., 2011; Huang et al., 2011; Nguyen et al., 2011), the HSP90 inhibitors analogue to geldanamycin (Chinnaiyan et al., 2005; Rao et al., 2008; Yu et al., 2011), radiation therapy (Chinnaiyan et al., 2005), anthracyclines (Munster et al., 2009) and tamoxifen (Munster et al., 2011; Thomas et al., 2011).

A recent development of interest is that of bivalent agents that combine two complementary active groups within a single molecular architecture. For example, the dual-acting histone deacetylase and topoisomerase II inhibitor derived from vorinostat and the anthracycline

daunorubicin, prototypical HDAC and topoisomerase II inhibitors, respectively (Guerrant et al., 2012).

As HDAC inhibitors are involved in modifying the MPR and its interaction with the ubiquitin proteasome system (UPS), combination studies of proteasome and HDAC inhibitors have been implemented. Bortezomib used in combination with romidepsin enhances the ability of FK228 to induce mitochondrial-dependent apoptosis. Co-treatment of bortezomib and vorinostat was shown to synergistically induce apoptosis in human leukemic cells, MM cells, non-small cell lung cancer (NSCLC) cells and hepatoma cells (Hideshima et al., 2011). Phase I and phase II studies are ongoing with the proteasome inhibitor bortezomib in combination with vorinostat or romidepsin, for the treatment of MM (Badros et al., 2009; Harrison et al., 2008; Weber et al., 2008). A possible explanation for these beneficial outcomes and synergistic effects could be that HDACs are also involved in protein quality control, influencing both the UPS (Fotheringham et al., 2009a) and alternative modes of proteasome inhibition.

1.7 Intracellular clearance mechanisms: autophagy, the ubiquitin proteasome system and the integrated regulation of cell fate

1.7.1 Introduction

A complex network of molecular chaperones exists that help proteins in folding and stabilise the transient conformations that proteins adapt for trafficking across membranes and during their assembly and disassembly into functional complexes (Driscoll and Chowdhury, 2012). The

homeostatic capability of the chaperone network can be overcome by various physiological and pathological conditions resulting in protein aggregation and proteotoxicity. In such circumstances, proteolytic systems eradicate the unstable proteins and recycle their amino acids. The two main proteolytic systems in cells are the UPS and autophagy. Together with molecular chaperones, these comprise crucial constituents of the cellular quality control system (Bukau et al., 2006).

There is a continuous turnover of all intracellular components including soluble proteins and organelles enabling the cell to maintain a state of self-renewal. Cellular degradative systems can be up-regulated in response to protein or organelle damage and to restock the intracellular reserve of free amino acids that maintain protein synthesis even in when nutrients are scarce. If these proteolytic systems fail to maintain basal cellular turnover or adapt to degradative needs of cells under stress conditions, cellular homeostasis is disrupted and the cellular energetic balance is compromised. This can result in intracellular accumulation of conformationally altered proteins that organise into insoluble oligomeric structures that are toxic and can result in cell death (Johnston et al., 1998; Kopito, 2000).

The two systems that manage the proteolytic cellular load, autophagy and the UPS, share a series of critical steps and components. These include cargo selection and tagging, cargo recognition and delivery to the proteolytic machinery, degradation in the proteolytic core and recycling of the constituent amino acids.

1.7.2 Autophagy

Autophagy (from the Greek “auto” meaning oneself and “phagy” meaning to eat) is an evolutionarily conserved major catabolic process where cytosolic components and invading pathogens are delivered to the lysosome for bulk degradation (Sridhar et al., 2012). Autophagy has a role in cellular quality control by removal of damaged long-lived proteins and organelles and their normal turnover. It is also a metabolic stress response providing an alternative source of energy by degrading intracellular materials.

The essential component of this proteolytic system is the lysosome (Repnik et al., 2012). Lysosomes are single membrane vesicles that contain intraluminal cellular hydrolases. The activity of intraluminal hydrolases is pH dependent and is increased in the acidic environment of the lysosomal lumen. An adenosine tri-phosphate (ATP)-dependent proton pump at the lysosomal membrane mediates acidification. Low lysosomal pH also facilitated partial unfolding of the substrate proteins enabling access by endoproteases to internal peptide bonds. Proteins are converted to small di- and tri-peptides and free amino acids that are released into the cytosol through permeases at the lysosomal membrane.

Three different types of autophagy exist: microautophagy, chaperone-mediated autophagy and macroautophagy and they differ in their mode of delivery to lysosomes (Janku et al., 2011a). Macroautophagy is the most relevant process to cancer biology and therapy and hereafter will be referred to as autophagy.

Autophagy regulates the levels of long-lived proteins and organelles and the UPS, by contrast, degrades short-lived proteins and autophagy may also work with the UPS in removal of potentially toxic protein aggregates as part of the MPR (Driscoll and Chowdhury, 2012). These aggregates accumulate at a storage site for degradation termed the aggresome and they are transported by retrograde microtubule transport via dynein motors (Kawaguchi et al., 2003a). The main mechanism of clearance of these inclusions is autophagy and suggests that in this circumstance, autophagy has a cytoprotective role. Aggresomes share features with inclusions that are formed during progression of several neurodegenerative conditions such as Parkinson disease and Huntington disease (Pandey et al., 2007a; Pandey et al., 2007b).

1.7.3 Signalling pathways in autophagy

Around 35 different genes (known as *Atg* or autophagy-related genes) participate in the execution and regulation of autophagy. Their protein products or Atg proteins organize into functional complexes that regulate each of the steps of autophagy (figure 1.5) (Klionsky et al., 2003). The major checkpoint in signalling pathways that regulate autophagy is the mammalian target of rapamycin complex 1 (mTORC1) and it integrates signalling through the phosphoinositide (PI3K)/Akt pathway and cellular nutrient status or energy levels which are sensed by adenosine monophosphate (AMP)-activated kinase (AMPK) (Janku et al., 2011a).

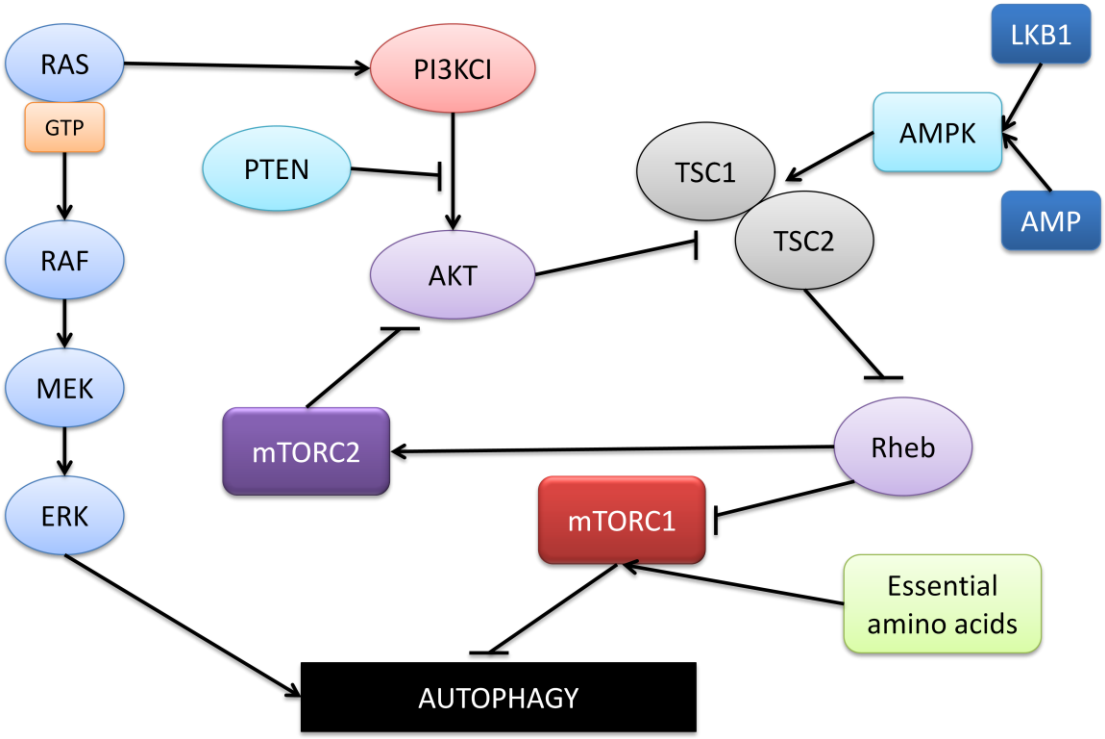


Figure 1.5: Regulation of autophagy

PI3KCI activates Akt which dampens the inhibitory effects of TSC1 and TSC2 by inhibiting their heterodimerisation via phosphorylation of TSC2. TSC1/2 inhibits the GTPase activity of Rheb. When this inhibitory signal is reduced, mTORC1 is activated resulting in autophagy inhibition. AMPK is activated by AMP or LKB1 and inhibits mTORC1 via TSC1/2. Activated mTORC1 downregulates autophagy by phosphorylating a complex of autophagy proteins (ULK1/2) which inhibits the downstream autophagy cascade. mTORC2 is also activated by this cascade which then phosphorylates Akt and provides a positive feedback loop of Akt activation that contributes to inhibition of autophagy. GTP-Ras activates PI3KCI as well as the RAF-MEK-ERK pathway and has an anti-autophagy effect. Cellular influx of amino acids also inhibits autophagy by activation of mTORC1 (adapted from (Janku et al., 2011a)).

Abbreviations: PI3KCI, phosphatidyl inositol 3-kinase; TSC, tuberous sclerosis protein; Rheb, ras homologue enriched in brain; mTORC: mammalian target of rapamycin; ULK, Unc-51-like kinase; AMPK, adenosine monophosphate-dependent kinase; LKB-1, liver kinase B-1

1.7.4 Cellular events and the machinery of autophagy

The autophagocytic process can be divided into several distinct phases (Xie and Klionsky, 2007). The first phase is the formation of the autophagosome at the phagophore assembly site (PAS) which is made up of forming phagophores (also called isolation membranes) and autophagy proteins. These phagophores start to sequester cytoplasmic constituents and once the edges of the phagophore are fused, a unique lipid bi-layer vesicular organelle is formed called an autophagosome. This engulfs the sequestrated cytoplasmic components, undergoes a maturation process by fusing with early and late endosomes and finally fuses with the lysosome. The contents of this autolysosome are degraded by lysosomal enzymes. There is a complex cascade of events (summarised in figures 1.6 and 1.7).

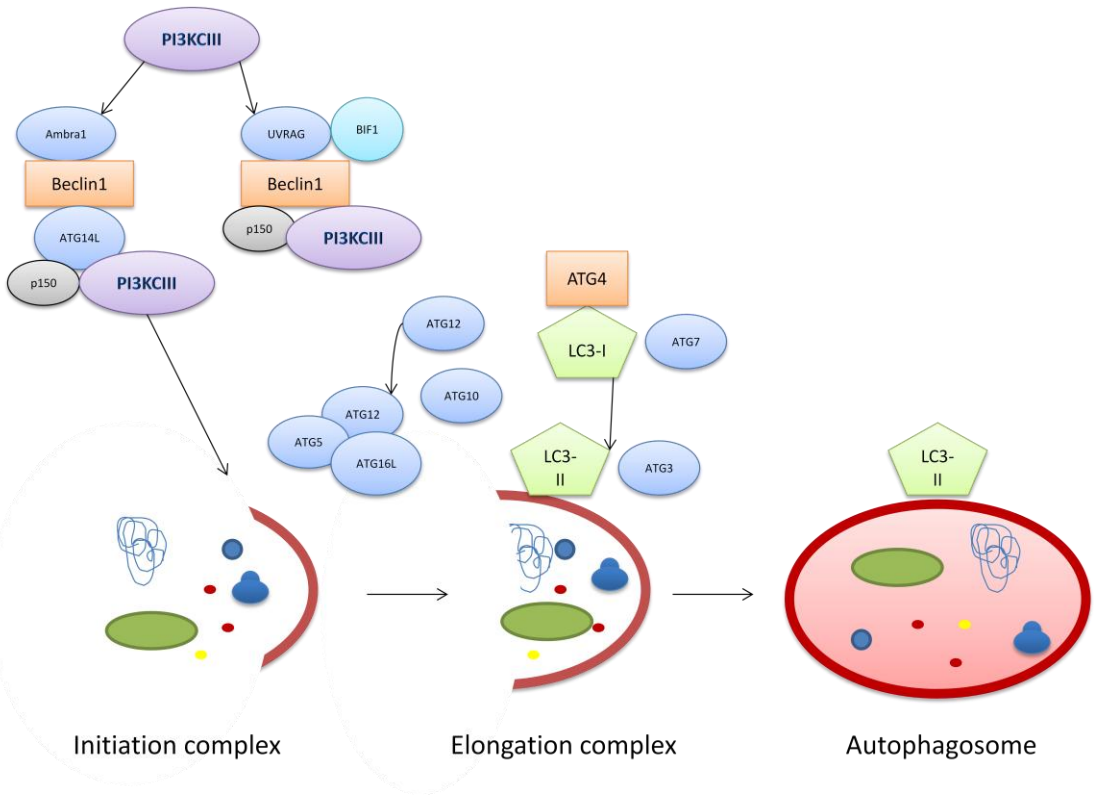


Figure 1.6: Autophagy cascade: initiation and elongation

The nucleation phase is controlled by a complex involving PI3KCIII with Beclin1–Atg14L–PI3KCIII–p150, Ambra1 or Beclin1–UVRAG–PI3KCIII–p150–Bif1. This step can be negatively regulated by the antiapoptotic protein Bcl-2. Atg9 and VMP1 are essential factors for autophagy. Atg9 has a role in phagophore expansion. The Atg12–Atg5 conjugate interacts with Atg16L, forming a large multimeric complex. LC3-I is conjugated to phosphatidylethanolamine in a reaction requiring Atg7 and Atg3. The lipidated form of LC3-I (LC3-II) is attached to both faces of the phagophore membrane. Abbreviations: Atg, autophagy-related gene; Bif1, endophilin-B1; LC3-I, microtubule-associated protein 1 light chain 3; mTORC1, mammalian target of rapamycin complex 1; PI3KCIII, phosphoinositide 3-kinase class III; UVRAG, UV radiation resistance

associated gene protein; VMP1, transmembrane protein 49 (adapted from (Sridhar et al., 2012)).

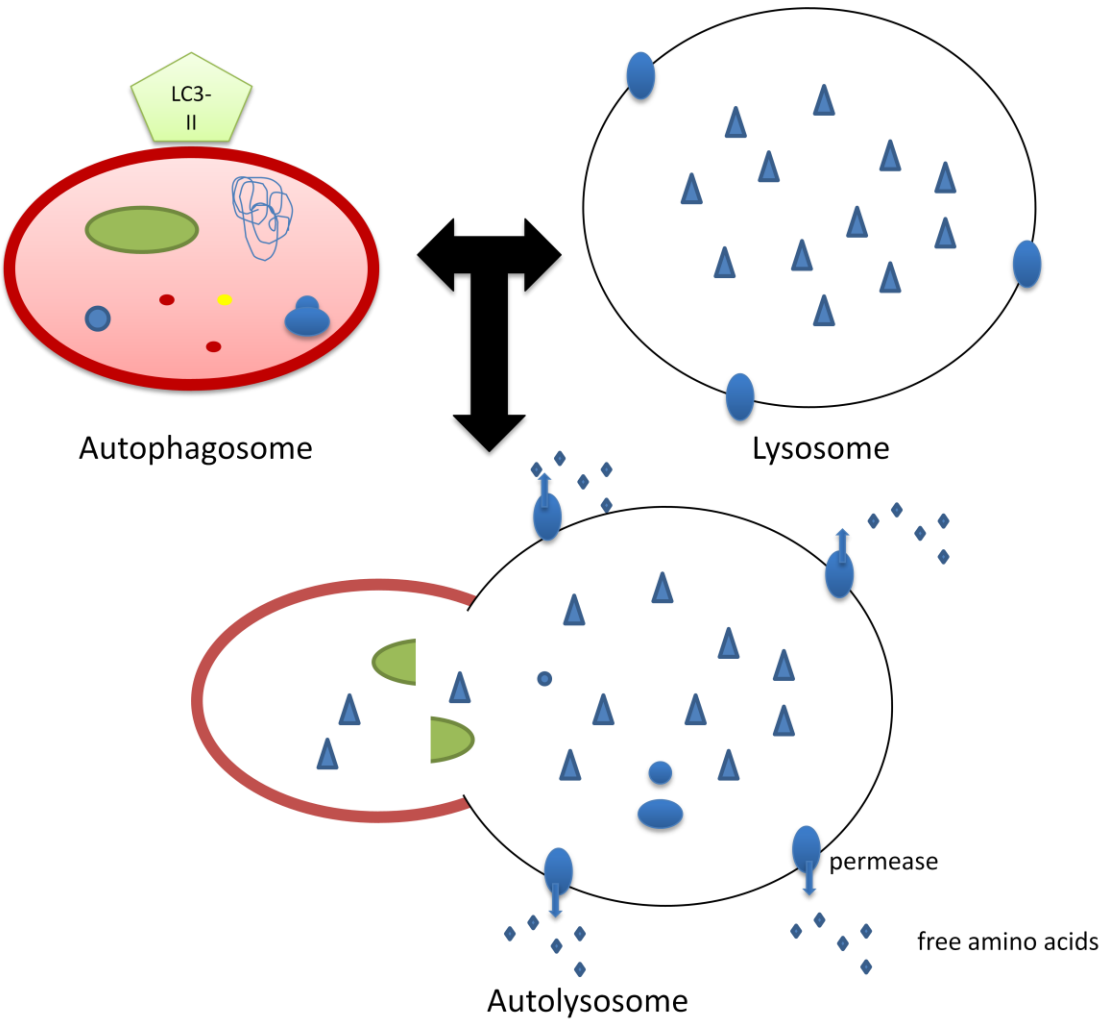


Figure 1.7: Autophagy cascade: maturation and lysosomal fusion

Recruitment of cargo from the cytoplasm requires autophagy receptors such as p62, Nbr1 or NIX. There is a final pathway that disassembles Atg protein complexes from matured autophagosomes that is mediated by Atg2, Atg9 and Atg18. The mechanisms by which the cargo is sealed by the isolation membrane are poorly characterised. Fusion of the complete double membrane autophagosome with endolysosomal compartments leads to

the breakdown of cargoes by acidic hydrolases such as the cathepsins. This fusion process requires the lysosomal membrane protein LAMP-2 and the small GTPase Rab7.

A complete double membrane autophagosome then fuses with the lysosome into the autophagolysosome, and the cargo-containing membrane compartment is lysed and degraded.

Abbreviations: Atg; autophagy-related gene; Nbr1: neighbour of BRCA-1 gene 1; LAMP-2, lysosomes associated membrane protein-2; GTPase: guanosine triphosphatase

1.7.5 Physiological functions of autophagy

In essence, there are four functions of autophagy: cell and tissue remodelling, cellular defence, quality control and cellular source of energy (Mizushima, 2005; Mizushima et al., 2008; Singh and Cuervo, 2011). Autophagy plays an important role in eliminating large portions of cytosol, organelles, plasma membrane and cellular corpses and therefore contributes to cellular differentiation, tissue remodelling and embryogenesis. Pathogens such as bacteria, viruses and parasites that reach the cellular cytoplasm through phagocytosis or directly across the plasma membrane can be eliminated by autophagy. Normal autophagic activity is essential for the maintenance of cellular homeostasis through continuous turnover of organelles and of damaged or altered proteins. Finally, autophagy may be a source of energy in situations of stress or nutrient deprivation. It is this final function of autophagy that may be significant in carcinogenesis (Degenhardt et al., 2006; Jin and White, 2008).

1.7.6. Autophagy and carcinogenesis

The PI3K/Akt/mTOR pathway regulates autophagy as previously described. It is frequently activated in cancer cells. Autophagy inhibition is an attractive anti-cancer target as it represents an important tumour survival mechanism (Sridhar et al., 2012). However, the situation is complicated by the fact that autophagy in areas of metabolic stress may also be a mechanism for limiting DNA damage caused by accumulation of reactive oxygen species and damaged organelles as well as removal of misfolded proteins (Karantza-Wadsworth et al., 2007).

A number of retrospective studies have shown that loss of the autophagy-related gene *Beclin 1* is associated with a poor prognosis in tumours. Low immunohistochemical expression of Beclin 1 in 115 node-positive colon cancer specimens was associated with a significantly worse 5-year overall survival (47% vs. 67%; p=0.011) (Li et al., 2009). In a study of squamous cell carcinoma of the oesophagus, 18 of 54 patients whose tumours did not express Beclin 1 as determined by immunohistochemistry had a significantly higher mortality (p=0.004) than those with normal expression (Chen et al., 2009). Loss of Beclin1 in breast cancer cell lines also resulted in resistance to the HER2 inhibitor lapatinib (Martin et al., 2009). By contrast, high Beclin 1 expression was associated with improved survival of patients with high-grade gliomas (p=0.03) and hepatocellular carcinoma (Ding et al., 2008; Pirtoli et al., 2009). However, in one analysis of patients with nasopharyngeal carcinoma treated with chemoradiation, elevated Beclin 1 expression strongly correlated with poor overall survival, progression-free survival and distant metastasis-free survival (Wan et al., 2010). A recent study found that mice with systemic mosaic deletion of the autophagy gene *atg5* or liver-specific deletion of *atg7* have a high incidence of

benign liver adenoma development, suggesting that autophagy suppresses tumour initiation (Takamura et al., 2011).

Autophagy was assessed in a small study of 13 malignant melanomas (Lazova et al., 2010). Tumour samples and florid melanoma in situ (MIS) showed over-expression of LC3 in contrast to early MIS and normal melanocytes suggesting that autophagy activation is a feature of more advanced disease. In contrast, a larger study of 149 melanoma samples demonstrated a significant decrease in beclin-1 protein and mRNA and LC3 mRNA with tumour progression with the lowest expression of cleaved LC3 in melanoma metastases (Miracco et al., 2010a). In an evaluation of 163 gastrointestinal tumour samples, overexpression of LC3 was observed in over half of the samples but did not correlate with survival outcomes (Yoshioka et al., 2008).

In a study of LC3 expression in 102 breast carcinomas, three distinct patterns of LC3 immunostaining were recognised: diffuse cytoplasmic, perinuclear and "stone-like" pattern which were described as dense, rounded amorphous structures enclosed within cytoplasmic vacuoles (Sivridis et al., 2010). The diffuse cytoplasmic and perinuclear patterns were associated with a favourable prognosis and an association with hormone receptors. The "stone-like" pattern of expression was associated with higher grade tumours and a poor prognosis. A further sixty epithelial non-breast tumours, breast cancer xenografts and HCT116 colon cancer spheroids were analysed and they displayed similar autophagic patterns. The authors concluded that the "stone-like" structures (SLS) may mark the completion of the autophagic process and that high autophagic activity may be associated with increased tumour aggressiveness and reduced long-term survival. These SLS may represent accumulation of debris and destruction of tumour cells.

The diffuse cytoplasmic and perinuclear staining patterns may be a feature of basal autophagy especially as these features were noted in non-neoplastic tissue.

In a follow on study, the same authors examined LC3 expression in colorectal cancer specimens from 155 patients (Giatromanolaki et al., 2010a). Similar analysis was carried out with respect to presence of SLS, diffuse cytoplasmic staining and perinuclear staining. Once again, high SLS counts were associated with a poorer prognosis while a perinuclear staining pattern was associated with significantly better prognosis. The cytoplasmic pattern was considered to be irrelevant. Indeed, a high SLS count with suppressed perinuclear expression was associated with a particularly poor prognosis and absence of SLS and intense perinuclear LC3 staining were associated with a particularly favourable prognosis. Multivariate analysis showed that SLS and perinuclear patterns were independent predictors of death events.

One of the conclusions drawn by the authors was that diffuse staining of LC3 in the cytoplasm reflected an intensified production of LC3-I and an early event in autophagosome formation. Once formed, the autophagocytic cargo would need to be delivered to lysosome-rich perinuclear area and so the perinuclear pattern may reflect basal functional autophagocytic machinery which is important for protein homeostasis in the cell.

1.7.7 Autophagy as a mechanism of tumour suppression

There is evidence that impaired autophagy may compromise the ability of the cancer cell to cope with metabolic stress and can lead to cell death (Jin et al., 2007). In such situations, necrosis can

result in an inflammatory response resulting in chronic tissue damage and genetic instability with a higher rate of oncogenic DNA mutations resulting in an enhanced malignant phenotype.

In mouse models with a mono-allelic deletion of *Beclin1* (*Beclin1*$^{+/-}$), there was a greater incidence of spontaneous tumours compared with *Beclin*$^{+/+}$ mice (Qu et al., 2003; Yue et al., 2003). There was decreased autophagy with no loss of heterozygosity and reduced but not absent expression of Beclin1. The Beclin1-/- phenotype was embryonically lethal. The suggestion was that *Beclin1* is a haplo-insufficient tumour suppressor gene. It has been proposed that in autophagy defective tumour cells, there is a failure to eliminate p62, endoplasmic reticulum chaperones and protein disulphide isomerases in response to stress and consequent protein quality control failure (Mathew et al., 2009). Persistence of p62 leads to increased oxidative stress, accumulation of damaged mitochondria and activation of the DNA-damage response.

In certain neurological disorders such as Parkinson disease and Huntington disease, pathogenesis is related to accumulation of misfolded proteins and impairment of autophagy and consequent protein degradation can accelerate neurodegeneration (Rubinsztein, 2006). Whether a similar phenomenon is observed in cancer and what its biological relevance is remains to be elucidated.

1.7.8. Measuring autophagy

There are two challenges in measuring autophagy: firstly use of static measurements of a dynamic process can be misleading and secondly, the detection of autophagy does not imply function. The gold standard method to measure autophagy is to detect autophagic vesicles using

electron microscopy and counting these in cells (Mizushima et al., 2010a). This is an expensive and laborious technique and less useful for the analysis of clinical tissues. Another standard technique for quantification of autophagy is antibody-based detection of LC3 protein which is constitutively expressed at low levels in most cells. This can be with fluorescence microscopy or immunoblotting. LC3-I and LC3-II can be discerned due to different mobility on immunoblotting or in fluorescent microscopy studies where LC3-I appears diffuse in the cytoplasm and LC3-II appears as distinct puncta indicative of formation of autophagosomes (Mizushima et al., 2010a). Although fluorescence microscopy is cheaper and more widely available, it is far more subjective and quantification can be challenging. Punctate structures representing autophagosomes are visualised but capturing the dynamic nature of autophagy can be challenging. Immunoblotting is a useful tool in preclinical studies but much less useful for clinical samples due to the large amounts of stromal tissue present.

Immunohistochemical detection of proteins involved in autophagosome formation has been used in studies of clinical tumour samples. Most studies published have used Beclin1 and LC3 (Chen et al., 2009; Giatromanolaki et al., 2010b; Kabeya et al., 2000; Koukourakis et al., 2010; Li et al., 2009; Miracco et al., 2010b; Pirtoli et al., 2009; Qu et al., 2003; Sivridis et al., 2010; Wan et al., 2010; Yoshioka et al., 2008; Yue et al., 2003). There are a number of drawbacks to this approach which include variations in sample preparation, antibody quality and use of arbitrary cut-offs and scoring systems. These scoring systems are at best semi-quantitative and to date, standard criteria have not been adopted.

Guidelines on general autophagy assays are available (Klionsky et al., 2008) and attempts have been made to standardise and validate immunohistochemical detection of LC3 (Holt et al., 2011; Ladoire et al., 2012).

1.7.9. Autophagy in anti-cancer therapeutics

1.7.9.1. Proteasome inhibitors and HDAC inhibitors

Proteasome inhibitors are emerging as effective anti-cancer agents especially in multiple myeloma (Wu et al., 2010). These agents can induce autophagy in cancer cell lines and combining proteasome and autophagy inhibition leads to greater cell death than each agent individually in cell lines (Driscoll and Chowdhury, 2012). When proteasome function is impaired, it appears that induction of autophagy is a possible compensatory mechanism. HDAC6 may have a role in this compensatory activation suggesting a rationale for combining proteasome and HDAC inhibitors.

As previously described, autophagy may be a mechanism of cancer cell survival in situations of metabolic stress. However, if these unfavourable conditions continue beyond a crucial point required for cell survival, autophagic cell death may occur. Inducers of autophagy may exploit this mechanism and a number of anti-cancer agents are known to induce autophagy including HDAC and proteasome inhibitors (Carew et al., 2008; Carew et al., 2010).

HDAC inhibition has been shown to induce autophagy in a number of studies. Recently, SAHA was shown to increase expression of LC3 and inhibit mTOR resulting in the dephosphorylation, and thus activation, of the autophagic protein kinase ULK1 (Gammoh et al., 2012). Inhibition of autophagy by RNAi in glioblastoma cells results in an increase in SAHA-induced apoptosis. Importantly, when apoptosis was pharmacologically blocked, SAHA-induced non-apoptotic cell death was also potentiated by autophagy inhibition.

1.7.9.2. Autophagy inhibitors

Tumour cells might use autophagy a means to survive metabolic stress encountered during radiation or systemic therapy. Autophagy inhibitors should therefore be able to potentiate cytotoxicity of cancer treatments. Chloroquine (CQ) and hydroxychloroquine (HCQ) are anti-malarial drugs that inhibit lysosyme acidification and degradation of autophagosomes (Ohkuma and Poole, 1981; Poole and Ohkuma, 1981). HDAC inhibitor-induced apoptosis is enhanced by co-administration with chloroquine in chronic myeloid leukaemia cells both in vitro and in primary cells from patients (Amaravadi et al., 2007; Bellodi et al., 2009). Similar results have also been seen in colon cancer cells, triple negative breast cancer cells and malignant peripheral nerve sheath tumours (Carew et al., 2010; Lopez et al., 2011; Rao et al., 2012). This enhanced toxicity may be mediated by altered cellular redox status induced by the combination of HDAC inhibitor and CQ and there is growing interest in combining anti-cancer therapies with CQ.

Lucanthone is used clinically in the treatment of schistosomiasis but also has inhibitory activity against topoisomerase II and has been reported to inhibit AP endonucleases 1, an important

enzyme in DNA base excision repair (Luo and Kelley, 2004). Based on these properties, lucanthone is currently being investigated as a sensitizer to chemotherapy and radiation. In breast cancer cells, lucanthone induced vacuolization, interfered with lysosomal function and led to the accumulation of undegraded proteins (Carew et al., 2011). In cells treated with lucanthone, there was increased expression and aggregation of p62, a protein that is degraded by autophagy. There were also synergistic effects on apoptosis when lucanthone was combined with vorinostat that were greater than with a chloroquine and vorinostat combination. The authors suggested that this agent could be a more potent and less toxic alternative to chloroquine in future cancer clinical trials.

Several autophagy inhibitors have been studied but these agents have nonspecific effects on other cellular functions, such as endocytosis (e.g., 3-methyladenine) and lysosomal function (e.g., bafilomycin A) (Janku et al., 2011b). Chloroquine itself impacts on normal lysosomal function as well as the function of endosomes and not all of its apparent cytotoxic effects may be attributed to autophagy inhibition (Solomon and Lee, 2009). Normal cells also use autophagy to maintain homeostasis and therefore, one potential danger of suppressing autophagy is the enhancement of organ specific toxicities which might limit the use of such combination therapies (Kimura et al., 2013).

Targeting key autophagy proteins would be a more potent and specific approach and several components of the autophagic machinery are druggable and serve as potential therapeutic targets (Yang et al., 2011). While the clinical relevance of HDAC inhibitor-induced autophagy remains

to be elucidated, modifying autophagy induction may be a novel way of improving HDAC inhibitor efficacy.

1.8. The ubiquitin-proteasome system

The UPS is the major pathway in eukaryotes that regulates extralysosomal degradation of cytosolic, nuclear and endoplasmic reticulum-associated proteins (Bedford et al., 2011). It also degrades misfolded or unassembled proteins via endoplasmic reticulum associated degradation (ERAD) (Meusser et al., 2005). Mostly short-lived proteins are degraded via a cascade of events that involve tagging of proteins by ubiquitin. This is a small (8.5kDa) globular, heat stable protein that is highly evolutionarily conserved and ubiquitously expressed in eukaryotic cells (Goldstein et al., 1975; Schlesinger et al., 1975). Once this is covalently linked to proteins, they are marked for elimination by the 26S proteasome, a highly conserved multi-catalytic ATP-dependent protease complex (Groll et al., 1997). The UPS enables rapid, precise and timely processing of a huge variety of cellular proteins that impacts on the control of critical cellular functions such as cell cycle progression, DNA repair, apoptosis, gene transcription, signal transduction, senescence, development, immune response, metabolism and protein quality control.

1.8.1 Cellular events and the machinery of the UPS

The UPS can be roughly divided into two successive steps: ubiquitylation and proteasomal degradation. Proteins that are destined for proteasomal degradation are earmarked through the

conjugation of ubiquitin polypeptides. These proteins are recognised by the presence of degradation signals which can be small motifs, molecular domains or misfolded structures (figure 1.8) (Ravid and Hochstrasser, 2008).

The polyubiquitin cascade is hierarchical with two E1 proteins, around one hundred E2 proteins and more than a thousand E3 proteins. The ubiquitinated substrate is then degraded by the 26S proteasome to form a number of small peptides and the release of free ubiquitin (Pickart, 2001). The small peptides are then further degraded by cellular proteases into their constituent amino acids.

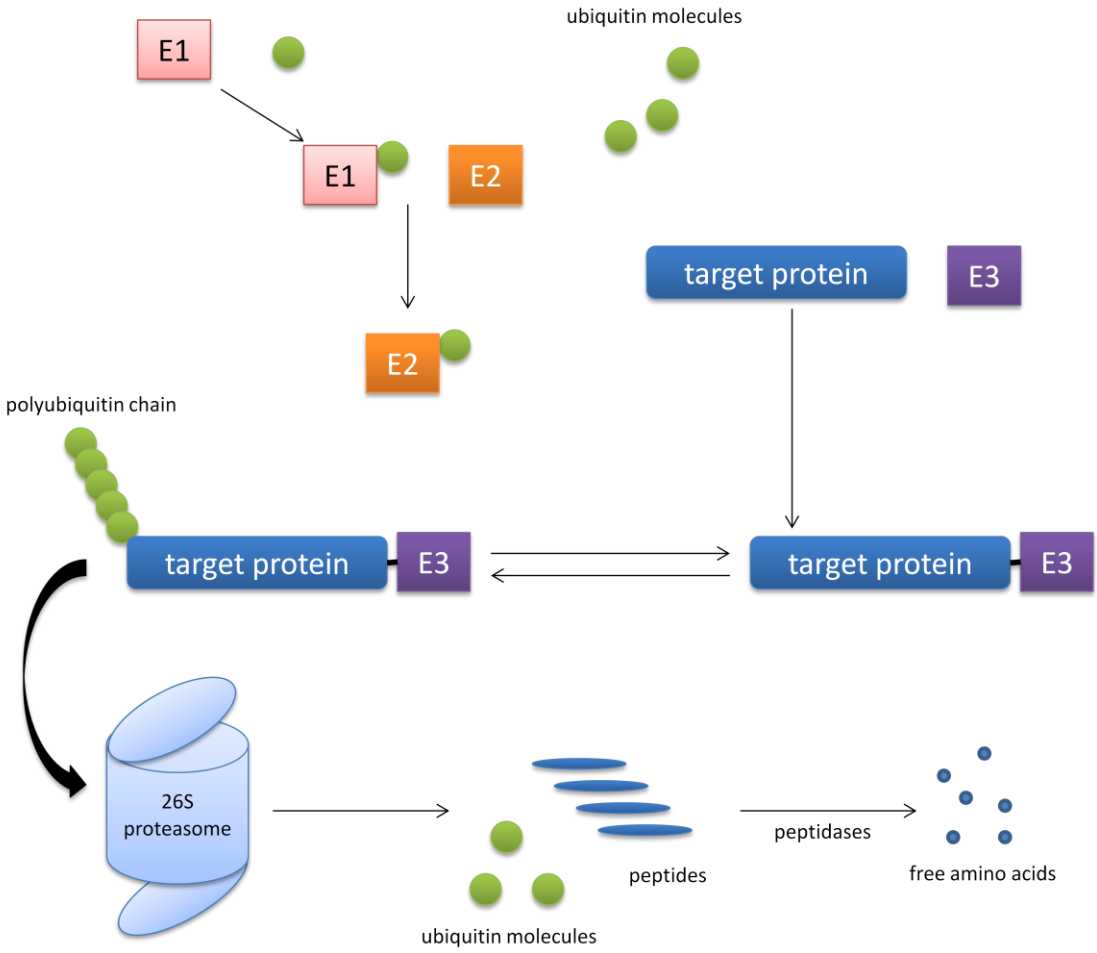


Figure 1.8: The ubiquitin proteasome pathway

Ubiquitin is activated by E1 ubiquitin-activating enzymes and subsequently transferred to E2 ubiqutin-conjugating enzymes. Target proteins for degradation are bound to their respective E3 ubiquitin ligase and the E3-substrate complex can then accept the ubiquitin from the E2 to form polyubiquitinated proteins which are then targeted to the 26S proteasome for degradation. Ubiquitin is then recycled for use in the degradation of further substrates and peptidases degrade peptides into free amino acids.

1.8.2. The 26S proteasome

The 26S proteasome is a large (~2.5 MDa) ATP-dependent multi-subunit protease complex that consists of a 20S catalytic core particle (CP) and one or two 19S regulatory particles (RP) (Glickman et al., 1998; Groll et al., 1997). The 20S CP is a barrel-shaped structure made up of 28 subunits organised in two outer α-rings and two inner β-rings, each comprising seven structurally similar α- and β-subunits respectively. The α-rings serve as a gate for substrate entry into the proteolytic chamber formed by the β-rings. The proteolytic activity of the proteasome is contained within the inside of the internal proteolytic chamber and is mediated by the threonine protease activity of the subunits β-1 (caspase-like), β-2 (tryptic-like) and β-5 (chemotryptic-like) (Groll et al., 2000; Groll et al., 1999; Heinemeyer et al., 1997).

The active sites are located on the inner surface of the proteolytic chamber and so the proteasomal substrates need to be transported here. This is regulated by the association of 19S RP which controls the opening and closing of the α-rings in the 20S CP (Ciechanover, 1994). The 19S RP is made up of 19 subunits organised as a lid and a base. The base subunit contains six ATPase and four non-ATPase subunits. The ATPase subunits provide energy needed for deubiquitination and unfolding of the protein substrates which is a required for threading through the narrow channel of the 20S CP as well as for α-ring opening. The lid subunit is comprised of eight non-ATPase subunits and the lid is found in both proteasome-bound and unbound forms. The exact function of the lid is unknown although it is necessary for proper degradation of polyubiquitinated substrates (Ciechanover and Ben-Saadon, 2004) .

The lid and base subunits of the 19S proteasome interact via an association with S5a, which is thought to be important for the stability of the regulatory particle of the proteasome and binds via a vonWillebrand factor A (VWA) domain (Fu et al., 2001). S5a has a high affinity for polyubiquitinated chains and binds these through an ubiquitin interacting motif (UIM). This domain is important in the recognition and binding of ubiquitinated substrates to S5a and the proteasome (Hofmann and Falquet, 2001).

1.8.3. Development of therapies targeting the UPS

The role of the UPS in various diseases makes it an obvious target for the development of therapeutic agents. The 26S proteasome regulates many cellular functions, the most prominent of which include the advancement through mitosis, growth, chemotaxis, antigen presentation, angiogenesis, apoptosis, and the expression of several genes which in turn regulate other processes (Ciechanover, 2005). These mechanisms influenced by the 26S proteasome are some of the processes altered or deregulated in cancers. Proteasome inhibitors have been developed and used with some degree of success in the treatment of cancer (Frankland-Searby and Bhaumik, 2012).

1.8.4. Small molecule inhibitors of proteasome catalytic activity

A number of small molecule inhibitors of the 20S catalytic core have been developed and the majority of these compounds function via binding to the active site of the catalytic core (Kisselev and Goldberg, 2001). Proteasome inhibitors can be grouped into peptide aldehydes (MG132),

peptide vinyl sulphones, peptide boronates (bortezomib), peptide epoxyketones (epoxomicin) and β-lactones (lactacystin and its derivatives) (Frankland-Searby and Bhaumik, 2012).

The proteasome inhibitor which has been most widely used clinically is bortezomib (also known as PS-341 or Velcade). It is a water-soluble dipeptide boronic acid which contains pyrazinoic acid, phenylalanine and leucine with boric acid instead of a carboxylic acid. It forms more stable tetrahedral intermediates with N-terminal threonine residues of the 20S catalytic core resulting in inhibition of chymotrypsin-like activity of the 20S proteasome (Groll et al., 2006). It has been investigated in a variety of phase II clinical trials in multiple myeloma and was approved in 2006 by the FDA for use in patients who have received at least one prior therapy (Kane et al., 2006; Richardson et al., 2003; Richardson et al., 2005). Combination treatment with melphalan has more recently demonstrated an overall survival benefit compared to melphalan alone (Mateos et al., 2010). Bortezomib is also clinically useful for relapsed and refractory mantle cell lymphoma (Kane et al., 2007) and has shown some efficacy in treatment for lung cancer (Scagliotti, 2006). The use of bortezomib in combination with other established chemotherapeutics has also been explored. There are several promising proteosome inhibitors that are currently in clinical trials and these include Carfilzomib (PR-171), ONX0912 (PR-047), Marizomib (NPI-0052), CEP-18770, and MLN9708 (Frankland-Searby and Bhaumik, 2012).

1.9. Regulated targeting of proteolytic substrates to the proteasome.

1.9.1. UbA/UbL domain containing proteins.

The targeting of ubiquitinated substrates to the proteasome is mediated by a family of proteins which contain an ubiquitin-binding domain (UbA) and ubiquitin-like domain (UbL) (Buchberger, 2002; Verma et al., 2004; Welchman et al., 2005). These were first characterised in *S. cerevisiae* and include the nucleotide excision repair (NER) protein Rad23, Dsk2, a protein important in spindle pole body duplication, Ddi1 and p62 (Dantuma et al., 2009; Watkins et al., 1993). Rad23 (Radiation sensitive) was originally identified as an important factor involved in the recognition of DNA lesions and was first identified while attempting to decipher the reason for a ultraviolet (UV) sensitivity phenotype observed in a particular mutated yeast strain (Watkins et al., 1993). Two adjacent genes on chromosome V were deleted and one of these, named Rad23, was accountable for the observed UV radiation sensitivity. Mutations in these genes encoding proteins involved in NER are linked to the xeroderma pigmentosum (XP) syndrome which is characterized by extreme UV sensitivity of the skin and predisposition to skin tumours.

Human rad23B (HR23B) is one of the human homologues of the *S. cerevisiae* protein Rad23. The identification of UbL and UbA led to its identification as having a role in the UPS pathway (figure 1.9). UbL domain binds to the 26S proteasome and the UbA domain specifically recognise polyubiquitin chains via the C-terminal UbA domains (Watkins et al., 1993; Wilkinson et al., 2001).

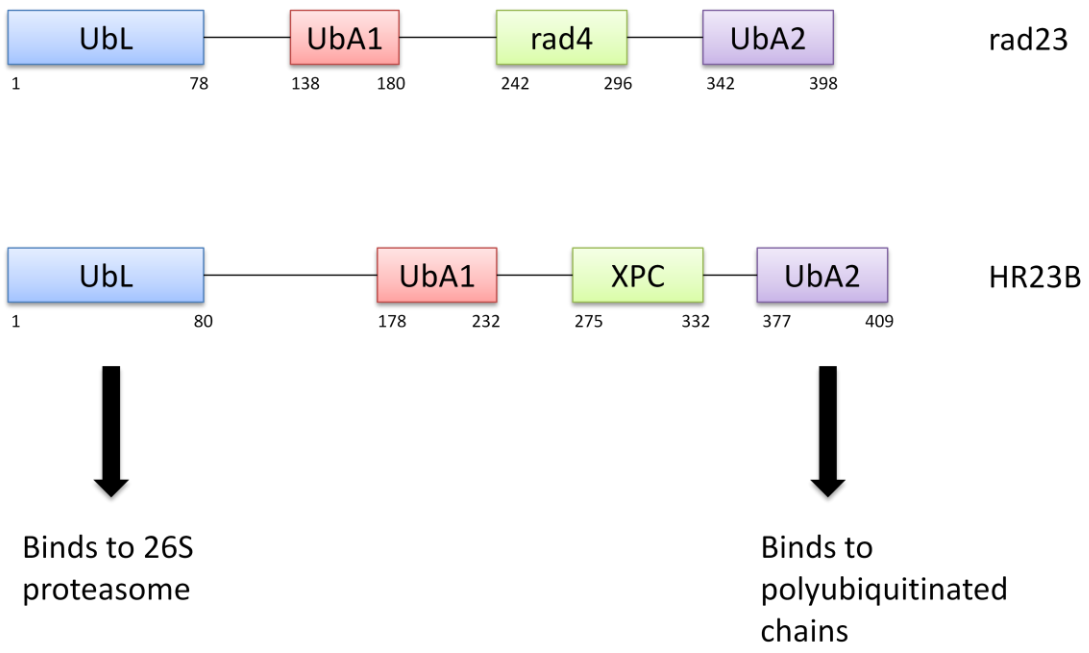


Figure 1.9: Rad23 and its human homologue HR23B

HR23B contain an N-terminal UbL domain, which is responsible for binding to the 26S proteasome and two ubiquitin associated UbA domains, which are involved in binding to the polyubiquitin chains. The C-terminal UbA domain is thought to preferentially bind polyubiquitinated substrates as it is adjacent to a glutamine rich region that has been identified as the binding site for HR23B's partner in NER, XPC

Abbreviations: HR23B, human Rad23B; UbL, ubiquitin-like; UbA, ubiquitin-associated, NER, nucleotide excision repair

Rad23 encodes an acidic protein comprising 398 amino acids with molecular weight of approximately 43kDa. The N-terminal portion of the protein comprised a basic region with the N-terminal residues 2-77 having an overall 29% identity to ubiquitin. The remainder of the protein consisted of an acidic region which was thought to form a compact globular domain with

affinity for basic target proteins. It lacks any type of enzymatic activity and it acts as a scaffold protein achieving its essential functions by binding target proteins via one its diverse binding molecules (Goh et al., 2008).

1.9.2. Rad23 in proteasomal degradation

The UbL domain makes up the first eighty amino acids of Rad23 (figure 1.9) and when the UbL domain is substituted for ubiquitin, the fusion protein is fully functional in DNA repair but interaction with the proteasome was impaired suggesting that this is its major function (Lambertson et al., 2003). The mechanism for substrate delivery to the proteasome is thought to be mediated via the UbL domain of Rad23 (Ghaboosi and Deshaies, 2007). The UbL domain of Rad23 binds to the Rpn1 subunit of the 19S regulatory particle and the Rpn1/Rpn2 subunits form a docking station for UbL domains (Elsasser et al., 2002; Saeki et al., 2002). These make up the base of the regulatory particle along with six AAA-ATPase subunits and they form a doughnut-like structure in which the Rpn1 subunit sits on top of the Rpn2 subunit. When the UbL domain binds to Rpn1, Rad23 is positioned centrally in the base close to the entrance of the core particle (figure 1.10). The human Rad23 proteins (HR23A and HR23B) interact with S5a which is an ubiquitin binding subunit of the proteasome via an interaction between the S5a ubiquitin interaction motif (UIM) and the human Rad23 UbL, and this complex is thought to regulate the targeting of polyubiquitinated substrates to the proteasome for degradation (Young et al., 1998).

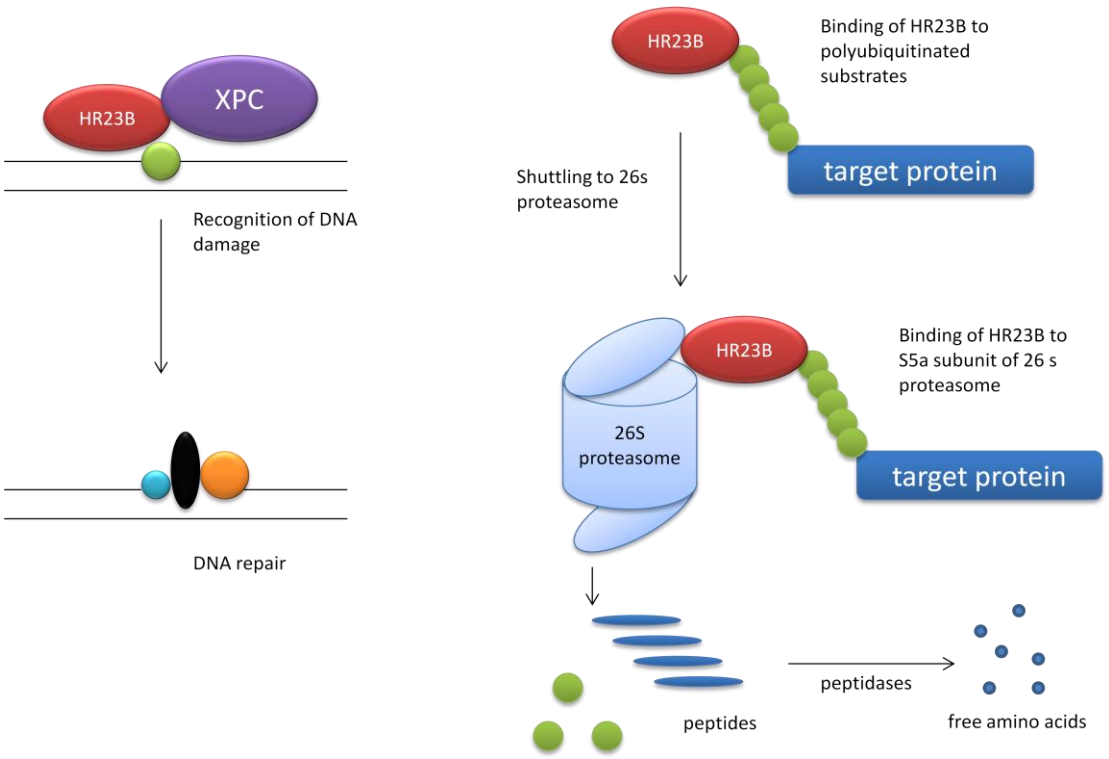


Figure 1.10: Functions of HR23B

HR23B has also been shown to have a function in NER where it forms a complex with the XPC protein which then recognises and integrates with damaged DNA and recruits the subsequent proteins necessary for repair of bulky DNA lesions. In human cells HR23B has an additional role where it binds to polyubiquitinated proteins and modulates their targeting to the 26S proteasome via binding to the S5a subunit.

Abbreviations: HR23B, human rad23B; NER, nucleotide excision repair, XPC, xeroderma pigmentosum complementation group C

Rad23 may alternatively recognise polyubiquitinated substrates via the UbA domain and shuttle these to the 26S proteasome (Madura, 2004). Rad23 contains a central UbA domain (UbA1) and a C-terminal UbA2 domain. Both bind mono- and polyubiquitin with distinct specificities (Raasi et al., 2005). There are four classes of UbA domains based on their binding affinities to ubiquitin

chains and Rad23's UBA1 is classified as a class II domain which binds Lys63-polyubiquitin chains in preference to Lys48 linked chains (Varadan et al., 2005). Most ubiquitin binding is thought to be UbA1 dependent based on domain deletion studies (Chen and Madura, 2002; Chen et al., 2001). However, the reasons for UbA-domain specificity are still not fully understood.

1.9.3. Role of Rad23 in protection of ubiquitinated substrates from proteolysis

The over-expression of both Rad23 and Dsk2 in yeast leads to inhibition of proteolysis, as binding of excess Rad23 or Dsk2 to the substrate bound polyubiquitin chain sequesters the substrate from the ubiquitination machinery and thus inhibits the ligation of additional ubiquitin molecules (Ortolan et al., 2004). Therefore, ubiquitylated proteins bound to UbA/UbL proteins in cellular excess may be protected from ubiquitin chain elongation and deubiquitylation. This so-called ubiquitin chain restriction may be important for unidirectional flow in substrate targeting as well as selective proteasomal degradation (Richly et al., 2005). These observations also generally highlight the importance of these proteins in proteasomal degradation pathways as their cellular levels appear to be critical.

1.9.4. Intramolecular interactions of the UbA and UbL domains and impact on function

The UbA domain does not exclusively bind ubiquitin. Rad23 can form homodimers and heterodimers with Ddi1. Binding of the UbL domain to the proteasome can disrupt this intramolecular binding and may result in open and closed conformations of Rad23. In the open conformation, the UbA domain can bind ubiquitinated substrates as it has a 10 fold higher affinity for these substrates than for the UbL domains, which would then allow the free UbL domain to bind to the proteasome (Ghaboosi and Deshaies, 2007).

Intramolecular interactions between the UbA/UbL domains may function to regulate protein activity. Full length Rad23 has a decreased affinity for the proteasome when compared to truncated Rad23 containing only the UbL domain. In addition, removal of the UbL from HR23A increases its affinity for free ubiquitin chains (Heessen et al., 2005). C-terminal UBA domains may guard ubiquitin receptors from destruction by preventing initiation of degradation at the proteasome. When unstructured polypeptides that were long enough to function as initiation sites for degradation were introduced, the protective effect of UBA domains was abrogated and conversely, degradation of substrates that contained an unstructured extension were attenuated by the introduction of C-terminal UBA domains (Heinen et al., 2011). These examples demonstrate that the intramolecular interactions between UbL and UbA domains may result in an inhibition of the intermolecular functions of these domains, altering the activity of these proteins in binding to both the proteasome and ubiquitin.

1.10. Biomarkers

1.10.1. Types of biomarkers

The Biomarkers Definitions Working Group defines a biomarker as "a characteristic that is objectively measured and evaluated as an indicator of normal biological processes, pathogenic processes, or pharmacologic responses to a therapeutic intervention" (2001). There are essentially three types of biomarker: prognostic, pharmacodynamic and predictive (La Thangue and Kerr, 2011). Predictive biomarkers anticipate the likely outcome of the illness and may determine if further therapy is required. Prognostic markers predict the likely course of disease in a defined population of patient irrespective of treatment. Pharmacodynamic (PD) biomarkers measure the effect of the drug on the disease, e.g. the level of apoptosis or proliferation in the tumour upon drug delivery, the degree of change on a substrate regulated by an enzymatic drug target.

Predictive biomarkers assess the likelihood that the tumour will respond to the drug and therefore forecast the likely response to treatment. It is these biomarkers that are of interest when one considers the possibility of personalising cancer therapy. There are some biomarkers that are both predictive and prognostic, such as hormone receptor status in breast cancer and *KRAS* status in colorectal cancer (Duffy, 2005; Karapetis et al., 2008). The EMA and FDA encourage drug developers to identify predictive biomarkers as a companion diagnostic. However, the majority of older classes of drugs that are employed in the treatment of most solid and haematological cancers are off patent so there is little commercial incentive to develop companion diagnostics

for these drugs. The newer targeted therapies are costlier and therefore development of a companion diagnostic may be justified.

A small number of predictive biomarkers have found clinical utility and these are summarised in table 1.6 (adapted from (La Thangue and Kerr, 2011)).

Table 1.5 Predictive biomarkers in clinical use in oncology

Biomarker	Tumour type	Drug	Target
ER	Breast	Tamoxifen	Oestrogen receptor
HER2		Trastuzumab	HER2
BRCA1/2		Olaparib, veliparib	PARP
EGFR	NSCLC	Erlotinib, gefitinib	EGFR
ALK		Crizotinib	ALK
EGFR* ± *KRAS	Colorectal	Cetuximab, panitimumab	EGFR
BRAF V600E	Melanoma	Vemurafenib	BRAF
BCR-ABL	CML	Imatinib, dasatinib, nilotinib	BCR-ABL
PML-RAR	APL	All trans retinoic acid	PML-RAR
KIT	GIST	Imatinib	KIT

Abbreviations: ER, oestrogen receptor, HER2, human epidermal growth factor receptor 2; PARP, poly (ADP-ribose) polymerase; EGFR, epidermal growth factor receptor, KRAS, Kirsten rat sarcoma viral oncogene homologue; NSCLC, non-small cell lung cancer; CML, chronic myeloid leukaemia; APL, acute promyelocytic leukaemia; GIST, gastrointestinal stromal tumour.

1.10.2 Prognostic relevance of tissue expression of HDACs

Altered expression, deregulation and mutations of HDAC genes have been linked to tumour development either through modification of gene transcription or through non-histone HDAC substrates. Somatic mutations of HDAC genes are rare but HDAC4 mutations have been identified in breast cancer (Sjoblom et al., 2006) and mutations resulting in HDAC2 protein truncation have been described in human epithelial cancer cell lines (Ropero et al., 2006). Numerous studies have been performed in which expression of HDACs have been assessed using immunohistochemistry (summarised in table 1.7 and reviewed in (Khan and La Thangue, 2012a)).

Table 1.6: Class I/II and IV HDACs; cancer associations

HDAC subunit	Deregulation in cancer
Class I	
1	Improved prognosis in breast cancer Upregulated in hormone-refractory prostate cancer, gastric cancer, colorectal cancer, SCC of the tongue, oesophageal and pancreatic cancer Associated with advanced stage in lung and oesophageal cancer
2	Upregulated in colorectal cancer, gastric cancer, cervical dysplasia and invasive carcinoma Associated with aggressive CTCL
3	Upregulated in lung cancer, prostate and colon cancer Poor prognostic indicator for post-liver transplantation HCC
8	Higher expression associated with poorer outcome in paediatric neuroblastoma
Class IIa	
4	Overexpressed in breast cancer
5	Downregulated in colon cancer and AML Low expression associated with poor prognosis in lung cancer
7	Overexpressed in colon cancer
9	Overexpressed in medulloblastoma/astrocytoma
Class Iib	
6	Conflicting prognostic interpretations in breast cancer Associated with favourable outcome in CTCL
10	Poor prognostic indicator in lung cancer Overexpressed in HCC
Class IV	
11	Overexpressed in breast cancer

Abbreviations: HDAC, histone deacetylase; SCC, squamous cell carcinoma; CTCL, cutaneous T cell lymphoma; HCC, hepatocellular carcinoma; AML, acute myeloid leukaemia

It has been suggested that assessing HDAC levels in patient tumour tissues may help identify patient sub-groups who could benefit from HDAC inhibitor treatment. Different expression profiles between different tissues and cancer types make it difficult to use them routinely as prognostic biomarkers. Advanced techniques, such as array systems and high throughput analyses, could give a more differentiated picture of the expression profiles within tissues and tumours.

1.10.3. Pharmacodynamic biomarkers

Histone acetylation is a direct downstream modification regulated by HDACs, and can be measured in both tumours peripheral blood mononuclear cells (Stimson and La Thangue, 2009a). It is induced by HDAC inhibitors in a dose and time dependent manner. However, histone acetylation and tumour response are not necessarily linked and therefore its predictive role has been questioned (Steele et al., 2008).

Other proteins that are known to be induced upon HDAC inhibitor treatment include p21 and HSP90 related proteins such as HSP72 and c-Raf (Stimson and La Thangue, 2009b). The predictive utility of these biomarkers remains to be determined and no clinical studies have been carried out so far that have utilised biomarkers to select patients or to predict response to HDAC inhibitor treatment.

1.10.4. Future clinical development of predictive biomarkers

Most biomarkers that are being utilized in the clinic were identified through retrospective analysis of clinical trial data and coincidental *ad hoc* genetic analysis. In most prospective clinical trials, companion biomarkers are rarely incorporated in clinical trial design (Buyse et al., 2011).

Newer techniques that have been used to identify biomarkers include high-throughput approaches including large scale DNA sequencing, single-nucleotide polymorphism analysis and transcript profiling by microarray and proteomics (Schilsky, 2010). These techniques produce correlative data that can identify genes and proteins that coincide with disease state or therapeutic response. It may be more challenging to integrate this information with the mechanisms involved in attaining the tumour phenotype or action of the drug. Research has therefore been focused on developing platforms that allow functionally relevant biomarkers to be identified which can then be rationalised in the context of the mechanism of tumour killing by the drug and used to support and refine its clinical development.

There are essentially two types of biomarkers that are likely to be clinically useful: biomarkers that inform on drug resistance and those that identify drug-responsive tumours. Genetic screens (at the genome wide level or on selective populations of genes by ribonucleic acid (RNA) interference) have facilitated the identification of both types of biomarkers (Mullenders and Bernards, 2009).

1.11. HR23B: a biomarker for HDAC inhibitors

1.11.1. Introduction.

HDAC inhibitors have generated a great deal of interest in the scientific and clinical arenas as they affect a multitude of cytotoxic pathways with relatively little effect on normal tissues. Despite this interest, in practical terms, there are only a few tumour types for which significant activity has been reported in single agent clinical trials. Experience in solid tumours has been particularly disappointing.

There is therefore a need for methods for identifying patients in whom HDAC inhibitors might be of greatest benefit. Understanding and elucidating the pathways through which these agents kill cells is of great importance. A genome-wide loss-of-function screen using small hairpin RNA (shRNA) of 8000 genes identified a group of genes that when silenced in the tumour cell prevented HDAC inhibitor-induced apoptosis (Fotheringham et al., 2009b). One of these, HR23B, shuttles ubiquitinated cargo proteins to the proteasome and has been validated as a sensitivity determinant for HDAC inhibitor-induced apoptosis. HR23B also governs tumour cell sensitivity to drugs that act directly on the proteasome and the level of HR23B was found to influence the response of tumour cells to HDAC inhibitors.

1.11.2. Objectives and achievements.

The main aim of this project was to further validate HR23B as a predictive biomarker for the ability of HDAC inhibitors to cause cell death by apoptosis. As the initial shRNA screen was performed in U2OS cells, it was important to validate HR23B in other cell lines, particularly in CTCL as clinically; HDAC inhibitors appear to have significant activity in this condition. A further important aim of the project was to determine the importance of the proteasome targeting ability of HR23B and its potential role in HDAC inhibitor-induced cell death. The effects of combining HDAC inhibitors and proteasome inhibitors in CTCL and solid tumour cell lines were also investigated and the results suggested a synergistic interaction that sheds light on a new mechanism for this combination.

Another important aim was to determine levels of HR23B in clinical tumour samples using immunohistochemistry. Using tissue microarrays, it was possible to screen relatively large numbers of tumours of different types and assess patterns of HR23B expression. More specifically, the levels of HR23B in CTCL were evaluated. It was vitally important to determine if HR23B expression in CTCL had a predictive role in patients treated with HDAC inhibitors. Clinical biopsies were therefore examined from such patients who were treated with HDAC inhibitors and in whom clinical outcome data was available. The aim of this approach was to retrospectively analyse expression of HR23B and investigate if there was any correlation with levels and clinical outcome.

In CTCL analysis of HR23B expression in biopsies taken from one of the pivotal phase II clinical trials (Duvic et al., 2007), an association was found between HR23B levels and clinical response to HDAC inhibitor therapy. This strengthened the hypothesis that HR23B is a clinically relevant biomarker of therapeutic response,

Treatment of tumour cells with HDAC inhibitors can result in a number of different outcomes including apoptosis, senescence, autophagy and cell cycle arrest. Given this variability in cellular response, the value of HR23B as biomarker of response could be enhanced if it were to have a role in dictating the biological consequence of HDAC inhibitor treatment. Therefore, another aim of this project was to explore the mechanistic role of HR23B in regulating the biological consequence of HDAC inhibitor treatment. HR23B levels impacts on autophagy and apoptosis and the mechanism responsible involves the interplay between HR23B and HDAC6 and specifically the ability of HDAC6 to counter-balance the pro-apoptotic effects of HR23B. Furthermore, expression of HR23B was correlated with LC3 expression (a marker of autophagy) and there was a frequent co-incidence of low HR23B and increased autophagy. Tumours with increased number of autophagocytic cells also had a poorer prognosis.

CHAPTER 2

MATERIALS AND METHODS

2.1. Cell culture.

Cells were cultured at 37^{o}C in a humidified 5% CO_2 incubator in DMEM (Invitrogen) (U2OS, A2058, GFPu1, HCT116, HCT15, WT and shRNA A549 cells, BL, 224), RPMI-1640 (Invitrogen) (A375) containing 10% FCS (Invitrogen). HUT 78, SeAX and MYLA cells were cultured in RPMI-1640 containing 20% FCS. All media contained 1% penicillin/streptomycin (Invitrogen). The GFPu1 cell line was derived from HEK293 cells (Bence et al., 2001) and was a kind gift from Ron Kopito.

A U2OS-TET-Flag-HR23B inducible cell line (Khan et al., 2010) was grown in DMEM containing 10% tetracycline-negative FCS (PAA Laboratories), hygromycin (Invitrogen), G418 (Promega) and 1% penicillin/streptomycin (Invitrogen). Flag-HR23B was induced by the addition of 1 µg/mL doxycycline to culture media. The shRNA A549 HDAC6 WT and KD cells were a kind gift from T.P. Yao (Kawaguchi et al., 2003b).

2.2. Compounds and drug treatments.

Cells were treated with compounds MG132, chloroquine valproic acid, (Sigma), suberoylanilide hydroxamic acid (SAHA) (Alexis Biochemicals), bortezomib (Millenium) and CXD101 (Celleron) at the indicated concentrations and for the indicated times before harvesting. Apart from valproic acid and chloroquine all compounds were solubilised in dimethylsulfoxide (DMSO) and added to media at a 1:1000 dilution to minimise vehicle effects. Valproic acid and chloroquine was made up fresh in media prior to use each time.

2.3. Transfection and small interfering RNA (siRNA)

For transient siRNA experiments, cells were transfected with siRNAs against HR23B P (5'-GAUGCAACGAGUGCACUUG-3', HDAC6 (00349900; Dharmacon) or non-targeting control siRNA #2 (Dharmacon, Perbio). siRNA sequences named P are sequences corresponding to those identified in the SAHA pRetroSuper shRNA screen (Fotheringham et al., 2009a). Another siRNA (II) and a pool of siRNA containing P and II were also tested but during optimisation, the greatest depletion of HR23B was seen using P and so subsequent experiments were all performed with this siRNA (appendix 1). Cells were transfected as indicated using Oligofectamine (Invitrogen) to a final concentration of 50nM before harvesting. Plasmids were transfected using Genejuice (Merck) according to manufacturer's instructions.

2.4 Electroporation

siRNA was introduced into CTCL cell lines using electroporation. 100nM HR23B siRNA (5'-GAUGCAACGAGUGCACUUG-3') or 100nM non-targeting (NT) control siRNA (Dharmacon) was added to 500µl of hypo-osmolar buffer and $1x10^6$ cells and the mixture incubated for 10 min at room temperature. An Eppendorf multiporator was then used to pulse cells at 1100V for 100µs and cells incubated for a further 10 min at room temperature. Cell culture media at 37^oC was then added and the mixture added to cell culture dishes. Cells were allowed to grow in media for 48h before a 1ml aliquot was removed to allow determination of protein depletion via immunoblotting. Cells were then treated with appropriate drug concentrations for a further 48h or 72h as indicated.

2.5. Flow cytometry

Cells were plated at approximately 50,000 cells per 10cm plate before drug treatment for appropriate time as indicated. Cells were harvested by scraping in phosphate-buffered saline (PBS). Harvested cells were washed twice in PBS and fixed in 70% ethanol/PBS overnight at $4^{o}C$ followed by incubation for 30 minutes at $4^{o}C$ with 1 x RNAse A and 20ng/ml propidium iodide (Sigma). Samples were run on a FACScan flow cytometer (BD Bioscience) and analysis was carried out using CellQuestPro software. Cell death was determined using propidium iodide staining to evaluate the percentage of cells with sub-diploidal (sub-G1) DNA content. Propidium iodide staining was measured by detection of fluorescence in the FL-2 channel. The cell populations were gated to include only events with FL2-W <400 to allow acceptance of only single cells in the analysis of propidium iodide staining as a representation of DNA content within each single cell. These single cells were then gated relative to total DNA content as measured by FL2-A to determine the percentage of cells in each phase of the cell cycle, where a DNA content of FL2-A<150 indicated subG1 phase (as a measurement of apoptosis). Cells were gated in each experiment with the parameters of DNA content 2n for G1 and 4n for G2 phase of the cell cycle.

The IC50 for apoptosis was defined as the concentration of drug at which there was 50% of the maximal response (ability to cause accumulation of cells in the subG1 phase of the cell cycle). These concentrations were utilised in all combination experiments.

2.6. Immunoblotting

Cells were washed with 1 x PBS and lysed in RIPA lysis buffer (50mM Tris pH 7.4, 150mM NaCl, 1mM EDTA, 0.25% sodium deoxycholate, 1.0% NP-40) and protease inhibitors at 4°C for 20 minutes. Cell lysate was normalised (Bradford assay) and equal protein loading was confirmed with Ponceau S staining. Cell lysates were loaded in a denaturing SDS loading buffer (3x) (375mM Tris pH6.8, 30% glycerol, 6% SDS, 0.015% bromophenol blue and 1% β-mercaptoethanol). Total protein was resolved by denaturing SDS–polyacrylamide gel electrophoresis (PAGE) before electrotransfer to Protran nitrocellulose membrane (Inverclyde Biologicals) or PVDF membrane and probed with antibody.

Primary antibodies used were anti-β-actin and anti-FLAG M2 (Sigma), anti-GFP and anti-LAMP1 (Santa Cruz Biotechnology), anti-HR23B and anti-PARP and anti-cleaved PARP (BD Biosciences), anti-cathepsin (Sigma), anti-LC3 (Nanotools and Upstate), anti-HDAC6 and anti-acetylated histone H3 (Upstate). Membranes were then washed 3 x 10 minutes in PBS 0.1% Tween-20 and subsequently probed with appropriate secondary HRP-antibody. Enhanced chemi-luminescence (Perbio) was used to visualize antibody binding.

2.7 Assay for proteasome activity

The proteasome activity assay kit used (Merck Millipore), assays intracellular proteasome activity by recognising the substrate LLVY (Meng et al., 1999). The assay is based on detection of the fluorophore 7-Amino-4-methylcoumarin (AMC) after cleavage from the labelled substrate

LLVY-AMC (Absorption=351nm. Emission=430nm). The free AMC fluorescence can be quantified using a 380/460 nm filter set in a fluorometer. The plate reader was calibrated using increasing concentrations of AMC and measuring arbitrary fluorescence units after one hour incubation (appendix 2a).

Cells were harvested after 16h treatment with HDAC inhibitor and the proteasome inhibitors MG132 (100nM) or bortezomib (100nM), or vehicle control. Following a wash in PBS, cells were resuspended in 130 ml HEPES buffer (5 mM HEPES, 1 mM EDTA [pH7.5]) and sonicated for 1 min. Samples were centrifuged for 10 min (13,200 rpm at 4ºC) and the supernatant was removed, stored on ice, and used immediately. Proteasome activity per sample was measured by adding 20 µl cell lysate to each well in triplicate. The volume needed was determined by measuring absorbance across a range of volume of lysates for untreated MYLA and A2058 cells (appendix 2b and 2c) Assay buffer (95µl) was added as a blank. Five µl of the fluorogenic substrate Suc-LLVY-AMC was added to all samples and incubated for 10 min at room temperature. The plate was read every 2 min for 1h on a plate reader (360 nm excitation, 460 nm emission, gain = 58).

2.8 Immunofluorescence

Cells were seeded onto coverslips which were washed in PBS and fixed in 3.7% formaldehyde for 15 minutes. Cells were permeabilised in PBS containing 0.5% Triton X100 for 5 minutes and then blocked in 5% FCS/PBS for 30 minutes at room temperature before incubation with primary antibody as indicated. Coverslips were washed in PBS containing 0.05% Tween-20 and

incubated with the corresponding secondary antibodies for 30 minutes at room temperature: Alexa Fluor 488 (green fluorescence) or Alexa Fluor 594 (red fluorescence) (Molecular Probes). Finally, coverslips were washed extensively in PBS containing 0.05% Tween-20 and mounted onto microscope slides using Vectashield containing DAPI (Vector Laboratories). Quantification of immunofluorescence was carried out by determining the proportion of cells with punctate staining (LC3) or strong staining (cleaved PARP) out of 500 cells counted.

2.9 Immunohistochemistry

Immunohistochemistry was performed using the VECTASTAIN® ABC system (Vector Labs) according to stated protocol. Paraffin-embedded formalin-fixed specimens were sectioned (5µm) onto glass slides, cleared of paraffin in Histoclear and rehydrated through graded alcohol baths. After a rinse in water, sections were ‘‘pressure-cooked’’ for 2 min in 1mM EDTA at pH8 for heat-induced epitope retrieval or heated to 98 degrees in a water bath for 20 minutes. Slides were incubated in 6% Methanol/H_2O_2 for 15 minutes to inactivate endogenous peroxidises and treated with normal blocking serum in PBS-Tween (PBST) for 20 minutes. The next step involved treatment with anti-HR23B or anti-LC3 overnight at 4ºC. HR23B antibody concentration was 1:400 and LC3 antibody concentration was 1:100. This was followed by biotinylated rabbit anti-mouse secondary antibody for 30 minutes at room temperature. Avidin DH (Reagent A) was mixed with its paired biotinylated enzyme (Reagent B) prior to use for 30 minutes followed by addition of DAB substrate. Slides were placed in haematoxylin (Sigma) for 30 seconds for nuclear counterstaining and then mounted with coverslips using AquaTex

(Merck). Sections were examined under a Zeiss Axioskop light microscope. Images were captured with MicroPublisher 5.0 RTV, and imaging was performed with Adobe Photoshop 8.0.

U2OS cells were plated and grown for 24 hours followed by treatment with DMSO or SAHA at 5 µM for 24 hours. Cells were then harvested, spun down and cell pellets were fixed in formalin and embedded in paraffin. Sections (5µm) were then placed on glass slides and staining was performed with anti-LC3 as described. Antibody titre optimisation was carried out using different dilutions of antibody and compared with the same dilution of species specific IgG (appendix 3). A punctate pattern of LC3 immunostaining was evident after SAHA treatment and the optimum antibody concentration was determined to be 1:100.

To establish the optimum concentration (titre) and incubation time for the anti-LC3 antibody, a series of colorectal adenocarcinomas were employed in a pilot study. The dilution giving the best contrast between the apparently positive malignant epithelial cells and the surrounding tumour stroma with minimal background staining was 1:100 after overnight incubation.

To establish the optimum concentration (titre) and incubation time for the anti-HR23B antibody, a series of normal skin and melanoma samples were employed in a pilot study. The dilution giving the best contrast between the apparently positive normal skin and malignant cells and the surrounding tissue stroma with minimal background staining was 1:400 after overnight incubation.

Normal mouse immunoglobulin-G (IgG) was substituted for the primary antibody as a negative control. Staining with omission of the primary antibody was also performed as a negative control (examples are shown in appendix 4).

2.10 Tissue sources and histopathology examination

All tissue microarrays (TMAs) apart from those from the VICTOR trial (Midgley et al., 2010) were obtained from Oxford Radcliffe Biobank (ethical approval reference: H/0606/5). The number of samples analysed per tissue microarray are detailed in table 2.1.Samples from patients treated with valproic acid were obtained from the VB-NEO trial (ethical approval reference: 08/H0606/111).

Table 2.1: Details of colorectal tissue microarrays with number of evaluable samples

Tissue microarray	Number of evaluable samples
Normal colon	79
Primary colorectal cancer	111
Colorectal lymph node metastases	27
Colorectal liver metastases	41
Primary melanoma	105
Melanoma metastases	99

Colorectal tissue was obtained from archived tissue microarrays from the VICTOR trial. These included patients who had undergone surgical resection with primary colorectal cancer (stage II or III) between 2001 and 2004. All tumour biopsies were analysed in triplicate and each patient had a matched normal tissue sample. Medical reports of clinical information, demographics, treatment details and patient outcome were available for all patients with follow up of nearly 5 years. This study was covered by ethical approval reference number MREC/00/7/412 VICTOR trial. Written informed consent was obtained from each patient.

CTCL tissues from the phase II clinical trial were obtained from the MD Anderson Cancer Center and use of human tissues was approved by the Institutional Review Board of the MD Anderson Cancer Center. Written informed consent was obtained from each patient.

2.11 Patients and methods (pilot trial)

2.11.1 Inclusion and exclusion criteria

Individuals over the age of 18 deemed to have a life expectancy of at least 12 weeks were eligible for the study. ECOG performance status of 1 or better, adequate hepatic (total bilirubin levels $\leq$ 1.2 x upper limit normal (ULN)) and bone marrow function (haemoglobin >10g/dL, absolute neutrophil count $\geq$ 1,500 /mm^3 and platelet count of $\geq$ 100,000 /mm^3) were required. Patients had to have resectable stage 3 or 4, histologically proven melanoma or unknown primary with melanoma metastases (palpable lymph nodes or limited stage 4 disease).

Patients were excluded if they had recent major thoracic or abdominal surgery; chemotherapeutic or investigational agents, or radiotherapy in the preceding 4 weeks; mitomycin C or nitrosureas within previous 6 weeks; an active infection or significant non-malignant intercurrent illness; known central nervous metastases; a history of seizures; unresolved gastrointestinal symptoms; were pregnant or lactating; were serologically positive for hepatitis B, hepatitis C or HIV; were unable to swallow capsules; or were receiving concurrent antacid medication. A negative serum pregnancy test was required in women with child-bearing potential and all patients were required to use medically approved contraceptive precautions during the study and for 4 weeks afterwards.

The study was conducted in accordance with the Principles of the International Conference on Harmonisation of Good Clinical Practice guidelines and the Declaration of Helsinki. The protocol was approved by an independent ethics committee, according to UK and local requirements. All patients enrolled in the study gave informed written consent.

2.11.2 Treatment

Patients received valproic acid (Sanofi-Aventis, Guildford, UK) at a dose of 30mg/kg orally as capsules thrice daily on days 1 to 5 prior to surgery. A dose of 75 mg/kg was selected per day to be administered over five days giving a total dose of 375 mg/kg. These doses were based on early phase trials (Munster et al., 2009; Munster et al., 2011; Rocca et al., 2009). For example in a phase I trial, the maximum-tolerated dose and recommended phase II dose was VPA 140 mg/kg per day for 48 hours and in another phase I/II trial a dose of 120 mg/kg/day VPA for 72 hours was well tolerated.

2.11.3 Study design

This was a pilot study of five patients Dose reduction of valproic acid by 50% was permitted in response to grade 3 drug related toxicity inadequately controlled by symptomatic treatment, or for any grade 4 drug related toxicity. Patients were followed up for 28 days after the last dose of study drug.

2.11.4 Specimen storage

Resected specimens were placed in formalin and then embedded in paraffin and stored in the Oxford Radcliffe Biobank (ORB) until required. Primary melanoma samples were also stored similarly after resection in the ORB.

2.12 VICTOR trial retrospective analysis: study design

This was a retrospective study based on archival material. The cases analysed represent patients enrolled onto the VICTOR trial. TMAs were selected randomly based upon availability. All patients in the series underwent surgery with a follow-up of at least 4 years after surgery. Patients with perioperative death and those with missing demographic or histopathological data were excluded from this study. The end points of analysis were the association of HR23B and LC3 expression with immunohistochemical variables and its impact on the progression-free and overall disease-specific survival.

2.13 Immunohistochemistry evaluation and scoring

For CTCL, a scoring system for HR23B was derived based upon the frequency of malignant cells in the dermis, the frequency and pattern of expression in the epidermis and the type of dermis infiltrate Intensity of expression was also categorised as described in table 2.2. The biopsies were scored blind by two independent pathologists and a semi quantitative analysis based upon intensity and frequency of HR23B staining and the type of dermal and epidermal infiltrate was performed on each biopsy (table 2.3). A total staining score (TSS) was determined out of 13, where a score of greater than or equal to 6 was considered to be strong HR23B staining. The threshold for differentiating between positive and negative immunostaining was set at a TSS of 6. This optimal cut-off was determined by the receiver operating characteristic curve distribution analysis. The TSS was then compared with clinical outcome, namely partial response (PR), stable disease (SD) or progressive disease (PD).

Table 2.2: Semi quantitative IHC staining evaluation of HR23B in CTCL biopsies

IHC STAINING EVALUATION FOR CTCL BIOPSIES	
Intensity (I)	
Epidermis and dermis	0 – negative
	1 – weakly positive
	2 – moderately positive
	3 – strongly positive
Frequency (F)	
Dermis	0 - <5% positive
	2 – 25-50% positive
	3 – 50-75% positive
	4 - >75% positive
Epidermis infiltrate	0 – none
	1 – few/sparse
	2 – many single
	3 – Pautrier's
Dermis Infiltrate Type	0 – normal
	1 – patch
	2 – plaque
	3 – tumour
Total Staining Scores (TSS)	1 – 13 Positive ≥6, Negative <6

For colorectal cancer, melanoma and the multi-tumour TMA, HR23B was scored by two assessors. Scoring criteria for HR23B were as follows; frequency was scored as the percentage of malignant cells per tissue section staining positive and intensity of staining was scored subjectively as the degree of staining for HR23B. The scoring system used for colorectal cancer and melanoma is summarised in table 2.4. The TSS was derived by adding frequency and intensity scores together. Results were obtained separately for nuclear and cytoplasmic staining. A positive TSS was considered to be 5-7 and a negative TSS was considered to be 0-4.

Table 2.3: IHC scoring system used for HR23B in melanoma, colorectal and multi-tumour TMA

Frequency (%)	Score	Intensity	Score
0	0	Negative	0
1-10	1	Weak	1
11-50	2	Medium	2
51-80	3	Strong	3
81-100	4		

Scoring criteria for LC3 were adapted from work carried out by Sivridis and colleagues (Giatromanolaki et al., 2010b). Cells with punctuate cytoplasmic staining of at least 10% of tumour cells with absence of perinuclear staining were considered to have high levels of autophagy and cells with absence or low levels of punctuate cytoplasmic staining and perinuclear staining were considered to have low or basal levels of autophagy.

The pathologists who performed the immunohistochemical assessment of HR23B and LC3 were blinded to the patient, histopathological and outcome data. Scores were compared between observers and kappa values were determined to assess the strength of agreement (appendix 5).

2.14: Statistical analysis

The data obtained are expressed as mean ± SD or ± SEM as indicated. Statistical evaluation of data was done with two-tailed Student's t test. P values <0.05 were considered statistically significant. The Mann-Whitney U test was used to evaluate non-parametric data and P values of <0.05 were considered statistically significant. Statistical analysis was conducted using Graph Pad Prism version 5.0 (GraphPad Software, La Jolla, Ca).

In the analysis of the CTCL clinical trial data, Fisher's exact t test was used to determine significance of the association (contingency) between response and HR23B TSS. Positive predictive value (PPV) was determined using the following equation:

$$PPV = \frac{\text{Number of true positives}}{\text{Number of true positives + number of false positives}}$$

Negative predictive value (NPV) was determined by the following equation:

$$NPV = \frac{\text{Number of true negatives}}{\text{Number of true negatives and number of false negatives}}$$

In the analysis of the VICTOR trial data, HR23B was analysed as a binary variable split into negative (score 0-4) or positive (score=5-7) staining. LC3 was analysed as a binary variable as negative, <10% punctate staining with presence of diffuse cytoplasmic staining and/or

perinuclear staining, or positive, ≥10% tumour cells with punctate staining. Demographic and survival information for all VICTOR patients, for those who provided samples and for those whose samples were included in this analysis were summarised.

The primary outcome, overall survival (OS) was defined as the time from randomisation until death from any cause with patients not reported as dead being censored at their last known date alive. Disease free survival (DFS), a secondary outcome, was defined as time from randomisation until recurrence or death from any cause where patients who were alive and recurrence-free were censored at their last known recurrence-free date.

Both OS and DFS were analysed using Kaplan Meier plots and log-rank tests by LC3 and HR23B expression. 3 and 5 year survival rates together with their 95% confidence intervals were presented overall and by LC3 and HR23B expression, where these were calculated from the Kaplan Meier curves taking into account both events and censoring. Multivariate analysis was carried out using the Cox proportional hazards model for LC3 expression and HR23B expression after adjusting for VICTOR treatment, gender, site (colon/rectum), stage (II/III), age and prior radiotherapy and chemotherapy. Hazard ratios and 95% confidence intervals were given for each LC3 and HR23B expression levels.

The analysis was repeated with HR23B and LC3 combined. Patients with positive HR23B and negative LC3 were compared with patients with negative HR23B and positive LC3. Statistical analysis was carried out using STATA 11.0.

CHAPTER 3

RESULTS

EFFECT OF HDAC INHIBITOR AND PROTEASOME INHIBITOR TREATMENT ON CTCL, COLORECTAL AND MELANOMA CELL LINES: CELL CYCLE EFFECTS AND EFFECTS ON HR23B EXPRESSION

3.1. Introduction

.

In a previous study, a genome-wide loss-of-function screen was used to identify genes that govern the sensitivity of tumour cells to HDAC inhibitor induced apoptosis and which might act as biomarkers for predicting response to HDAC (Fotheringham et al., 2009a). The screen identified HR23B which, in cell culture, sensitises osteosarcoma cells to HDAC inhibitor-dependent apoptotic cell death. One of the human homologues of the *S. cerevisiae* protein Rad23, HR23B, was first identified as playing a role in nucleotide excision repair, when identified as a component of an essential NER factor in a cell free repair system along with XPC (Masutani et al., 1994). It was further identified as having a role in the UPS after the identification of two distinct domains, the UBL domain, which was shown to bind to the 26S proteasome (Schauber et al 1998) and the UBA domain, which was found to specifically recognise polyubiquitin chains via the C-terminal UBA domains (Bertolaet et al 2001). At a mechanistic level, HR23B has an important role in shuttling ubiquitinated cargo proteins to the proteasome (Chen et al 2001, Chen and Madura 2002). Indeed, proteasomes display reduced activity in tumour cells treated with HDAC inhibitors, and HR23B is in part responsible for the aberrant proteasome activity (Fotheringham et al 2009).

It was important to determine whether the effects seen in osteosarcoma cells were reproducible in a variety of other cell lines including haematological cell lines especially as HDAC inhibitors in clinical trials have shown greater efficacy in the treatment of haematological malignancies as compared to solid tumours. Furthermore, the effects of different HDAC inhibitors on these cell

lines were also investigated. Ideally other readouts of HDAC inhibitor therapy should have also been investigated, such as effects on cell proliferation, angiogenesis and senescence but time limitations prevented this. Furthermore, apoptosis was considered to be one of the more clinically important mechanisms through which HDAC inhibitors cause cell death as well as being the mechanism of cell death measured in the initial genome wide screen through which HR23B was identified.

3.2. Effects of HDAC inhibitor treatment on apoptosis in tumour cell lines

Melanoma cell lines were sensitive to apoptosis (determined by flow cytometry) induced by SAHA in a dose-dependent manner, although A375 cells were most sensitive to SAHA, followed by SKMel28, with BL and A2058 cells being less sensitive (figure 3.1). 224 cells were the most resistant to SAHA treatment. CTCL cell lines were also sensitive to apoptosis after SAHA treatment and HUT78 and SeAX cells appeared to be considerably more sensitive than MYLA cells (figure 3.1). Colorectal cell lines were also sensitive to apoptosis after SAHA treatment with HCT116 cells being more sensitive. In A375, HUT78 and SeAX cells, concentrations of SAHA greater than 10μM did not result in a further increase in sub-G1 (data not included in the figure).

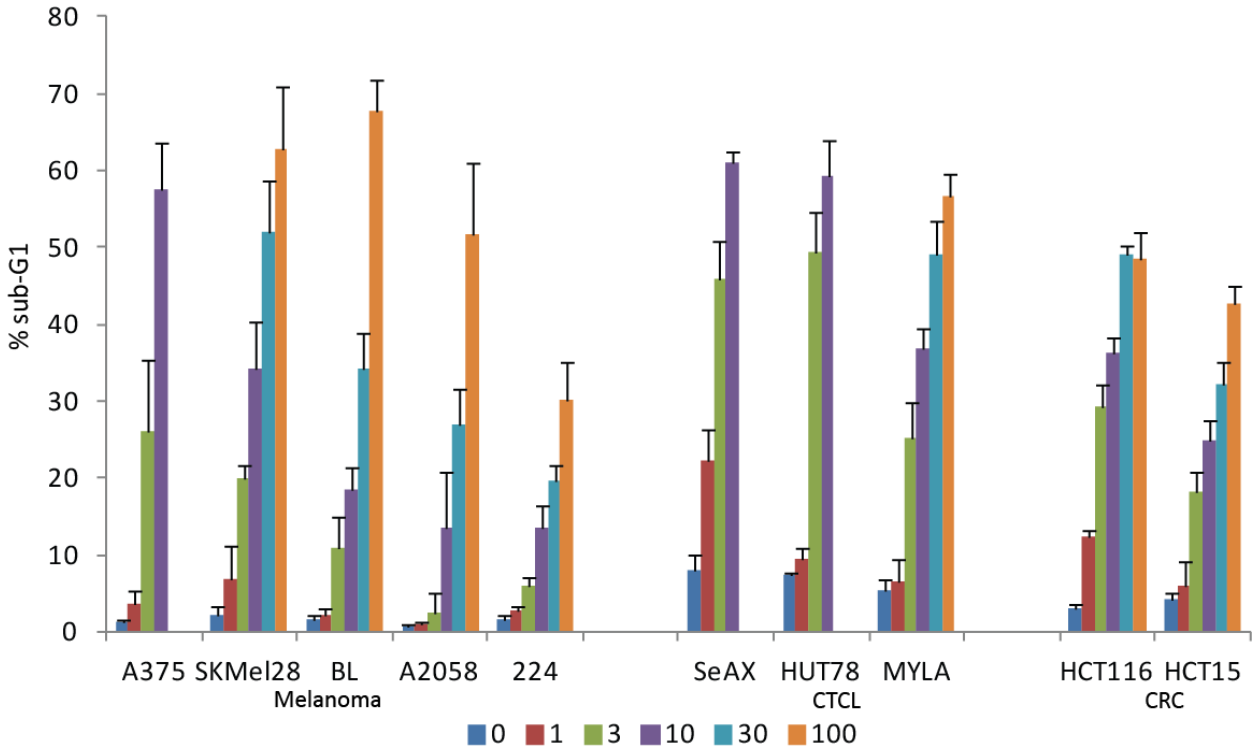


Figure 3.1

Effect of HDAC inhibitors on apoptosis in tumour cell lines

The levels of sub-G1 apoptotic cells determined by FACS analysis after treating melanoma, CTCL and colorectal (CRC) cell lines as indicated for 48 hours with SAHA at the indicated doses in µM (n=3, error bars: SD).

Poly-ADP ribose polymerase (PARP) is a substrate for certain caspases (for example, caspase 3 and 7) activated during early stages of apoptosis. These proteases cleave PARP to fragments of approximately 89 kD and 24 kD (Soldani and Scovassi, 2002). Detection of the 89 kD PARP fragment with anti-PARP thus serves as an early marker of apoptosis. This was measured to further substantiate the sub-G1 assay as an indicator of apoptosis (figure 3.2) and the 89 kD fragment was easily detectable at concentrations of SAHA treatment that resulted in a high

percentage of cells in sub-G1 in A2058, MYLA, HCT116 cells (figures 3.2 a-c). A similar effect was seen in U2OS cells treated with CXD101 indicating that this phenomenon was observed in cell lines treated with another HDAC inhibitor (figure 3.2d).

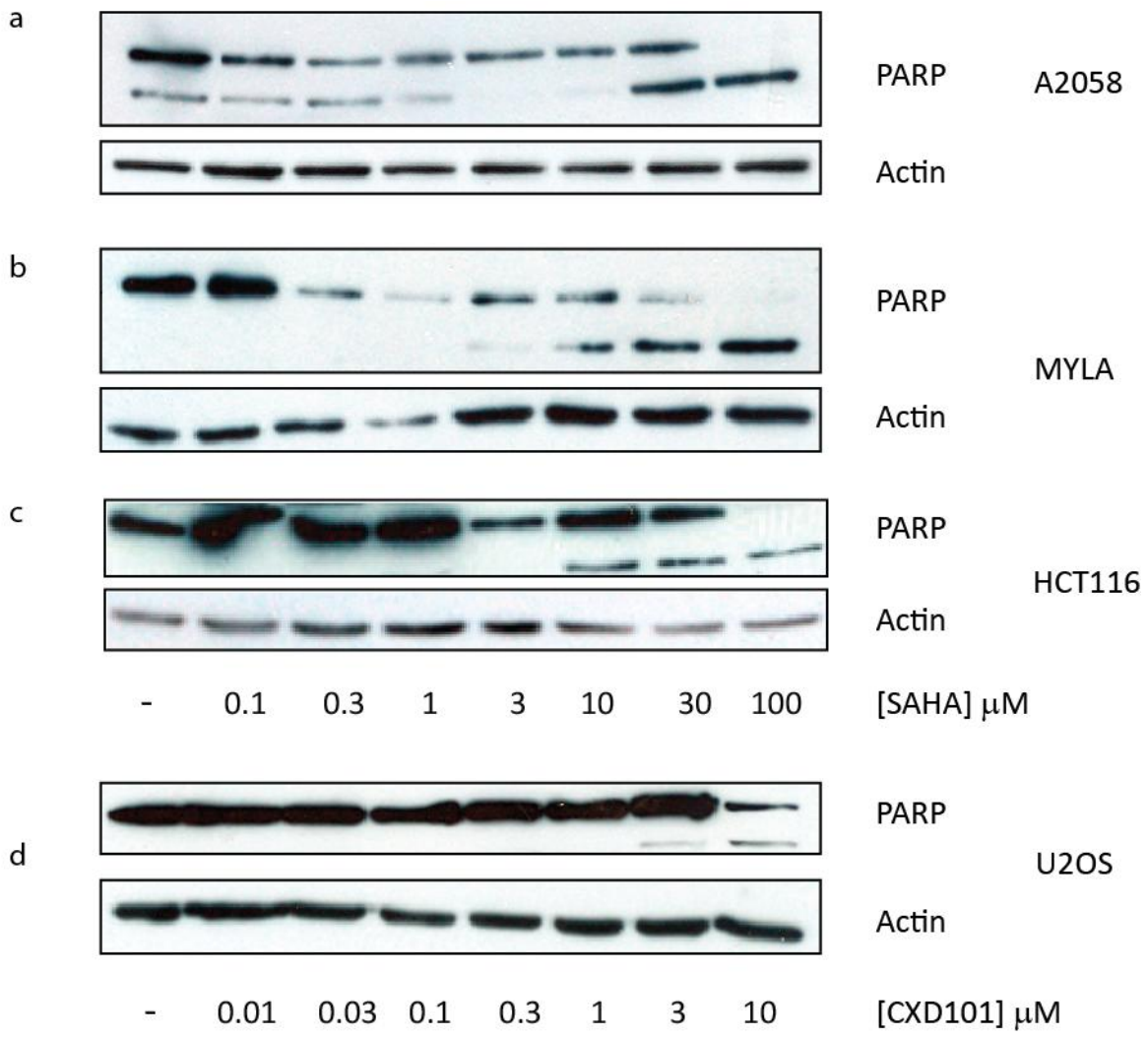


Figure 3.2

Protein expression of PARP and cleaved PARP upon HDAC inhibitor treatment as an indicator of apoptosis

(a-c) Immunoblots showing protein levels of cleaved and uncleaved PARP in the A2058, MYLA and HCT116 cell lines after treatment for 48h with SAHA at the indicated doses.

(d) Immunoblot showing protein levels of cleaved and uncleaved PARP in the U2OS cell line after treatment for 48h with CXD101 at the indicated doses. Actin is shown as loading control.

Although there was some overlap in sensitivities, melanoma cell lines required higher concentrations of SAHA to achieve similar levels of apoptosis when compared to CTCL cell lines. The notable exception was the A375 cell line. This was more clearly demonstrated when sub-G1 levels at 10μM of SAHA treatment were compared (figure 3.3). The mean sub-G1 percentage for melanoma cell lines at this dose of SAHA was significantly lower than CTCL cell lines (24.8% vs. 45.5%, $p<0.05$). This probably reflects the clinical situation where CTCL is a tumour that is relatively more sensitive to HDAC inhibitor treatment. Sensitivity to HDAC inhibitor therapy of colorectal cell lines lay somewhere in between that of melanoma and CTCL cell lines. While this was an interesting observation, a larger panel of cell lines should ideally be used to make more definitive conclusions.

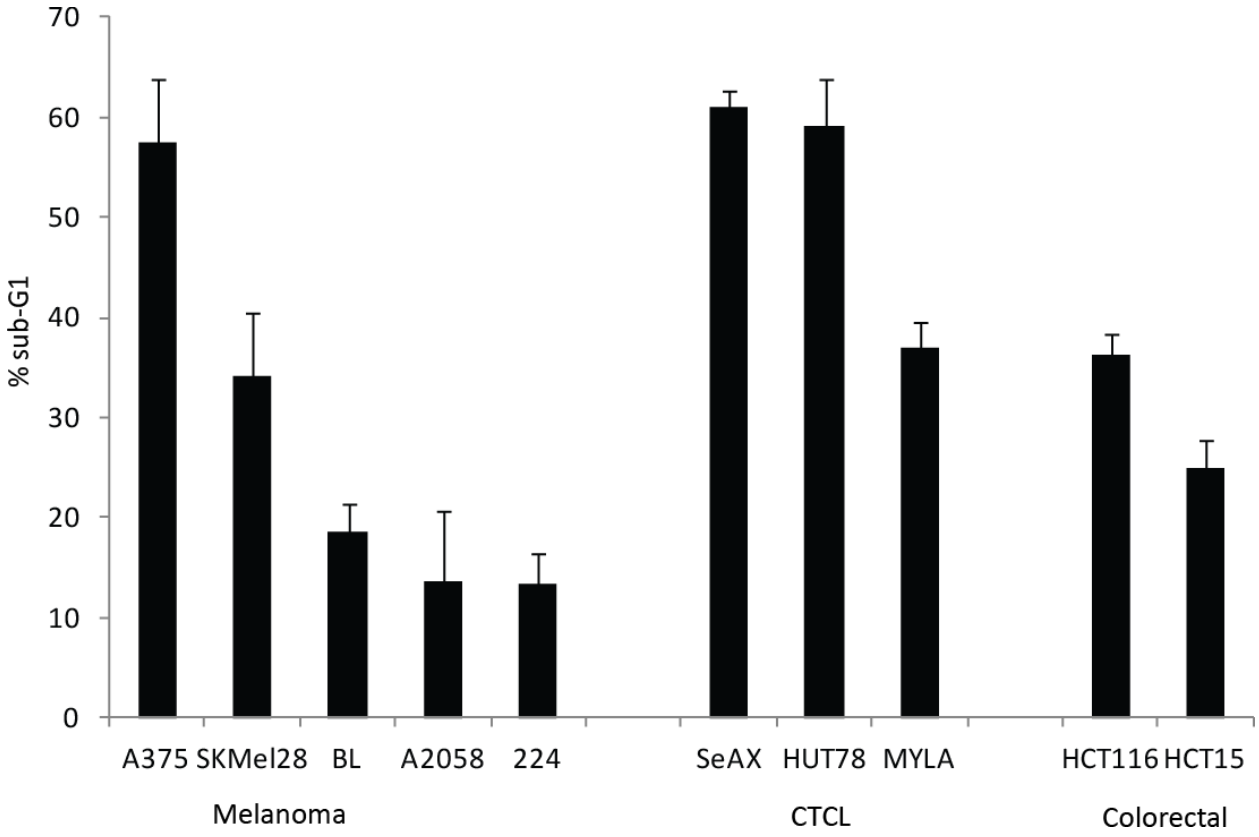


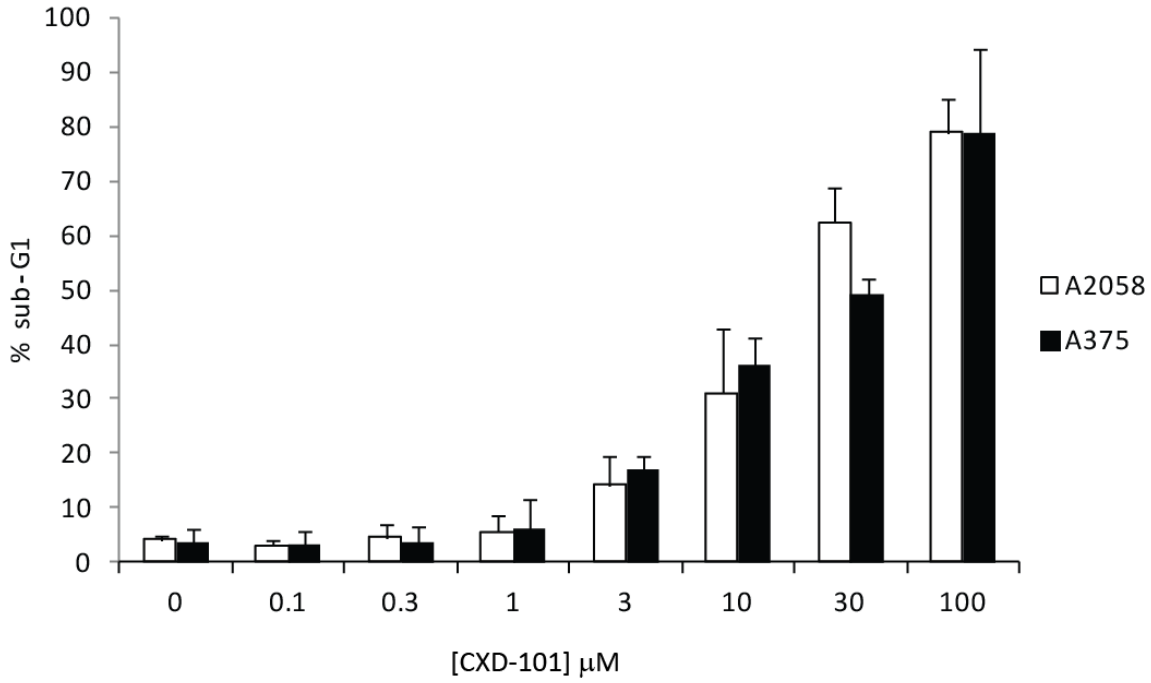
Figure 3.3

Comparison of apoptosis induced by SAHA at one concentration across different cell lines

The levels of sub-G1 apoptotic cells after treatment of melanoma, CTCL and colorectal cell lines as indicated for 48h with 10µM SAHA (n=3, error bars: SD).

Melanoma cell lines were sensitive to apoptosis induced by other HDAC inhibitors such as CXD101 and valproic acid (VPA) (figure 3.4). The enhanced sensitivity of A375 cells was less apparent with VPA treatment and not seen with CXD101 treatment. Drug concentrations of VPA in the millimolar range were required to achieve the same percentage of cells in sub-G1 compared to CXD101 and SAHA which were potent in the micromolar range reflecting the clinical situation.

a


100
90
80
70
60
50
40
30
20
10
0
% sub-G1
0
0.1
0.3
1
3
10
30
100
[CXD-101] μM
A2058
A375

b

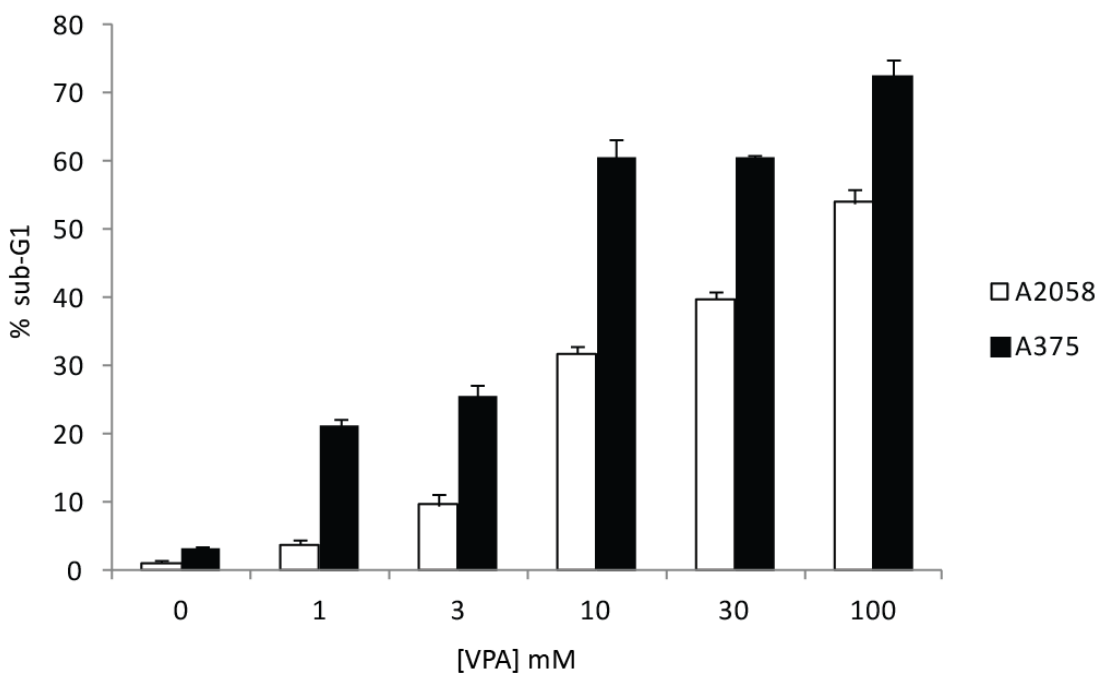

80
70
60
50
40
30
20
10
0
% sub-G1
0
1
3
10
30
100
[VPA] mM
A2058
A375

Figure 3.4

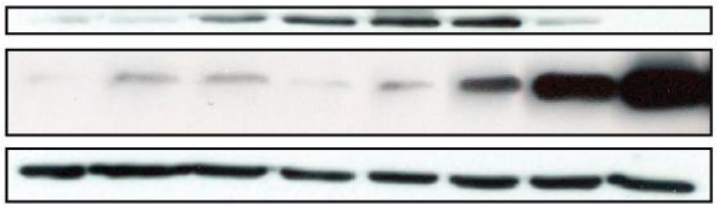
Effect of other HDAC inhibitors on induction of apoptosis in melanoma cell lines

The levels of sub-G1 apoptotic cells determined by FACS analysis after treating melanoma cell lines as indicated for 48h with CXD101 (a) and valproic acid (b) at the indicated doses (n=3, error bars: SD).

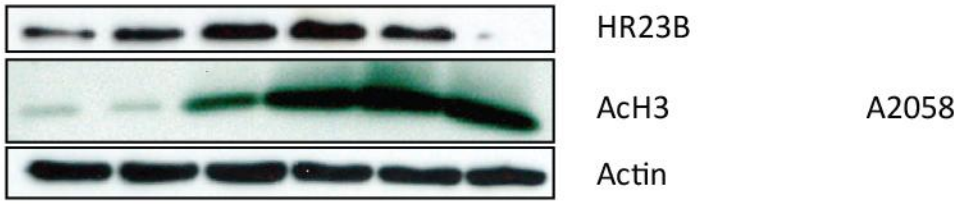
3.3. Effects of HDAC inhibitors on the expression of HR23B

It has been previously demonstrated that HR23B protein levels increase upon SAHA treatment in U2OS cells (Fotheringham et al., 2009a). The expression of HR23B, as determined by immunoblotting, increased with escalating dose of HDAC inhibitor and at highest concentrations, the levels decreased substantially. This observation was apparent in different cell lines treated with different HDAC inhibitors including SAHA, valproic acid and CXD101 (figure 3.5 a-d). Surprisingly, HR23B protein levels were also increased after proteasome inhibition with a subsequent reduction in protein levels at the highest doses (figure 3.6). Interestingly, this phenomenon occurred across a range of different tumour cell lines including melanoma, colorectal cancer and CTCL (figures 3.6a-e).

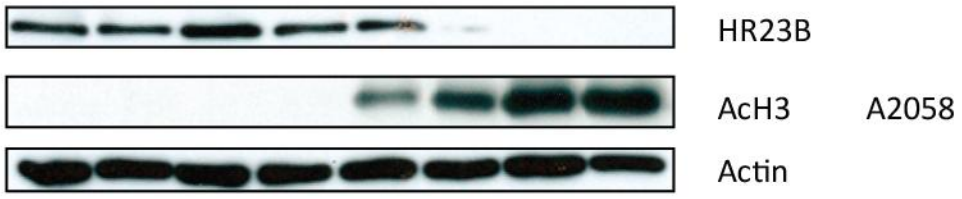
a


HR23B
AcH3
A375
Actin
0 0.01 0.03 0.1 0.3 1 3 10 [SAHA] µM

b


HR23B
AcH3
A2058
Actin
0 0.1 0.3 1 3 10 [VPA] mM

c


HR23B
AcH3
A2058
Actin
0 0.1 0.3 1 3 10 30 100 [CXD101] µM

d

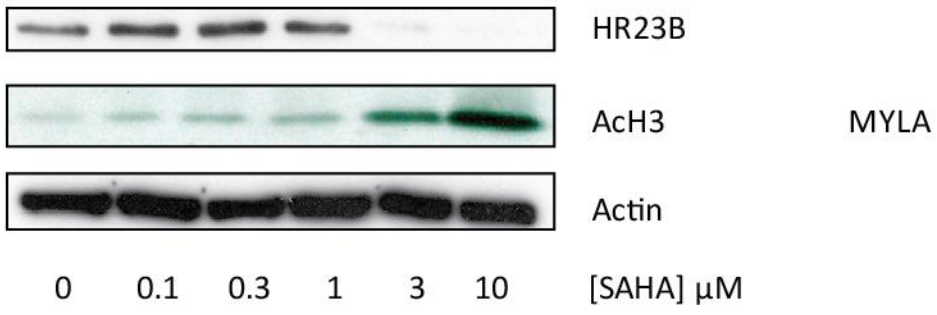

HR23B
AcH3
MYLA
Actin
0 0.1 0.3 1 3 10 [SAHA] µM

Figure 3.5

Effect of HDAC inhibitors on expression of HR23B

Immunoblots showing protein levels of HR23B in the melanoma cell lines A375 (a) and A2058 (b,c) and the CTCL cell line MYLA (d) treated with the indicated dose of SAHA (μM), valproic acid (mM) and CXD101 (μM) for 48h. Anti-acetylated H3 and anti-actin (loading control) are shown for comparison. The examples shown are representative of three different experiments.

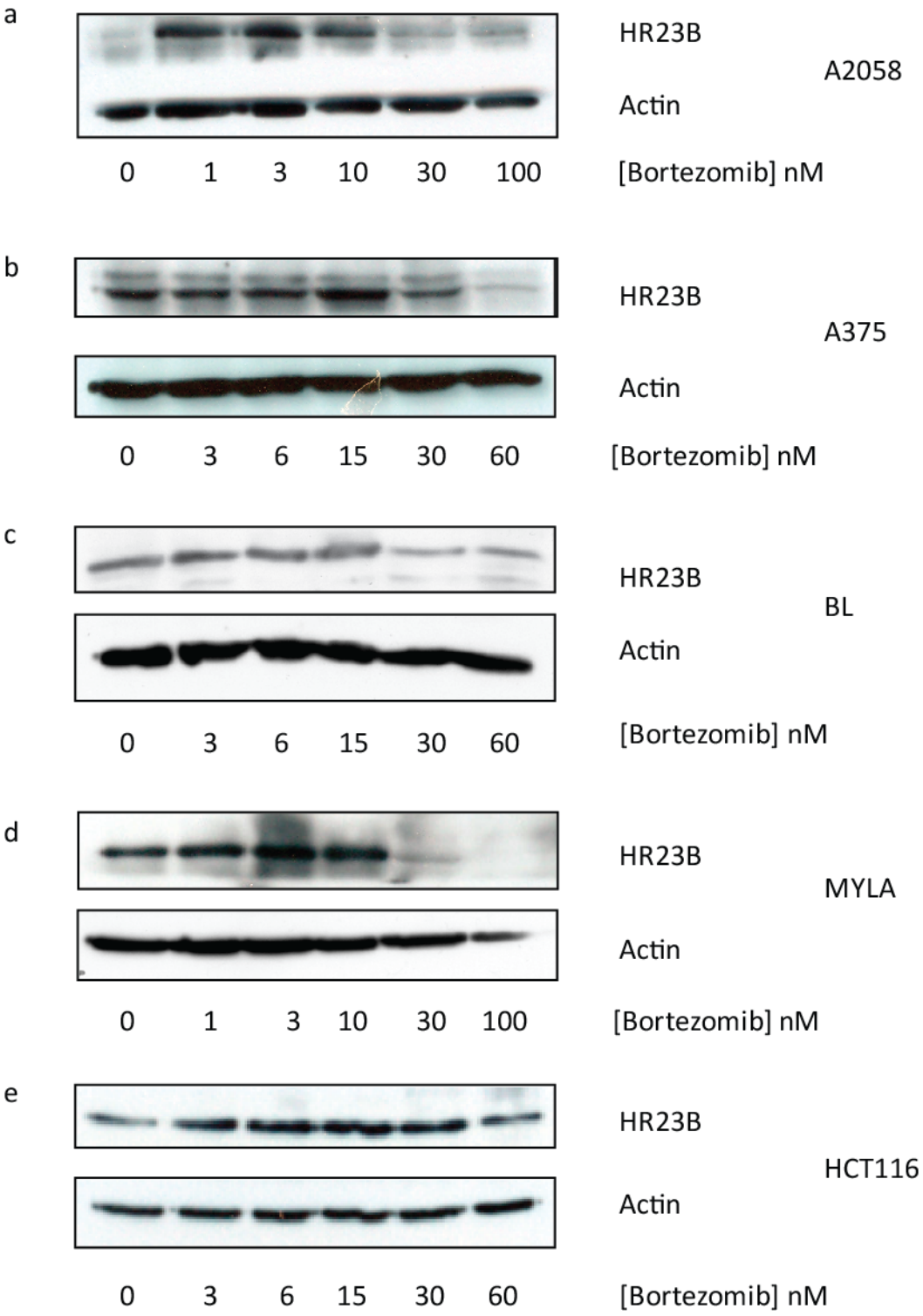

a
HR23B
A2058
Actin
0 1 3 10 30 100
[Bortezomib] nM
b
HR23B
A375
Actin
0 3 6 15 30 60
[Bortezomib] nM
c
HR23B
BL
Actin
0 3 6 15 30 60
[Bortezomib] nM
d
HR23B
MYLA
Actin
0 1 3 10 30 100
[Bortezomib] nM
e
HR23B
HCT116
Actin
0 3 6 15 30 60
[Bortezomib] nM

Figure 3.6

Effect of bortezomib on expression of HR23B

Immunoblots showing protein levels of HR23B in the melanoma cell lines A2058 (a), A375 (b) and BL (c), the CTCL cell line MYLA (d) and the colorectal cell line HCT115 (e) treated with the indicated dose of bortezomib (nM) for 48h. Anti-actin (loading control) is shown for comparison. The examples shown are representative of at least three different experiments.

To further investigate this observation, the levels and localisation of HR23B were investigated by immunofluorescence. Cells were treated with 10μM SAHA for 24 h and coverslips were then analysed by fluorescence microscopy. HR23B appears to be expressed mainly in the nucleus of untreated cells at relatively low levels, and after treatment with 10 μM SAHA cytoplasmic expression of HR23B increased in U20S and HCT116 cells (figures 3.7a and b). A shorter incubation time to the immunoblotting experiments was required because cell death was considerably higher at 48h with most cells no longer adherent to the coverslips. Increased protein expression of HR23B as determined by immunoblotting was noted after 24h incubation of drug but this was not as consistent across all cell lines (data not shown).

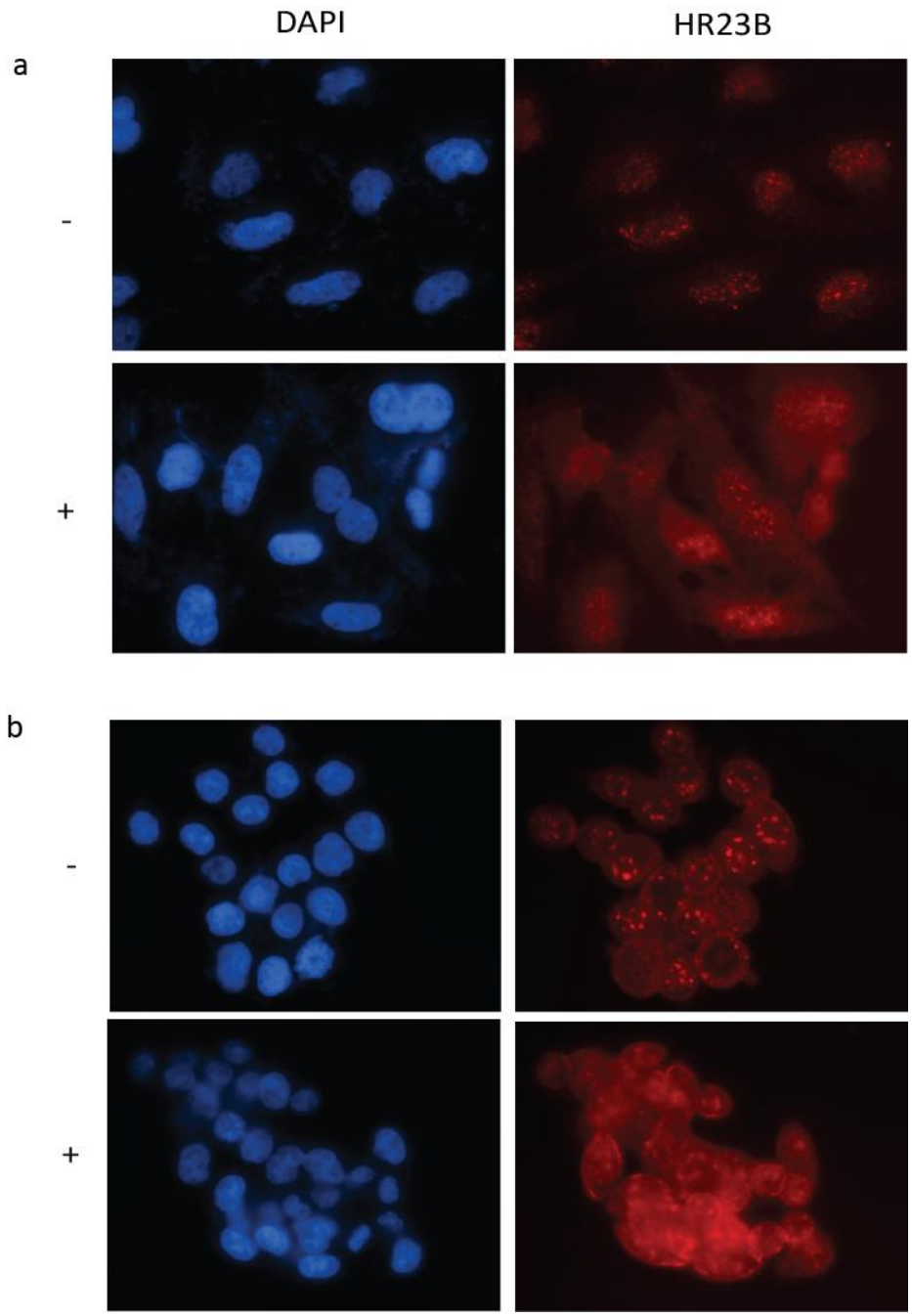


Figure 3.7

Effect of HDAC inhibitors on cellular localisation and expression of HR23B

Cells were treated with 10μM SAHA for 24h and coverslips were then analysed by fluorescence microscopy for HR23B (red). Immunostaining shows the level of HR23B in U2OS cells (a) and in HCT116 cells (b) before and after treatment with 10 μM SAHA (+) for 24h. Nuclei were

located by comparison to DAPI staining. The images shown are representative of 3 independent experiments.

The actual protein levels of HR23B after drug treatment are perhaps not as important as the baseline levels pre-treatment in determining sensitivity to HDAC inhibitors; the hypothesis being that high levels correspond to increased sensitivity and vice versa. The baseline expression of HR23B in different cell lines was investigated and correlated with sensitivity. There appeared to be some association in CTCL, colorectal cancer and melanoma (figure 3.8) although the results were not reliably reproducible. Nevertheless, it was difficult to make a comparison with only a few cell lines for each tumour type.

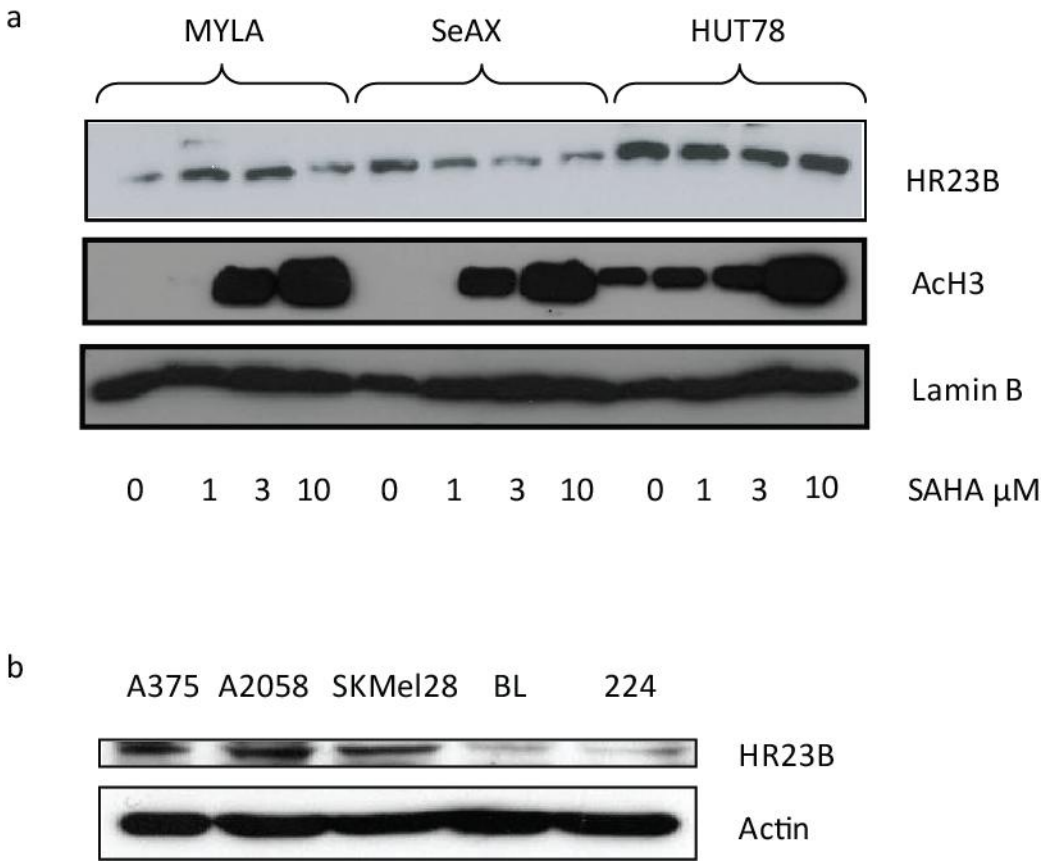


Figure 3.8

Basal levels of HR23B in CTCL and melanoma in cell lines

(a) Immunoblot showing protein levels of HR23B in the CTCL cell lines MYLA, SeAX and HUT78 treated with the indicated doses of SAHA (µM) for 48h. Acetylated H3 and lamin (loading control) are shown for comparison. HR23B expression with no drug treatment is lowest in the more resistant cell line (MYLA) and higher in the more sensitive cell lines. Lamin B was used as loading control due to lack of expression of actin by HUT78 cells

(b) Immunoblot showing protein levels of HR23B in the melanoma cell lines A375, A2058, SKMel28, BL and 224 after treatment with DMSO for 24h to demonstrate baseline expression of HR23B. In this example, HR23B expression is lower in the more resistant cell lines. Actin levels are shown as loading control. The immunoblot is representative of three different experiments.

3.4. Alteration in pre-treatment HR23B levels impacts on HDAC inhibitor-mediated apoptosis

To gain a better understanding of the role of HR23B in apoptosis after HDAC inhibitor treatment, levels were modified before treatment. Firstly, the effect of depleting HR23B was examined to assess whether it was a sensitivity determinant for HDAC inhibitors in melanoma and CTCL cells. The introduction of siRNA against HR23B RNA reduced the level of endogenous HR23B compared to the siRNA control treatment (figures 3.9a and 3.9c), and HR23B depletion coincided with reduced sensitivity to apoptosis as determined by measuring the percentage of cells in the sub-G1 fraction. This was evident in A2058 and MYLA cells upon SAHA treatment (Figure 3.9b and 3.9d). In A2058 cells, the difference between the control and HR23B siRNA was statistically significant when cells were treated with 10μM SAHA but not quite significant at 30μM. In MYLA cells, the difference was statistically significant only at 30μM. These data corroborated data from similar experiments in U2OS cells (Fotheringham et al., 2009).

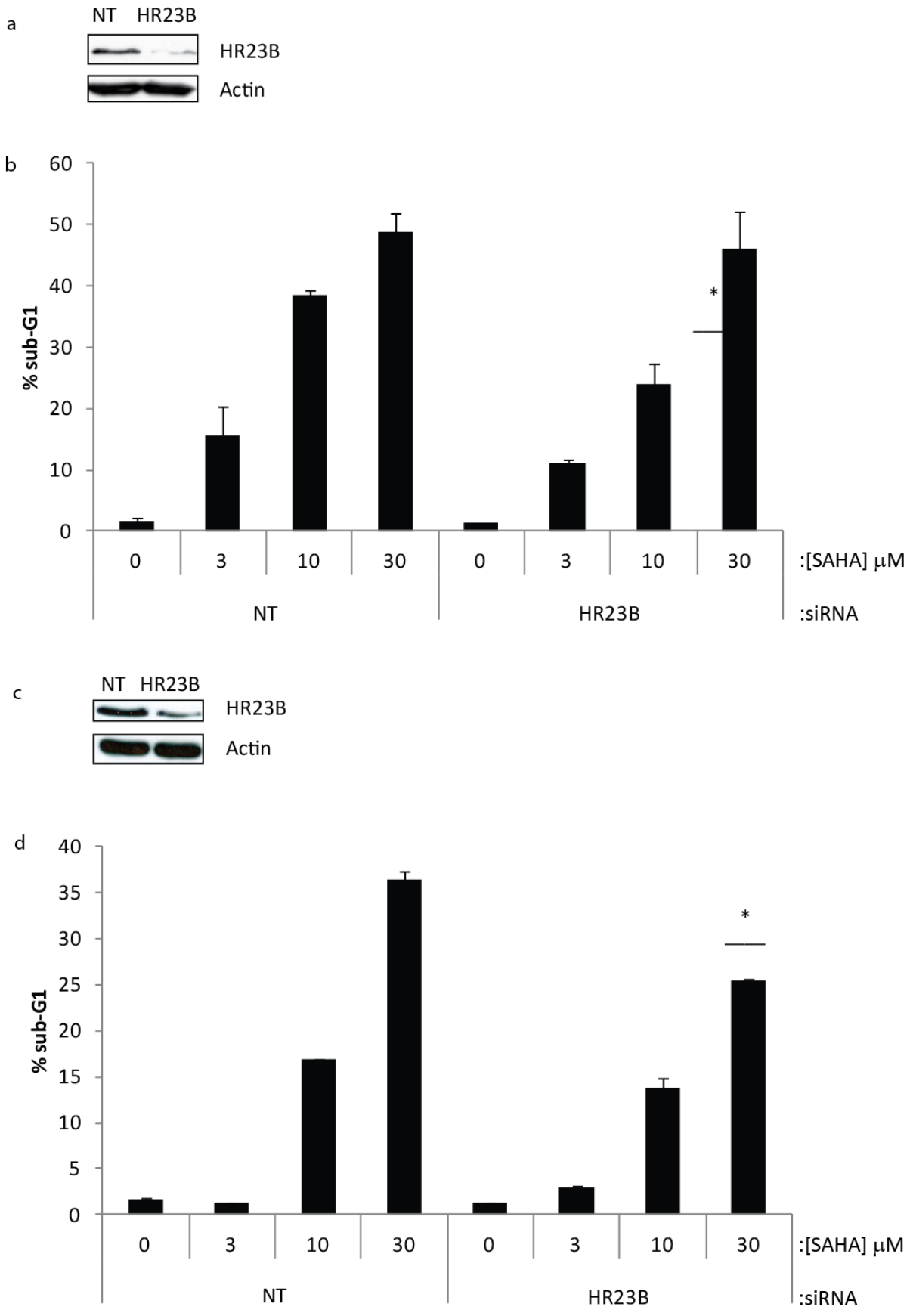
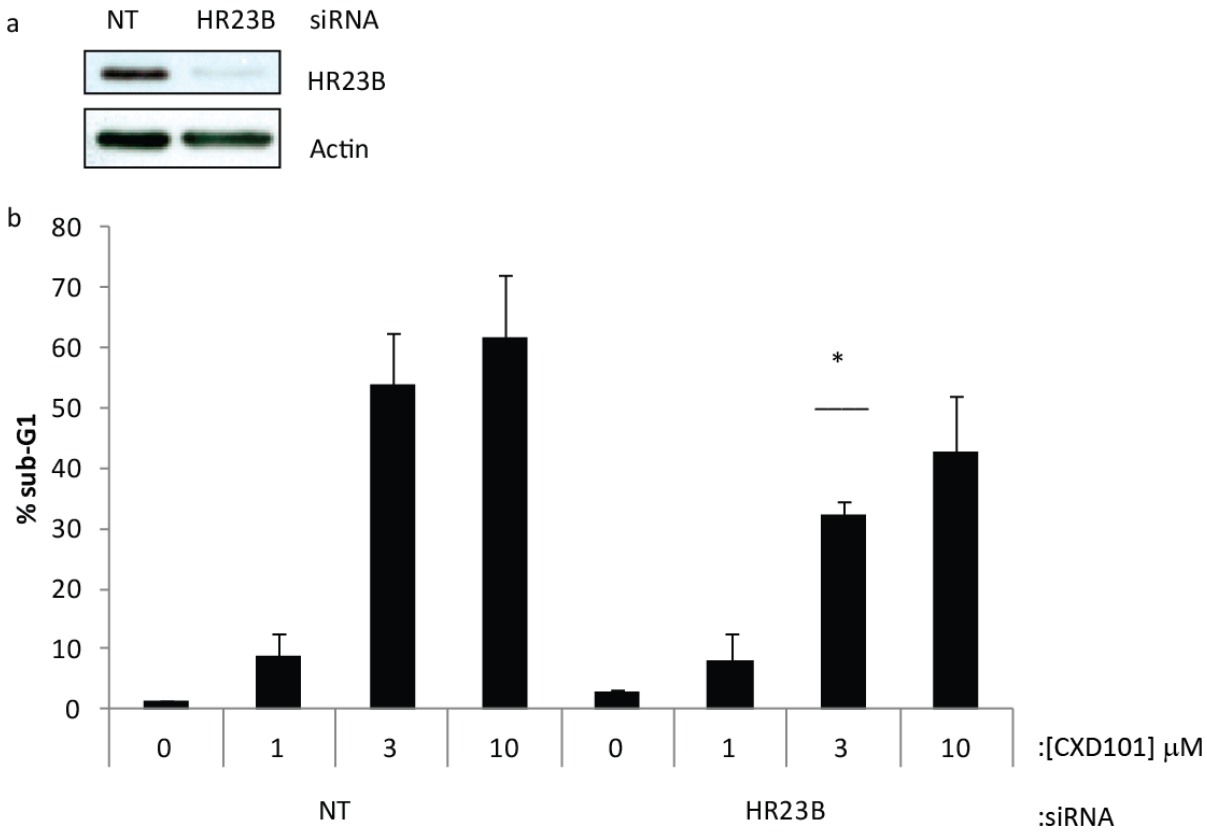

a
NT
HR23B
HR23B
Actin
b
% sub-G1
60
50
40
30
20
10
0
*
0
3
10
30
0
3
10
30
:[SAHA] μM
NT
HR23B
:siRNA
c
NT
HR23B
HR23B
Actin
d
% sub-G1
40
35
30
25
20
15
10
5
0
*
0
3
10
30
0
3
10
30
:[SAHA] μM
NT
HR23B
:siRNA

Figure 3.9

Effect of depleting HR23B using siRNA in melanoma and CTCL cells upon HDAC inhibitor-induced apoptosis

A2058 cells (a) and MYLA (c) cells were treated with HR23B or non-targeting control (NT) siRNA for 48h, followed by immunoblotting. Actin served as the loading control. The levels of sub-G1 A2058 cells (b) and MYLA cells (d) determined by FACS after treatment with HR23B siRNA or non-targeting control (NT) siRNA for 48h followed by treatment with DMSO control or increasing concentrations of SAHA (μM) as indicated for 48h (* significance in two-tailed Student's t test; *$P < 0.05$; n=3, error bars = SD).

Rescue from apoptosis was also seen in U2OS cells pre-treated with HR23B siRNA followed by CXD101 treatment with the difference between control and HR23B siRNA seen at 3 μM and 10 μM although the latter difference was not statistically significant (figure 3.10b). Furthermore, treatment of HR23B-depleted cells with VPA also resulted in rescue from apoptosis that was statistically significantly different at 10 mM (figure 3.10d). However, this phenomenon was not observed in all cell lines; e.g. in HCT116 colorectal cancer cells and in A375 melanoma cells, apoptosis, as measured by the sub-G1 fraction, was no different at varying concentrations of SAHA under non-targeting and HR23B siRNA treatment (appendix V1).


a
NT
HR23B
siRNA
HR23B
Actin
b
% sub-G1
80
70
60
50
40
30
20
10
0
*
0
1
3
10
0
1
3
10
:[CXD101] μM
NT
HR23B
:siRNA

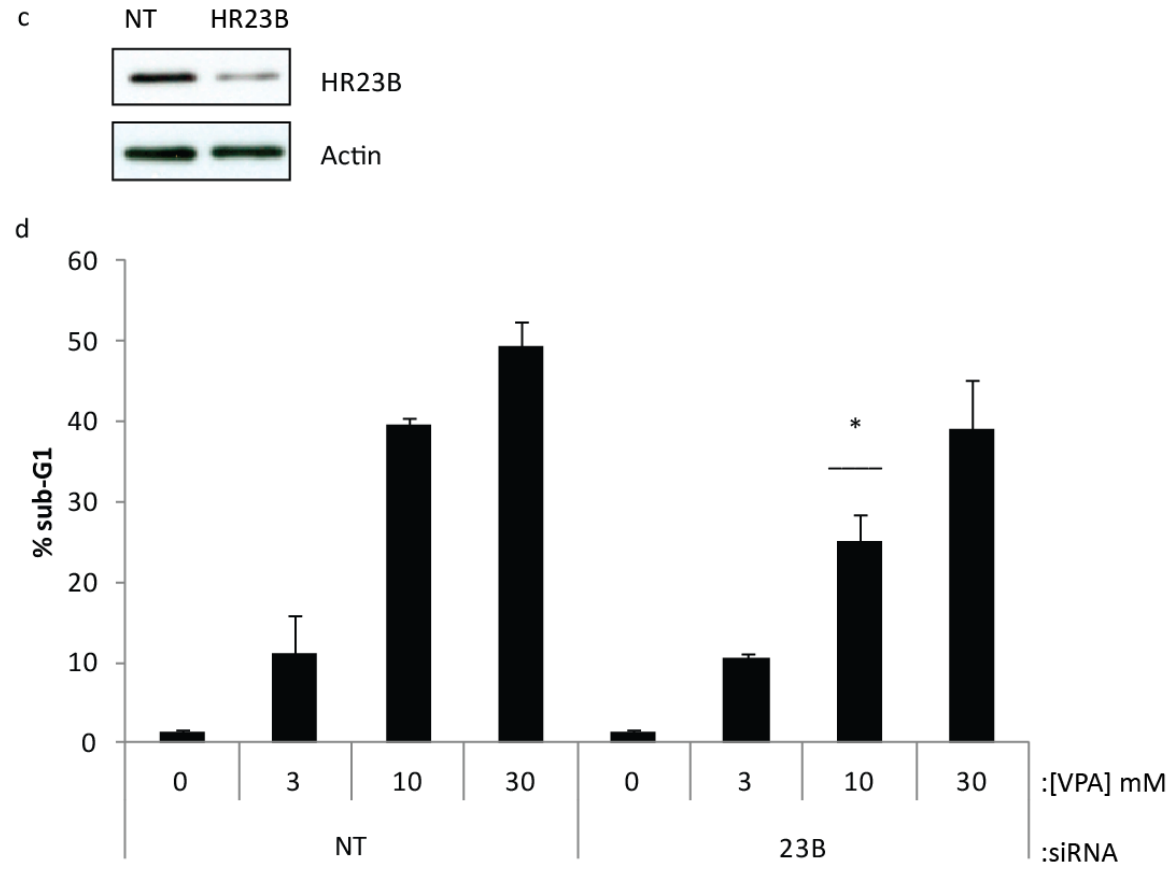

c
NT
HR23B
HR23B
Actin
d
% sub-G1
60
50
40
30
20
10
0
*
0
3
10
30
0
3
10
30
:[VPA] mM
NT
23B
:siRNA

Figure 3.10

Effect of depleting HR23B using siRNA in U2OS and melanoma cells on HDAC inhibitor-induced apoptosis

(a) Immunoblot showing the expression of HR23B, with actin as a loading control, for the experiment in (b)

(b) The levels of sub-G1 in U2OS cells determined by FACS after treatment with HR23B siRNA or non-targeting control (NT) siRNA for 48h followed by treatment with DMSO control or increasing concentrations of CXD101(μM) as indicated for 48h (* significance in two-tailed Student's t test; *P < 0.05; n=3, error bars = SD).

(c) Immunoblot showing the expression of HR23B, with actin as a loading control, for the experiment in (d)

(d) The levels of sub-G1 in A2058 cells determined by FACS after treatment with HR23B siRNA or non-targeting control (NT) siRNA for 48h followed by treatment with increasing concentrations of valproic acid as indicated for 48h (* significance in two-tailed Student's t test; *P < 0.05; n=3, error bars = SD).

In stable U2OS cell lines in which the expression of stable ectopic HR23B was under conditional control (induction upon doxycycline treatment), there was a statistically significant increase in sensitivity to HDAC inhibitors in cells where HR23B levels were induced compared to the uninduced cells (figure 3.11). There was increased apoptosis at both 3 and 10 μM of SAHA treatment indicated by increased proportion of cells in the sub-G1 phase as well as increased PARP cleavage. There was no increase in HR23B levels in the parental cells upon doxycycline treatment (Khan et al., 2010).

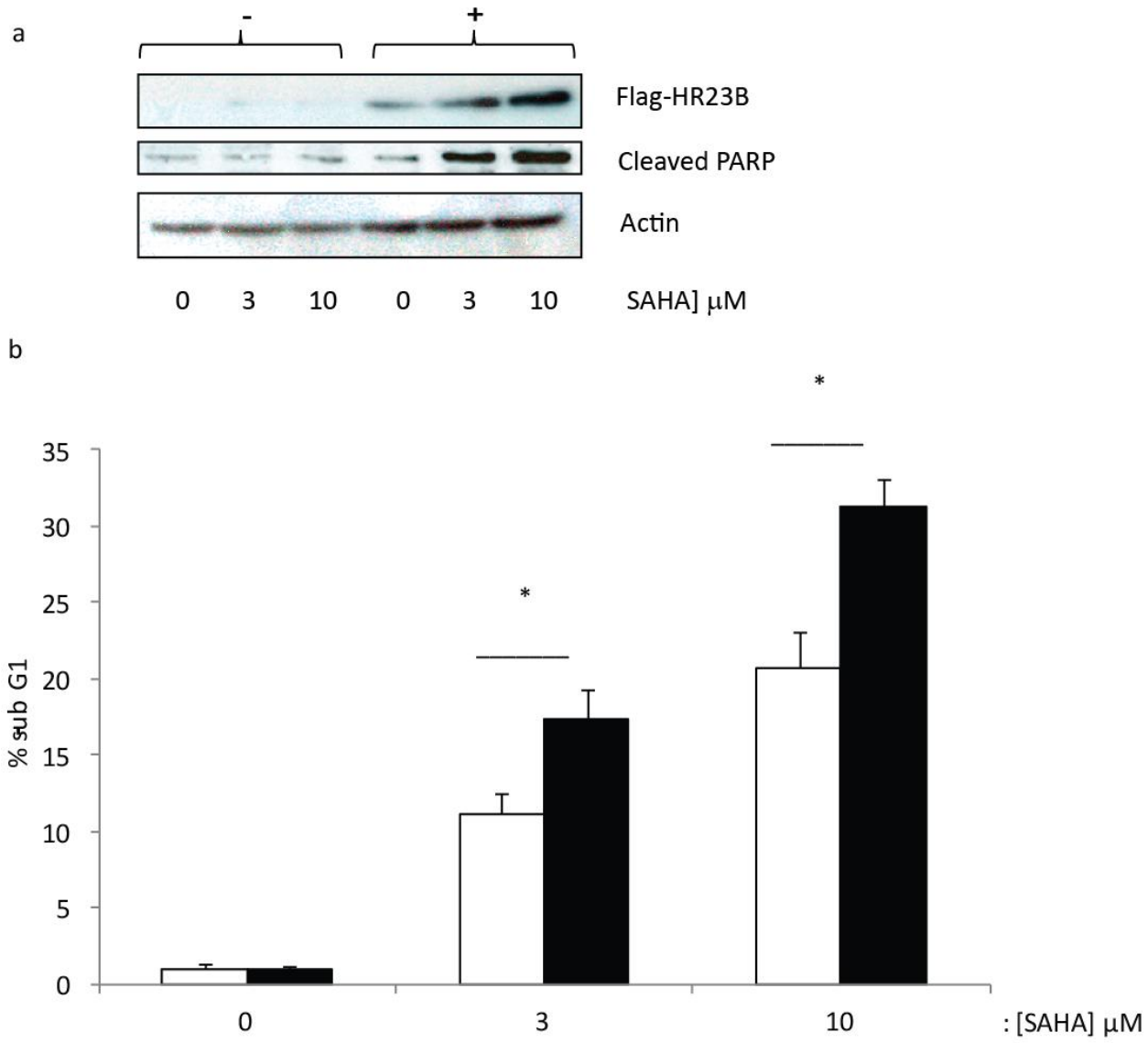


Figure 3.11

Effect of over-expression of HR23B on HDAC-inhibitor induced apoptosis

U2OS-TET cells expressing ectopic FLAG-HR23B were treated with doxycycline for 16 h before an additional 48h treatment with SAHA (3, 10 μM) or DMSO control (0).

(a) Immunoblot showing protein levels of FLAG-HR23B in uninduced (−) and induced (+) U2OS-TET cells and cleaved PARP. Actin was used as a loading control.

b) Graph showing the percentage sub-G1 cells in induced (black bar) cell lines treated with SAHA compared with DMSO control (clear bar) (* significance in two-tailed Student's t test; *$P < 0.05$; n=3, error bars = SD).

3.5. Conclusion.

Increase in HR23B protein levels along with altered cellular localisation after HDAC inhibitor treatment suggests a change in HR23B function under these conditions. Its more cytoplasmic localisation in some cell lines after SAHA treatment could suggest that under SAHA treatment, HR23B exerts a more proteolytic role. The fact that HR23B protein levels increase after HDAC inhibitor and proteasome inhibitor treatment implies that the role of HR23B in the degradation of proteins may be important for the ability of SAHA to cause apoptosis in tumour cell lines.

There is some evidence that baseline levels in HR23B levels in different cell lines corresponds to sensitivity to HDAC inhibitors and this is evident when HR23B levels are either decreased or increased before HDAC inhibitor treatment. The rescue from apoptosis upon depleting HR23B before HDAC inhibitor treatment is evident across a variety of different cell lines as well as with different HDAC inhibitors but is by no means universal. These findings support the role of HR23B as a sensitivity determinant in HDAC inhibitor treated cells at certain concentrations in some but not all cell lines. .

CHAPTER 4

RESULTS

PROTEASOME ACTIVITY IN CTCL AND MELANOMA CELL LINES TREATED WITH HDAC INHIBITORS

4.1. Introduction

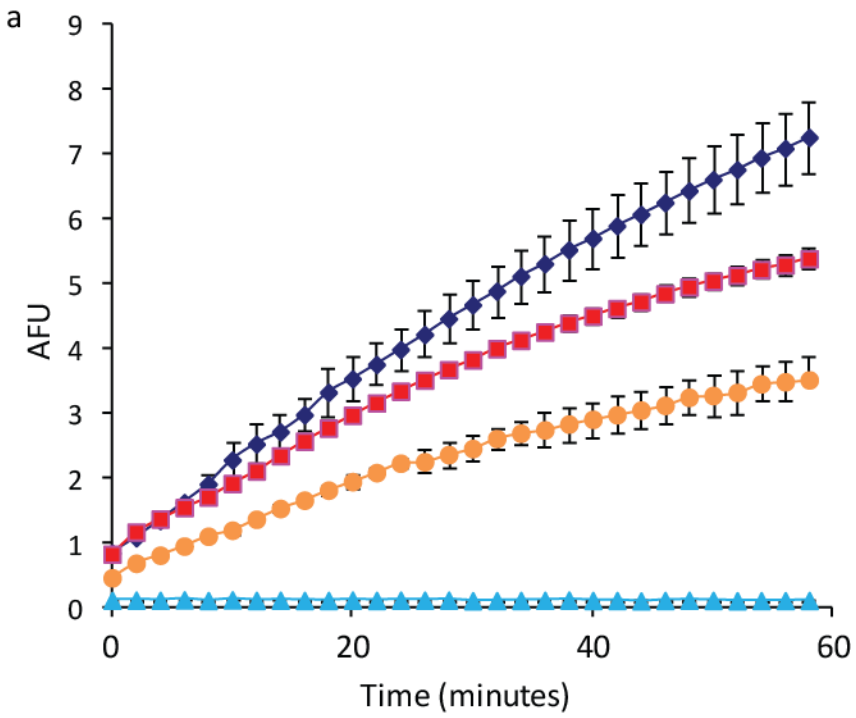
At a mechanistic level, HR23B has an important role in shuttling ubiquitinated cargo proteins to the proteasome (Chen et al 2001, Chen and Madura 2002, Marks and Breslow 2007). Indeed, proteasomes display aberrant activity in osteosarcoma cells treated with HDAC inhibitors, and HR23B is in part responsible for the effect on proteasome activity (Fotheringham et al., 2009a). In U2OS cells treated with HDAC inhibitors, HR23B contributed to the inhibition of proteasome activity. It was essential to establish whether there were mechanistic parallels in other tumour cell lines, and therefore proteasome activity in CTCL and melanoma cells upon HDAC inhibitor treatment was evaluated.

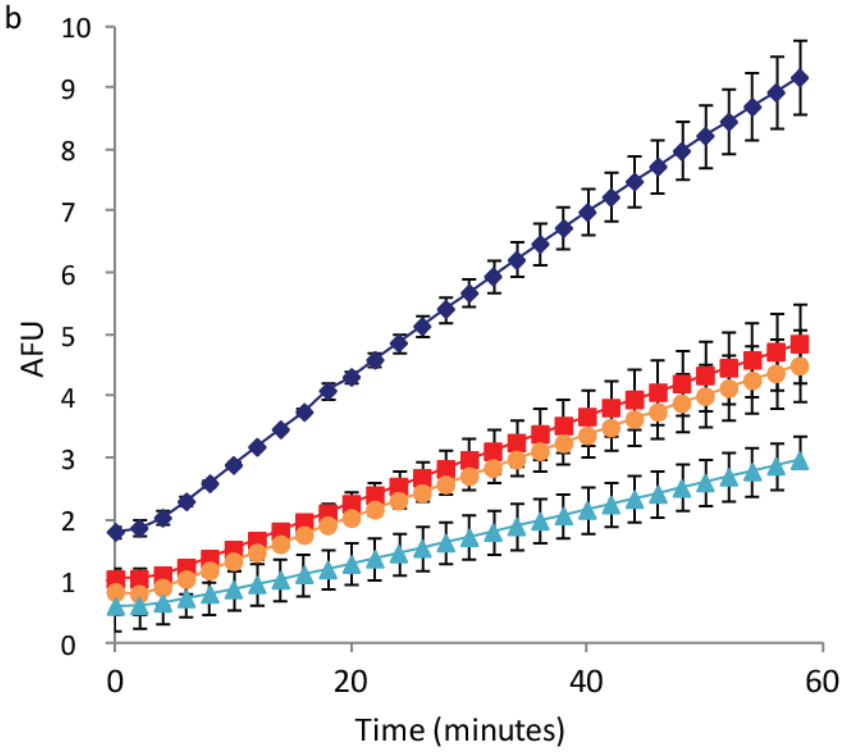
A number of reports have described the anti-cancer effects of combining an HDAC inhibitor with a proteasome inhibitor, the most studied of which is bortezomib (Stimson et al., 2009). Given the shared effect of HDAC and proteasome inhibitors on HR23B together with the role of HR23B in conferring drug sensitivity in tumour cells, it is crucial to test whether the level of HR23B might influence the outcome of the combined treatment and, possibly, provide an instructive biomarker that informs on the outcome of the combination treatment.

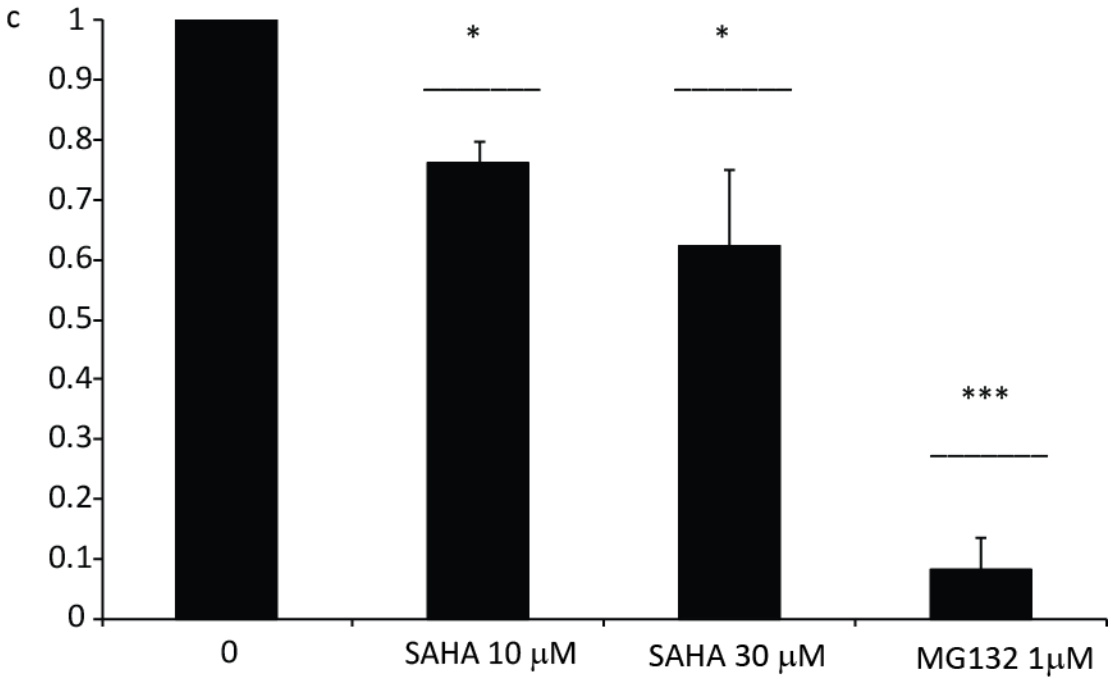
4.2. HDAC inhibitor treatment causes a decrease in proteasomal activity

When centrifuged lysates containing proteasomes were obtained from SAHA treated A2058 and MYLA cells and protease activity measured *in vitro* using a fluorogenic substrate peptide (Meng et al., 1999), a significant decrease in catalytic activity was apparent compared to the control

treatment (figures 4.1a and 4.1b). The inhibition of proteasome activity was both concentration of drug and time of treatment dependent. The reduction in catalytic activity after SAHA treatment was statistically significant at both 10μM and 30μM in both cell lines when compared to the DMSO control (figures 4.1c and 4.1d).


a
AFU
Time (minutes)
0
1
2
3
4
5
6
7
8
9
0
20
40
60


b
AFU
Time (minutes)
0
1
2
3
4
5
6
7
8
9
10
0
20
40
60


c
1
0.9
0.8
0.7
0.6
0.5
0.4
0.3
0.2
0.1
0
*
*
***
0
SAHA 10 μM
SAHA 30 μM
MG132 1μM

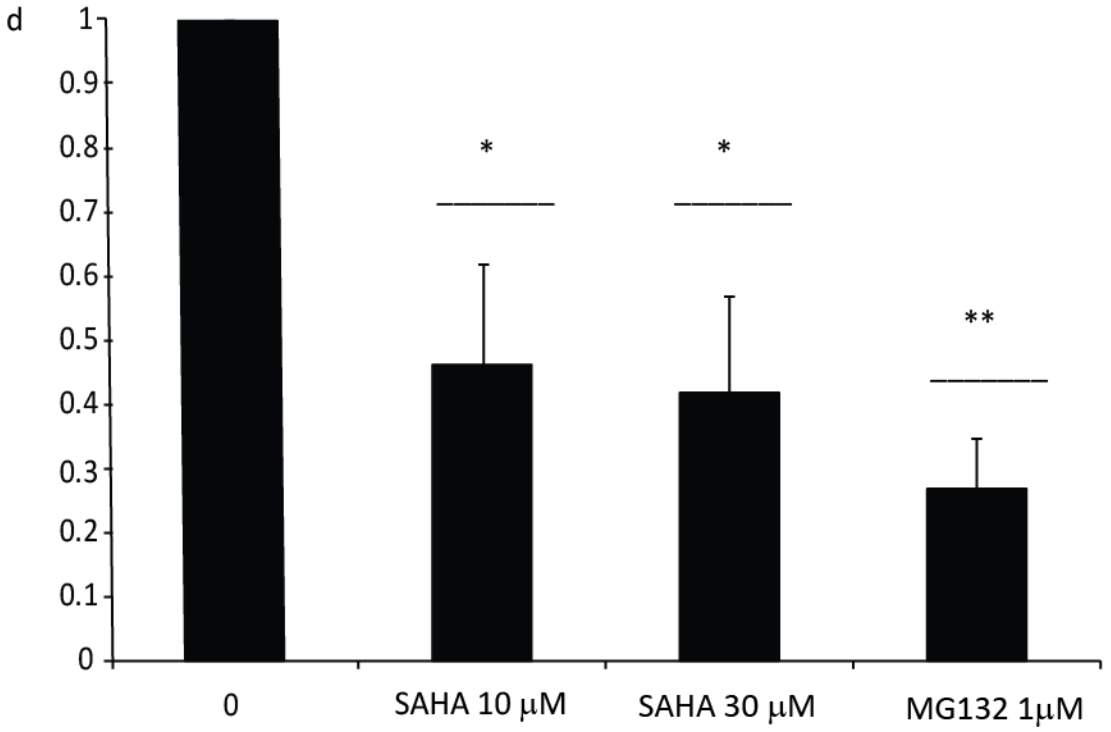
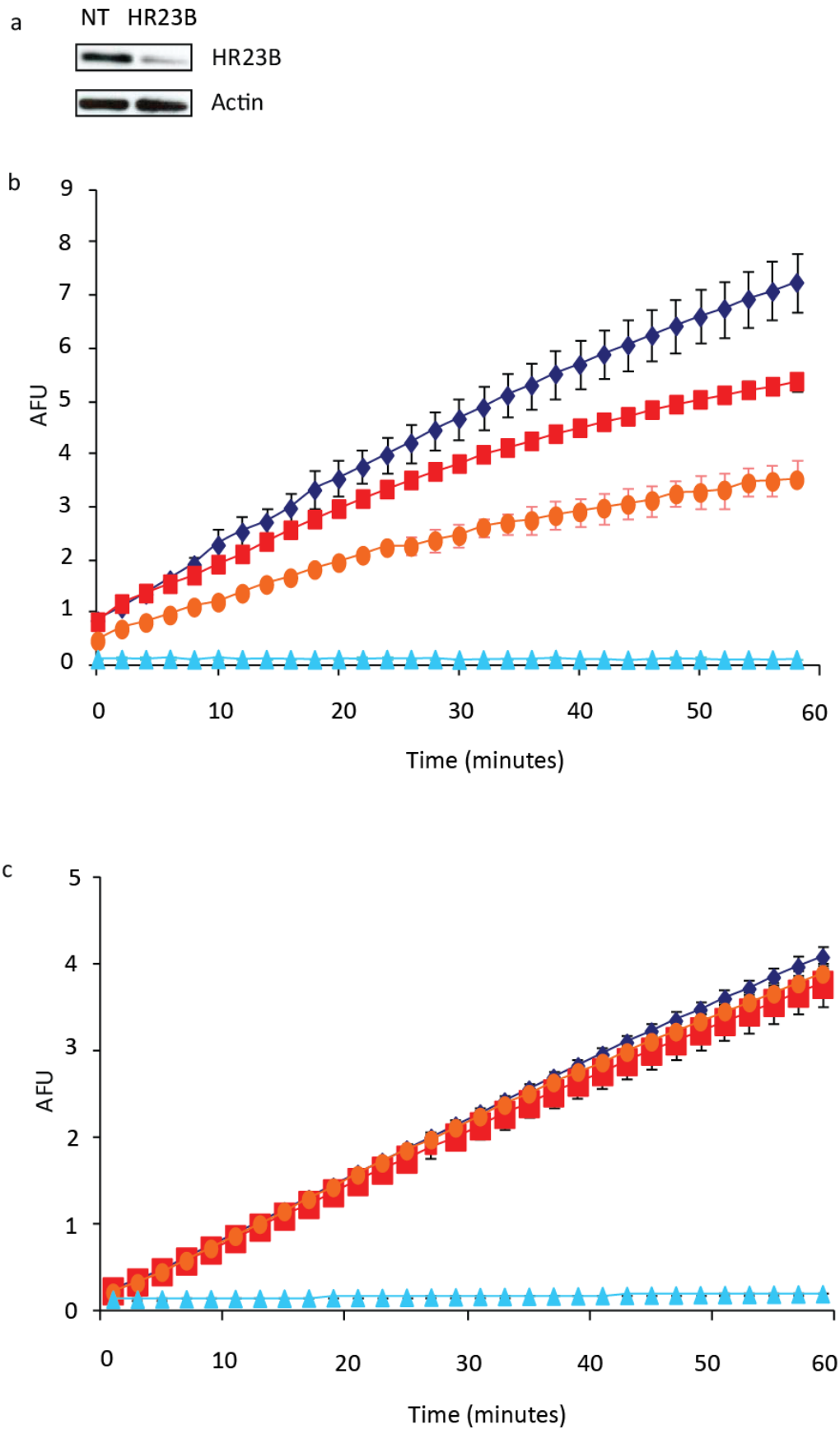

d
1
0.9
0.8
0.7
0.6
0.5
0.4
0.3
0.2
0.1
0
*
*
**
0
SAHA 10 μM
SAHA 30 μM
MG132 1μM

Figure 4.1

Proteasome activity in CTCL and melanoma cells treated with HDAC inhibitors

MYLA cells (a) and A2058 cells (b) were treated with DMSO (blue), SAHA 10μM (red), SAHA 30μM (orange) or MG132 1μM (cyan) and harvested at 24h. Cleaved substrate (as arbitrary fluorescence units; AFU) representative of active proteasome was measured at 2 min intervals for 60 min. (experiment performed in triplicate, error bars = SD). Inhibition of catalytic activity normalised to the DMSO treatment is indicated for SAHA and MG132 treatment of MYLA (c) and A2058 (d) cell lines (* significance in two-tailed Student's t test; * $P < 0.05$, ** $P < 0.005$; *** $P < 0.0005$; n=3, error bars = SD).

To assess the role of HR23B in regulating proteasome activity, HR23B was depleted in HDAC inhibitor-treated MYLA cells using siRNA (figure 4.2a), and then proteasome activity measured *in vitro*. Under non-targeting siRNA control conditions, the reduction in catalytic activity was similar to that seen in cells treated with no siRNA (figures 4.2b and 4.2d). However in conditions of HR23B depletion, the decrease in proteasome activity was no longer apparent (figure 4.2c); this suggests that proteasome activity in HDAC inhibitor treated cells is in part influenced by HR23B. When this difference was quantified by normalising values to the DMSO control, there was a highly statistically significant difference at the SAHA concentration of 30 μM (figure 4.2d). It was notable that the concentration of SAHA at which there was a statistically significant difference in catalytic activity between the non-targeting siRNA and the HR23B siRNA treated cells was the same at which rescue from apoptosis was seen, i.e. 30μM. (figure 3.9d).


a
NT HR23B
HR23B
Actin
b
AFU
Time (minutes)
c
AFU
Time (minutes)

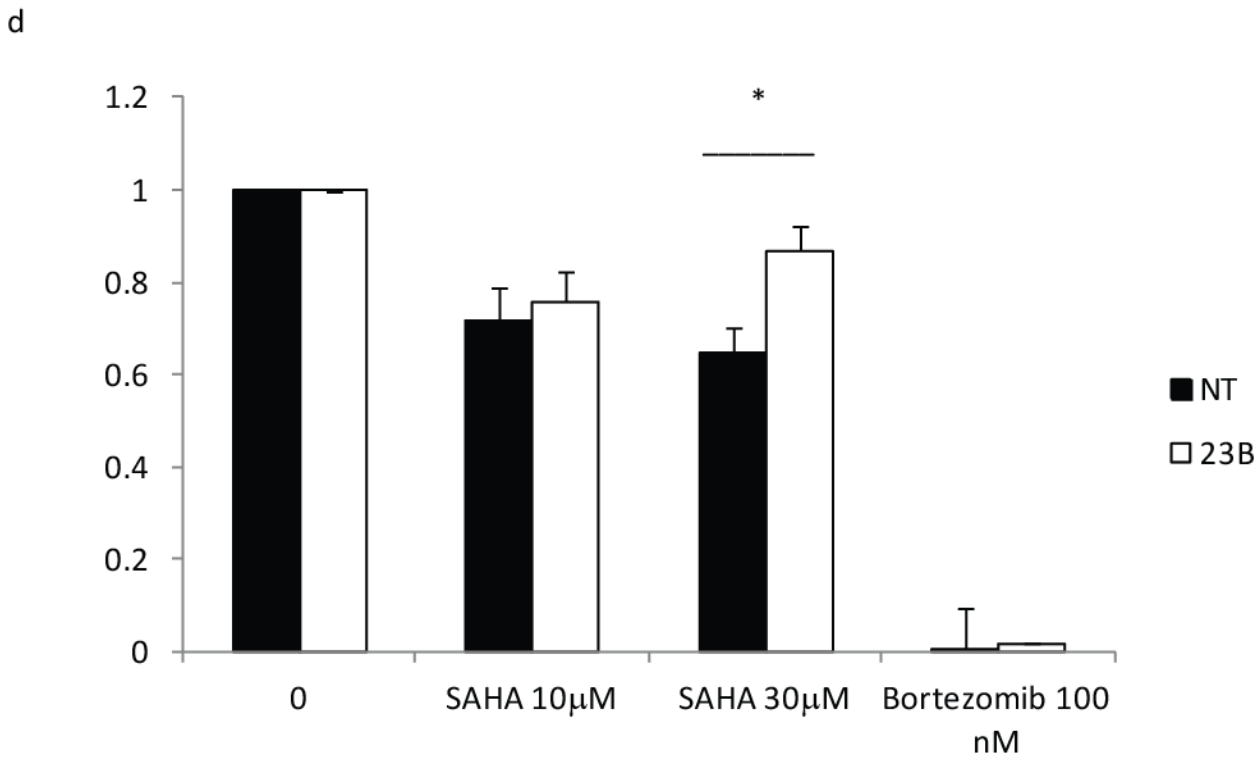


Figure 4.2

Effect of depleting HR23B on proteasome activity in MYLA cells

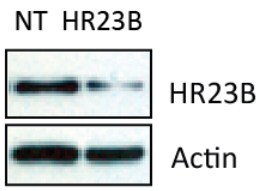
(a) Immunoblot showing the expression of HR23B, with actin as a loading control, for the experiments in (b) and (c).

MYLA cells were treated with non-targeting (b) or HR23B siRNA (c) for 48h followed by a subsequent 24h treatment with DMSO (blue), SAHA 10µM (red), SAHA 30µM (orange) or bortezomib 100nM (cyan) and harvested at 24h. Cleaved substrate representative of active proteasome was measured at 2 min intervals for 60 min (experiment performed in triplicate, error bars = SD).

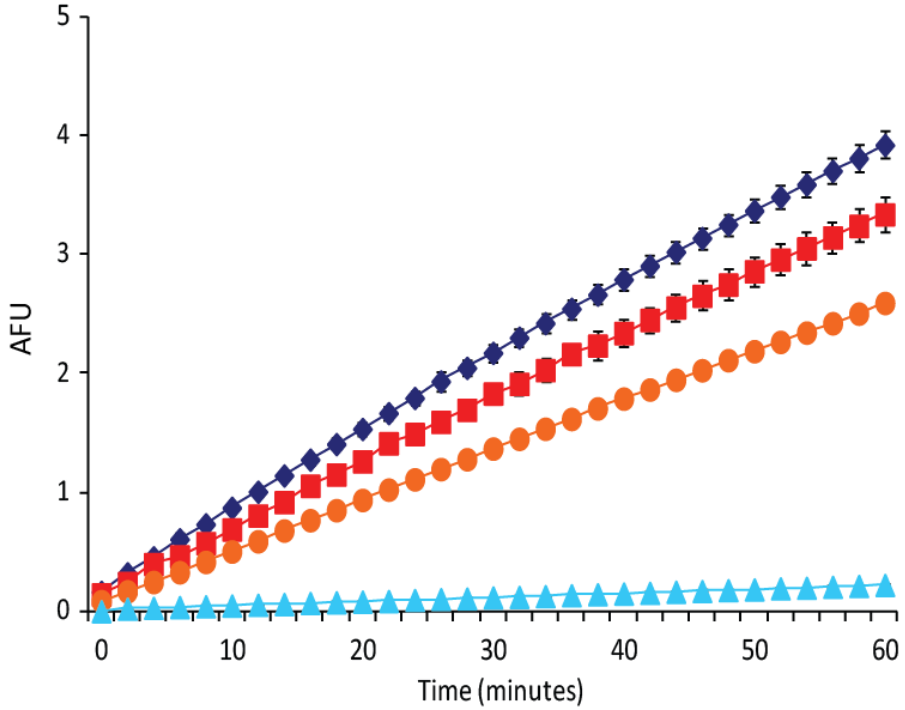
(d) Inhibition of catalytic activity normalised to the DMSO treatment is indicated for SAHA and proteasome inhibitor treatment of MYLA cell lines under non-targeting (NT) or HR23B siRNA conditions (* significance in two-tailed Student's t test; * $P < 0.005$, n=3, error bars = SD).

When the same experiment was performed in A2058 cells (figure 4.3), there was reduced catalytic activity when cells were treated with non-targeting siRNA at both 10 μM and 30 μM concentrations of SAHA but the differences were not statistically significant. The same experiment in A375 cells revealed no difference in catalytic activity between cell treated with non-targeting siRNA and HR23B siRNA (data not shown).

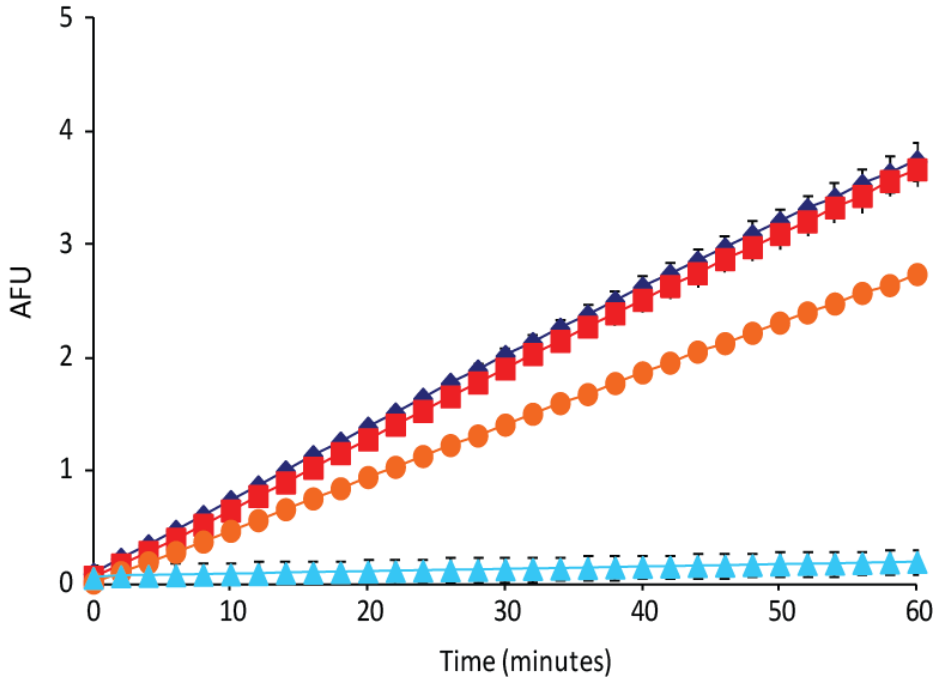
a


NT HR23B
HR23B
Actin

b


AFU
Time (minutes)
0
1
2
3
4
5
0
10
20
30
40
50
60

c


AFU
Time (minutes)
0
1
2
3
4
5
0
10
20
30
40
50
60

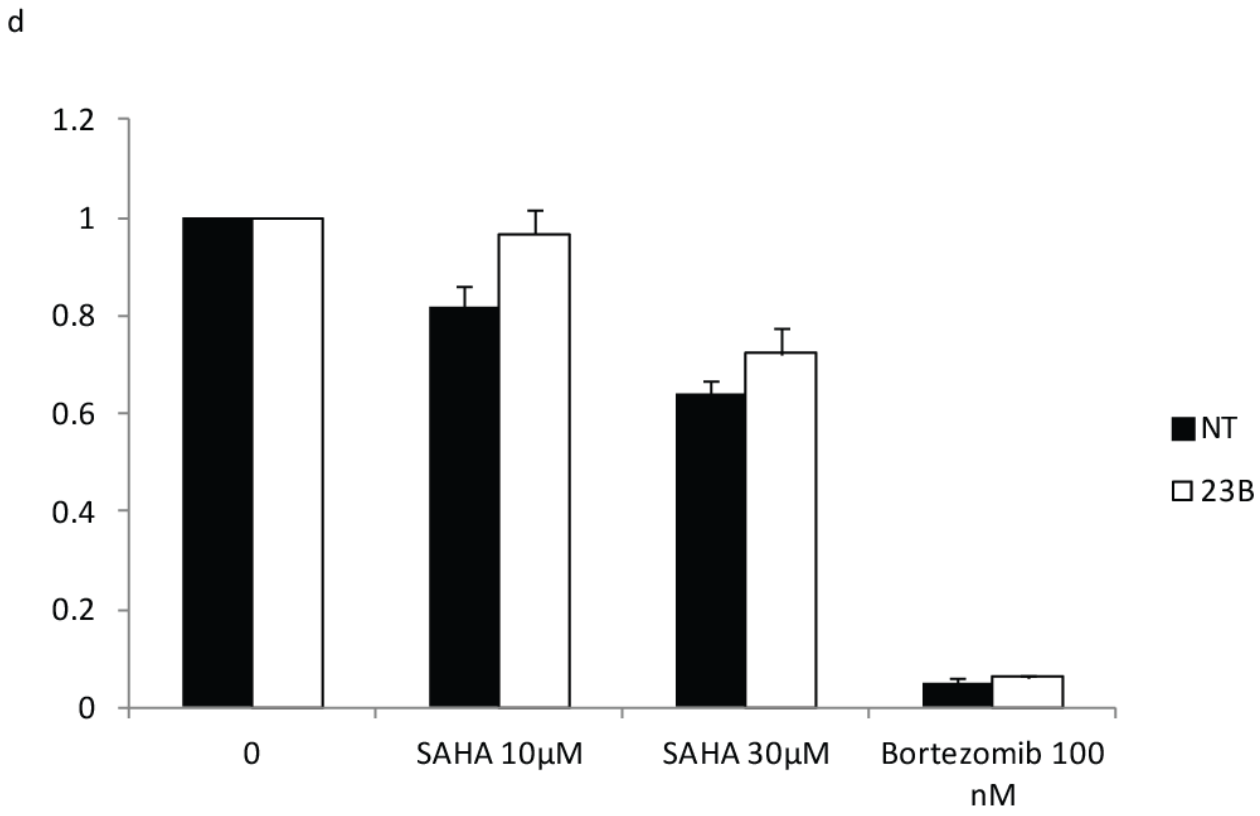


Figure 4.3

Effect of depleting HR23B on proteasome activity in A2058 cells

(a) Immunoblot showing the expression of HR23B, with actin as a loading control, for the experiments in (b) and (c).

A2058 cells were treated with non-targeting (b) or HR23B siRNA (c) for 48h followed by a subsequent 24h treatment with DMSO (blue), SAHA 10µM (red), SAHA 30µM (orange) or bortezomib 100nM (cyan) and harvested at 24h. Cleaved substrate representative of active proteasome was measured at 2 min intervals for 60 min (experiment performed in triplicate, error bars = SD).

(d) Inhibition of catalytic activity normalised to the DMSO treatment is indicated for SAHA and proteasome inhibitor treatment of A2058 cell lines under non-targeting (NT) or HR23B siRNA conditions (not statistically significant in two-tailed Student's t test; n=3, error bars = SD).

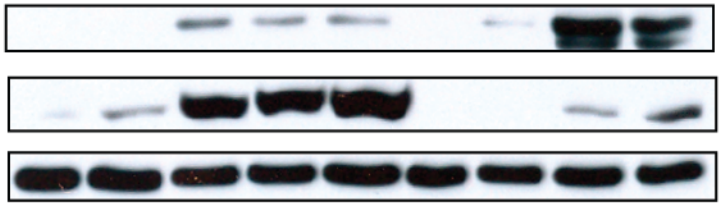
In GFPu1 HEK293 cells, GFP is targeted to the proteasome for degradation via a Ch1 degron sequence which is a proteasome targeting sequence (Gilon et al., 1998), and thus the level of GFP provides a surrogate and independent measure of proteasome activity (Bence et al., 2001). In previous studies treating GFPu1 HEK293 cells with SAHA caused an increase in the level of GFP which does not result from increased RNA levels (Fotheringham et al., 2009a), indicating that proteasome activity is under aberrant control in SAHA-treated cells. As expected, bortezomib treatment led to a decrease in proteasome activity, reflected in the coincident increase in the level of the GFP protein (figure 4.4a). Although the effect of SAHA on GFP levels was less marked than that observed for bortezomib, there was nevertheless an inhibitory effect on proteasome activity which was dose-dependent (figure 4.4a).

At a concentration of 10nM, combining bortezomib with SAHA resulted in a greater than additive effect on proteasome inhibition, reflected by the increased level of GFP (figures 4.4b). When GFPu1 was transiently transfected into A2058 cells, GFP expression increased when cells were treated with bortezomib at a similar level to transfected controls and absent in untreated conditions (figure 4.4c). Interestingly, when GFPu1 transfected A2058 cells were treated with a combination of SAHA and bortezomib, there appeared to be a dose-dependent and synergistic increase in GFP expression (figure 4.4d). This suggests that the effects seen in a stably transfected cell line (HEK293-GFPu1), when compared to another tumour type, namely melanoma, can be reproduced in conditions of transient GFPu1 transient transfection.

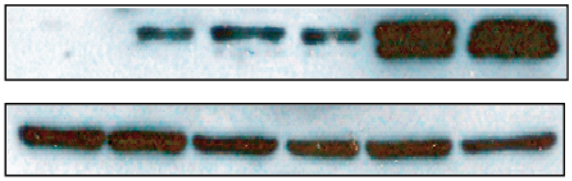
Further, in conditions where endogenous HR23B was depleted with siRNA in HEK293 cells (figure 4.4e), proteasome inhibition was less apparent under combined treatment conditions

(GFP levels reduced by about 50%; figure 4.4f and 4.4g). These results therefore support the hypothesis that the apoptotic effects of HDAC and proteasome inhibitors are at least partially mediated via the proteasome, and further suggest that HR23B levels impact on proteasome activity in treated cells.

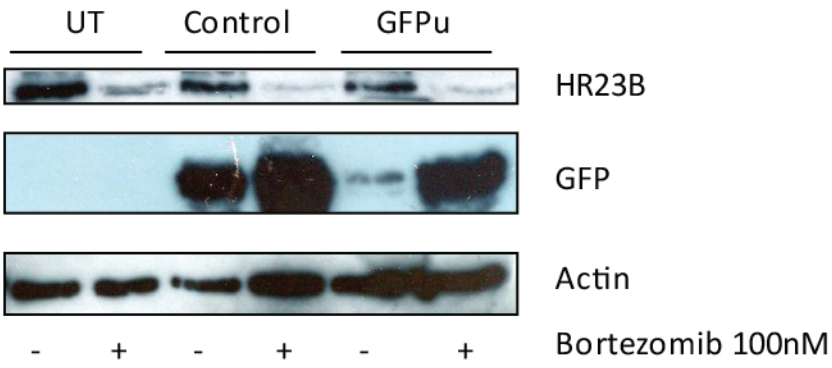
a


GFP
Ac H3
Actin
0 3 10 30 100 – – – –
[SAHA] μM
0 – – – – 3 10 30 100

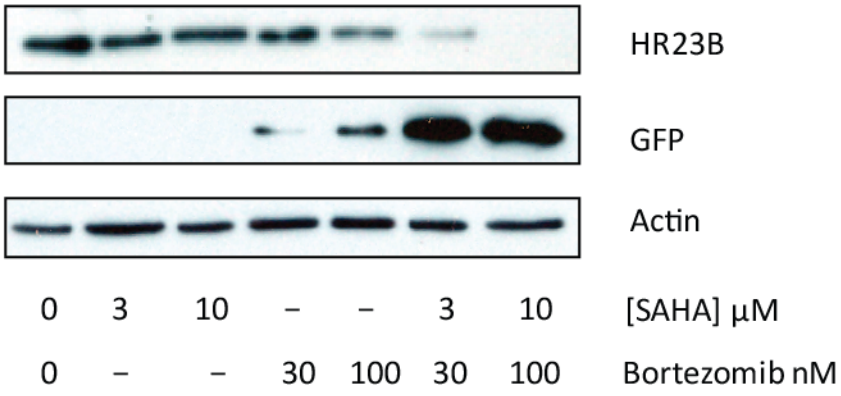
b


GFP
Actin
0 30 100 - 30 100
[SAHA] μM
0 – – + + +
Bortezomib 10nM

c


UT
Control
GFPu
HR23B
GFP
Actin
- + - + - +
Bortezomib 100nM

d


HR23B
GFP
Actin
0 3 10 – – 3 10
[SAHA] μM
0 – – 30 100 30 100
Bortezomib nM

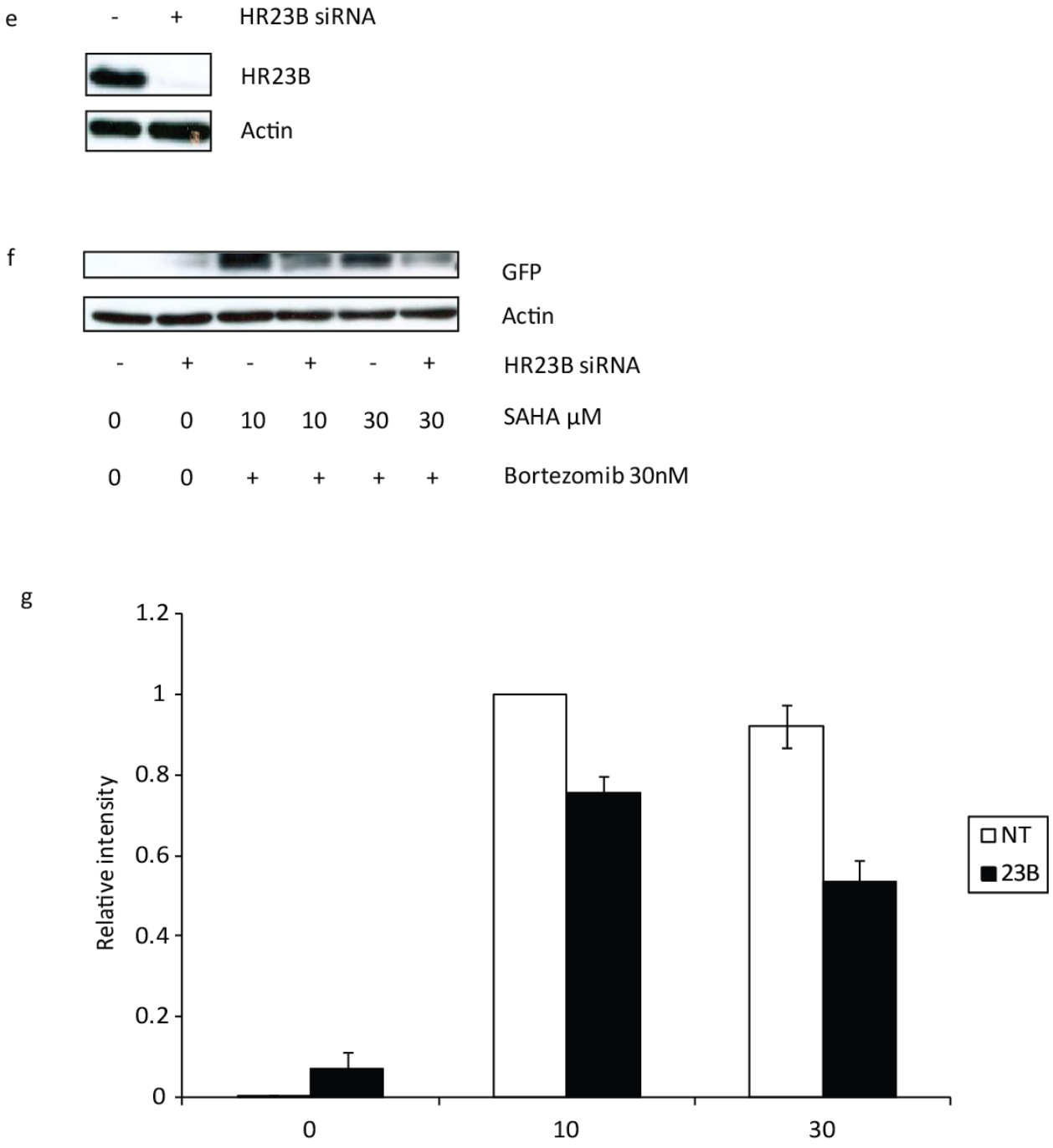


Figure 4.4

Measuring proteasome function after HDAC inhibitor, proteasome inhibitor or combination treatment using GFPu1 cells and cells transiently transfected with GFPu1

(a) Immunoblot showing the level of GFP protein, with actin as a loading control. GFPu1 cells were either untreated (-) or treated with increasing concentrations of SAHA or

bortezomib as indicated for 48h. Acetylated H3 (AcH3) is shown for comparison. The example shown is representative of three independent experiments.

(b) Immunoblot showing the expression of GFP, with actin as a loading control. GFPu1 cells were either untreated (-) or treated with the indicated concentrations of SAHA (μM) combined with bortezomib as indicated for 48h. The example shown is representative of three independent experiments.

(c) Immunoblot showing the expression of GFP and HR23B, with actin as loading control in A208 cells transiently transfected with GFP and GFPu1 followed by treatment with bortezomib as indicated for 24 hours. Untransfected (UT) cells are shown for comparison.

(d) Immunoblot showing the expression of GFP and HR23B, with actin as loading control in A2058 cells transiently transfected with GFPu1 followed by treatment with SAHA, bortezomib or a combination as indicated for 24h. The example shown is representative of three independent experiments.

(e) Immunoblot showing the level of HR23B in GFPu1 cells treated as described in (e).

(f) Immunoblot showing the expression of GFP, with actin as a loading control. HEK293 GFPu1 cells were either treated with NT (−) or HR23B (+) siRNA for 48h followed by a subsequent 48h treatment with DMSO or medium containing bortezomib (in nM), SAHA (in μM) or both drugs in combination as indicated. The example shown is representative of three different experiments.

(g) Graphical representation of GFP levels in (e) after quantitation; the level of GFP is shown by the bars in cells treated with control (clear) or HR23B (black) siRNA. (n=3, error bars = SD).

4.3. A reduction in HR23B protein levels rescues both HDAC inhibitor- and proteasome inhibitor-mediated apoptosis

The proteasome is becoming increasingly recognised as a viable cancer target, and a variety of small molecule drugs that interfere with proteasome activity are either in development or already approved for clinical use. In a similar way to HDAC inhibitors, proteasome inhibitors cause profound apoptosis in tumour cells. Since HR23B is likely to be responsible for the altered proteasome activity observed in HDAC inhibitor treated cells, this would suggest that HR23B might also influence the sensitivity of cells to proteasome inhibitors. Indeed, HR23B siRNA significantly reduced the level of apoptosis induced by the proteasome inhibitor bortezomib (Figure 4.5b). Furthermore, HR23B was induced upon treating tumour cells with bortezomib (Figure 4.5c), where it reached similar levels to that seen in cells treated with HDAC inhibitors (figure 3.5). HR23B may therefore be functionally important in mediating cell sensitivity to both HDAC and proteasome inhibitors.

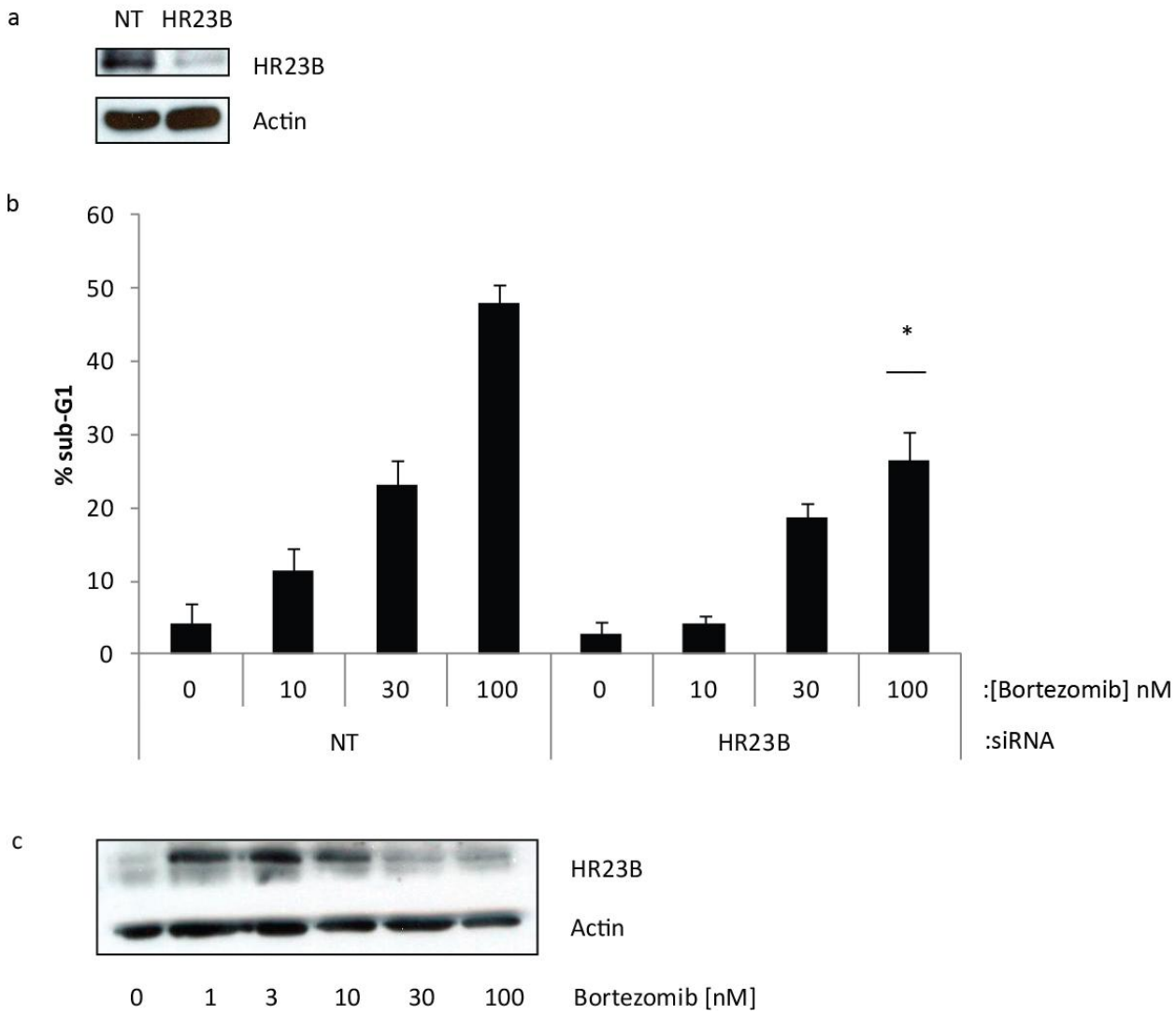


Figure 4.5

Effects of bortezomib treatment on HR23B expression in A2058 melanoma cells and impact of depletion of HR23B on apoptosis

(a) Immunoblot showing the expression of HR23B, with actin as a loading control, for the experiment in (b)

(b) The levels of sub-G1 in A2058 cells determined by FACS after treatment with HR23B siRNA or non-targeting control (NT) siRNA for 48h followed by treatment with DMSO

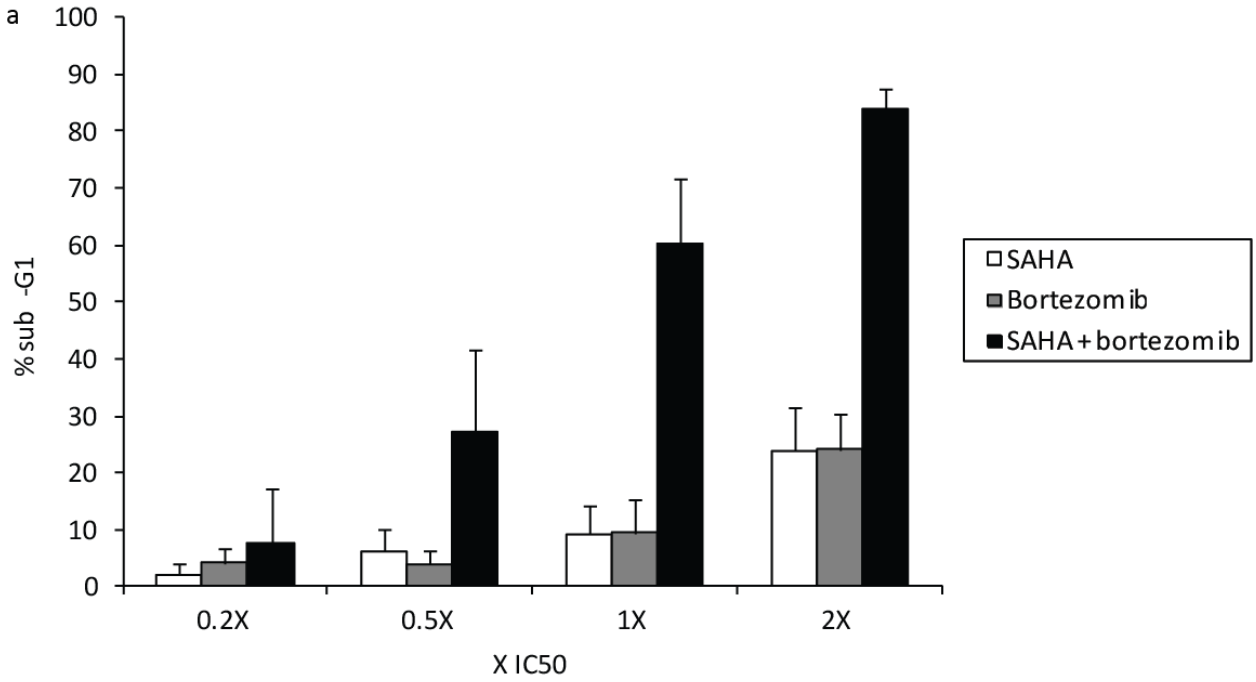
control or increasing concentrations of bortezomib (nM) as indicated for 48h (* significance in two-tailed Student's t test; *P < 0.05; n=3, error bars = SD).

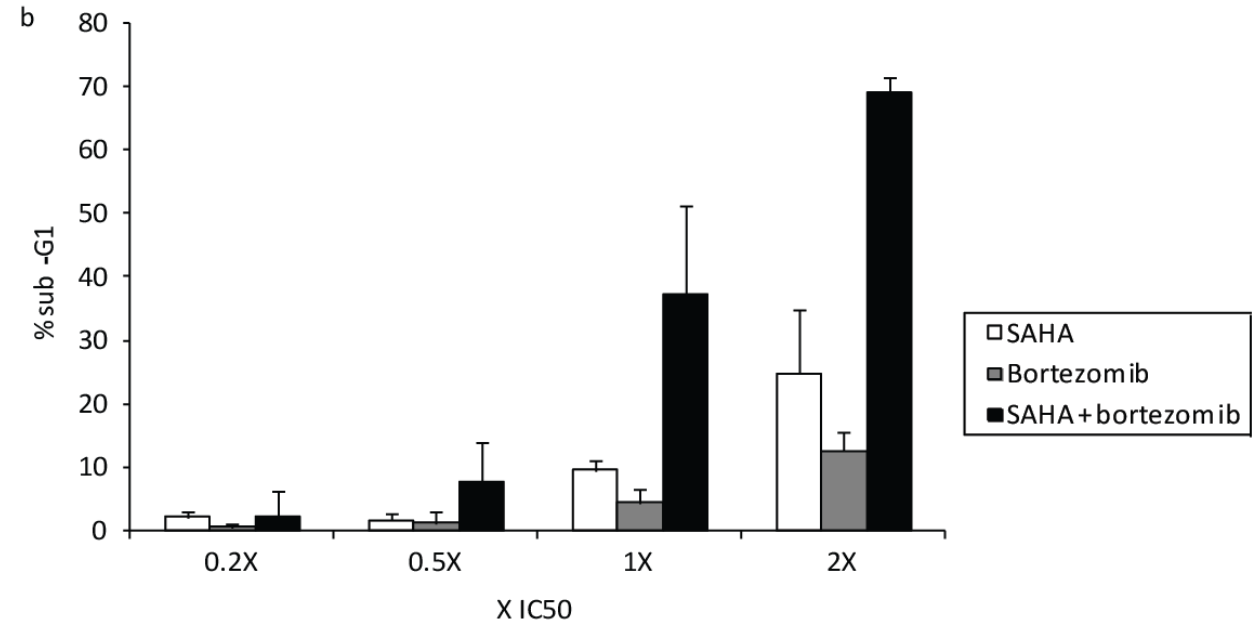
(c) Immunoblots showing protein levels of HR23B in the melanoma cell line A2058 treated with the indicated dose of bortezomib (nM) for 48h. Actin (loading control) is shown for comparison. The example shown is representative of three different experiments.

4.4. HDAC inhibitor and proteasome inhibitors synergize at low concentrations to cause similar levels of apoptosis as at higher concentrations of single inhibitor treatment

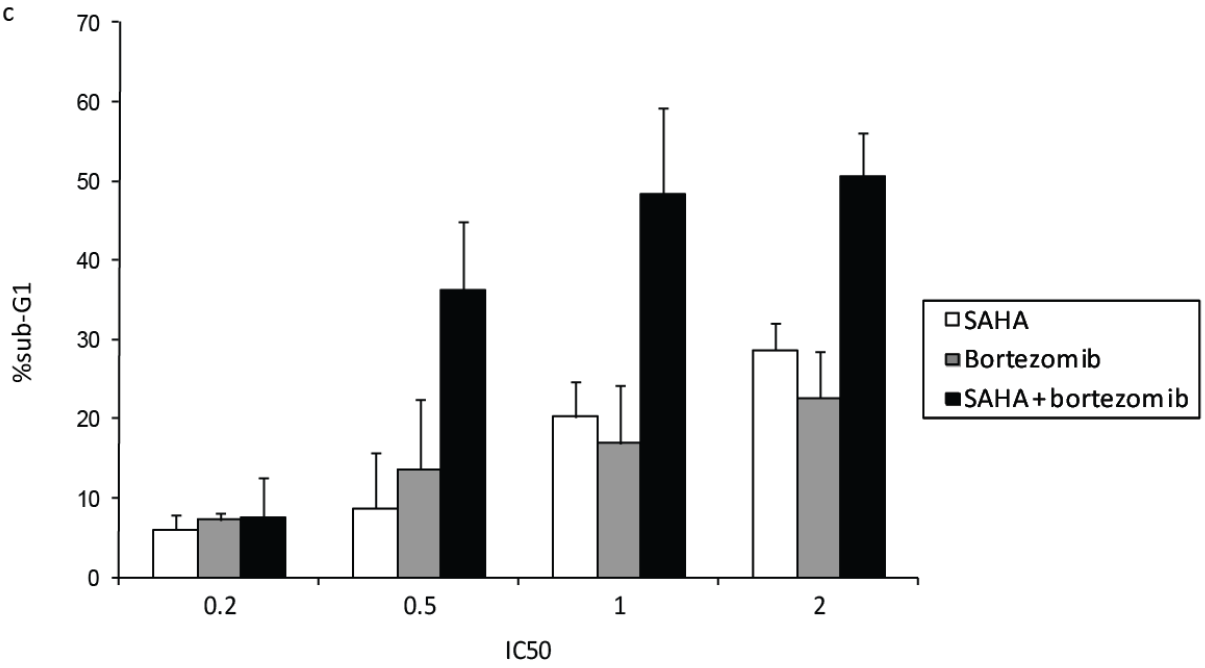
The effects of combining different doses of HDAC and proteasome inhibitor on apoptosis were investigated in MYLA, A2058 and A375 cells. Each inhibitor was combined at concentrations lower than those required to elicit 50% of maximal sub-G1 (IC_{50} for apoptosis) to both SAHA and bortezomib in order to discover whether use of these compounds at suboptimal concentrations in combination may cause similar effects to their use alone.

This resulted in increased levels of apoptosis (figures 4.6a-c). In MYLA cells the outcome appeared to be additive but in A2058 and A375 cells, the combination appeared to be synergistic especially at 0.5X and 1X the IC_{50} for each individual drug. Indeed, even after 24h treatment with the combination, there was a very marked increase in sub-G1 apoptotic cell population (data not shown). This phenomenon was also observed when valproic acid and bortezomib were combined in A2058 cells although the combination seemed to be additive (figure 4.6d).


a
100
90
80
70
60
50
40
30
20
10
0
% sub -G1
0.2X
0.5X
1X
2X
X IC50
SAHA
Bortezomib
SAHA + bortezomib


b
80
70
60
50
40
30
20
10
0
% sub -G1
0.2X
0.5X
1X
2X
X IC50
SAHA
Bortezomib
SAHA + bortezomib

c


70
60
50
40
30
20
10
0
%sub-G1
0.2
0.5
1
2
IC50
SAHA
Bortezomib
SAHA+bortezomib

d

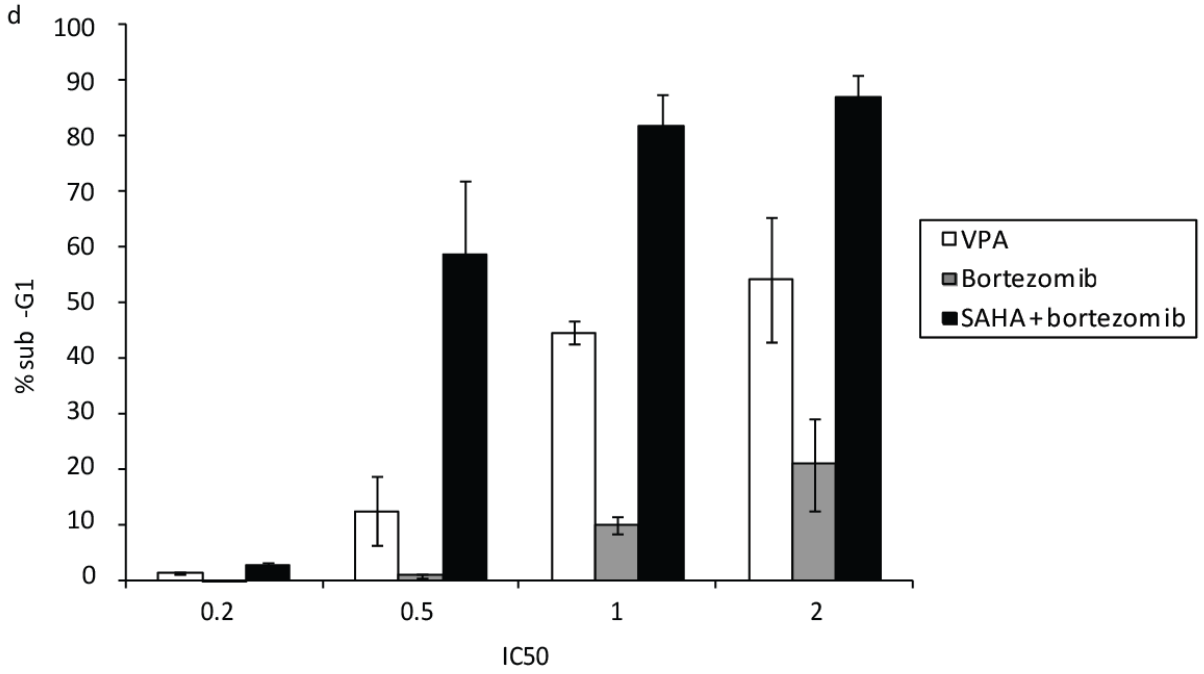

100
90
80
70
60
50
40
30
20
10
0
% sub -G1
0.2
0.5
1
2
IC50
VPA
Bortezomib
SAHA+bortezomib

Figure 4.6

Effects of combining SAHA and bortezomib on apoptosis in different cell lines

(a) The levels of sub-G1 cells determined by FACS after treating A2058 cells with increasing concentrations of SAHA (clear) and bortezomib (grey) [0.2, 0.5, 1, and 2× IC50 (1× IC50 = 10 μM SAHA and 50 nM bortezomib)] or a combination (black) for 48 h (n = 3; error bars, SD).

(b) The levels of sub-G1 cells determined by FACS after treating A375 cells with increasing concentrations of SAHA (clear) and bortezomib (grey) [0.2, 0.5, 1, and 2× IC50 (1× IC50 = 3 μM SAHA and 20 nM bortezomib)] or a combination (black) for 48 h (n = 3; error bars, SD).

(c) The levels of sub-G1 cells determined by FACS after treating MYLA cells with increasing concentrations of SAHA (clear) and bortezomib (grey) [0.2, 0.5, 1, and 2× IC50 (1× IC50 = 5 μM SAHA and 50 nM bortezomib)] or a combination (black) for 48 h (n = 3; error bars, SD).

(d) The levels of sub-G1 cells determined by FACS after treating A2058 cells with increasing concentrations of VPA (clear) and bortezomib (grey) [0.2, 0.5, 1, and 2× IC50 (1× IC50 = 5 mM VPA and 50 nM bortezomib)] or a combination (black) for 48 h (n = 3; error bars, SD).

When the effects of combination treatment on HR23B protein levels were investigated, at concentrations where synergy was observed, HR23B protein levels actually decreased significantly (Figure 4.7a, 4.7b). This effect was also seen to a lesser extent with either SAHA or bortezomib treatment alone at the highest concentrations. It was also apparent in both MYLA

and A2058 cells. This could be a result of HR23B becoming insoluble or the fact that only cells highly resistant to apoptosis remain viable and their expression of HR23B might be low or absent. It also raises the possibility that the basal levels of HR23B may be more important in terms of cellular responses to these compounds rather than the protein levels induced by treatment as discussed in chapter 3. There also appeared to be a greater than additive effect on acetylated histone H3 protein levels in both cell lines when SAHA and bortezomib treatment were combined. PARP cleavage was also evident with increasing concentrations of either SAHA or bortezomib and both in combination in MYLA cells (figure 4.7b) with a greater than additive effect seen at 0.5X IC50 of both drugs combined. This reflected the increased percentage of cells in sub-G1 seen at these combination concentrations in MYLA cells (figure 4.6c).

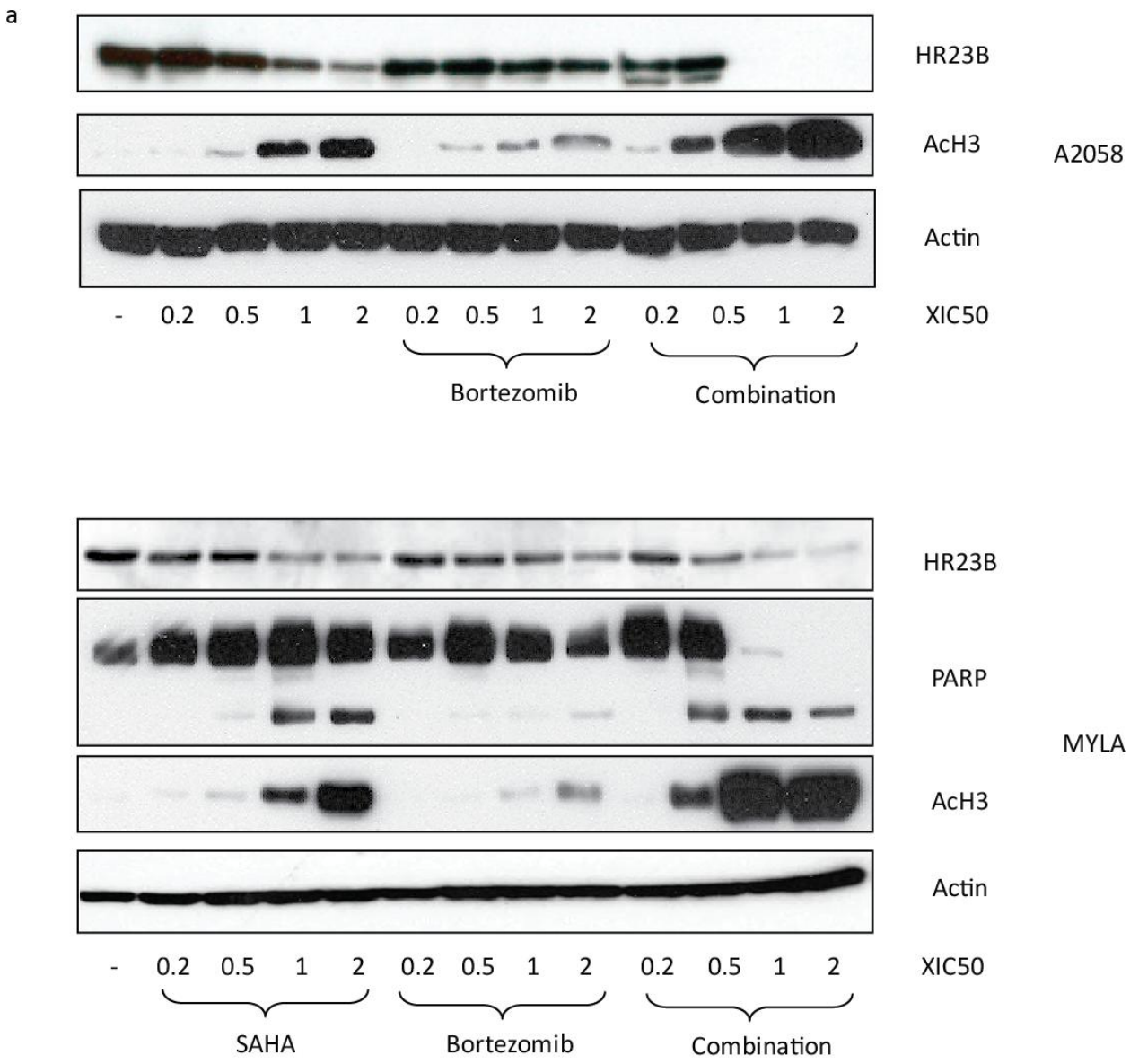


Figure 4.7

Effects of combination dosing of SAHA and bortezomib on HR23B, PARP and acetylated histone H3 expression

(a) Immunoblot showing effects of treatment with SAHA, bortezomib and combination of both on expression of HR23B, acetylated histone H3 (AcH3) in A2058 cells with actin as loading control. A2058 cells were with increasing concentrations of SAHA and

bortezomib [0.2, 0.5, 1, and 2× IC50 (1× IC50 = 10 μM SAHA and 50 nM bortezomib)] or a combination for 48 h. Immunoblot shown is representative of 3 experiments.

(b) Immunoblot showing effects of treatment with SAHA, bortezomib and combination of both on expression of HR23B, PARP, acetylated histone H3 (AcH3) in MYLA cells with actin as loading control. MYLA cells were with increasing concentrations of SAHA and bortezomib [0.2, 0.5, 1, and 2× IC50 (1× IC50 = 5 μM SAHA and 50 nM bortezomib)] or a combination for 48 h. Immunoblot shown is representative of 3 experiments.

The sequence of combining SAHA and bortezomib was investigated by treating A2058 cells with 24 hours of SAHA followed by 24 hours bortezomib in combination at 0.5X the IC_{50} for apoptosis for each individual drug and the reverse as well as combining both drugs for 48 hours (figure 4.8). Interestingly, pre-treatment with SAHA appeared to result in significantly more apoptosis than pre-treatment with bortezomib. In fact, if cells were pre-treated with bortezomib the effects of the combination treatment were not even additive. This suggests that SAHA somehow sensitises cells to induction of apoptosis by bortezomib and informs on optimal sequencing of both these agents in clinical trials.

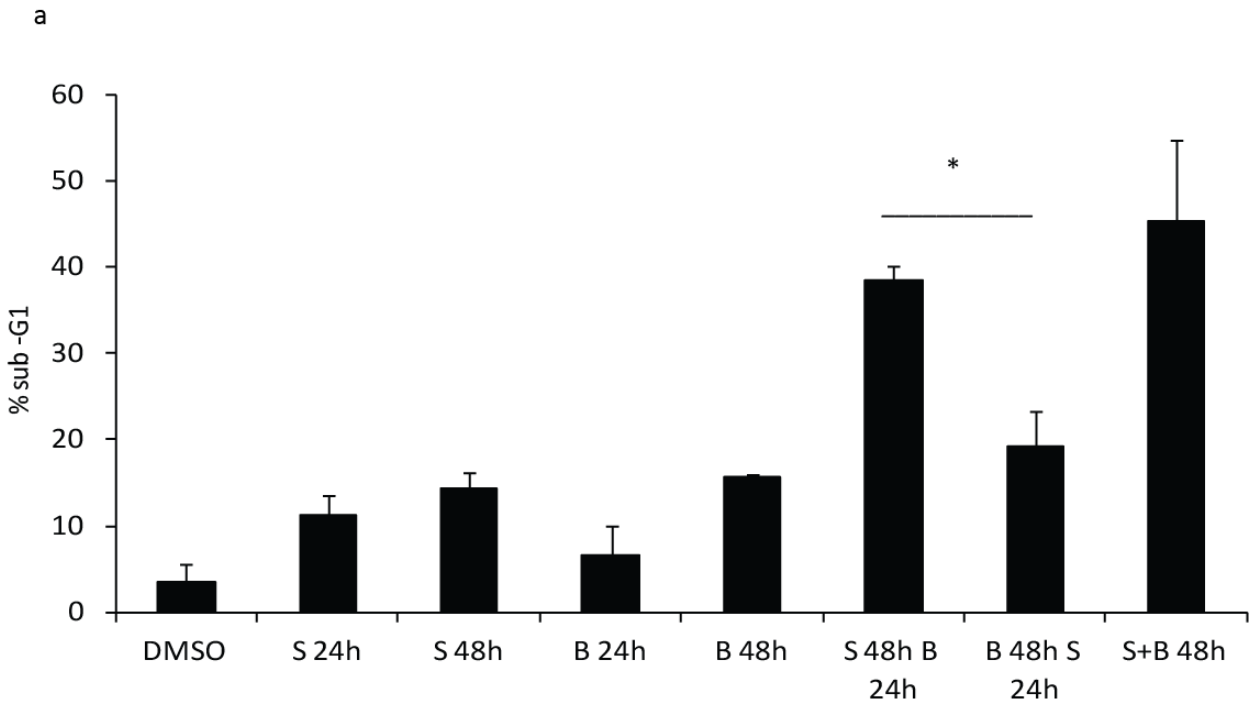


Figure 4.8

Effects of sequential and concurrent combination dosing of SAHA and bortezomib on apoptosis

The levels of sub-G1 cells determined by FACS after treating A2058 cells with either SAHA (S) or bortezomib (B) alone or in combination concurrently or sequentially as indicated at 0.5X IC_{50} for 24h or 48h (* significance in two-tailed Student's t test; * $P < 0.05$, n=3, error bars = SD).

To assess whether HR23B is a sensitivity determinant for the combined treatment, HR23B was depleted using siRNA followed by treatment with the combination of HDAC inhibitor and proteasome inhibitor at 1X IC_{50} for both drugs in A2058 cells (figure 4.9a,b). This resulted in a significantly reduced percentage of cells in the sub-G1 phase when the drugs were combined and HR23B was depleted (figure 4.9c). Surprisingly there was no difference seen in the percentage of cells in the sub-G1 phase of the cell cycle in the experiment where cells were treated with HDAC inhibitor alone when the non-targeted control treatment was compared with HR23B-depleted cells. The likeliest explanation for this is that cells in this particular experiment were treated at

different doses of HDAC inhibitor when compared to experiments where differences in the sub-G1 population were seen (figure 3.9, pg 100-101).

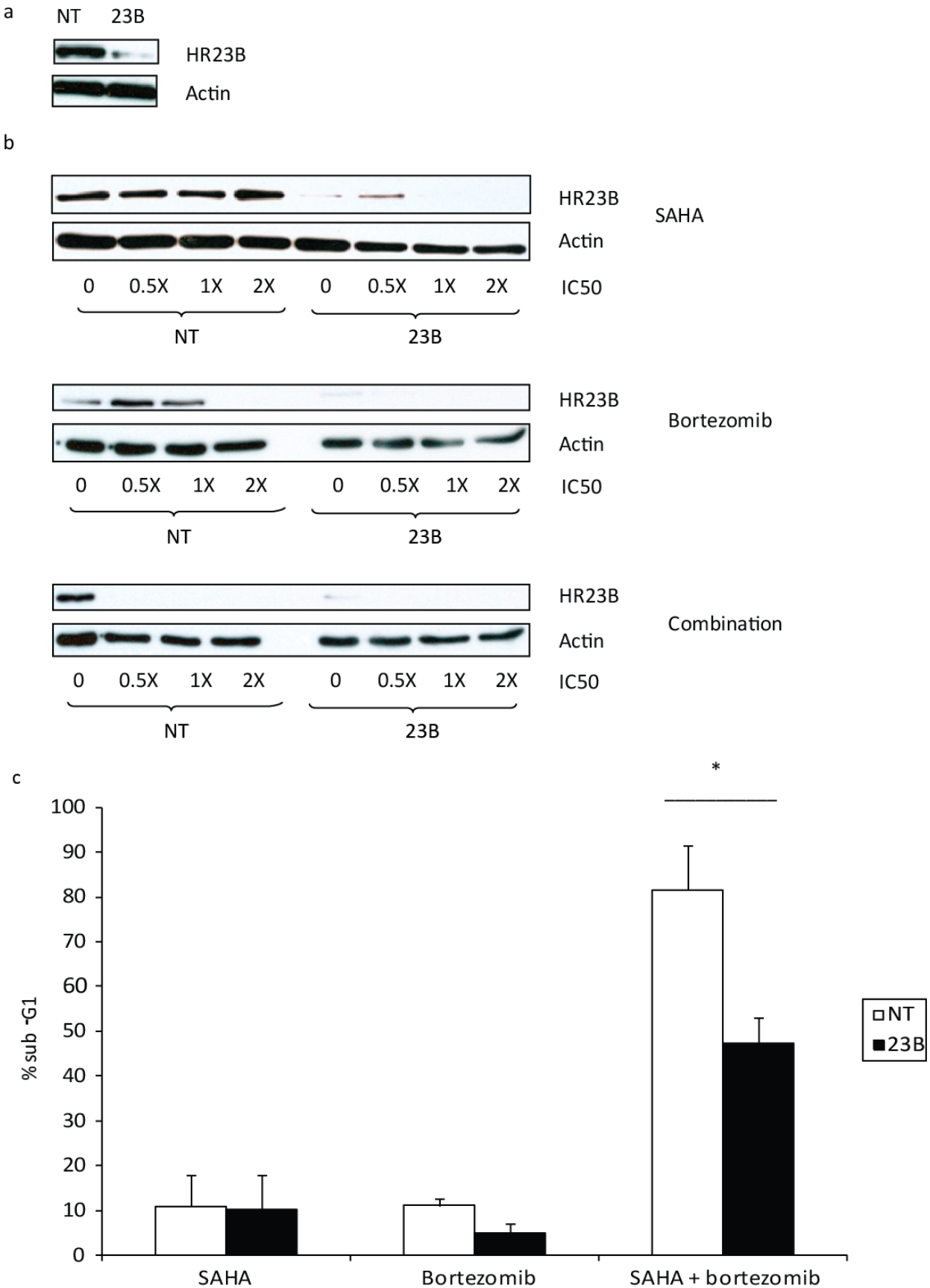

a
NT
23B
HR23B
Actin
b
HR23B
Actin
SAHA
0
0.5X
1X
2X
0
0.5X
1X
2X
IC50
NT
23B
HR23B
Actin
Bortezomib
IC50
NT
23B
HR23B
Actin
Combination
IC50
NT
23B
c
*
% sub -G1
100
90
80
70
60
50
40
30
20
10
0
NT
23B
SAHA
Bortezomib
SAHA + bortezomib

Figure 4.9

Effects of depletion of HR23B on apoptosis induced by SAHA and bortezomib in combination

a) Immunoblot showing the expression of HR23B, with actin as a loading control, for the experiment in (c).
b) Immunoblots showing the expression of HR23B with SAHA, bortezomib and combination treatment at varying concentrations as indicated, with actin as a loading control. The example shown is representative of three different experiments.
c) The levels of sub-G1 A2058 cells determined by FACS after treatment with HR23B siRNA (clear) or non-targeting control (NT: black) siRNA for 48h followed by treatment with SAHA and bortezomib (1x IC50) or a combination for 48h (* significance in two-tailed Student's t-test; * $P < 0.05$, n=3, error bars = SD).

The effect of the combination treatment was also studied in stable inducible HR23B cell lines (figure 4.10a). Ectopic HR23B increased the level of apoptosis in combined SAHA/bortezomib treatment for both drugs (figure 4.10b).

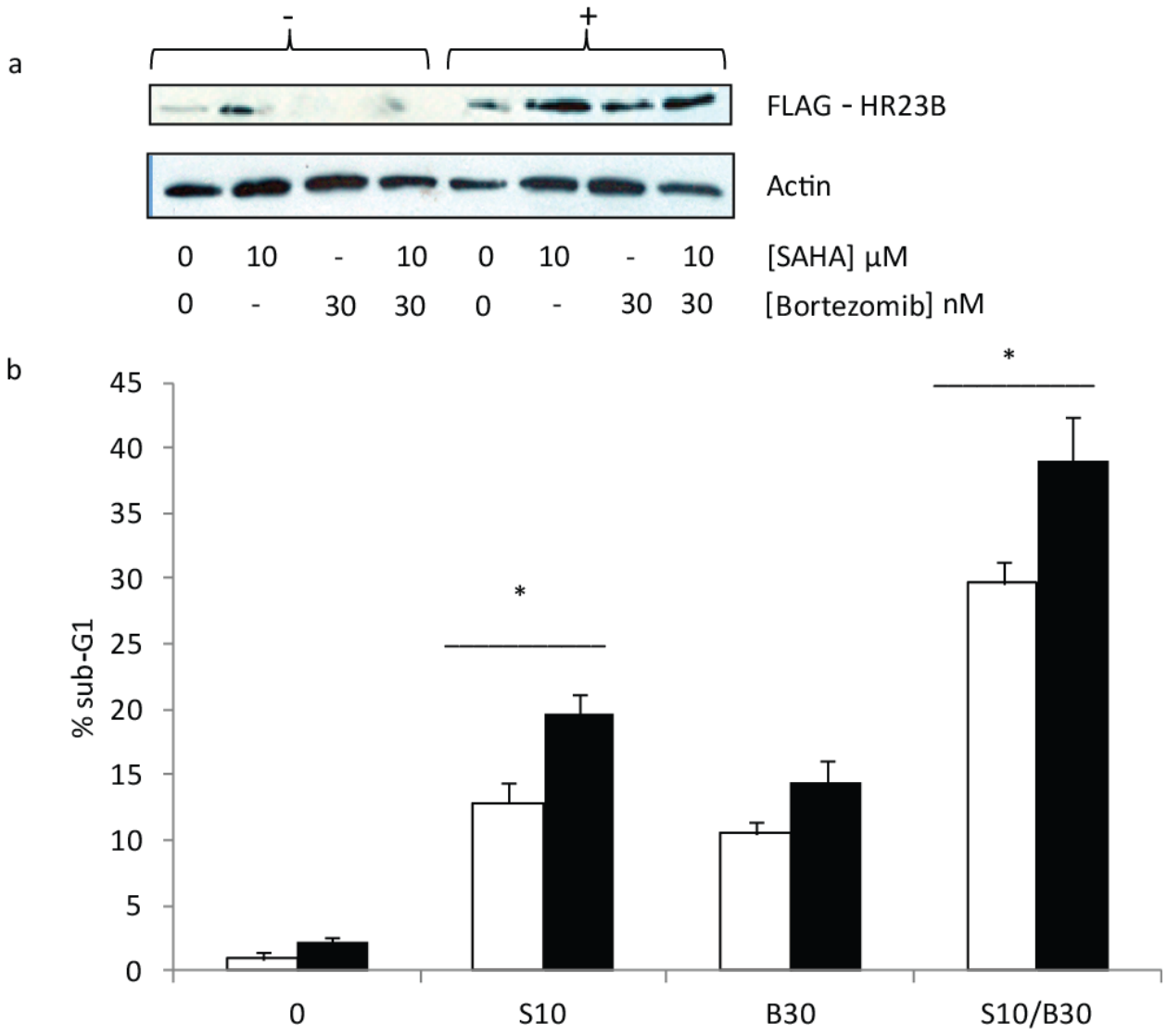


Figure 4.10

Effects of varying levels of HR23B expression on apoptosis induced by SAHA and bortezomib alone and in combination.

a) U2OS cells stably expressing inducible HR23B were either untreated (-) or treated with SAHA, bortezomib and in combination as indicated (in µM for SAHA and nM for bortezomib for 24h) under non-induced (-) or induced (+) doxycycline (dox) treatment conditions. Cells were harvested and immunoblotted with (for ectopic HR23B (ant-flag)),

anti-LC3 and anti-actin as indicated. Result shown is representative of three independent experiments

b) The levels of sub-G1 cells determined by FACS in induced (black) or uninduced (white) followed by treatment with SAHA and bortezomib as indicated alone or in combination for 24h (* significance in two-tailed Student's t-test; * $P < 0.05$, n=3, error bars = SD).

The synergy identified between SAHA and bortezomib at low concentrations together with the results from the GFPu1 cell line (Figure 4.3) suggests that these compounds have an inhibitory effect on the proteasome and provides a rational basis for their use in combination for therapeutic purposes.

4.5. Conclusion

The importance of the proteasome in the cellular response to SAHA was confirmed when siRNA mediated loss of HR23B also rescued proteasome inhibitor mediated apoptosis (figure 4.5b). Furthermore, in a functional and a surrogate assay, HDAC inhibitors have been shown to inhibit the proteasome in a dose and time-dependent fashion. Levels of HR23B appear to impact on the degree of proteasome inhibition giving further support to the hypothesis that HDAC inhibitors exert their cellular response, at least in part, via the proteasome (figures 4.2-4.4). The observed additive effects or synergy between these compounds and the possible importance of corresponding HR23B levels (figures 4.6, 4.7, 4.9 and 4.10) may also prove to be interesting in terms of the treatment of patients with these drugs in combination and the potential use of HR23B as a predictive biomarker.

CHAPTER 5

RESULTS

AUTOPHAGY IN HDAC INHIBITOR TREATED CELLS: INTERPLAY BETWEEN HR23B AND HDAC6

5.1. Introduction

Treatment of tumour cells with HDAC inhibitors can result in a number of different outcomes, including apoptosis, senescence, autophagy and cell cycle arrest (Khan and La Thangue, 2012b; Marks, 2010b). Given this variability in cellular response, the value of HR23B as a responsive biomarker would be enhanced if it were to have a role in dictating biological consequence of HDAC inhibitor treatment.

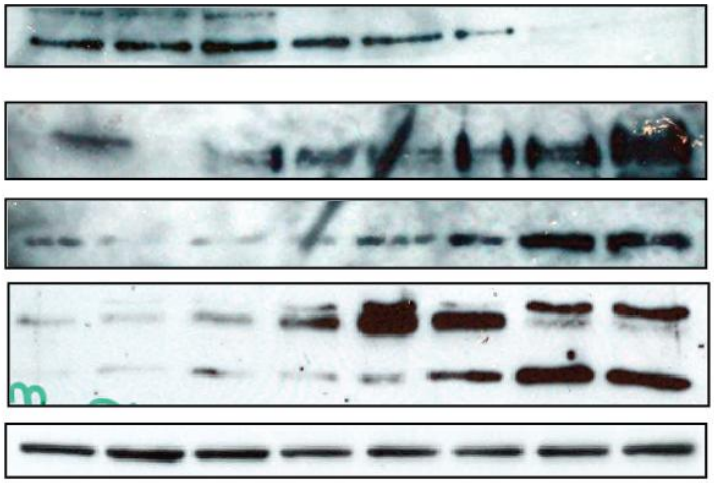
It has been clearly demonstrated that HDAC inhibitors can induce autophagy in cancer cells (Gammoh et al., 2012; Shao et al., 2010). Autophagy is a complex recycling system in which the cell's proteins and organelles are sequestered in autophagosomes and degraded after fusing with lysosomes (Janku et al., 2011a). Autophagy may function as a tumour suppressor pathway by degrading cellular components that are damaged or no longer required. However, once cancer has developed activation of the autophagy pathway may be utilized to generate ATP via protein recycling to overcome metabolic/hypoxic stress and maintain survival. Thus, autophagy may mediate cell death but it may in fact be a mechanism of tumour resistance to HDAC inhibitors.

Chloroquine (CQ) is a weak base that inhibits lysosomal acidification, which prevents the fusion of autophagosomes with lysosomes and subsequent autophagic degradation (Ohkuma and Poole, 1981; Poole and Ohkuma, 1981). HDAC inhibitor-induced apoptosis is enhanced by co-administration with chloroquine in chronic myeloid leukemia cells both *in vitro* and in primary cells from patients (Carew et al., 2008).

5.2. HR23B influences autophagy

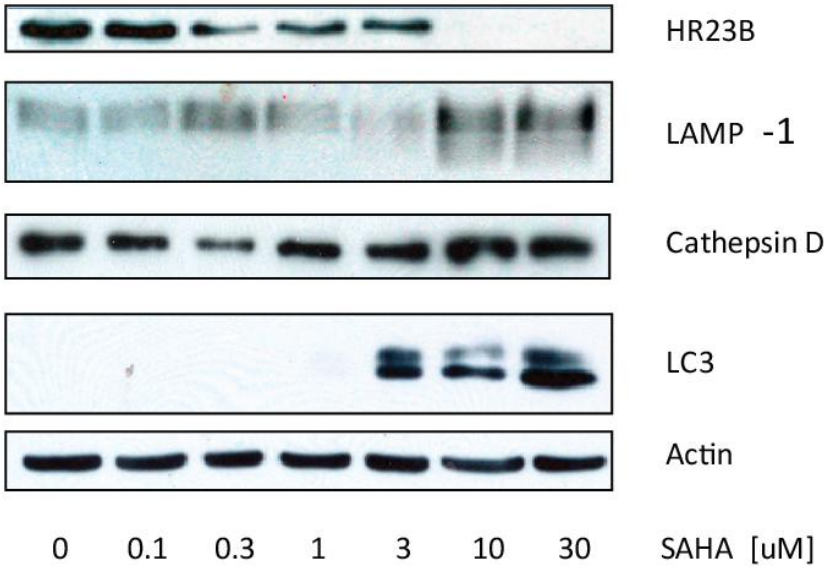
The effects on different autophagy markers of HDAC inhibitor treatment of a number of different cell lines were investigated. HDAC inhibitors caused LC3 cleavage as well as the appearance of LAMP1 and cathepsins D in diverse tumour cell lines such as HCT15, HCT116 (colorectal), A2058 (melanoma) and MYLA (CTCL) (figure 5.1). This phenomenon was observed with other HDAC inhibitors such as valproic acid (figure 5.2).

a



A2058

b



MYLA

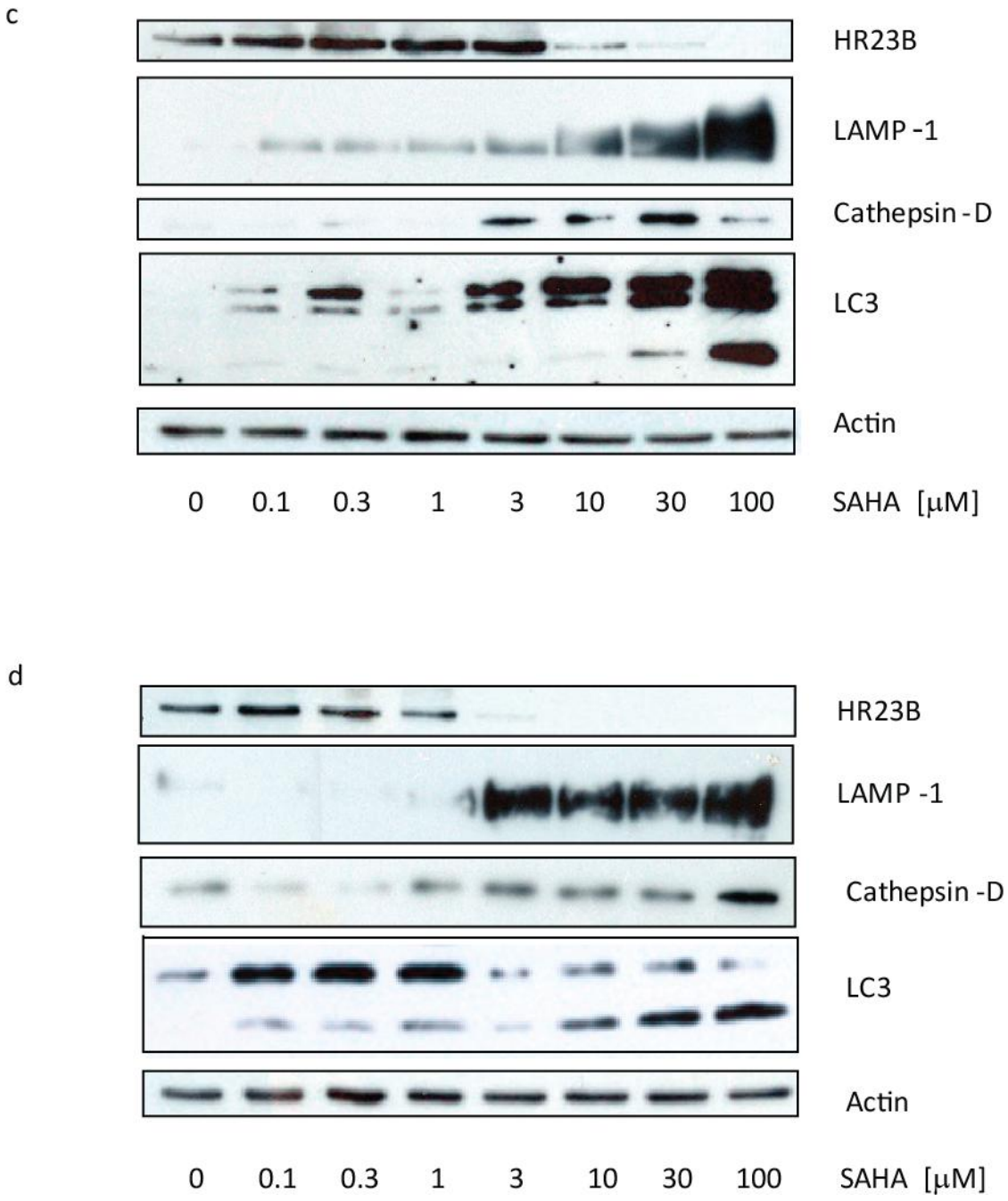


Figure 5.1

Autophagy and HR23B expression in cancer cells treated with HDAC inhibitors

A2058 (a), MYLA (b), HCT15 (c) and HCT116 (d) were each treated with SAHA at the indicated concentrations (μM) for 48h (72h A2058 and MYLA) and harvested and immunoblotted with anti-HR23B, anti-LC3, anti-LAMP-1, anti-cathepsin D and anti-actin

antibodies as indicated. Note the appearance of the cleaved (lower band) form of LC3 and increased overall LC3 level are indicative of autophagy. Immunoblots are representative of at least three independent experiments.

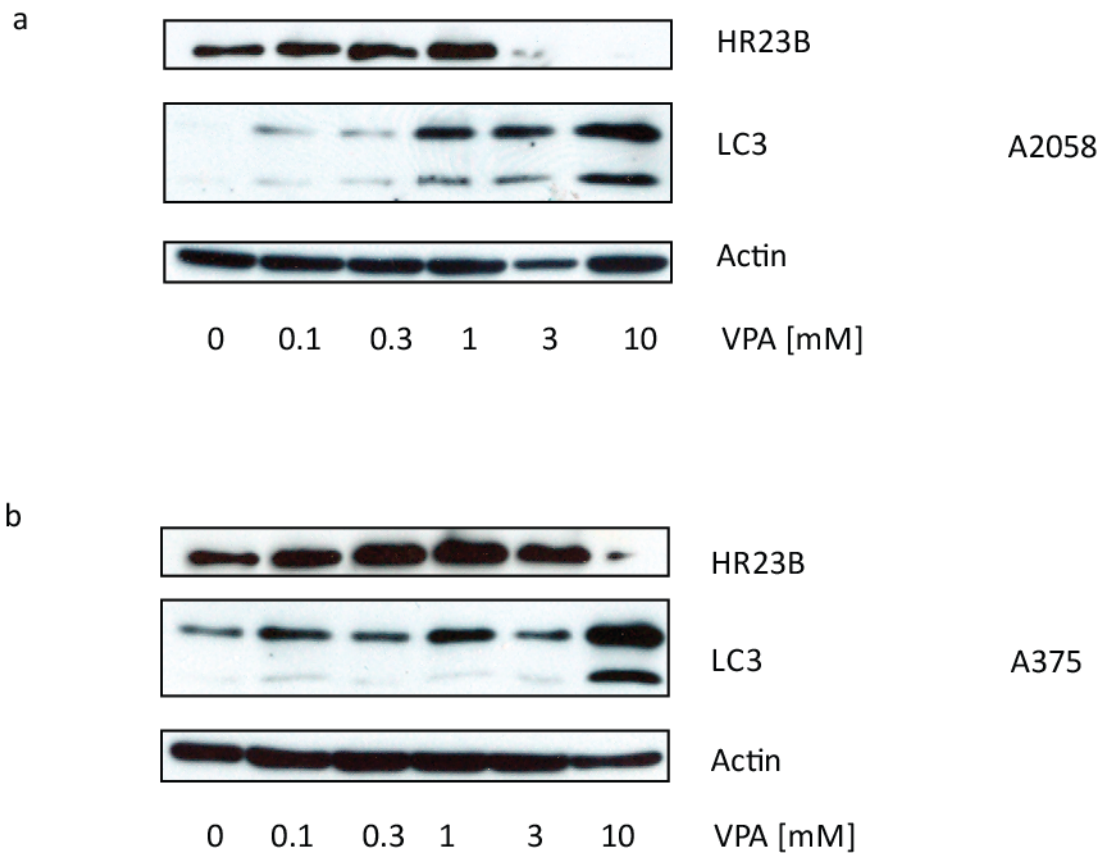


Figure 5.2

Autophagy and HR23B in cells treated with valproic acid

A2058 (a) and A375 (b) were each treated with valproic acid at the indicated concentrations (mM) for 72h and harvested and immunoblotted with anti-HR23B, anti-LC3 and anti-actin antibodies as indicated. Immunoblots are representative of at least three independent experiments.

The increase in autophagy protein markers coincided with the visual appearance of autophagosomes in cells in a variety of different cell lines (figure 5.3). These were represented by a so-called punctate cytoplasmic appearance. In addition to their well-established ability to induce apoptosis, HDAC inhibitors also enhanced autophagy. Interestingly, HR23B expression in U2OS and A2058 cells was not altered after SAHA treatment in these examples but in SAOS2 cells, there was increased cytoplasmic expression. Treatment duration was 24 hours compared to 48 hours in the immunoblotting experiment and this may be the reason why HR23B expression was not altered in the immunofluorescence experiment. The reason for the difference in incubation times was a practical one as at 48 h treatment; there were no adherent cells on the coverslips in the immunofluorescence experiment.

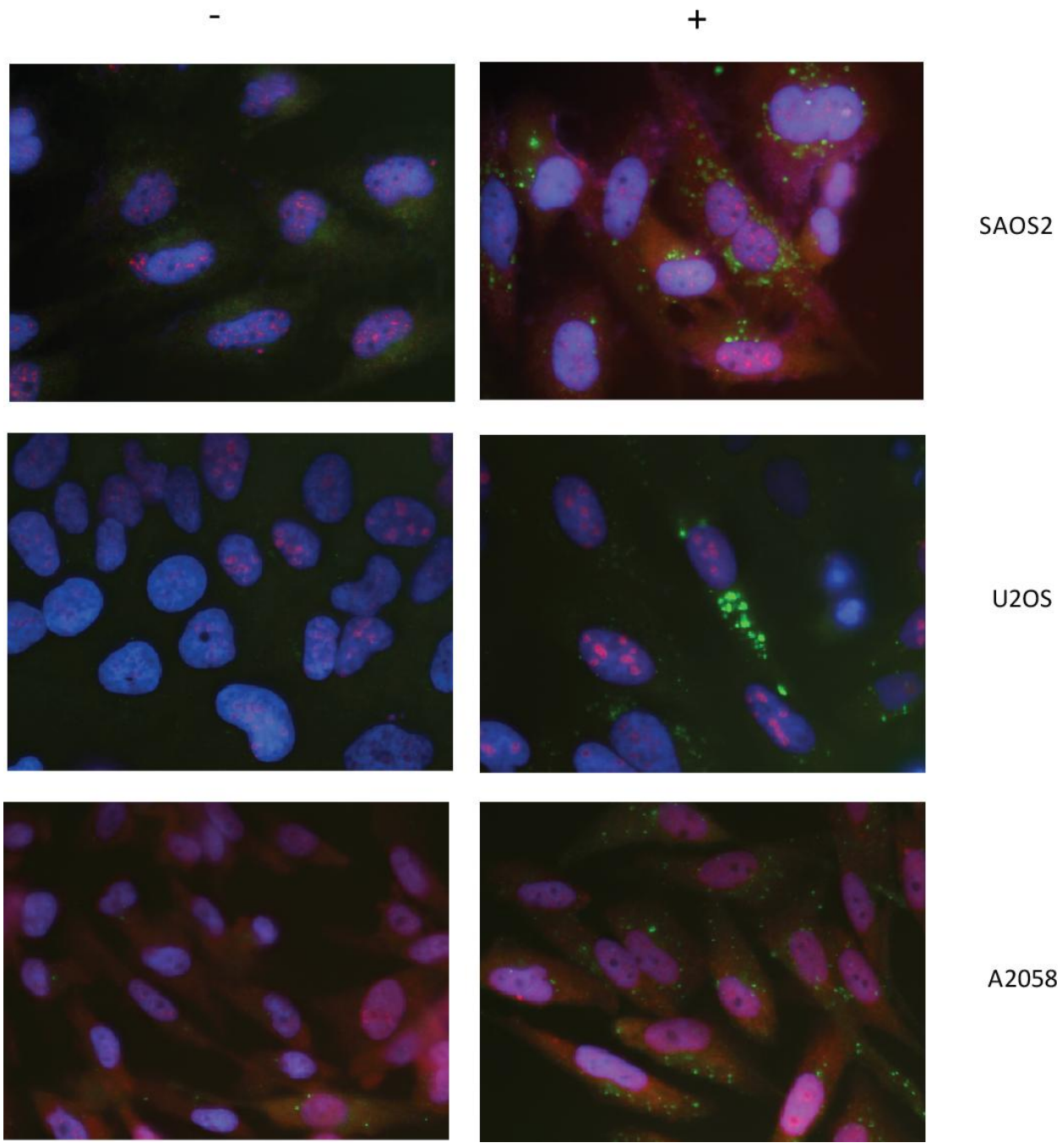


Figure 5.3

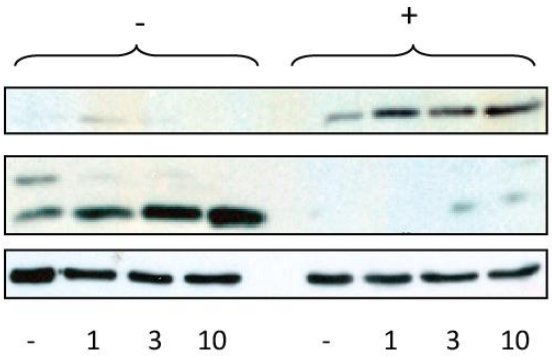
HR23B and LC3 expression using immunofluorescence in cells treated with SAHA

The appearances of autophagosomes in SAOS2, A2058 and U2OS cells treated with DMSO (-) or SAHA at 10μM (+) for 24h is shown by immunostaining (anti-LC3; green, anti-HR23B; red).

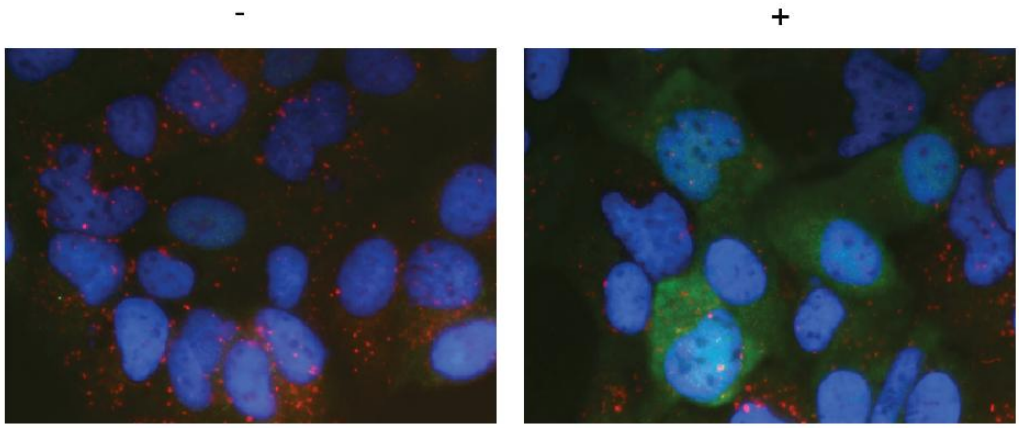
Counterstain with DAPI was superimposed for each image. Experiments were repeated at least three times.

When levels of HR23B were high, via expression of ectopic HR23B in stable cell lines, there were reduced or absent levels of LC3 upon HDAC inhibitor treatment (figure 5.4a). By immunostaining, autophagosomes apparent in SAHA treated cells were less evident when ectopic HR23B was expressed (figure 5.4b). LC3 expression was also virtually undetectable upon ectopic HR23B induction and SAHA treatment when measured using immunoblotting and there was a corresponding increase in cleaved PARP levels (figure 5.4c). Autophagosome expression was quantified and the difference between induced and non-induced conditions was statistically significant with the percentage of cells with autophagosomes significantly lower in conditions of HR23B induction. These phenomena were not observed when cells in which ectopic HR23B was expressed were treated with 5-fluorouracil suggesting that the effect was HDAC inhibitor-specific (figure 5.5).

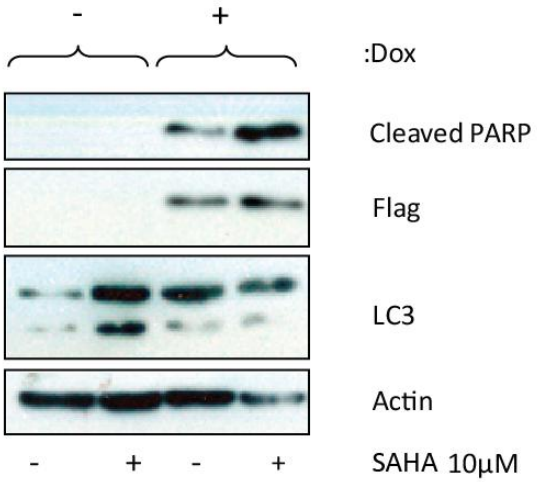
a


-
+
:Dox
Flag - HR23B
LC3
Actin
- 1 3 10 - 1 3 10
[SAHA] μM

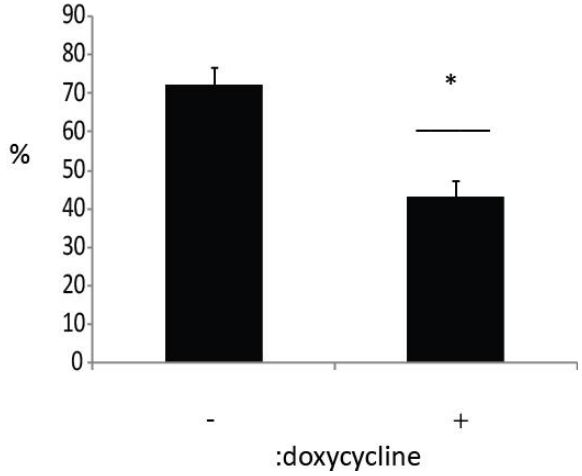
b


-
+

c


-
+
:Dox
Cleaved PARP
Flag
LC3
Actin
- + - +
SAHA 10μM

d


90
80
70
60
50
40
30
20
10
0
%
*
-
+
:doxycycline

d

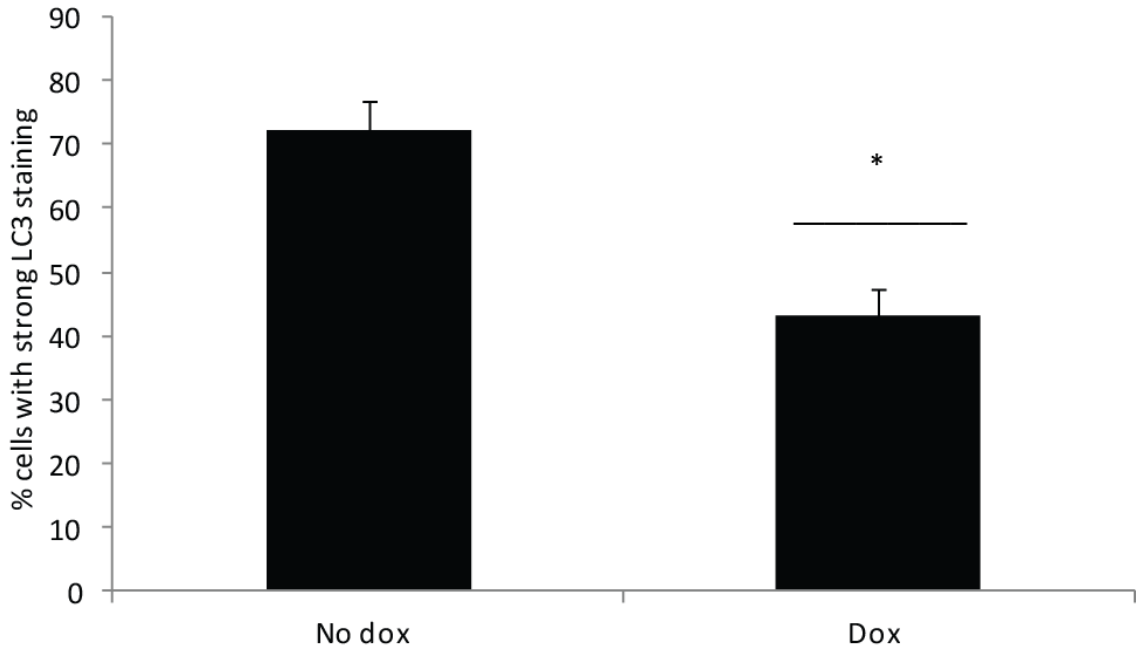


Figure 5.4

Effects of varying levels of HR23B on autophagy and apoptosis after HDAC inhibitor treatment.

(a) U2OS cells stably expressing inducible HR23B were either untreated (-) or treated with SAHA as indicated (in μM for 48h) under non-induced (-) or induced (+) doxycycline (dox) treatment conditions (1μg/ml; induction for 72h). Cells were harvested and immunoblotted with anti-FLAG (for ectopic HR23B), anti-LC3 and anti-actin as indicated. Result shown is representative of three independent experiments

(b) Autophagosomes in U2OS cells stably expressing inducible HR23B were visualized by immunostaining with anti-LC3 (red) after treatment with SAHA (10 μM for 18h) in the presence (+) or absence (-) of doxycycline. (FLAG-HR23B; green, counterstain with DAPI was superimposed for each image). Result shown is representative of three independent experiments.

(c) The protein levels of HR23B and LC3 from (b) were analysed by immunoblotting, cleaved PARP levels are also shown. Actin levels are indicated as loading control. Result shown is representative of three independent experiments.

(d) Quantification of autophagosomes from (b) is shown (* significance in two-tailed Student's t test; * $P < 0.05$, n=3; error bars, SD).

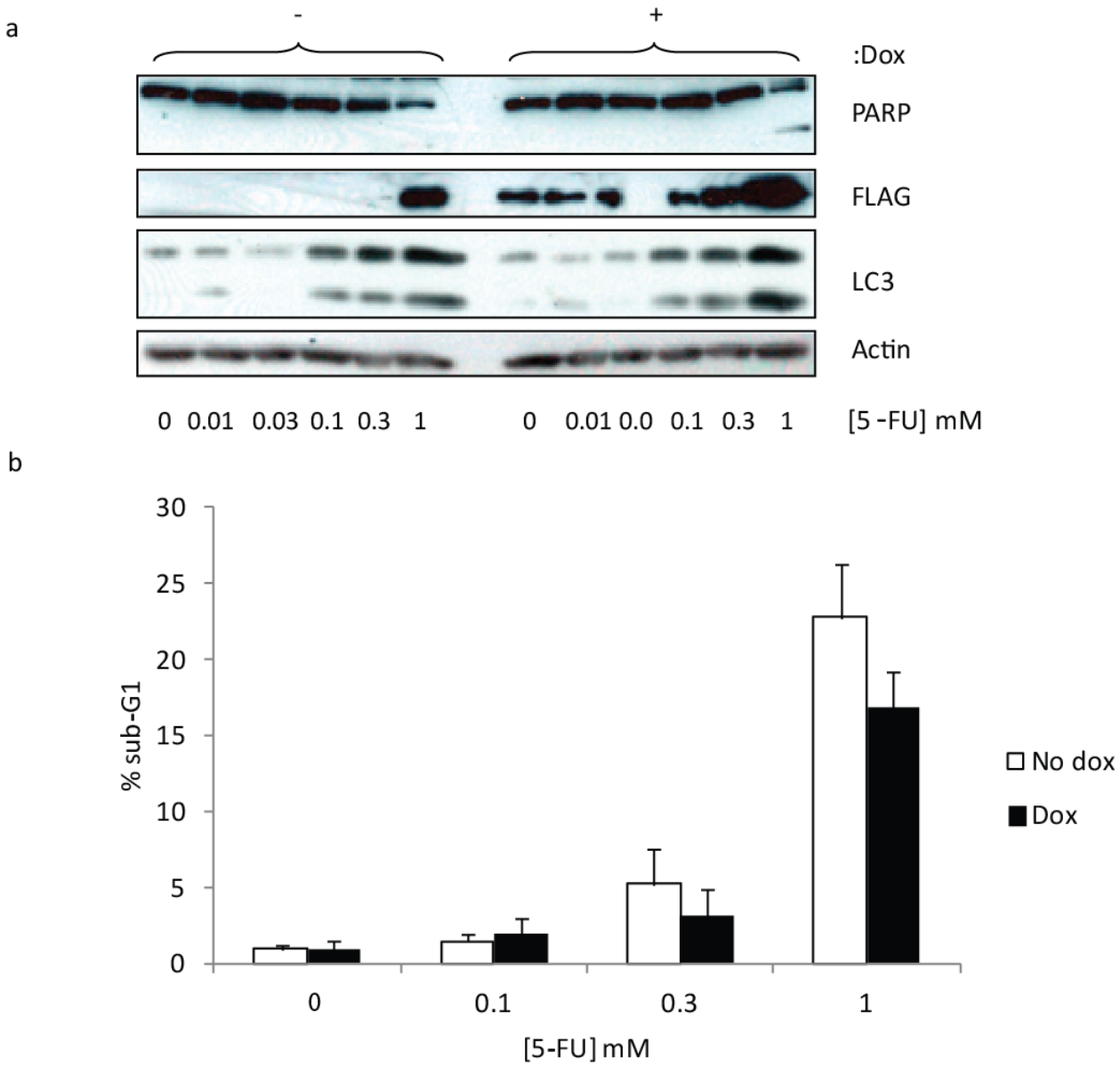


Figure 5.5

Effects of varying levels of HR23B on autophagy after 5-fluorouracil (5-FU) treatment.

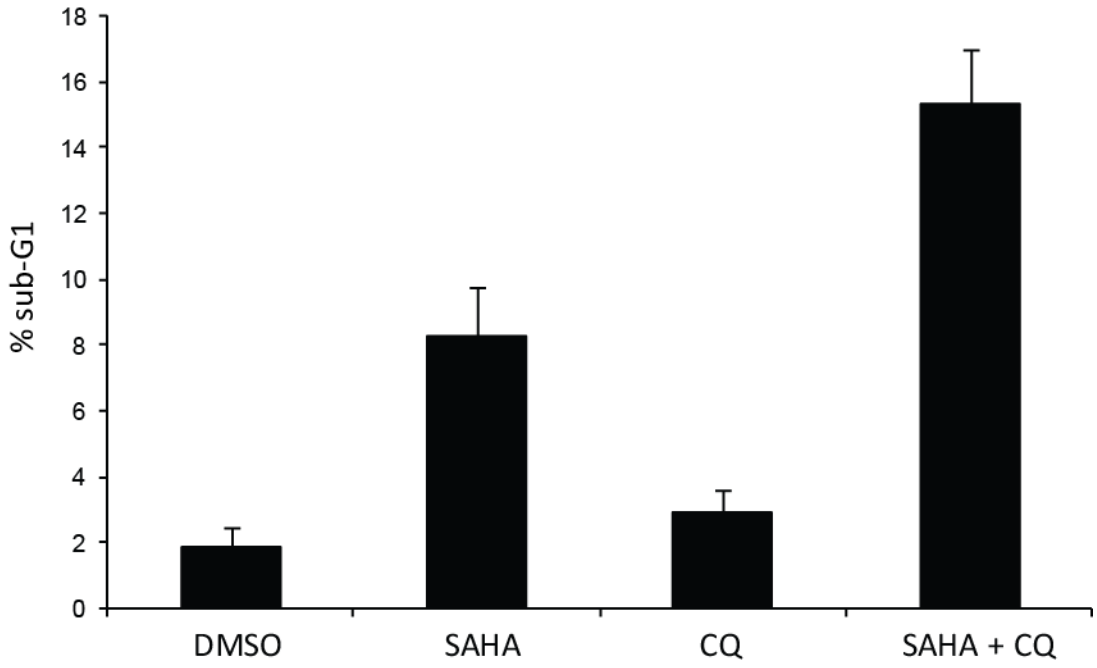
(a) U2OS cells stably expressing inducible HR23B were either untreated (-) or treated with 5-FU as indicated (in mM for 48h) under non-induced (-) or induced (+) doxycycline treatment conditions (1µg/ml; induction for 72h). Cells were harvested and immunoblotted with (for ectopic HR23B (anti-FLAG)), anti-LC3 and anti-actin as indicated. Result shown is representative of three independent experiments.

(b) Levels of sub-G1 cells from (a) were measured by flow cytometry, non-induced (clear), induced (black) with 5-FU concentrations as indicated in mM (n=3; error bars, SD).

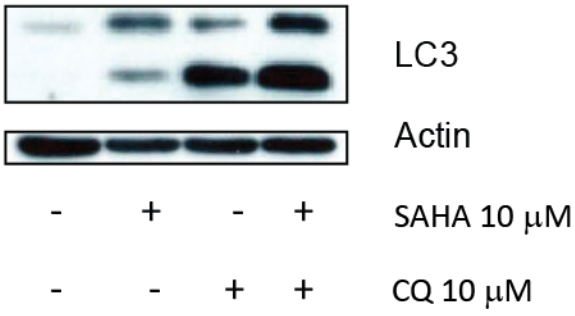
5.3. Effects of inhibiting autophagy on apoptosis

CQ was used as an inhibitor of autophagy and the effect of combining SAHA and CQ was a greater than additive increase in the percentage of sub-G1 cells (figure 5.6a, 5.6c). Interestingly, there appeared to be an increase in LC3 cleavage when SAHA and CQ were combined (figure 5.6 b, 5.6d). This presumably occurred because CQ inhibits autophagy downstream of the cellular events that result in LC3 cleavage, resulting in an accumulation of autophagosomes.

a


% sub-G1
18
16
14
12
10
8
6
4
2
0
DMSO
SAHA
CQ
SAHA + CQ

b


LC3
Actin
- + - +
SAHA 10 μM
- - + +
CQ 10 μM

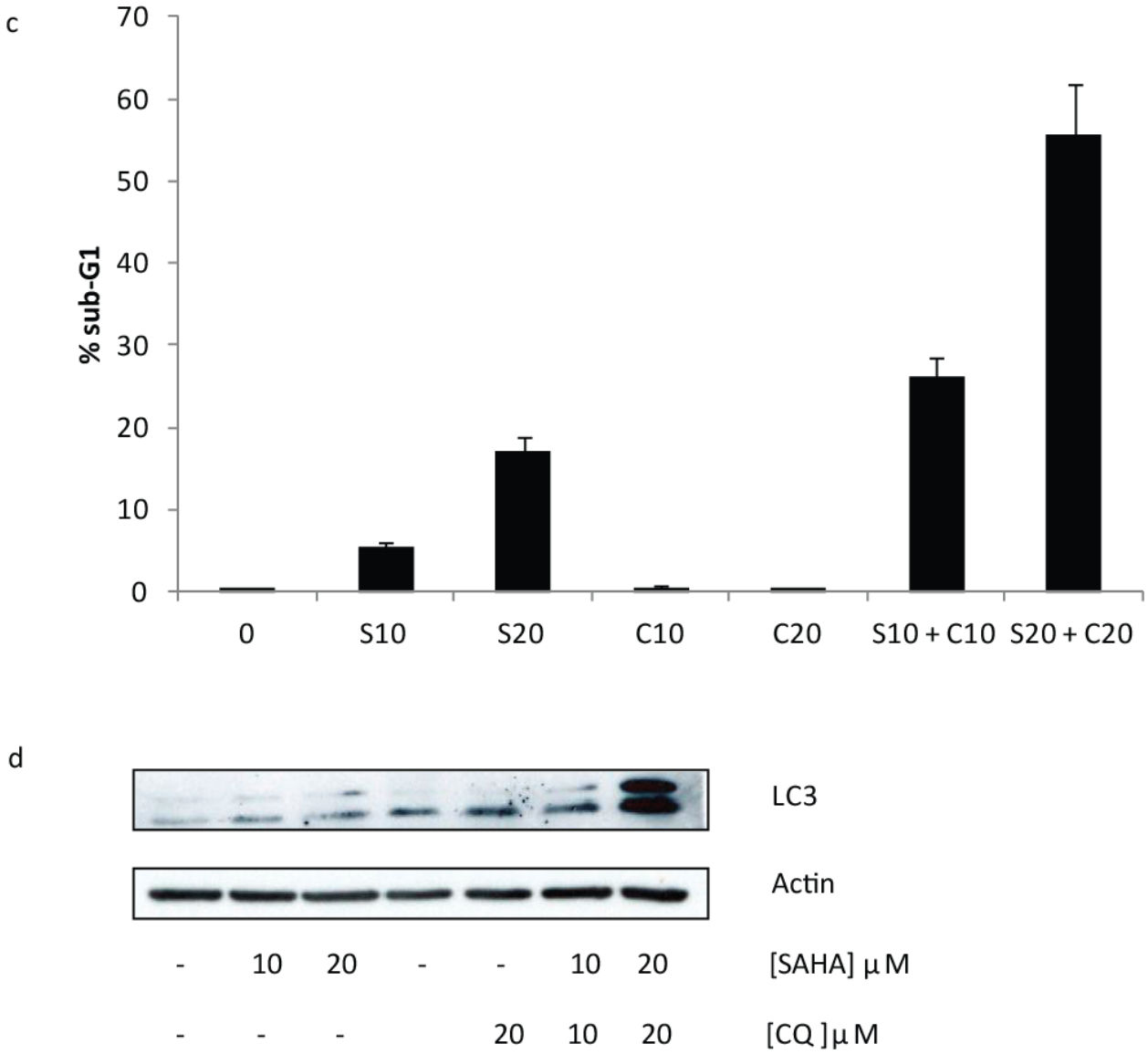


Figure 5.6

Effects of combining SAHA and chloroquine on apoptosis and autophagy

(a) U2OS cells were treated with SAHA or chloroquine (CQ) or in combination at the indicated doses for 24h and thereafter the level of sub-G1 cells were measured by flow cytometry (n=3; error bars: SD)

(b) Extracts from (a) were prepared and immunoblotted with anti-LC3 and anti-actin. Result shown is representative of three independent experiments.

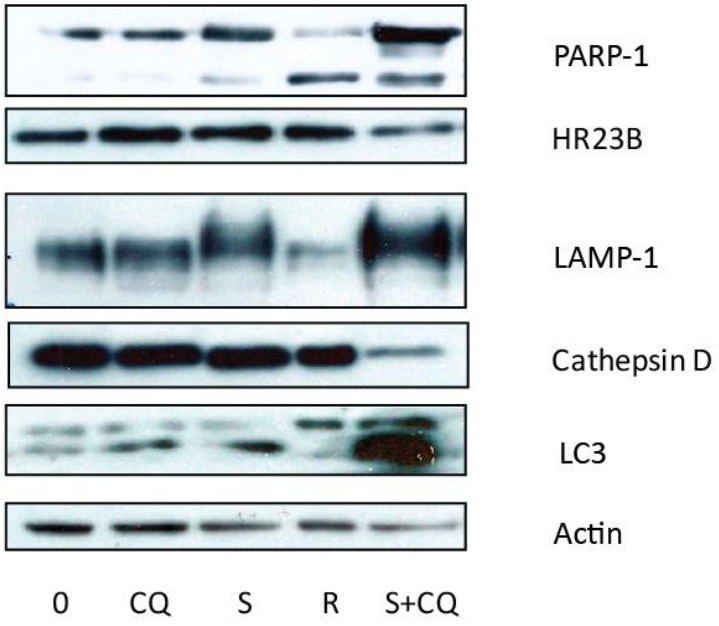
(c) MYLA cells were treated with SAHA (S) or chloroquine (C) in combination at the indicated doses in μM for 48h and thereafter the level of sub-G1 cells were measured by flow cytometry.

(d) Extracts from (c) were prepared and immunoblotted with anti-HR23B, anti-LC3 and anti-actin. Result shown is representative of two independent experiments.

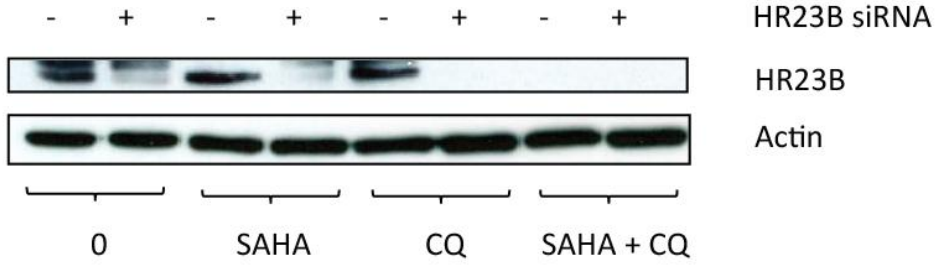
When A2058 cells were treated with CQ, LAMP-1 levels were also higher but cathepsin D levels were markedly reduced along with increased PARP cleavage (figure 5.7a). Cathepsin D is a lysosomal enzyme and low levels after treatment with SAHA and CQ in combination reflect an inhibition of autophagosome and lysosomal fusion. Rapamycin is an mTOR inhibitor and hence an inducer of autophagy and was incorporated as a positive control. However there was little effect seen on autophagy as measured in this experiment. Increased concentrations of rapamycin were used but also did not result in a significantly greater induction of autophagy (results not shown).

When HR23B levels were depleted using siRNA and cells were treated in combination with SAHA and CQ, the rescue from apoptosis seen in cells treated with SAHA alone was reversed (figure 5.7b). In fact, there was a greater percentage of sub-G1 cells in the cells treated with HR23B siRNA followed by SAHA and CQ treatment although this was not statistically significant. This suggested that the rescue from apoptosis upon HR23B depletion was in part related to the induction of autophagy and provided further evidence to support the hypothesis that resistance to HDAC inhibitor therapy may be mediated by induction of autophagy.

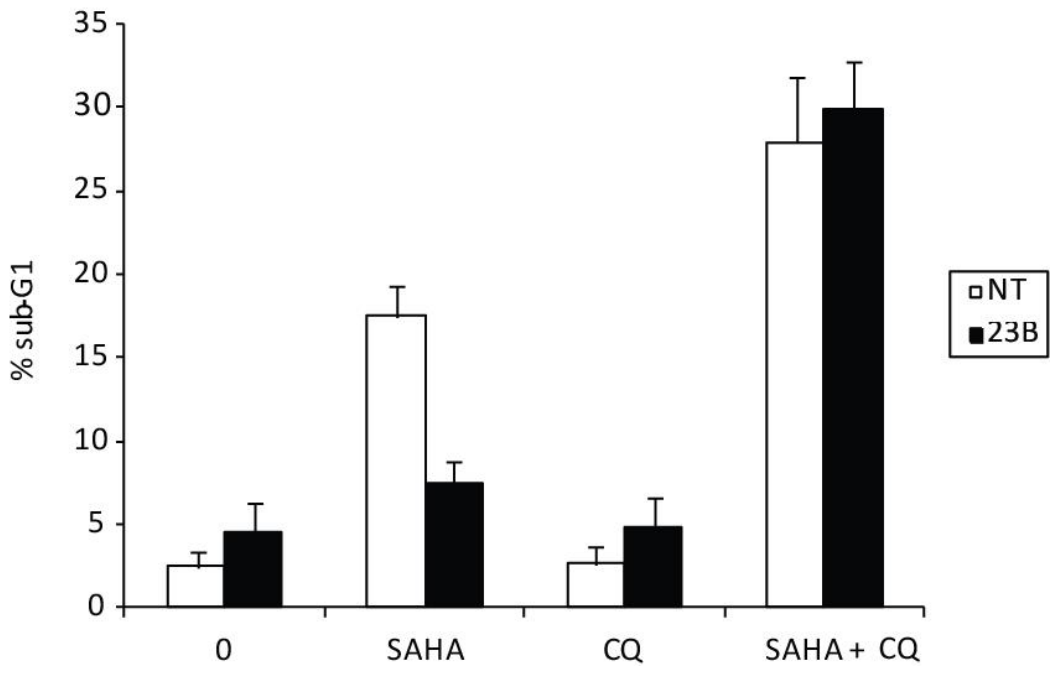
a


PARP-1
HR23B
LAMP-1
Cathepsin D
LC3
Actin
0
CQ
S
R
S+CQ

b


- + - + - + - +
HR23B siRNA
HR23B
Actin
0
SAHA
CQ
SAHA + CQ

c


% sub-G1
35
30
25
20
15
10
5
0
0
SAHA
CQ
SAHA + CQ
NT
23B

c

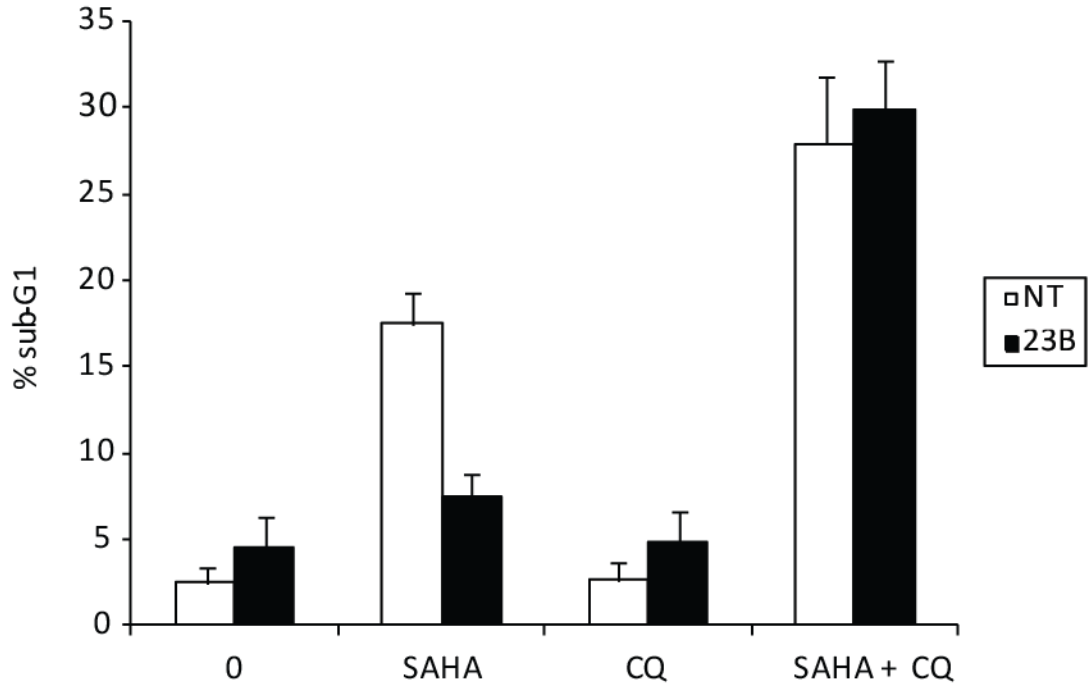


Figure 5.7

Effects of combining SAHA and chloroquine on apoptosis and autophagy in A2058 cells

(a) A2058 cells were treated with SAHA (S) at 10 μM or CQ at 10 μM, in combination or with Rapamycin (R) at 2 μM for 48h and extracts from were prepared and immunoblotted with anti-PARP, anti-HR23B, anti-LAMP-1, anti-cathepsin D, anti-LC3 and anti-actin as indicated.

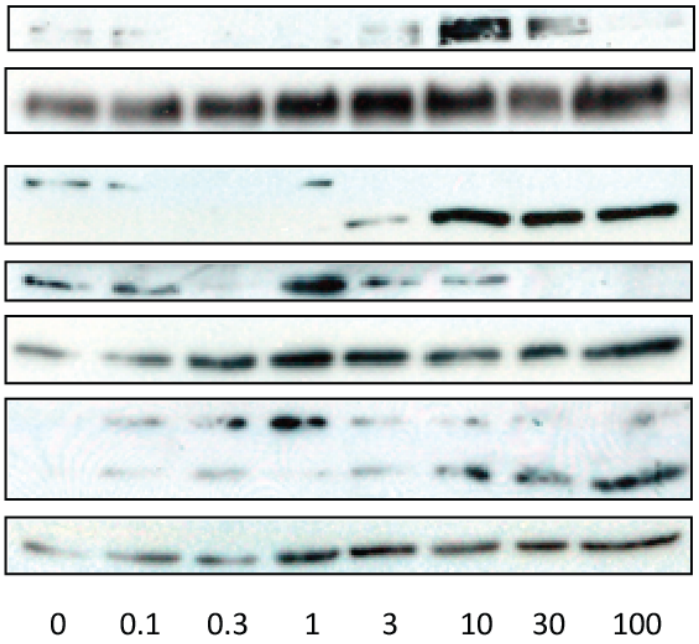
(b) U2OS cells were treated with HR23B or non-targeting (NT) control siRNA (50nM) for 48h and then treated with SAHA (10 μM) or CQ (10 μM) or in combination. Extracts were immunoblotted with anti-HR23B and anti-actin as indicated. Result shown is representative of three independent experiments.

(c) Levels of sub-G1 from (b) were measured using flow cytometry (n=3; error bars, SD).

5.4. Interplay between HR23B and HDAC6

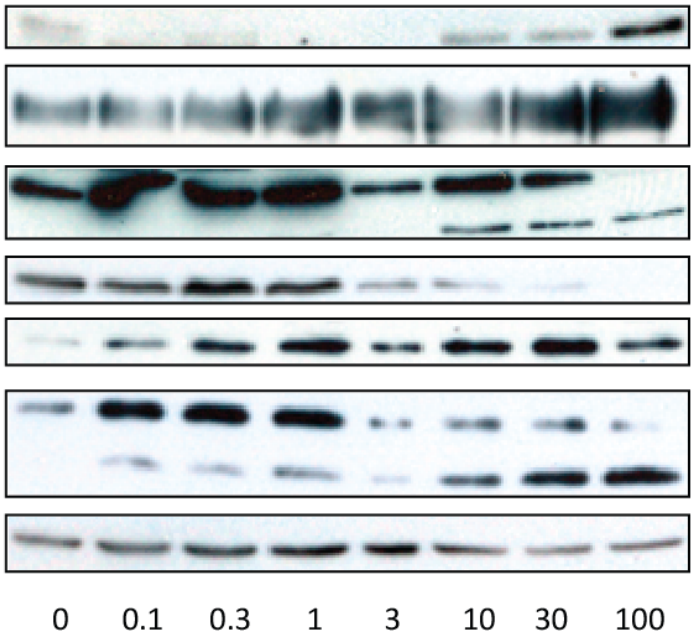
HDAC6 has an important function in protein turnover and autophagy. It was noted that HDAC6 levels were elevated at the higher concentrations of HDAC inhibitor therapy in A2058 and HCT116 cells which corresponded to low HR23B levels and high levels of autophagy markers (figure 5.8a, 5.8b). HR23B and HDAC6 were found to interact in immunoprecipitation assays in cells as well as with ectopic proteins (New et al., 2013).

a



A2058

b



HCT116

Figure 5.8

Expression of HDAC6, autophagy and apoptosis markers and HR23B expression in cancer cells treated with SAHA

(a) A2058 cells were treated with SAHA at the indicated concentrations (μM) for 48h and harvested and immunoblotted with anti-HDAC6, anti-LAMP-1, anti-cleaved PARP, anti-HR23B, anti-cathepsin D, anti-LC3 as indicated. Anti-actin was used as loading control. Immunoblots are representative of three independent experiments.

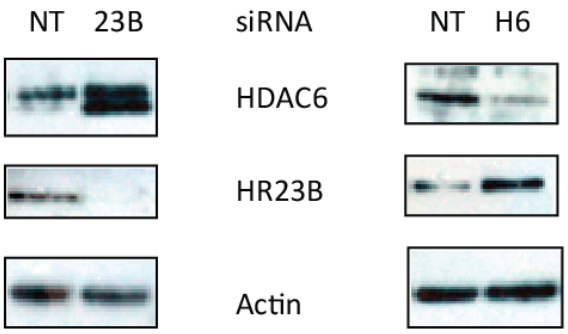
(b) HCT116 cells were treated with SAHA at the indicated concentrations (μM) for 48h and harvested and immunoblotted with anti-HDAC6, anti-LAMP-1, anti-PARP, anti-HR23B, anti-cathepsin D, anti-LC3 as indicated. Anti-actin was used as loading control. Immunoblots are representative of three independent experiments.

When HDAC6 levels were depleted using siRNA in U2OS cells levels of HR23B were induced (figure 5.9a). The reverse was also observed; HDAC6 levels were induced upon HR23B depletion (figure 5.9a). This phenomenon was also observed in wild type A549 cells (designated A549 WT) when compared to cellular counterparts stably expressing HDAC6 shRNA where HDAC6 levels were very low (designated A549 -/-). The level of HR23B was markedly higher in the HDAC6 deficient cells compared to normal control A549 cells (figure 5.10b). Overall, a biochemical relationship appears to exist between HR23B and HDAC6 in which HDAC6 interacts with and negatively regulates the level of HR23B.

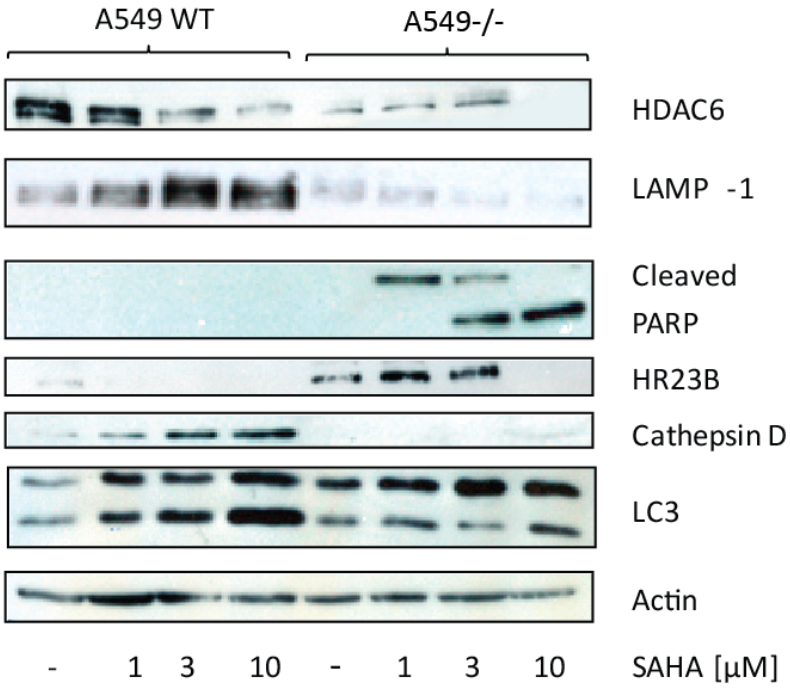
Because the level of HR23B appears to be influenced by HDAC6 and high HR23B levels sensitise cells to apoptosis, the absence of HDAC6 might impact on cell sensitivity to HDAC

inhibitors. In contrast to A549 WT cells, where low basal level apoptosis was apparent and a significant increase in apoptosis occurred upon HDAC inhibitor treatment (about 40-fold), A549 -/- cells had a high basal level of apoptosis (25-fold higher than normal cells) and a low relative increase in apoptosis (about 2- to 3- fold) upon HDAC inhibitor treatment (figures 5.9c, d; apoptosis measured as the sub-G1 population by flow cytometry). The enhanced level of apoptosis in the A549 -/- cells reflected increased levels of HR23B and PARP cleavage (figure 5.9b). There were also reduced levels of autophagy markers including LAMP-1, cathepsin-D and reduced LC3 cleavage.

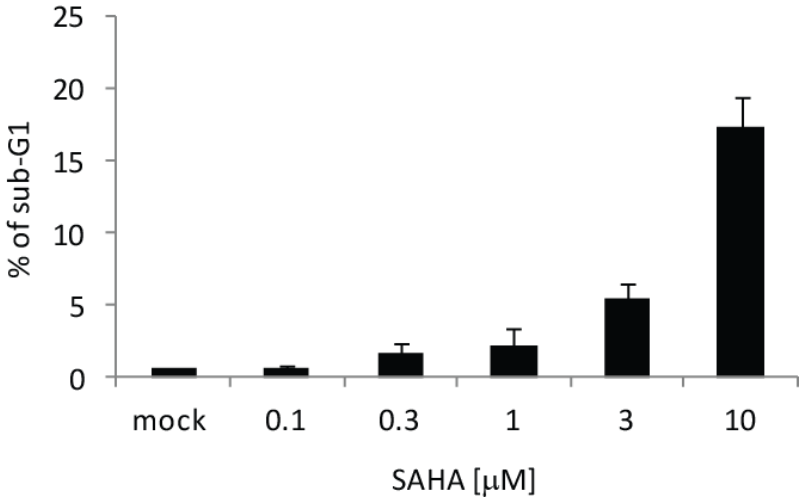
a


NT 23B
siRNA
NT H6
HDAC6
HR23B
Actin

b


A549 WT
A549-/-
HDAC6
LAMP -1
Cleaved PARP
HR23B
Cathepsin D
LC3
Actin
- 1 3 10 - 1 3 10
SAHA [μM]

c


25
20
15
10
5
0
% of sub-G1
mock
0.1
0.3
1
3
10
SAHA [μM]

d

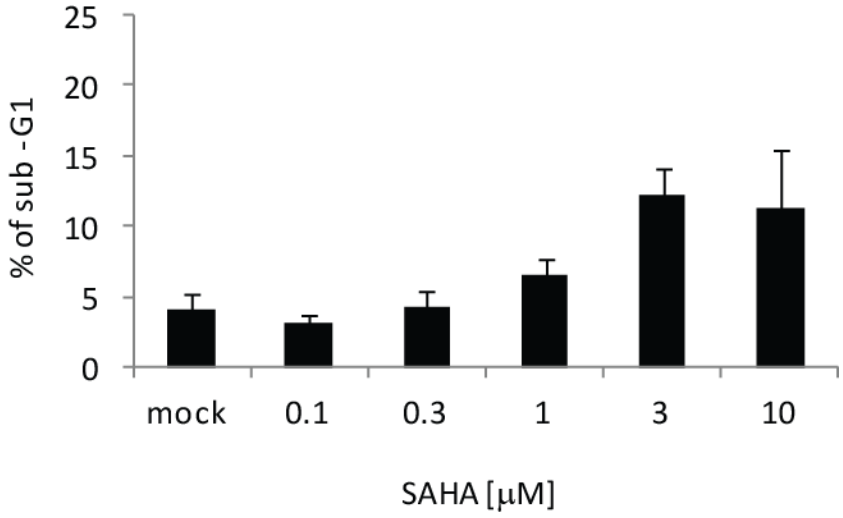


Figure 5.9

Effects of manipulating levels of HR23B and HDAC6 on expression of autophagy markers and apoptosis

(a) U2OS cells were transfected with either HR23B siRNA (23B), HDAC6 siRNA (H6) or non-targeting (NT) control siRNA (50nM) for 48h as indicated. Extracts were immunoblotted with anti-HR23B, anti-HDAC6 and anti-actin as indicated.

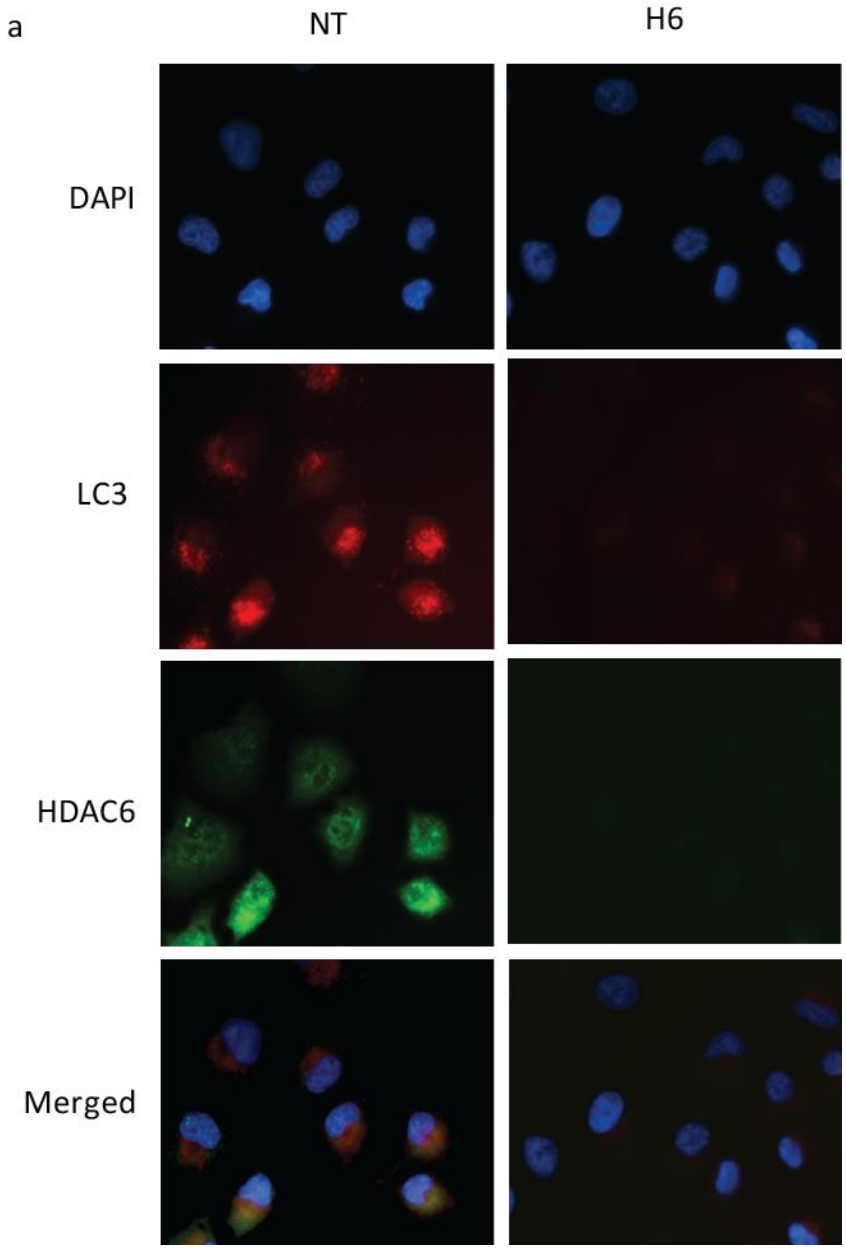
(b) Either wild-type (WT) or HDAC6$^{-/-}$ KD A549 cells were treated with SAHA as indicated and extracts were prepared and immunoblotted with antibodies to cathepsin-D, PARP, LAMP-1 and LC3 to assess levels of apoptosis and autophagy in addition to HR23B, HDAC6 and actin.

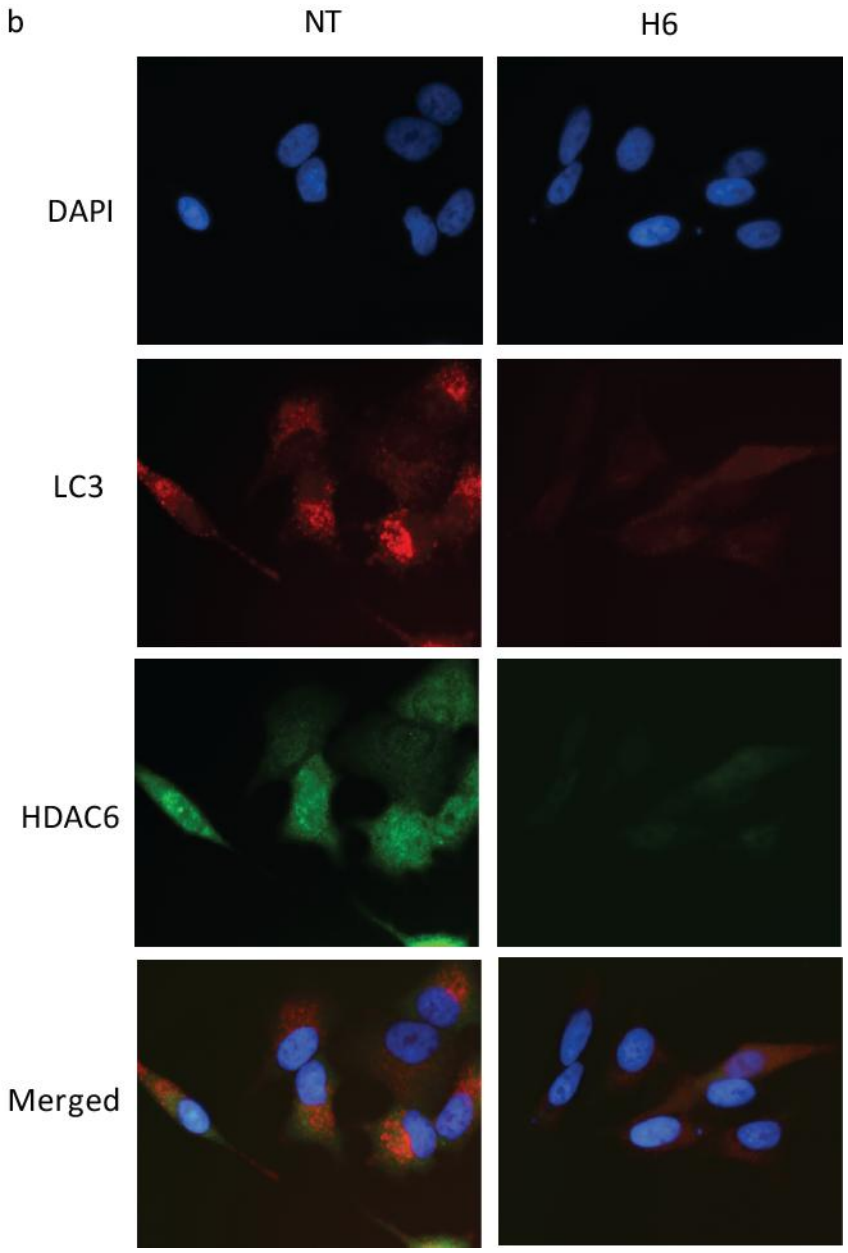
(c) The levels of sub-G1 cells measured by flow cytometry from the A549 WT cells treated with SAHA in (b) (n=3; error bars, SD)

(d) The levels of sub-G1 cells measured by flow cytometry from the A549 $^{-/-}$ cells treated with SAHA in (b) (n=3; error bars, SD).

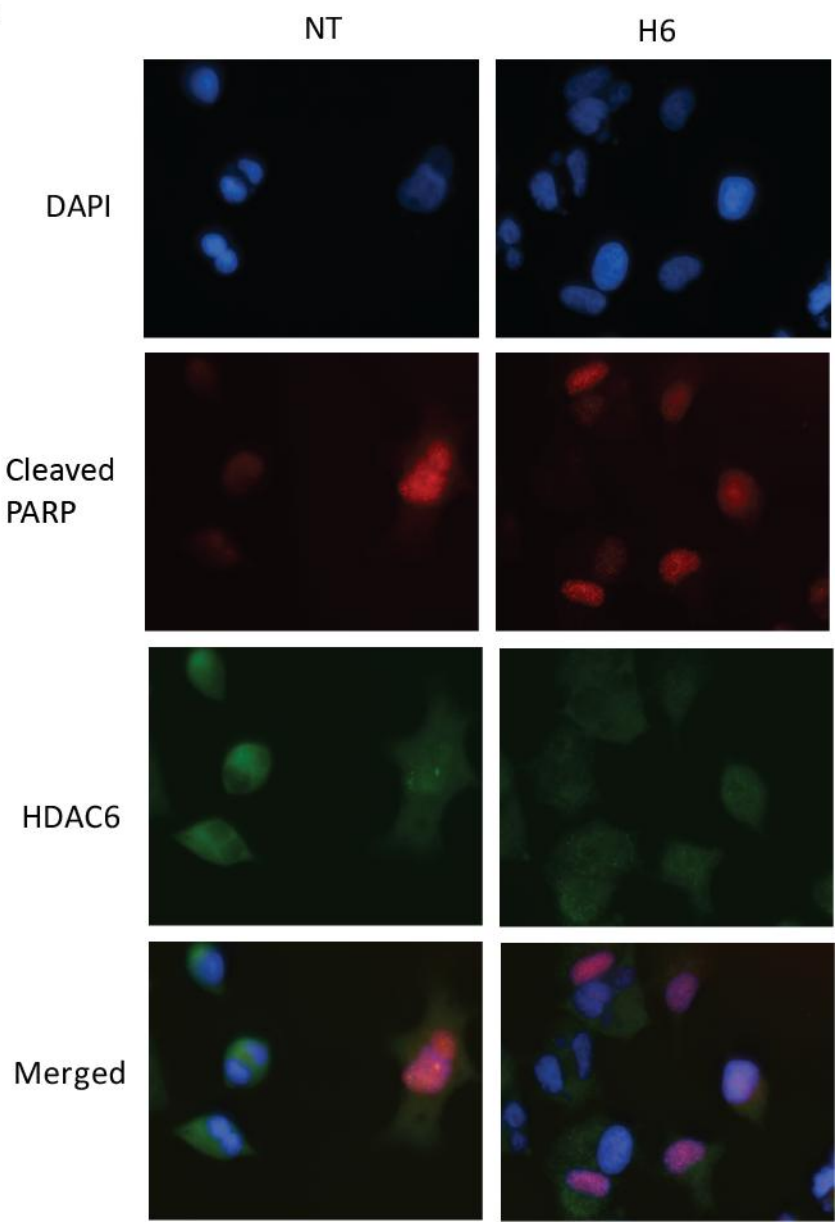
When HDAC6 was depleted transiently in A549 cells with siRNA, there appeared to be increased basal autophagy in the A549 WT cells which was reversed with HDAC6 siRNA treatment even without HDAC inhibitor treatment (figure 5.10a). There was also a decrease in autophagosome formation when HDAC6 was depleted transiently with siRNA and cells were treated with SAHA when compared to the non-targeting control (figure 5.11b). Conversely, there appeared to be an increase in apoptosis (as evidenced by cells expressing cleaved PARP on immunostaining) after HDAC6 siRNA treatment followed by HDAC inhibitor treatment (figure 5.11c). These differences were quantified in figure 5.11d and 5.11e and the differences were statistically significant (significance in two-tailed Student's t test; $p < 0.05$ at least). Overall,

these results suggest that HDAC6 may be a negative regulator of HR23B protein levels, which could couple HDAC6 activity (via its interplay with HR23B) to the apoptotic and autophagocytic outcome of treatment with HDAC inhibitors.

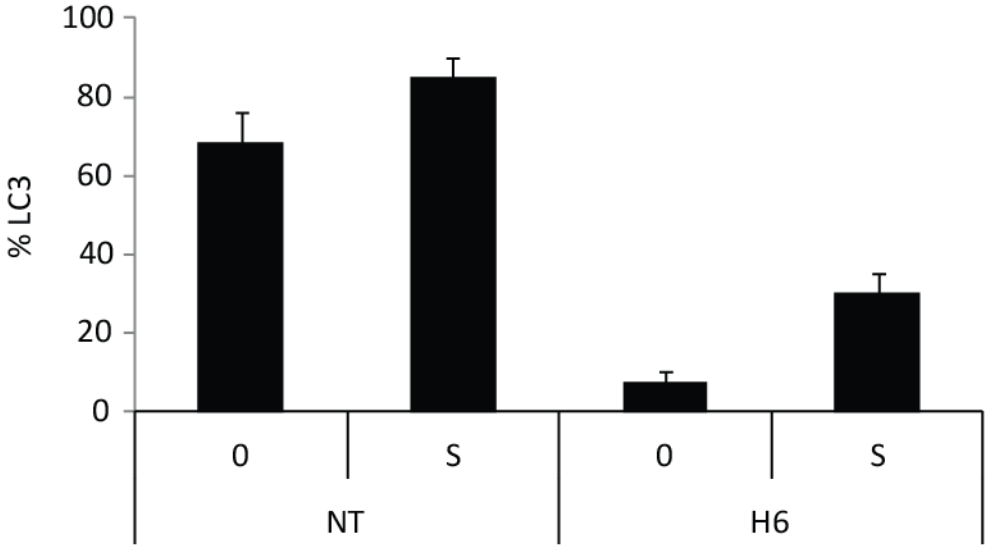



b
NT
H6
DAPI
LC3
HDAC6
Merged

c



d


100
80
60
40
20
0
% LC3
0
S
0
S
NT
H6

e

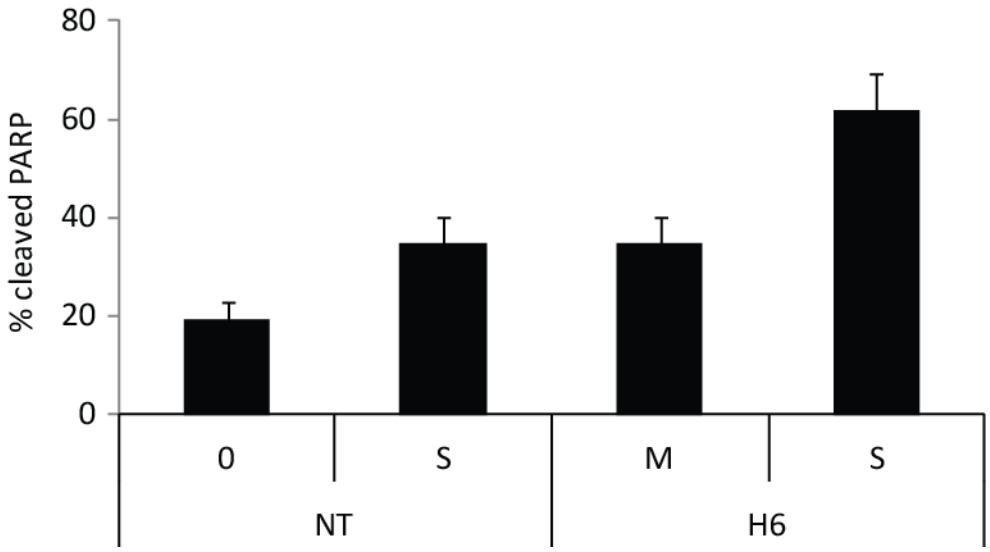

80
60
40
20
0
% cleaved PARP
0
S
M
S
NT
H6

Figure 5.10

Effects of manipulating levels of HDAC6 on expression of autophagy markers and apoptosis as determined by immunofluorescence

(a) A549 cells were transfected with control (NT) or HDAC6 siRNA (H6) at 50nM for 48hr followed by treatment with DMSO for 24h and thereafter immunostained with anti-LC3 (red) and HDAC6 (green) and counterstained with DAPI. The merged images are shown. Results shown are representative of three independent experiments.

(b) A549 cells were treated with control (NT) or HDAC6 siRNA (H6) at 50nM for 48hr followed by treatment with SAHA (10μM) for 24h and thereafter immunostained with anti-LC3 (red) and HDAC6 (green) and counterstained with DAPI. The merged images are shown. Results shown are representative of three independent experiments.

(c) A549 cells were treated with control (NT) or HDAC6 siRNA (50nM) for 48hr followed by treatment with SAHA (10μM) for 24h and thereafter immunostained with anti-cleaved PARP (red) and HDAC6 (green) and counterstained with DAPI. The merged images are shown. Results shown are representative of three independent experiments.

(d) A549 cells were treated with control (NT) or HDAC6 siRNA (H6) at 50nM for 48hr followed by treatment with DMSO (0) or SAHA 10 μM (S) for 24h. LC3 expression was quantified by counting 500 cells and noting the number of cells expressing autophagosomes from (a) and (b). Graphical representation of the percentage of LC3 staining cells in the NT relative to HDAC6 siRNA treatment (n=3; error bars, SD).

(e) Cleaved PARP expression was quantified by counting the number of cells expressing cleaved PARP from (c). Graphical representation of the percentage of cleaved PARP staining cells in the NT relative to HDAC6 siRNA treatment (n=3; error bars, SD).

5.5. Conclusion

Protein levels of HR23B have an impact on two known effects of HDAC inhibitor treatment, namely apoptosis and autophagy. Altering HR23B levels has an effect on HDAC inhibitor-induced autophagy such that increased levels result in fewer autophagocytic cells. Combining an HDAC inhibitor with an autophagy inhibitor may result in greater apoptosis than with the HDAC inhibitor alone reflected in both the increase in percentage of sub-G1 cells as well as increased PARP cleavage. This effect appears to be abrogated when HR23B is depleted before treatment with the combination. Modifying autophagy induction in combination with HDAC inhibitor therapy may be a novel way of improving HDAC inhibitor efficacy.

Increased levels of HR23B coincide with apoptosis whereas low level expression is frequently associated with autophagy. HR23B and HDAC6 interact and HDAC6 may be a negative regulator of apoptosis and a positive regulator of autophagy and through its ability to down-regulate HR23B, may impact on the cellular outcome of HDAC inhibitor treatment.

CHAPTER 6

RESULTS

EXPRESSION PATTERNS OF HR23B IN HUMAN TUMOUR TISSUES AND HR23B AS A PREDICTIVE BIOMARKER FOR RESPONSE TO THERAPY IN CTCL

6.1. Introduction

Cutaneous T cell lymphomas (CTCLs) are a heterogeneous group of extranodal non-Hodgkin's lymphomas in which malignant, clonal T lymphocytes present in the skin (Khan and La Thangue, 2008). The most common type of CTCL is mycosis fungoides (MF) which is an indolent form and constitutes approximately half of all cases. Sézary syndrome (SS) is an aggressive leukemic form of the disease and accounts for 4% of all cases. CTCL is of relevance as, to date, the only HDAC inhibitors which have received regulatory approval have been for the treatment of this rare condition (Whittaker et al., 2010).

The aetiology of CTCL is not clear; no definitive environmental, genetic or infective factors have been identified. The malignant clonal T lymphocytes in CTCL—which probably arise from normal skin lymphocytes—are CD4+, epidermotrophic (skin-homing) T cells. In normal skin, CD4+ helper T cells are activated in response to stimulation by antigen presenting cells. Constitutive activation of a population of CD4+ T cells in MF and SS is seen but the trigger is unknown and as the disease progresses the malignant clone dominates resulting in a skewed T helper 2 (Th2) cytokine profile ultimately resulting in inflammation and immune disarray (Kim et al., 2005).

The malignant T-cell tethers and rolls along the endothelial cell by virtue of interaction between cutaneous lymphocyte antigen (CLA) and E-selectin and the CC chemokine receptor 4 (CCR4) and CC chemokine ligand 17 (CCL17) (Khan and La Thangue, 2008). Clustering occurs around immature dendritic (Langerhan's) cells forming the characteristic Pautrier's microabscess. This

leads to activation and clonal expansion of malignant T-cells. Activated T-cells produce a variety of cytokines that lead to an increased Th2 phenotype and subsequent defective cellular immunity.

Naturally occurring regulatory T cells (Tregs) maintain immunological tolerance by suppressing the activity of other immune cells and these are deregulated in CTCL (Krejsgaard et al., 2012). Indeed, in early cutaneous lesions in patients with MF, there is a preponderance of Tregs that decrease in more advanced lesions. These may suppress tumour proliferation and levels correlate with improved survival. Patients with SS have very low levels of Tregs but high levels of malignant T cells expressing a Treg phenotype (FOXP3+CD25-). These cells express cytotoxic T lymphocyte antigen-4 (CTLA-4), IL-10 and transforming growth factor-β which suppress host immunity and decrease the anti-tumour response.

HR23B protein levels in a number of human cell lines have been investigated using immunoblotting techniques. From these data, there is a suggestion that levels of HR23B may provide predictive information on response to HDAC inhibitor therapy. Immunohistochemistry (IHC) refers to the process of detecting antigens (e.g., proteins) in cells of a tissue section by exploiting the principle of antibodies binding specifically to antigens in biological tissues. Immunohistochemical staining is widely used in the diagnosis of abnormal cells such as those found in cancerous tumours. Specific molecular markers are characteristic of particular cellular events such as proliferation or cell death (apoptosis). IHC is also widely used in basic research to understand the distribution and localization of biomarkers and differentially expressed proteins

in different parts of a biological tissue. To date, expression of HR23B has never been extensively investigated using IHC.

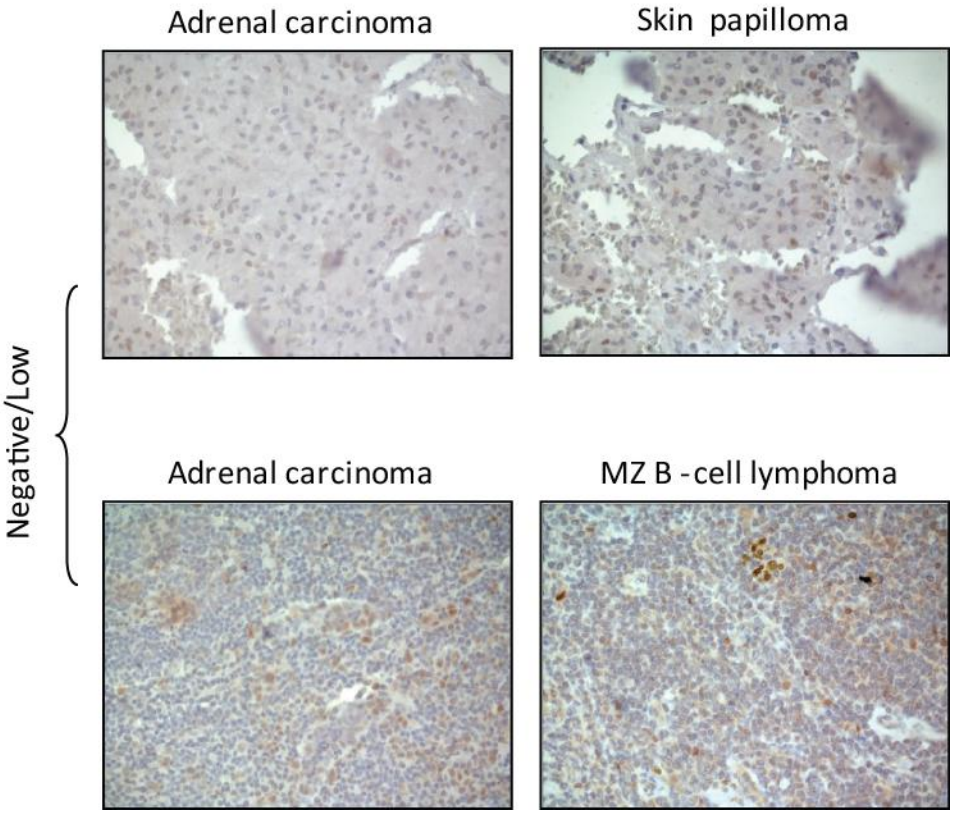
Expression of HR23B across a multi-tumour tissue TMA was investigated. As CTCL is the only tumour type for which HDAC inhibitors have received treatment approval, the expression in this tumour type was also assessed. Furthermore, expression patterns of HR23B in normal colon were compared to different stages of colorectal cancer. Colorectal cancer was selected as representative of solid tumours as it is one of the commonest tumour types and due to the availability of numerous histological specimens with associated clinical data.

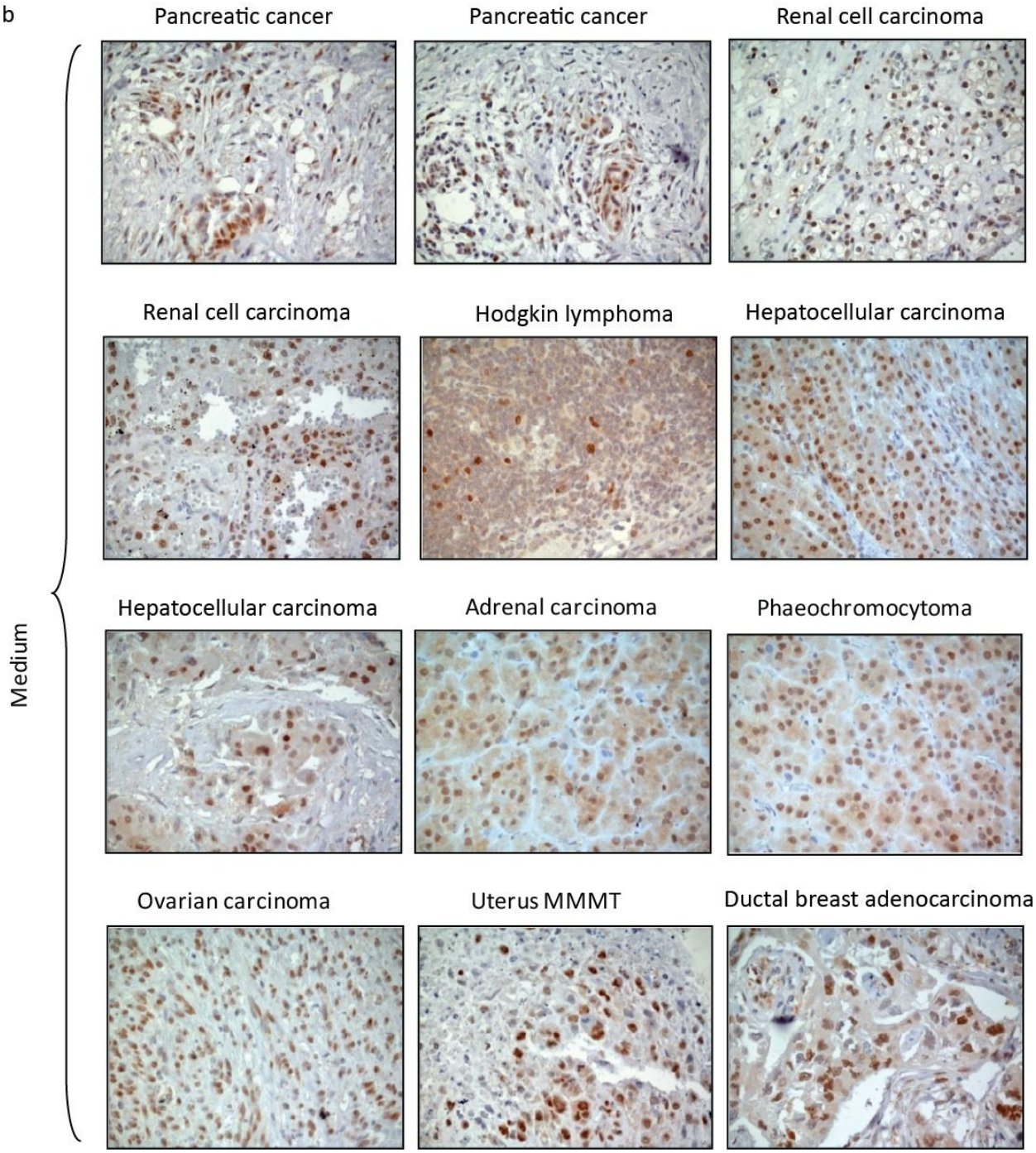
Because HR23B governs the sensitivity of tumour cells to HDAC inhibitors *in vitro*, it was reasoned that HR23B might find utility as a predictive biomarker in the clinical setting. The role of HR23B as sensitivity determinant for response to HDAC inhibitors in CTCL cell lines has been established. CTCL biopsies were obtained from one of the pivotal phase II clinical trials which led to FDA approval of SAHA for the treatment of CTCL (Duvic et al., 2007). Expression of HR23B was determined in these biopsies as well as a smaller cohort of biopsies from other clinical trials with different HDAC inhibitors.

6.2. HR23B expression is variable across different tumour types

HR23B expression was assessed in a multi-tumour TMA of twenty two different tumours and expression was assessed according to frequency (number of tumour cells expressing HR23B) and intensity of expression. Samples were then categorized based on low, intermediate and high expression (figure 6.1). Variability of expression appeared to be greatest in nuclear expression although there was also cytoplasmic expression.

a




b
Pancreatic cancer
Pancreatic cancer
Renal cell carcinoma
Renal cell carcinoma
Hodgkin lymphoma
Hepatocellular carcinoma
Hepatocellular carcinoma
Adrenal carcinoma
Phaeochromocytoma
Ovarian carcinoma
Uterus MMMT
Ductal breast adenocarcinoma
Medium

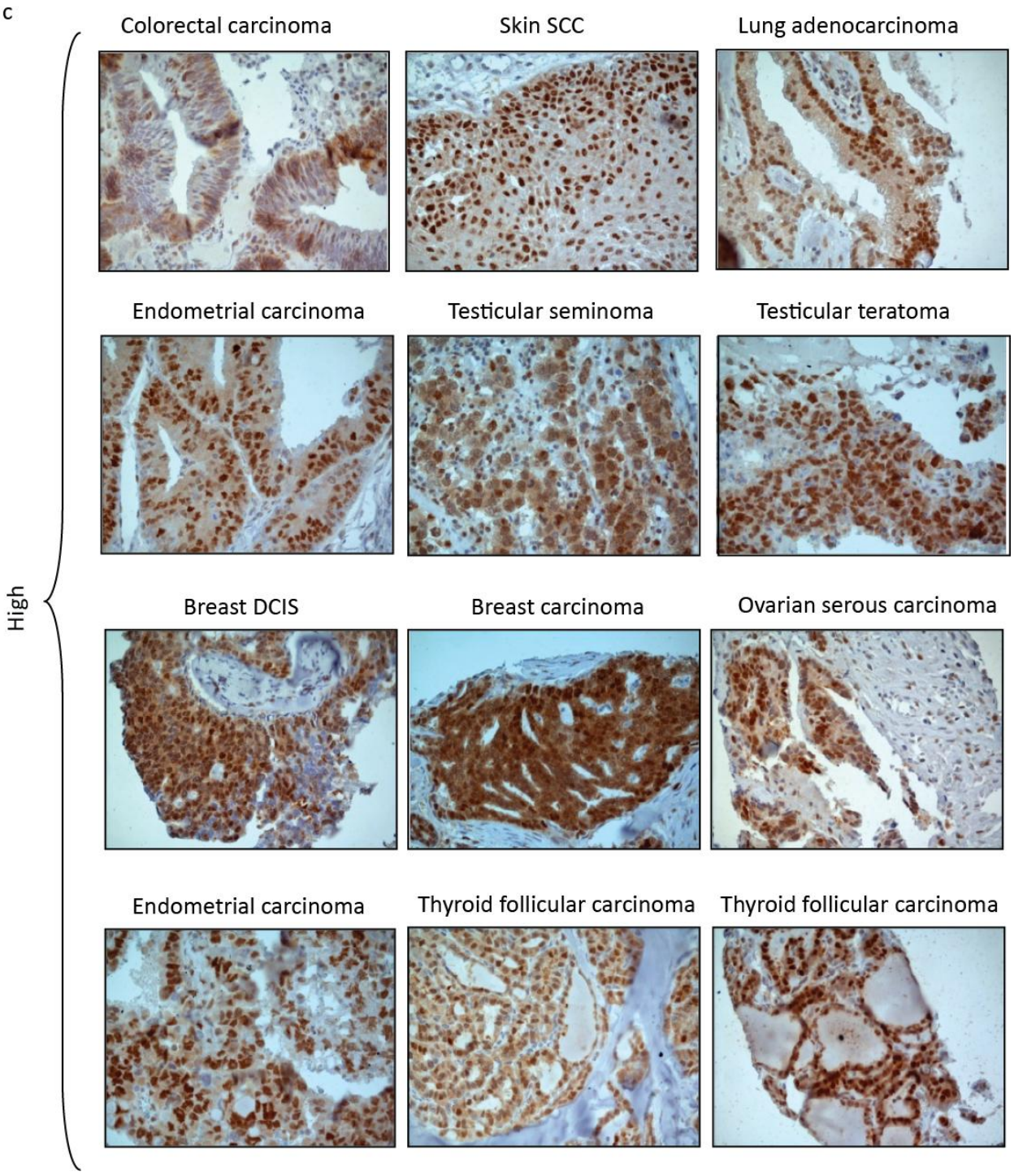

c
High
Colorectal carcinoma
Skin SCC
Lung adenocarcinoma
Endometrial carcinoma
Testicular seminoma
Testicular teratoma
Breast DCIS
Breast carcinoma
Ovarian serous carcinoma
Endometrial carcinoma
Thyroid follicular carcinoma
Thyroid follicular carcinoma

Figure 6.1

HR23B expression in multiple tumour types

A multi-tumour tissue microarray was stained with HR23B and the frequency and intensity of expression was assessed and categorised into low, intermediate and high HR2B immunostaining.

(a) Examples of tumours with low or absent HR23B immunostaining

(b) Examples of tumours with intermediate HR23B immunostaining

(c) Examples of tumours with high HR23B immunostaining

Abbreviations: MZ: marginal zone, DCIS: ductal carcinoma *in situ*, MMMT: mixed Müllerian cell tumour, SCC: squamous cell carcinoma

6.3. HR23B expression in CTCL

HR23B levels in tumour cell lines derived from haematological malignancies were evaluated and thereafter their sensitivity to HDAC inhibitors. In a small panel of cell lines derived from CTCL, HR23B levels correlated with sensitivity to SAHA (figure 3.8a). Following on from this, it was of interest to examine HR23B in clinical biopsies taken from patients with CTCL. By IHC biopsy-verified CTCL, including mycosis fungoides and its leukemic variant Sézary syndrome, HR23B was expressed at high levels (Table 6.1).

Table 6.1: Summary of HR23B expression in CTCL together with characteristics of neoplastic cells

Histology number	CTCL diagnosis	Neoplastic cells positive for HR23B	Neoplastic cells negative for HR23B
1	Mycosis fungoides		+
2	Mycosis fungoides	+	
3	Mycosis fungoides	+	
4	Mycosis fungoides	+	
5	Mycosis fungoides	+	
6	Mycosis fungoides	+	
7	Mycosis fungoides	+	
8	Mycosis fungoides	+	
9	Mycosis fungoides	+	
10	Mycosis fungoides	+	
11	Cutaneous cytotoxic T cell lymphoma	+	
12	Cutaneous anaplastic large cell lymphoma	+	
13	CLD	+	
14	CLD	+	
15	CLD	+	

Abbreviation: CLD, cutaneous lymphoproliferative disorder

The expression of HR23B was found to be localized to malignant CD3-positive T cells and areas of tumour mass (figure 6.2). Most but not all CTCL biopsies expressed high levels of HR23B (table 1, figure 6.2d), and so HR23B expression was not considered to be a general feature of CTCL. Moreover, HR23B levels were low in non-malignant tissue in which activated T cells were present (according to anti-CD3 staining), such as chronic dermatitis or non-malignant perivascular T cell infiltrate (figure 6.3), and thus HR23B expression was not considered to be a marker of activated T cells. HR23B was therefore found to be highly expressed in malignant T cells in CTCL *in situ*, which represents a malignancy that is known to be sensitive to HDAC inhibitor-based therapies.

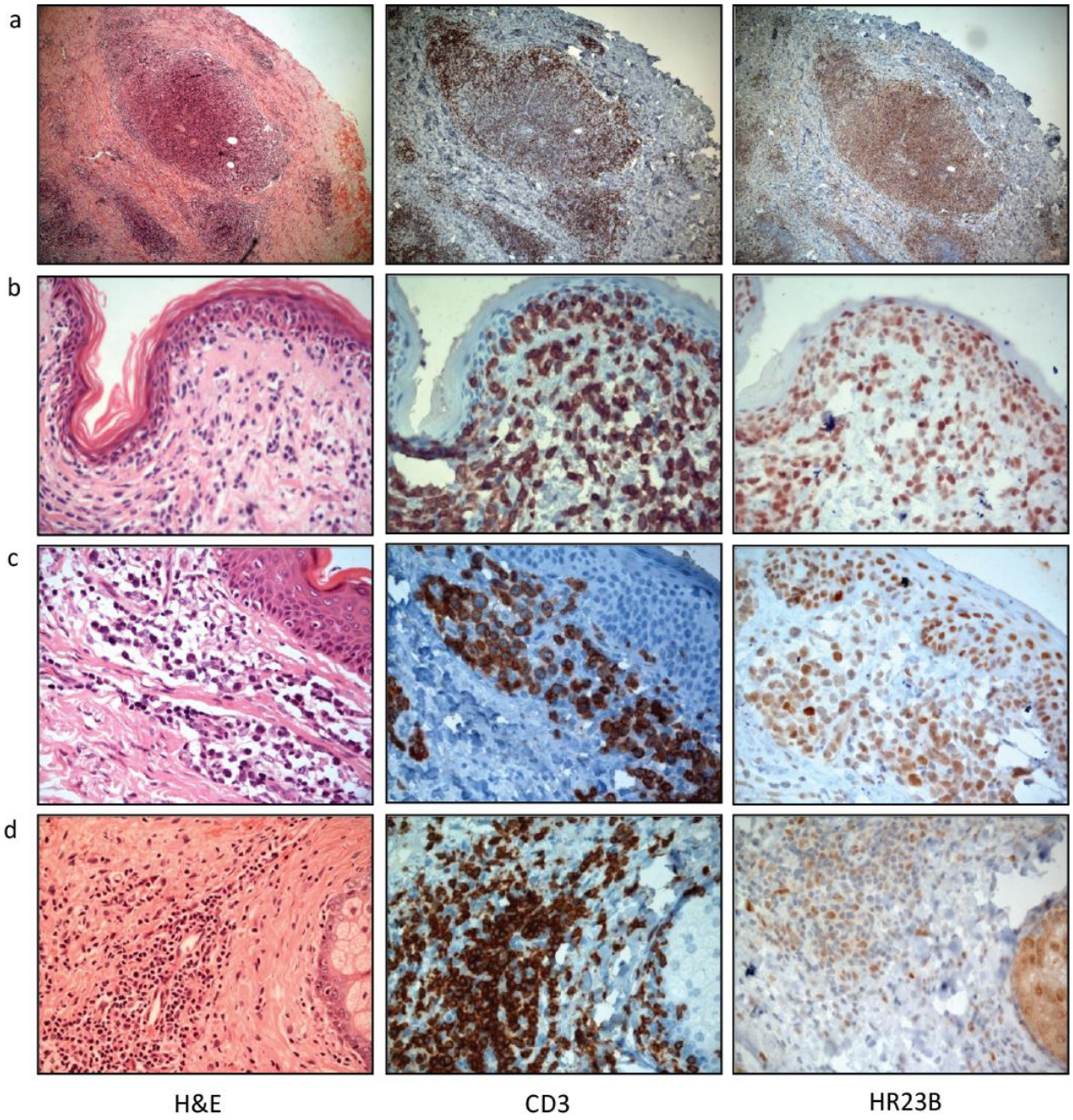


Figure 6.2

Expression of HR23B in cutaneous T cell lymphoma (CTCL)

A selection of CTCL biopsies were prepared and stained with haematoxylin and eosin (H&E), anti-CD3 and anti-HR23B as indicated.

(a) Cutaneous lymphoproliferative disorder (histology number 13).

(b) Cutaneous cytotoxic T cell lymphoma (histology number 11).

(c) Mycosis fungoides (histology number 7).

(d) Mycosis fungoides (histology number 1)

Each image in the triplet represents a separate serial section from the biopsy.

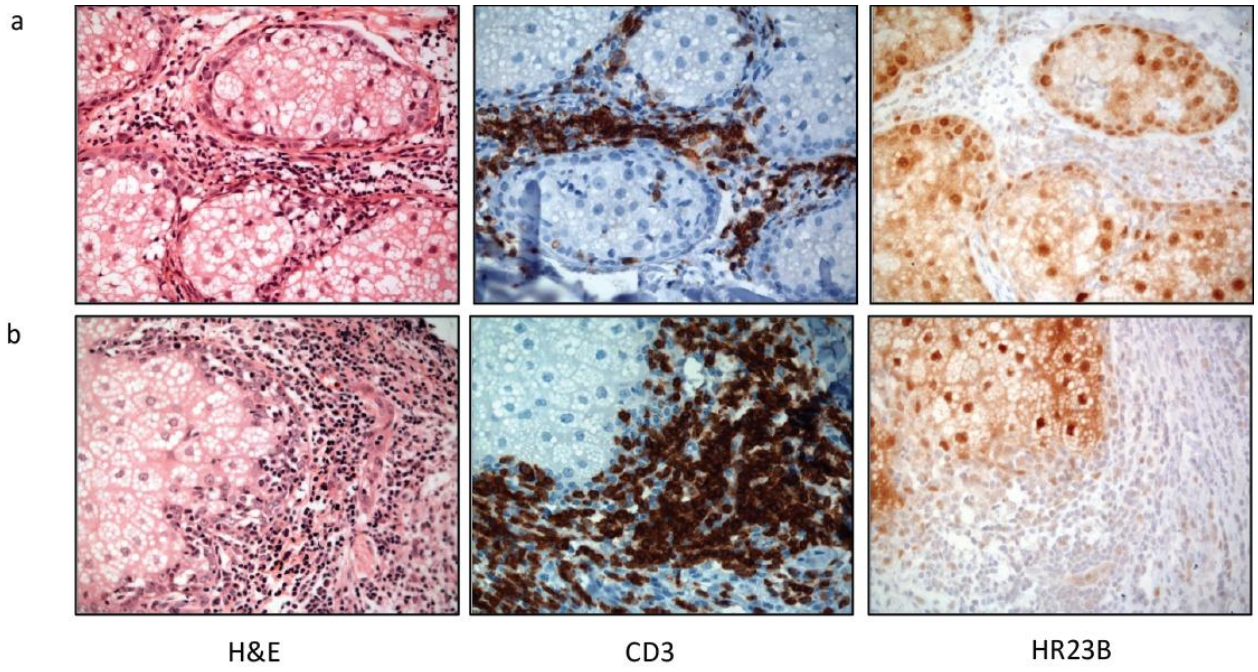


Figure 6.3

Expression of HR23B in non-malignant T cells

A-b: examples of tissue sections taken from biopsies showing haematoxylin and eosin (H&E) staining, anti-CD3 immunostaining and anti-HR23B immunostaining as indicated, images are from non-malignant tissues biopsied concurrently with CTCL.

(a) Non-malignant perivascular T cell infiltrate surrounding an apocrine gland.

(b) Chronic dermatitis (histology number 17)

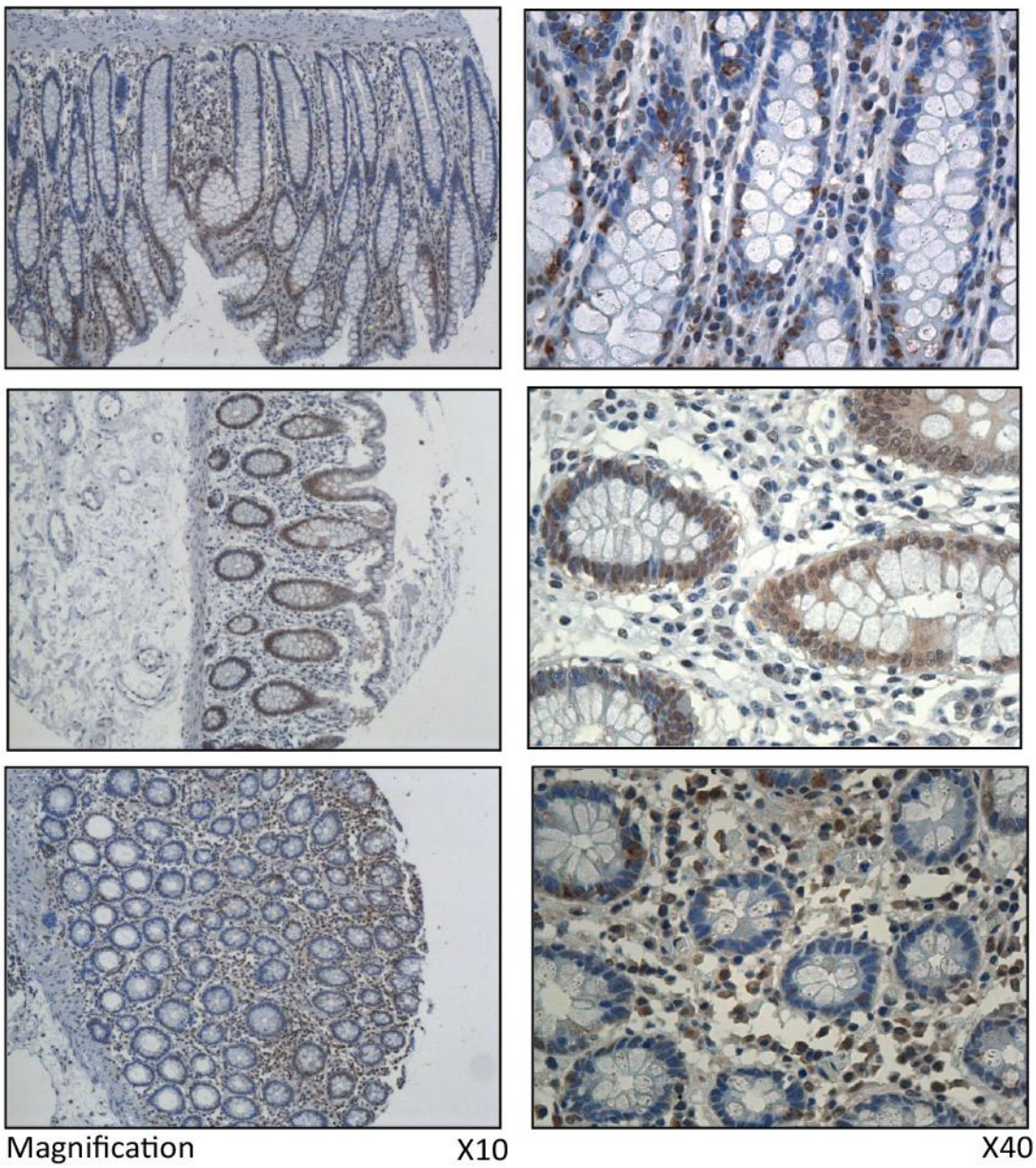
Each image in the triplet represents a separate serial section from the biopsy.

6.4. HR23B expression in normal colon and colon cancer

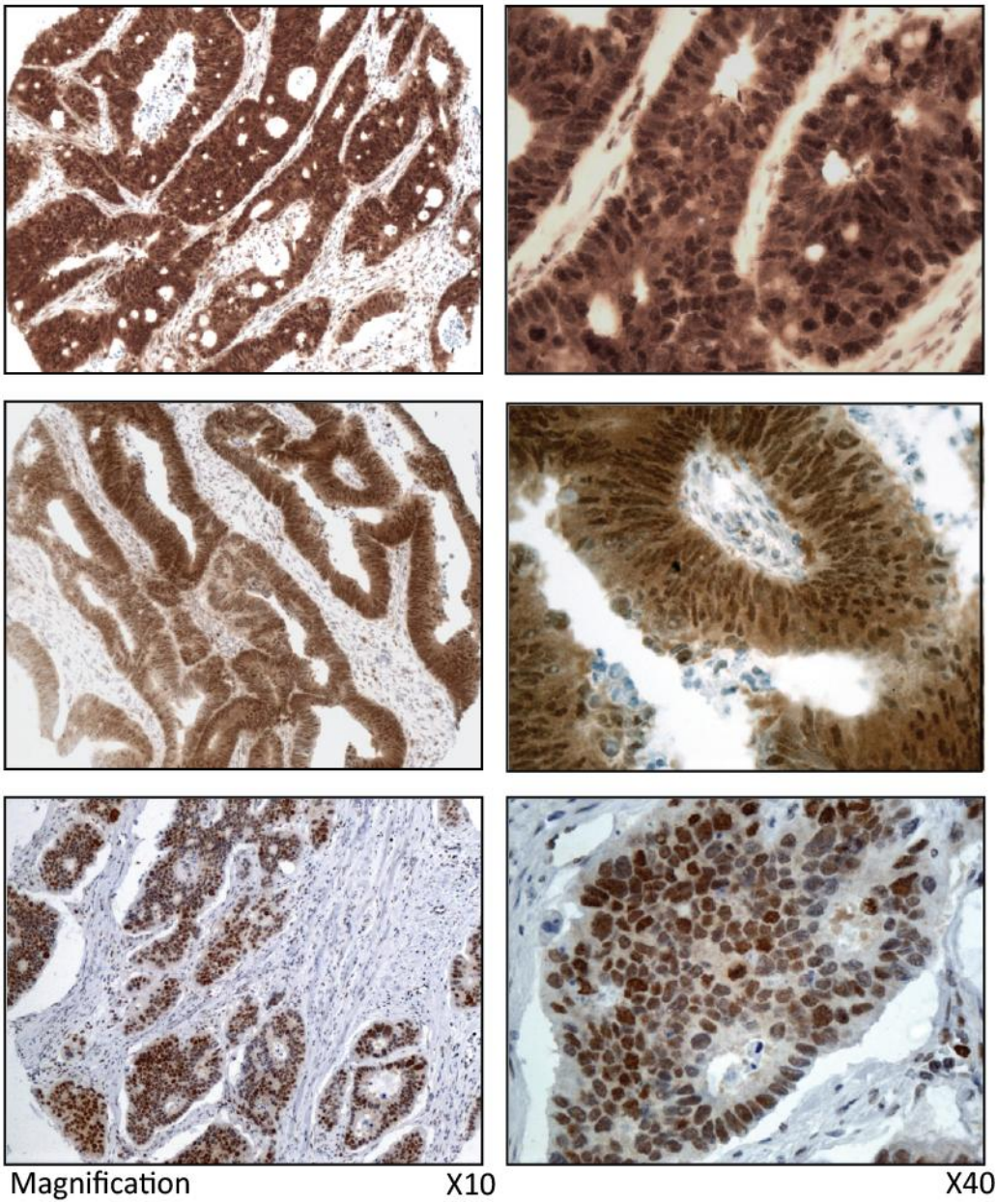
It was important to assess the expression of HR23B in a solid tumour as well as haematological cancers. Expression in colorectal cancer was initially investigated using TMAs of primary colon tumours, lymph node metastases from colorectal cancer and liver metastases from colorectal cancer. Samples were unpaired and nuclear and cytoplasmic expression was assessed separately. In addition, expression of HR23B in normal colon was also investigated.

Although there was evidence of variable staining in normal colon as well as in malignant tissue, certain patterns of expression were evident (figure 6.4).

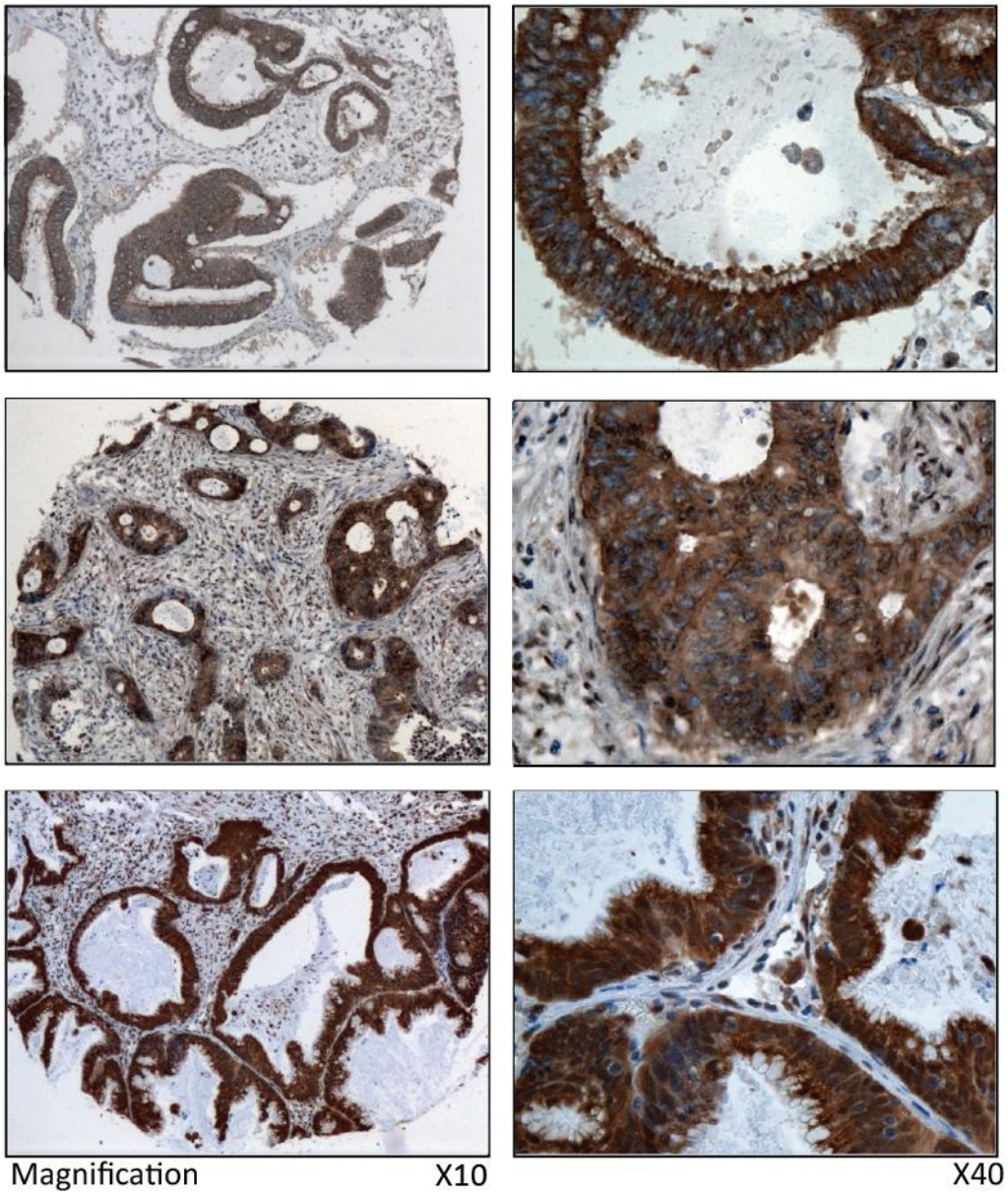
a



b



c



d

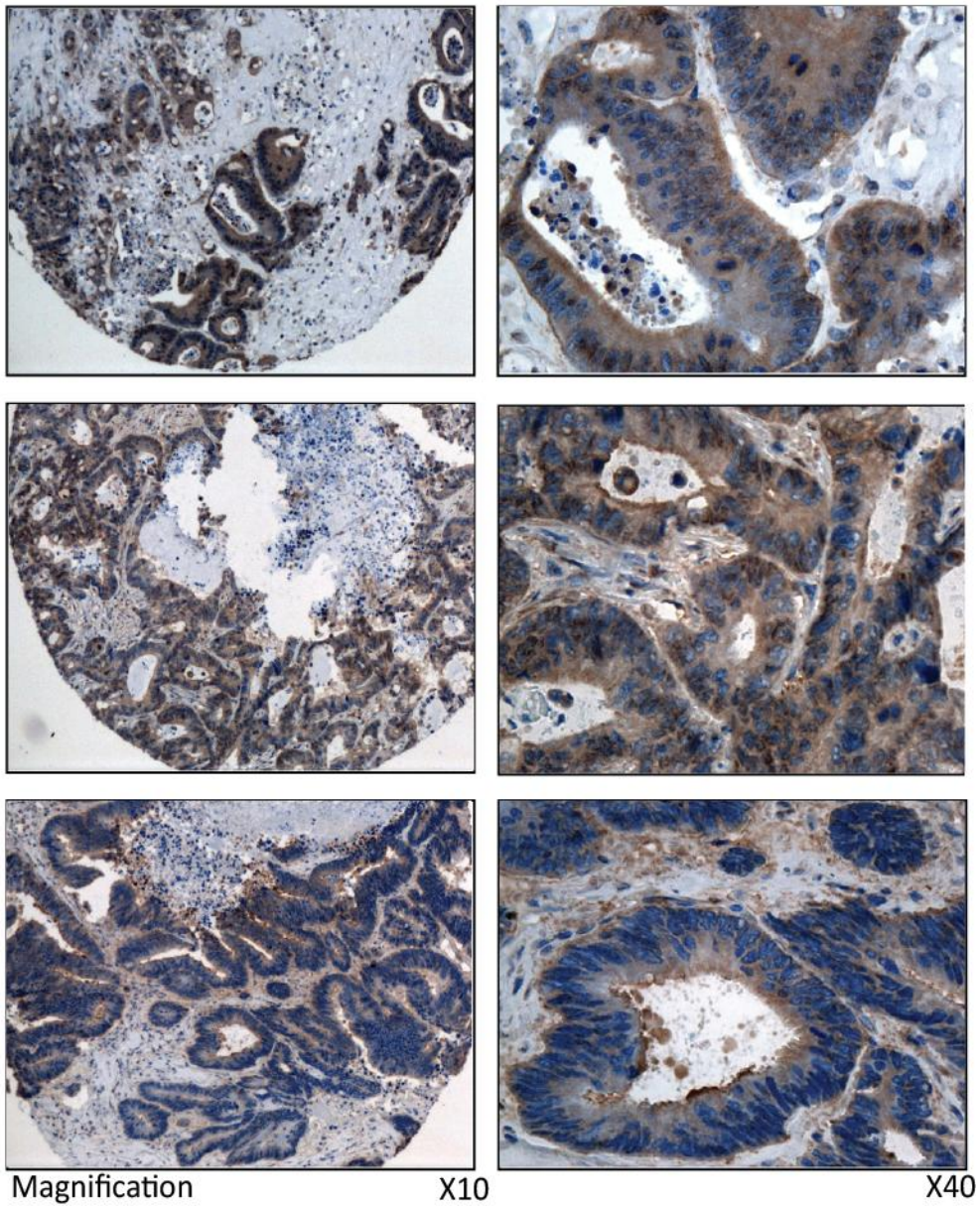


Figure 6.4

Expression of HR23B in normal colon tissue, primary colon cancer, nodal and liver metastases

Tissue microarrays of normal colon tissue, primary colon cancer, nodal and liver metastases were prepared and immunostaining with anti-HR23B was performed.

(a) Examples of HR23B expression in normal colon. HR23B expression is variable but generally weak.

(b) Examples of HR23B expression in primary colon cancer. Strong nuclear expression of HR23B is apparent.

(c) Examples of HR23B expression in nodal metastases from colon cancer. Loss of nuclear expression of HR23B is apparent at higher magnification.

(d) Examples of HR23B expression in liver metastases from colon cancer. Loss of nuclear expression of HR23B is apparent at higher magnification.

Nuclear and cytoplasmic expression of HR23B in normal colon tissues was statistically significantly less than in primary colon cancer suggesting that HR23B expression is upregulated in malignant tissues in this tumour type (figure 6.5). Nuclear expression was weaker in lymph node and liver metastases (figures 6.4c and 6.4d). Further analysis of this differences showed that the mean expression of nuclear HR23B appears to be statistically significantly lower in more advanced disease when compared to the primary colon cancer specimens although there were no differences seen in cytoplasmic staining (figure 6.5).

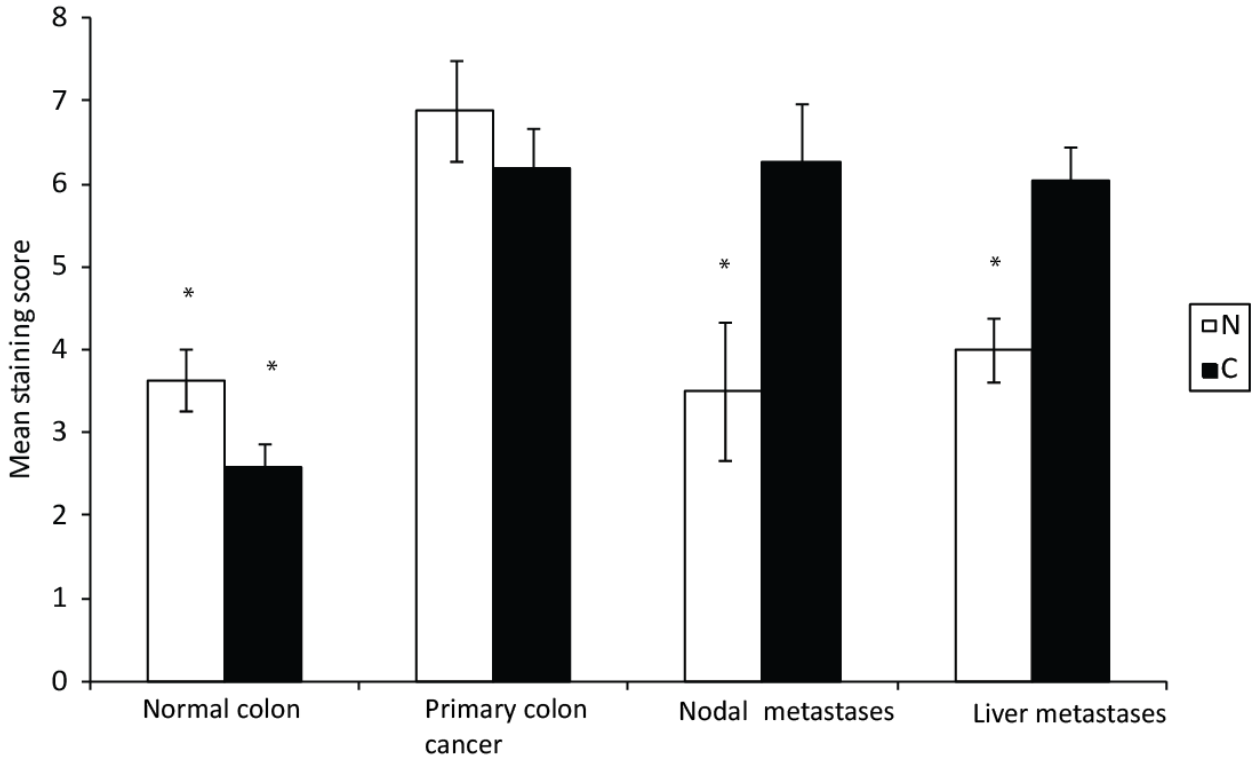


Figure 6.5

HR23B staining scores in normal colon tissue compared to primary colon cancer, nodal metastases and liver metastases (unpaired samples)

A mean staining score was derived for nuclear (n) and cytoplasmic (c) HR23B immunostaining from data collected from tissue microarrays. This was based on frequency and intensity of staining. Cytoplasmic staining was statistically significantly lower in normal colon versus malignant samples. Nuclear staining was also statistically significantly lower in normal colon versus primary colon cancer but this difference was no seen in samples from nodal and liver metastases (* significance in Mann-Whitney U non-parametric test; * $P < 0.05$, error bars, SEM).

6.5. HR23B expression in CTCL biopsies from a phase II clinical trial with SAHA

To determine whether the expression level of HR23B is a clinically useful biomarker for the response of CTCL to HDAC inhibitor therapy, an analysis was performed on a collection of CTCL biopsies taken from a phase II clinical trial of SAHA (Duvic et al., 2007). Paired skin-lesion biopsies from before and after SAHA treatment were assessed in 20 out of the 33 trial patients, using immunohistochemistry on paraffin-embedded formalin-fixed tissue. A total of 21 samples were available for analysis of pre-treatment expression because one patient (patient 8) had two distinct courses of treatment with SAHA and was therefore counted twice (table 6.2). Total staining scores for expression of HR23B in pre-treatment biopsies from patients with advanced CTCL from the phase II trial were determined. The clinical and pathological criteria assessed to define partial response (PR), stable disease (SD), or progressive disease (PD) were as described in the clinical trial. To determine the TSS, HR23B expression was assessed in the malignant lymphocytes in each biopsy.

A further 44 post treatment biopsies taken from patients undergoing active SAHA therapy were also analysed for HR23B expression, giving a total of 65 biopsies from the phase II clinical trial.

Table 6.2: Summary of phase II clinical trial patients, total staining score, and clinical outcome

Patient number	Total staining score	Outcome
1	7	PR
2	8	PD
3	7	PD
4	6	PD
5	8	PR
6	7	PR
7	6	PR
8a	9	PR
8b	5	PD
9	5	SD
10	10	SD
11	8	PD
12	5	PD
13	8	SD
14	7	PD
15	7	PR
16	6	SD
17	8	PR
18	5	SD
19	7	PR
20	5	PD

Abbreviations: PR, partial response; SD, stable disease; PD, progressive disease

The biopsies were scored blind by two independent pathologists and a semi quantitative analysis based upon intensity and frequency of HR23B staining and the type of dermal and epidermal infiltrate was performed on each biopsy (Table 2.2 materials and methods). A total staining score (TSS) was determined out of 13, where a score of greater than or equal to 6 was considered to be

strong HR23B staining. The threshold for differentiating between positive and negative immunostaining was set at a TSS of 6. This optimal cut-off was determined by the receiver operating characteristic curve distribution analysis. The TSS was then compared with clinical outcome, namely PR, SD, or PD (table 6.2).

Using pre-treatment expression of HR23B in the 20 trial patients, the proportion of patients with strong staining who had a clinical response was 68.8% (table 6.3). Therefore, the positive predictive value (PPV) of HR23B in this sample set was determined to be 68.8%. When the pre- and post treatment biopsies were combined (a total of 65 biopsies), a similar PPV was evident at 71.7% (table 6.4).

Table 6.3: Summary of TSS for pre-treatment expression of HR23B in biopsies from phase II clinical trial. Distribution of patients categorized as having high (≥ 6) or low (< 6) TSS for HR23B according to response to treatment (PR/SD) or no response to treatment (PD) in patients from the phase II trial. Values relating to the pre-treatment expression of HR23B are shown. Statistical significance was assessed using Fisher's exact test. Positive predictive value: 68.8%; one-tailed P = 0.262126; two-tailed P = 0.325372.

TSS	PR/SD	PD	Total
≥ 6	11	5	16
< 6	2	3	5
Total	13	8	21

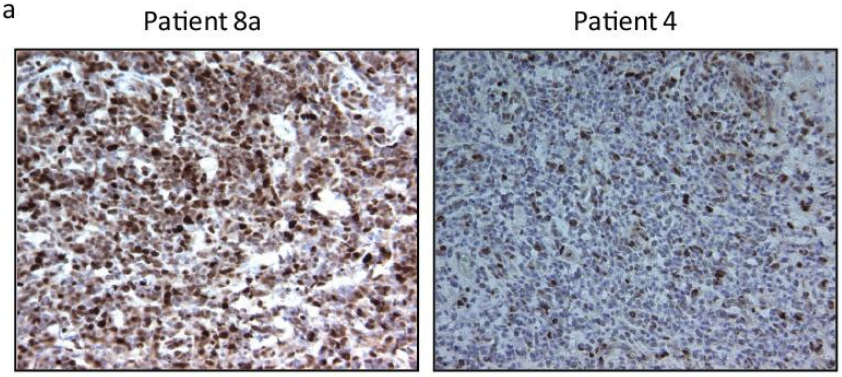
Table 6.4: Summary of TSS for pre-treatment and post treatment expression of HR23B in biopsies from phase II clinical trial. Distribution of patients categorized as having high (≥ 6) or low (< 6) TSS for HR23B according to response to treatment (PR/SD) or no response to treatment (PD) in patients from the phase II trial treated with SAHA. Values for pre-treatment and post-treatment expression of HR23B are shown. Statistical significance was assessed using Fisher's exact test. Positive predictive value: 71.7%; one-tailed P = 0.0522323; two-tailed P = 0.0874581.

TSS	PR/SD	PD	Total
≥ 6	38	15	53
< 6	5	7	12
Total	43	22	65

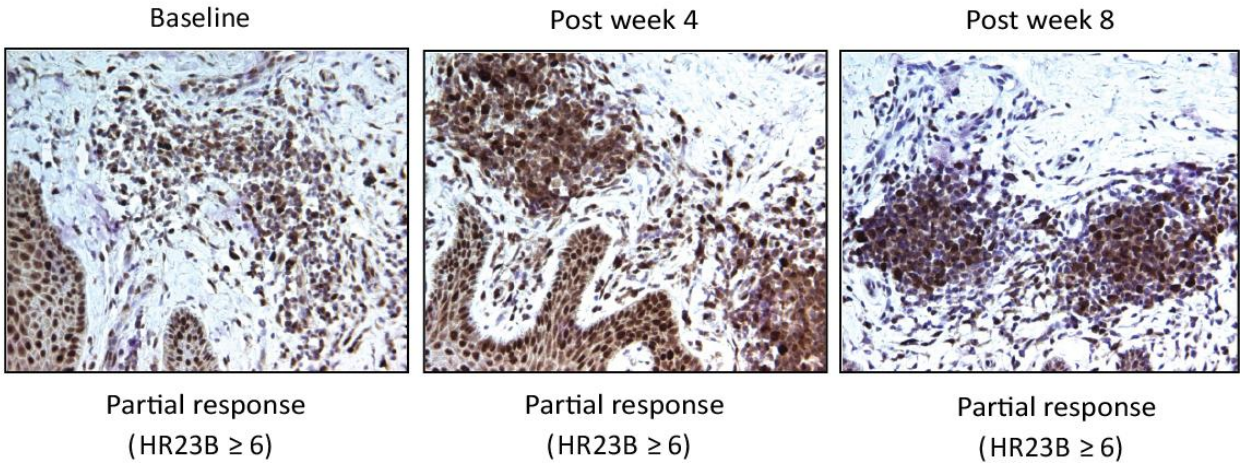
The PPVs of both pre-treatment and pre- and post-treatment samples were not statistically significant. This is likely to be due to the small sample sizes in both groups analysed. However, a PPV of around 70% can be considered to be clinically significant in a rare tumour type and it is conceivable that in future studies using larger sample sizes, statistical significance may be achievable.

Pre-treatment expression of HR23B in patient 8a provided an example of a high level of expression where a partial response to SAHA was observed and, by contrast, expression in patient 4 was low and this patient's disease progressed after SAHA treatment (Fig. 6.6a). Biopsies from patient 15 demonstrated that expression of HR23B remained high throughout the time that the patient was undergoing a partial response to SAHA (Fig. 6.6b). Very interestingly, the expression of HR23B coincided with both a response and lack of response in the same patient who was treated with two separate courses of SAHA (Fig. 6.6c). Thus, patient 8 had high baseline expression of HR23B and derived clinical benefit from SAHA after the first course of treatment, undergoing a partial response. However, 6 weeks into the second course of treatment, the patient's disease became unresponsive and progressive disease was apparent. This lack of response coincided with an almost complete absence of HR23B expression in the tumour mass (Fig. 6.6c). Together, these results suggest that HR23B may be an informative biomarker to identify CTCL patients who will undergo a favourable clinical response to SAHA.

a



b Patient 15



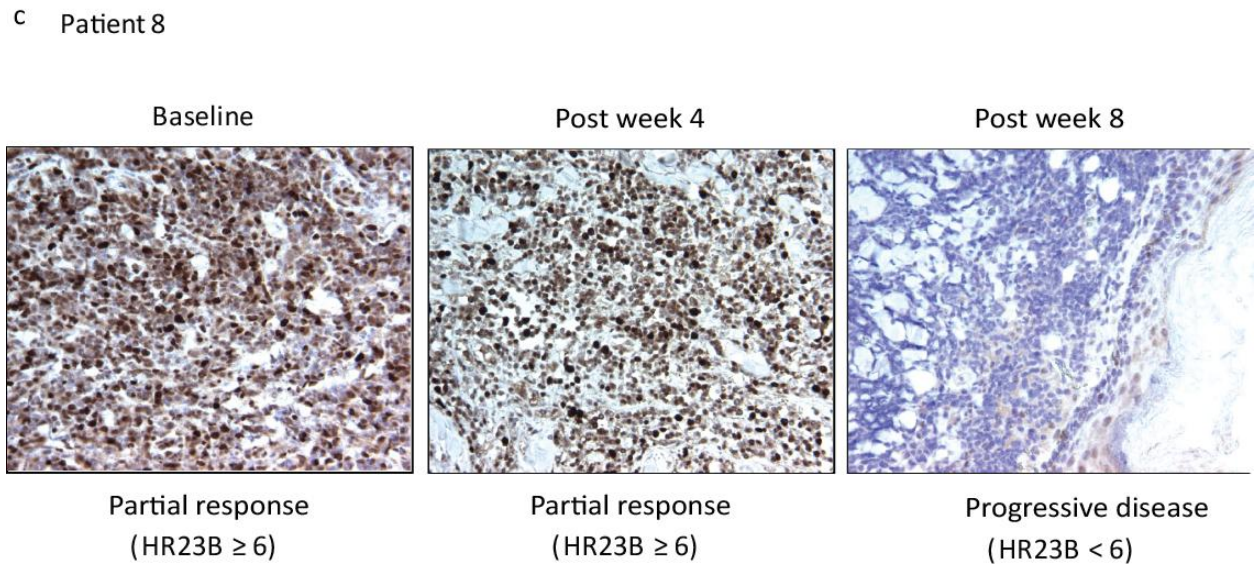


Figure 6.6

HR23B expression in SAHA-treated CTCL biopsies

(a) Representative images of the CTCL biopsies for patient 8a, who underwent a partial response (PR) following treatment with SAHA for 27 weeks before relapsing, and patient 4, who exhibited progressive disease (PD) following 2 weeks on SAHA. Note that HR23B immunostaining is noticeably stronger in the former compared with the latter. The TSS for HR23B is shown in brackets.

(b) Representative images of HR23B immunostaining in CTCL biopsies performed on pre-treatment and week-4 and week-8 biopsies from patient 15, who presented with Sézary syndrome and underwent a PR throughout SAHA treatment. The TSS for HR23B is indicated.

(c) Representative images of HR23B immunostaining in CTCL biopsies performed on pre-treatment and post treatment week-8 biopsies from patient 8, who underwent a PR following SAHA treatment. Following 27 weeks of SAHA treatment, the patient underwent PD and was subsequently placed on a different dose of SAHA. The patient

exhibited PD after 6 weeks of treatment. HR23B immunostaining performed on post treatment week-6 biopsy from this second dose of SAHA is illustrated. The TSS for HR23B is indicated.

HR23B expression in CTCL patients treated with HDAC inhibitors other than SAHA was analysed and pre-treatment biopsies taken from CTCL patients treated with PXD101 (1 patient), depsipeptide/FK228 (2 patients), and LBH589 (4 patients), both pre- and post treatment. A total of 21 biopsies were tested and ranked according to the HR23B TSS as described earlier (table 6.5).

Table 6.5: Summary of TSS in CTCL biopsies taken from patients treated with PXD101 and depsipeptide. Distribution of patients categorized as having high (≥ 6) or low (< 6) TSS for HR23B according to response to treatment (PR/SD) or no response (PD) in patients treated with PXD101, depsipeptide, or LBH589. Positive predictive value: 64.7%.

TSS	PR/SD	PD	Total
≥ 6	11	6	17
< 6	3	1	4
Total	14	7	21

One of the patients provided an example of pre-treatment HR23B staining and following treatment with PXD101 after 7 cycles (figure 6,7a). The pre-treatment HR23B TSS was greater than 6, when the patient underwent a partial response. This contrasted with later during the treatment regime (cycle 7), when the TSS was less than 6, which coincided with disease progression. Another patient provided an example of HR23B biopsy staining and TSS score after treatment with depsipeptide (figure 6.7b). HR23B remained high during the time when the patient underwent a partial response to depsipeptide (pre-treatment and cycle 2), and was low at drug cycle 3 when it coincided with disease progression. A total of 21 biopsies were characterized according to HR23B TSS (table 6.5). Comparing the TSS value with clinical outcome gave a PPV of 64.7%. This value rests on a smaller number of biopsies analyzed compared with the SAHA trial biopsies (table 6.4), and as a consequence was not open to statistical analysis. Nevertheless, the PPV continues to support the favourable coincidence between HR23B levels and clinical outcome. Thus, HR23B might be considered as a biomarker for HDAC inhibitor-based therapies in addition to SAHA.

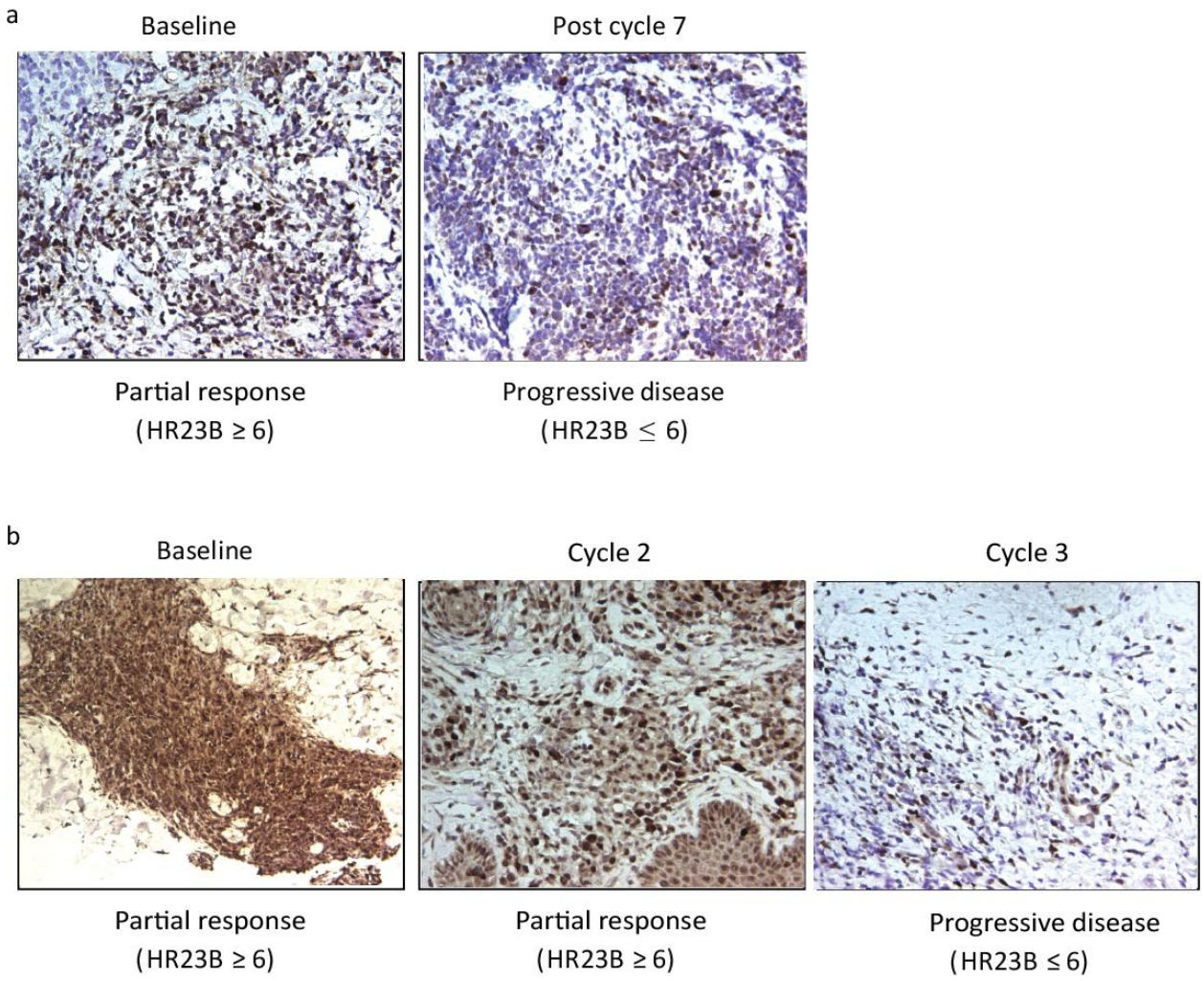


Figure 6.7

HR23B expression in PXD101 and depsipeptide-treated CTCL biopsies

(a) Representative images are shown of the CTCL biopsies from a patient treated with PXD101 who underwent a partial response following treatment but relapsed when the disease progressed after treatment with seven cycles of PXD101. Note that HR23B immunostaining is noticeably stronger at pre-treatment compared with when the patient's disease was progressing (after seven cycles of treatment). The TSS for HR23B is shown in parentheses.

(b) Representative images of HR23B immunostaining performed on pre-treatment and after cycle-2 and cycle-3 biopsies from a patient who underwent a partial response following depsipeptide treatment for two cycles but then the disease progressed after the third cycle of treatment. Note that HR23B immunostaining is noticeably stronger at pre-treatment and up to cycle 2 compared with when the patient's disease was progressing after cycle 3. The TSS for HR23B is shown in parentheses.

The negative predictive value (NPV) is defined as the proportion of subjects with a negative test result who are correctly diagnosed. This was determined for each of the three groups of patients (table 6.6). These values need to be interpreted with caution as the numbers of patients are very small (5 in the pre-treatment group, 14 in the all biopsies group and 7 in the other HDAC inhibitor-treated group). The NPV is lower than the PPV and this therefore suggests that measuring HR23B using the scoring system described is not as efficient at identifying patients with low expression who do not respond to therapy than those with high expression who respond.

Table 6.6: Negative predictive value of HR23B in retrospective analysis of SAHA treated CTCL patients

Patient group	Negative predictive value (%)
Pre-treatment biopsies (phase II clinical trial)	60
All biopsies from phase II clinical trial	50
Other HDAC inhibitor treated patient biopsies	14.3

6.6. Conclusion.

HR23B expression using immunohistochemistry shows intra-tumour and inter-tumour variability. Expression is both within the nucleus and cytoplasm although there is more variability in nuclear expression. Expression appears to be higher in malignant cells as evidenced by data in CTCL and colorectal cancer when compared to non-malignant tissues. In colorectal cancer, there appears to be a loss of nuclear HR23B staining with more advanced disease and cytoplasmic staining is similar in unpaired samples across the different disease stages.

There was a frequent coincidence between HR23B and clinical response to HDAC inhibitor therapy, supporting the idea that HR23B may be a clinically useful biomarker. HR23B represents a biomarker defined through a functional loss-of-function screen that may find clinical utility as a predictor of therapeutic response.

CHAPTER 7

RESULTS

DETECTION OF HR23B AND LC3 EXPRESSION IN HUMAN TUMOURS AND THEIR PROGNOSTIC ROLE IN COLORECTAL CANCER

7.1. Introduction.

HR23B levels impact on the outcome of treatment with HDAC inhibitor therapy. It is crucial to evaluate the significance of these findings in the context of the pathology of clinical disease. HR23B expression using immunohistochemistry has been evaluated and it is known that LC3 is a marker for autophagocytic cells (Kabeya et al., 2000). Previous studies have demonstrated that LC3 can be utilized as a marker of autophagy using immunohistochemistry (Mizushima et al., 2010b). Therefore, HR23B and LC3 expression were evaluated in the same biopsies from colorectal cancer.

Additionally, the effect of the HDAC inhibitor valproic acid (VPA) was explored in the clinical setting, specifically with respect to the pathology of HR23B and LC3 expression in tumour biopsies taken pre- and post-treatment in melanoma patients undergoing resection of either lymph nodes and/or metastases. The aim of this analysis was to determine if there were any parallels seen in expression of HR23B and LC3 in human tissues when compared to expression of both these proteins after HDAC inhibitor treatment assessed using immunoblotting.

Autophagy is being increasingly recognised as a mechanism that cancer cells use to survive under adverse conditions, for example chemotherapy. It is therefore plausible that tumours exhibiting different levels of HR23B and LC3 may differ in their clinical course and prognosis, reflecting the detrimental effect that autophagocytic tumour cells might have on therapeutic response. HR23B and LC3 expression were therefore evaluated in a collection of stage II and III colorectal cancer biopsies from a phase III, randomised, double blind, placebo-controlled study

of rofecoxib in colorectal cancer patients following potentially curative therapy (Midgley et al., 2010).

7.2. HR23B expression and autophagy in human tumours

TMAs of primary colorectal cancer and primary melanoma were selected and expression of HR23B and LC3 in was assessed (table 2.1). There was considerable variation on expression of both HR23B and LC3 in the same collection of colorectal cancer biopsies (figure 7.1). An expression profile of positive HR23B and negative LC3, and conversely negative HR23B and positive LC3 was evident (18% and 16% respectively of the total analysed). Thus, the relationship between HR23B and LC3 observed in cell line experiments, where the level of HR23B impacts on the propensity of cells to enter autophagy (measured by LC3 levels), was apparent *in situ*.

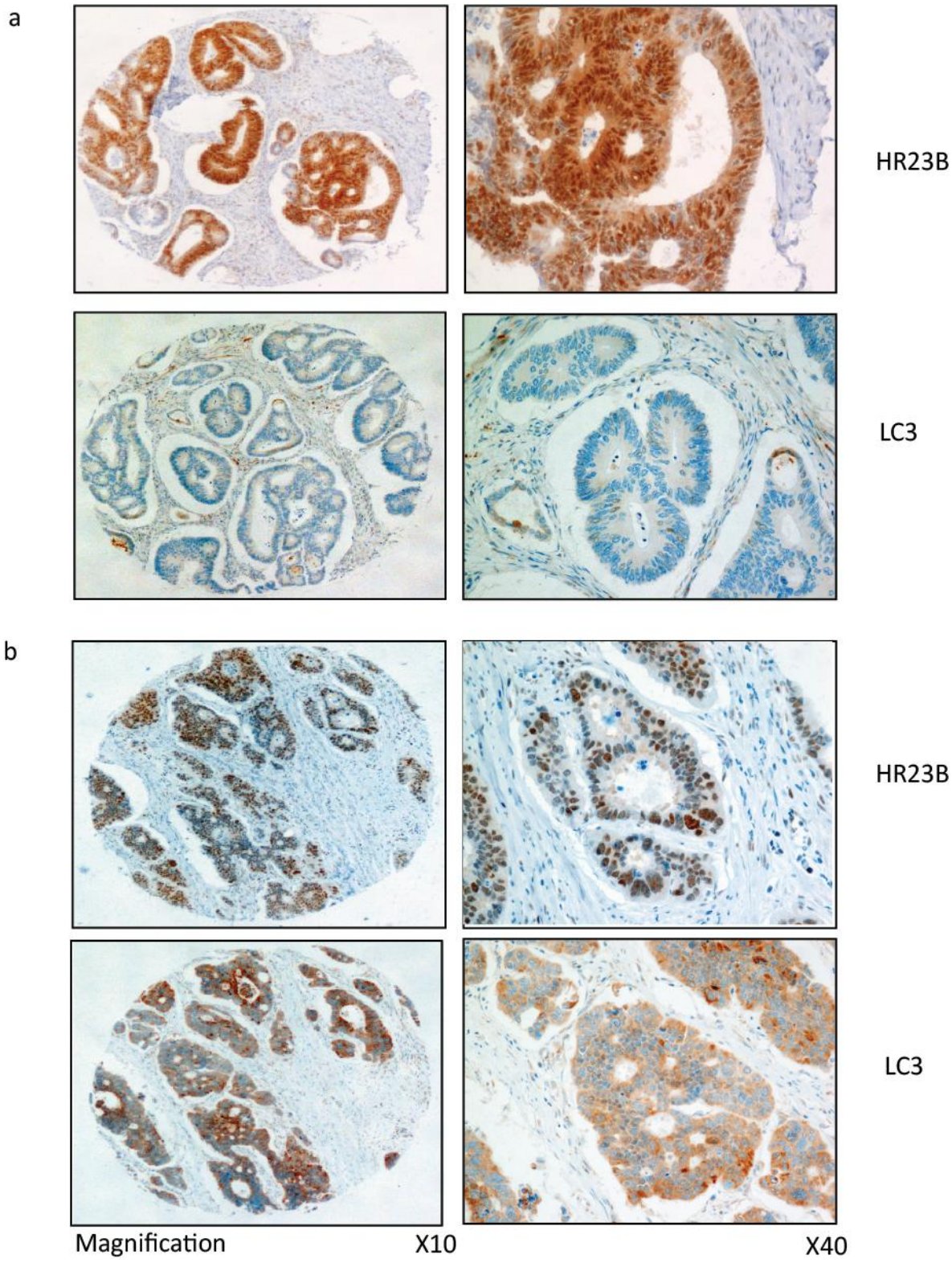

a
HR23B
LC3
b
HR23B
LC3
Magnification
X10
X40

Figure 7.1

HR23B and LC3 expression in colorectal cancer

Serial samples from a TMA of primary colorectal cancer were immunostained with anti-HR23B and anti-LC3 and strong and weak staining specimens were identified according to frequency and intensity of staining.

(a) Examples of neoplastic colorectal cancer cells staining positively for HR23B (top panel) and negatively for LC3 (bottom panel).

(b) Examples of neoplastic colorectal cells staining negatively for HR23B (top panel) and positively for LC3 (bottom panel).

Each image in the doublet represents a separate serial section from the biopsy.

Expression of HR23B and LC3 was also determined in melanoma specimens to investigate if this phenomenon is observed in another tumour type. In primary melanoma, heterogeneity in staining was also observed (figure 7.2). Tumours positive for HR23B and negative for LC3, and others negative for HR23B and positive for LC3 were again observed (11% and 14% respectively). Therefore, across both types of tumours examined, subgroups of tumours positive for HR23B and negative for LC3 and negative for HR23B and positive for LC3 were apparent.

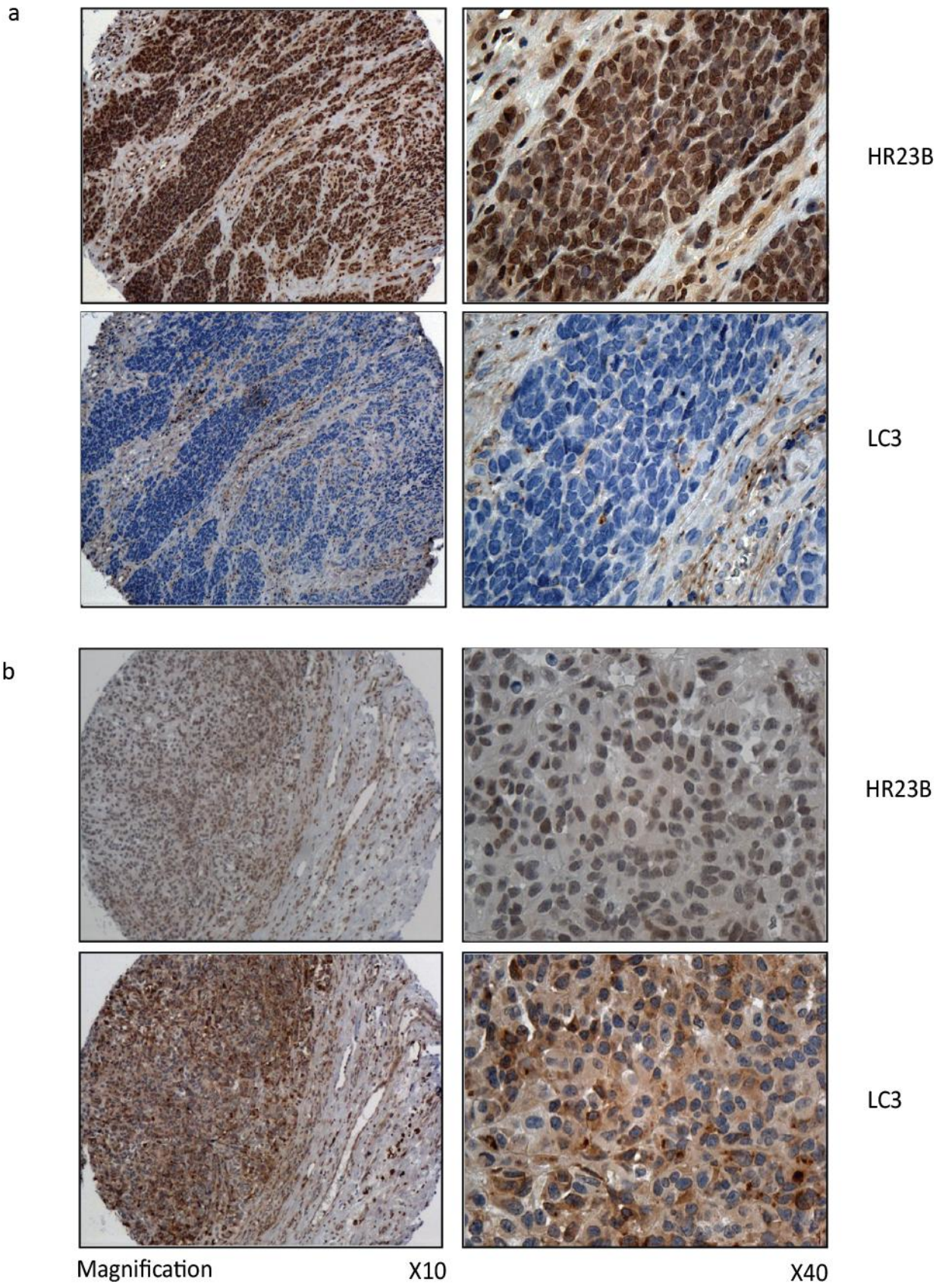

a
HR23B
LC3
b
HR23B
LC3
Magnification
X10
X40

Figure 7.2

HR23B and LC3 expression in primary melanoma

Serial samples from a TMA of primary melanoma were immunostained with anti-HR23B and anti-LC3 and positive and negative staining specimens were identified according to frequency and intensity of staining.

(a) Examples of neoplastic melanoma cells staining positively for HR23B (top panel) and negatively for LC3 (bottom panel).

(b) Examples of neoplastic melanoma cells staining negatively for HR23B (top panel) and positively for LC3 (bottom panel).

Each image in the doublet represents a separate serial section from the biopsy.

7.3. Autophagy during HDAC inhibitor treatment in patients

A small pilot study was performed where HR23B and LC3 expression were analysed in a series of biopsies from melanoma patients due to have lymph node surgery or excision of subcutaneous metastases pre-treated with valproic acid. Selected pre-treatment biopsies were available for comparison with post-treatment specimens.

In one patient where pre-treatment biopsies were available, HR23B expression was negative and LC3 expression was also negative (figure 7.3). This pattern contrasted with biopsies taken from patients treated with valproic acid; there were changes in the overall pathology of the tumour but also in the pattern of immunostaining (figure 7.4). Separate and alternate zones with positive and negative HR23B immunostaining were apparent, contrasting with the negative staining seen in

the pre-treatment biopsy. Interestingly, the post-treatment biopsy had closely demarcated zones where a punctate cytoplasmic pattern of LC3 was evident (considered to be positive). In these areas, HR23B expression was frequently negative. Positive expression of HR23B frequently coincided with negative LC3 immunostaining.

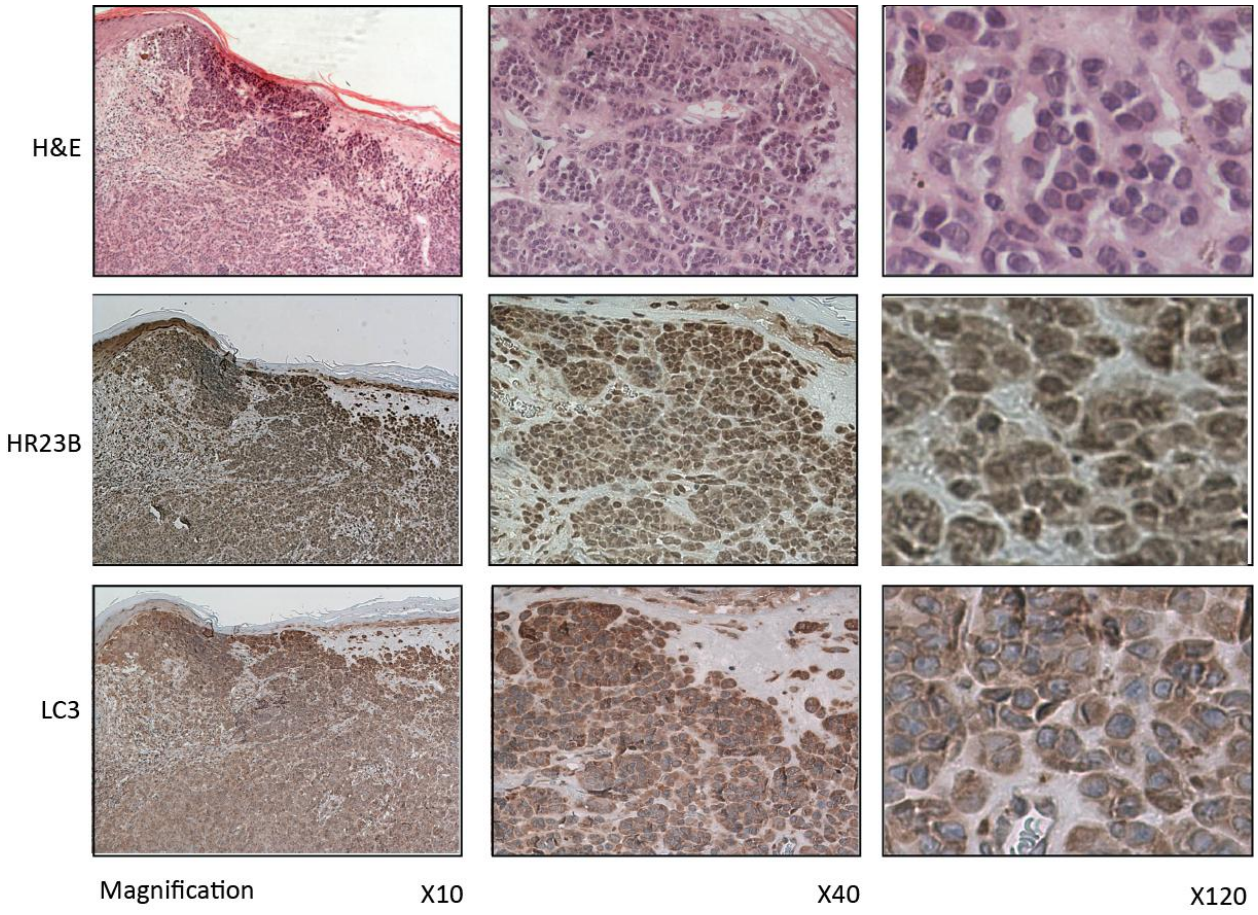


Figure 7.3

HR23B and LC3 expression in primary melanoma samples

Biopsies were obtained from patients with primary melanoma and serial sections were stained with H&E, anti-HR23B and anti-LC3. Examples of neoplastic melanoma cells stained with H&E, HR23B and LC3 as indicated.

Each image in the triplet represents a separate serial section from the biopsy.

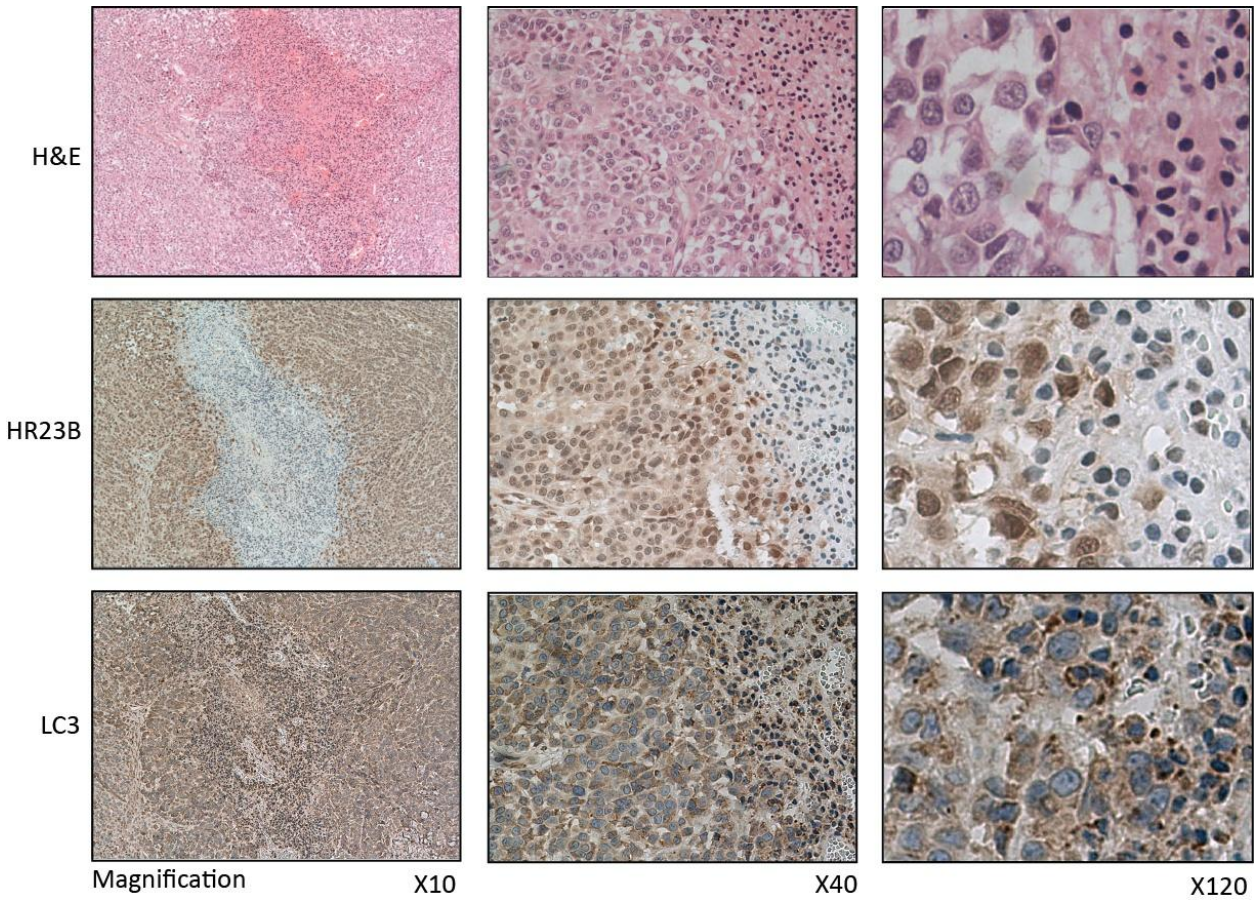


Figure 7.4

HR23B and LC3 expression in melanoma samples treated with valproic acid

Biopsies of melanoma metastases from patients pre-treated with valproic acid (VPA) were obtained and serial sections were stained with H&E, anti-HR23B and anti-LC3. Examples of neoplastic melanoma cells stained with H&E, HR23B and LC3 as indicated at different magnifications as shown. A section of tumour tissue is indicated which are negative for HR23B and is correspondingly positive for LC3 expression. There is also a rim of tissue adjacent where nuclear HR23B expression appears to be positive.

Each image in the triplet represents a separate serial section from the biopsy.

Further post-treatment biopsy specimens were available from two individual patients (figure 7.5). In both of these specimens, HR23B expression was generally negative and this coincided with positive LC3 expression. In one final patient where both pre- and post-treatment biopsy specimens were available, HR23B expression was positive both pre- and post-treatment and corresponding LC3 expression was negative (figure 7.6).

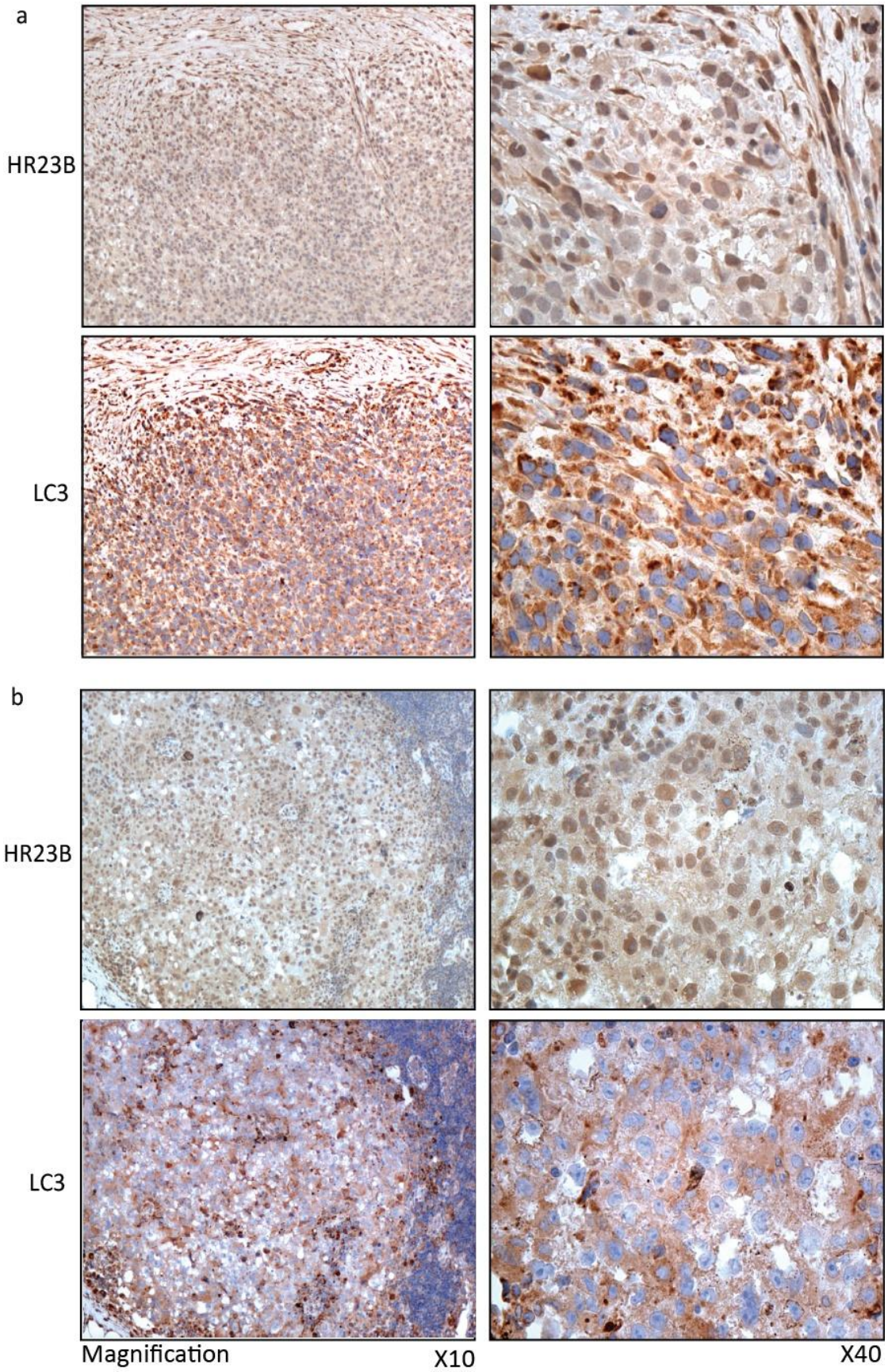

a
HR23B
LC3
b
HR23B
LC3
Magnification
X10
X40

Figure 7.5

HR23B and LC3 expression in melanoma samples treated with valproic acid from pilot clinical trial

Biopsies of melanoma metastases from two patients pre-treated with valproic acid (VPA) were obtained and serial sections were stained with H&E, anti-HR23B and anti-LC3. Examples of neoplastic melanoma cells stained with H&E, HR23B and LC3 as indicated at different magnifications as shown. In both examples, HR23B expression is negative and LC3 expression is positive.

(a) Examples of neoplastic melanoma cells stained with HR23B and LC3 as indicated.

(b) Second example of neoplastic melanoma cells stained with HR23B and LC3 as indicated.

Each image in the doublet represents a separate serial section from the biopsy.

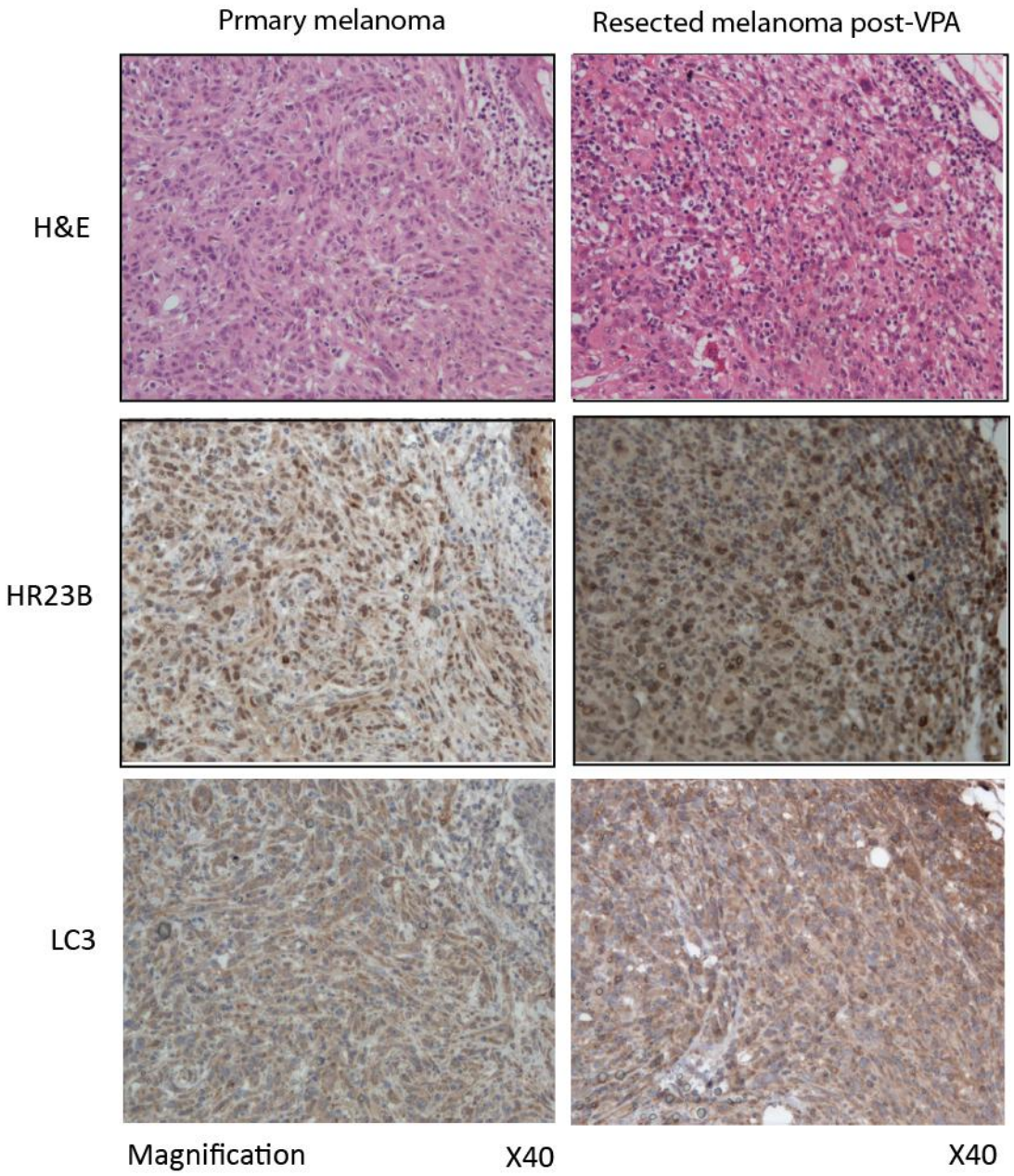


Figure 7.6

HR23B and LC3 expression in resected primary melanoma samples and resected metastases post-treatment with valproic acid (VPA)

Examples of neoplastic melanoma cells from primary resected melanoma stained with H&E, anti-HR23B and anti-LC3 as indicated (left panel)

Examples of neoplastic melanoma cells from resected metastases post-treatment with the HDAC inhibitor valproic acid; stained with H&E, anti-HR23B and anti-LC3 as indicated (right panel). Note that both HR23B and LC3 immunostaining remains similar when pre-treatment and post-treatment specimens are compared.

These results, derived from studying the expression of HR23B and LC3 in human subjects treated with an HDAC inhibitor are thus consistent with the hypothesis that HR23B influences the outcome of treatment. In a similar manner to the effect of HR23B on apoptosis and autophagy observed in tumour cell lines, a coincidental relationship was apparent between the expression of HR23B and the presence of autophagocytic tumour cells.

7.4. Prognostic significance of HR23B and LC3

HR23B and LC3 levels were assessed in a collection of stage II and III colorectal cancer tumour specimens from the VICTOR trial. Demographic and treatment details for all trial patients as well as the patients' samples available for immunohistochemical analysis are provided in table 1. A total of almost 300 patient samples were stained and results for both proteins were available from 204 patients. A total of around 1200 biopsies were screened (samples in triplicate with matched normal colon biopsies) and given a score reflecting the overall staining characteristics of HR23B and LC3 which was then related to clinical outcome (disease free survival; DFS and overall survival; OS). In the original trial about half of the patients had stage II and the other half had stage III disease; in the samples available for immunostaining, almost two thirds of samples were from patients with stage III disease.

Table 7.1: Baseline patient of VICTOR trial patients. Details provided of all patients and those who did and did not provide samples for research and those with evaluable samples for immunostaining

		VICTOR patients (N=2434) N (%)	Patients without Samples (N=1428) N (%)	Patients with samples (N=1006) N (%)	Patients to be analysed (N=204) N (%)
Cancer Site	Colon	1592 (65.41)	914 (64.01)	678 (67.40)	138 (67.65)
	Junction	181 (7.44)	102 (7.14)	79 (7.85)	15 (7.35)
	Rectum	661 (27.16)	412 (28.85)	249 (24.75)	51 (25.00)
Stage	Stage II	1159 (47.62)	667 (46.71)	492 (48.91)	64 (31.37)
	Stage III	1275 (52.38)	761 (53.29)	514 (51.09)	140 (68.63)
Chemotherapy	None	1580 (64.9)	943 (66.04)	369 (36.68)	58 (28.43
	Yes	854 (35.1)	485 (33.96)	637 (63.32)	146 (71.57)
Radiotherapy	Yes	299 (12.3)	191 (13.38)	108 (10.74)	18 (8.82)
	None	2135 (87.7)	1237 (86.62)	898 (89.26)	186 (91.18)
Gender	Male	1560 (64.09)	650 (64.61)	910 (63.73)	129 (63.24)
	Female	874 (35.91)	656 (35.39)	518 (36.27)	75 (36.76)
Age	Age (mean (SD))	63.78 (9.68)	63.52 (9.54)	64.15 (9.87)	64.91 (10.14)
Treatment	Placebo	1217 (50.0)	722 (50.6)	706 (49.4)	97 (47.55)
	Vioxx	1217 (50.0)	495 (49.2)	511 (50.8)	107 (52.45)

7.4.1 HR23B expression

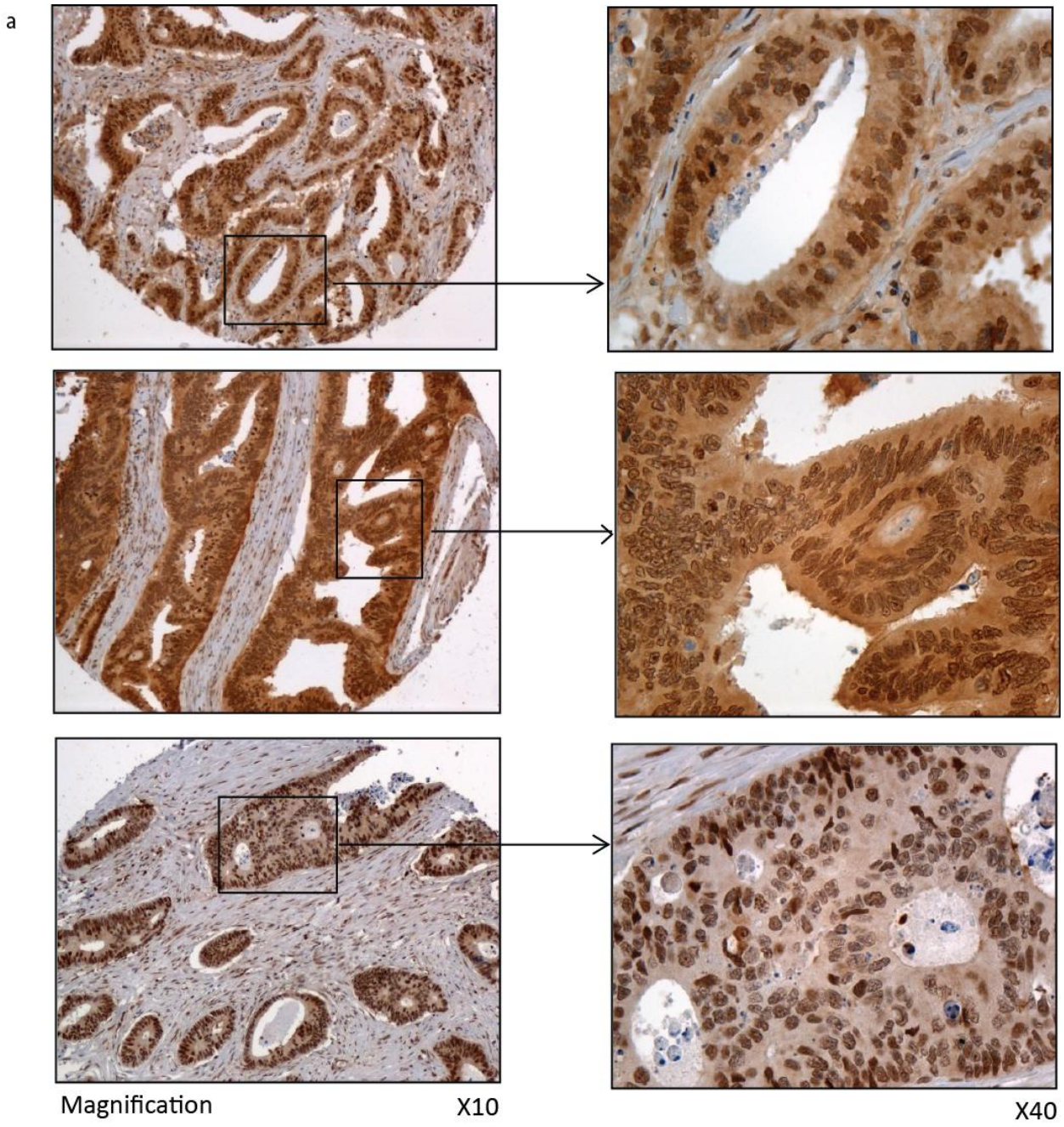
The number of deaths and recurrences as well as overall and disease free survival of the patients whose samples were stained for HR23B was similar when compared to the total patient population (table 7.2).

Table 7.2: Survival characteristics of VICTOR trial patients (HR23B). Details provided of all patients and those who did and did not provide samples for research and those with evaluable samples for HR23B immunostaining

	VICTOR Patients (N=2434)	Patients without samples (N=1428)	Patients with samples (N=1006)	Patients with HR23B-stained samples (N=204)
Deaths: n (%)	487 (20.0)	294 (20.59)	193 (19.18)	42 (20.59)
Recurrences/deaths (any cause)	704 (28.92)	427 (29.90)	277 (27.53)	59 (28.92)
Overall Survival (3-year % (95%CI))	87.3 (85.8, 88.6)	86.6 (84.7, 88.3)	88.1 (85.9, 90.0)	87.0 (81.4, 90.9)
Overall Survival (5-year % (95%CI))	78.2 (76.3, 78)	77.0 (74.5, 79.4)	79.7 (76.8, 82.2)	79.0 (72.1, 84.4)
Disease Free Survival (3-year % (95%CI))	74.6 (72.7, 76.3)	73.5 (71.0, 75.8)	76.1 (73.2, 78.7)	74.0 (67.2, 79.6)
Disease Free Survival (5-year % (95%CI))	66.5 (64.3, 68.7)	65.3 (62.4, 68.1)	68.2 (64.5, 71.5)	66.4 (57.7, 73.7)

There were populations of patients with positive and negative HR23B expression (figure 7.7). Almost 30% of patient samples were scored negative and the remainder were scored as positive.

Variation of expression was seen predominantly in nuclear expression of HR23B. HR23B expression was scored according to frequency and intensity of expression and total staining score (TSS) was derived. Patients were then divided into those who had developed a recurrence during the follow up period and those who had remained disease free.



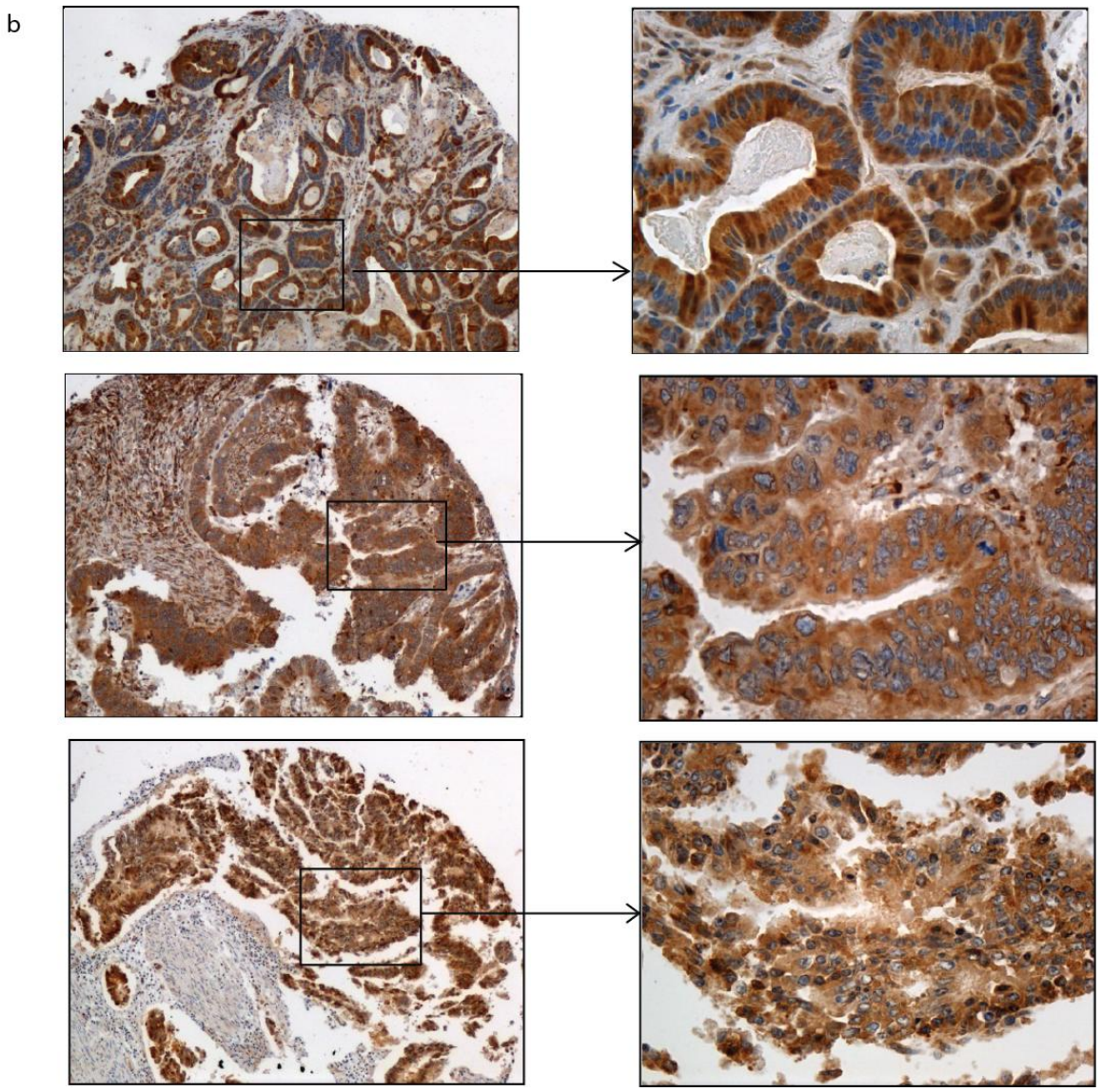


Figure 7.7

Examples of HR23B expression in colorectal cancer specimens from patients in VICTOR trial

TMAs of patient samples from the VICTOR trial were prepared and stained with anti-HR23B. Frequency and intensity of expression was assessed and in (a), nuclear HR23B expression was positive with most of the cells expressing the protein whereas in (b), nuclear expression was negative.

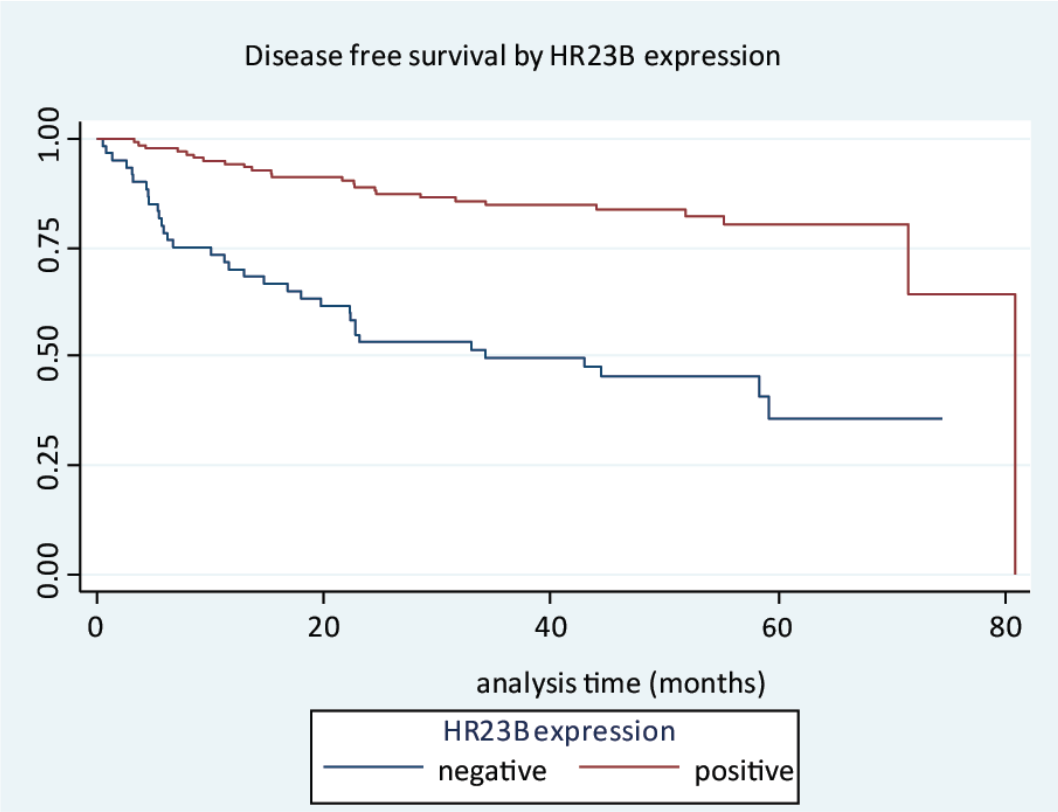
Tumours positive for HR23B had an improved DFS and OS compared to those that were negative (table 7.3). Kaplan-Meier survival curves for both disease free and overall survival demonstrated this difference (figure 7.8). Cox models showed a significant difference between negative HR23B and positive HR23B expression for overall survival and disease free survival (table 7.3). Patients with negative HR23B expression had a worse overall survival and recurrence free survival than patients with positive HR23B expression.

Table 7.3: Overall and disease free survival stratified according to HR23B expression in VICTOR trial patients. 3 and 5 year DFS and OS in months with confidence intervals for patients scoring negative or positive for HR23B

HR23B score	3-year DFS (months) (95% CI)	5-year DFS (months) (95% CI)	3-year OS (months) (95% CI)	5-year OS (months) (95% CI)
Negative	49.7 (36.6, 61.7)	35.9 (20.8, 51.2)	72.0 (58.8, 81.5)	56.5 (42.5, 68.4)
Positive	84.8 (77.4, 89.9)	80.4 (71.3, 86.9)	93.4 (87.7, 96.5)	89.4 (82.3, 93.8)

Abbreviations: DFS, disease free survival, OS, overall survival, CI, confidence intervals

a


Disease free survival by HR23B expression
1.00
0.75
0.50
0.25
0.00
0
20
40
60
80
analysis time (months)
HR23B expression
negative
positive

b

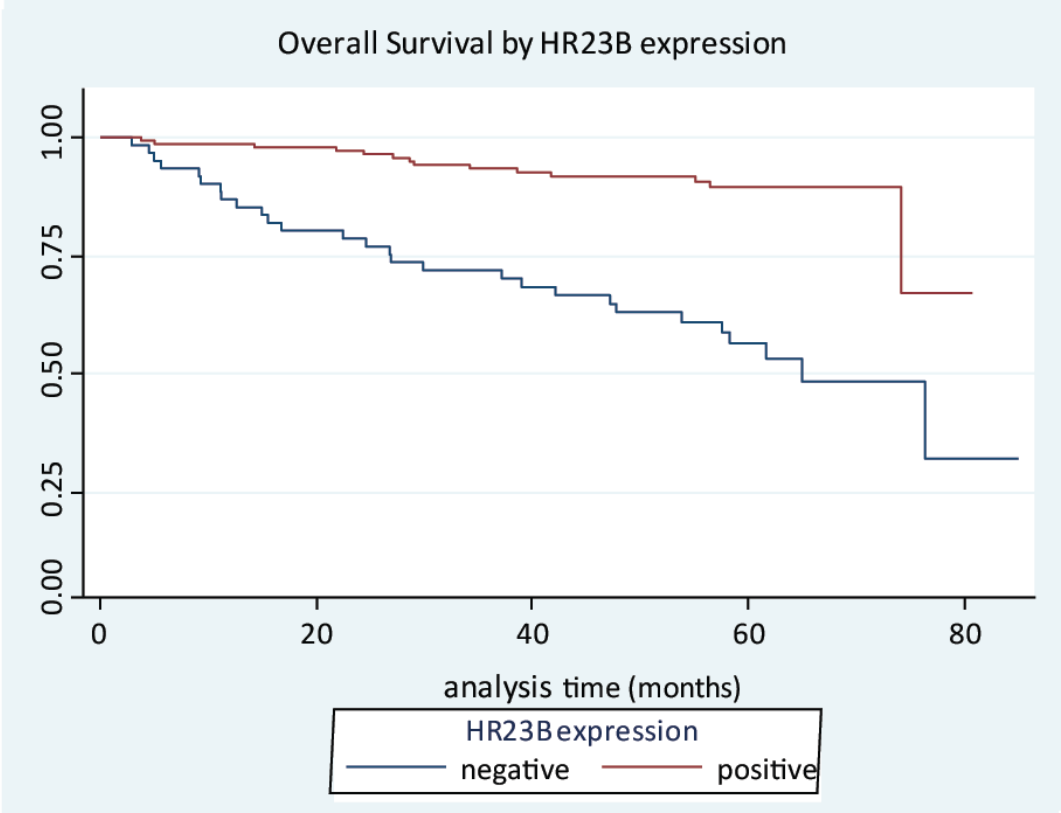

Overall Survival by HR23B expression
1.00
0.75
0.50
0.25
0.00
0
20
40
60
80
analysis time (months)
HR23B expression
negative
positive

Figure 7.8

Disease-free and overall survival in patients from VICTOR trial stratified according to HR23B expression

Nuclear HR23B expression was determined according to frequency and intensity and patients and a total staining score (TSS) was derived. Patients were thus stratified as negative or positive for HR23B expression.

(a) Kaplan –Meier plot of disease free survival stratified by expression of HR23B (assessed using TSS) over time (months). Log-rank test $p<0.001$.

(b) Kaplan-Meier plot of overall survival stratified by expression of HR23B (assessed using TSS) over time (months). Log-rang test $p<0.001$.

Table 7.4: Results of three separate univariate Cox models estimating effect of HR23B on disease free and overall survival. Hazard ratios are in comparison to a negative (0) score.

HR23B	Explanatory variable	Univariate analysis		Multivariate analysis*	
		Hazard ratio (95% CI)	p-value	Hazard ratio (95% CI)	p-value
DFS	Positive vs. negative	0.23 (0.14, 0.39)	<0.001	0.24 (0.14, 0.41)	<0.001
OS	Positive vs. negative	0.19 (0.10, 0.37)	<0.001	0.21 (0.11, 0.40)	<0.001

Abbreviations: DFS, disease free survival, OS, overall survival

*age at randomisation, gender, chemotherapy, radiotherapy, treatment, disease site and stage were also included in the multivariate analysis.

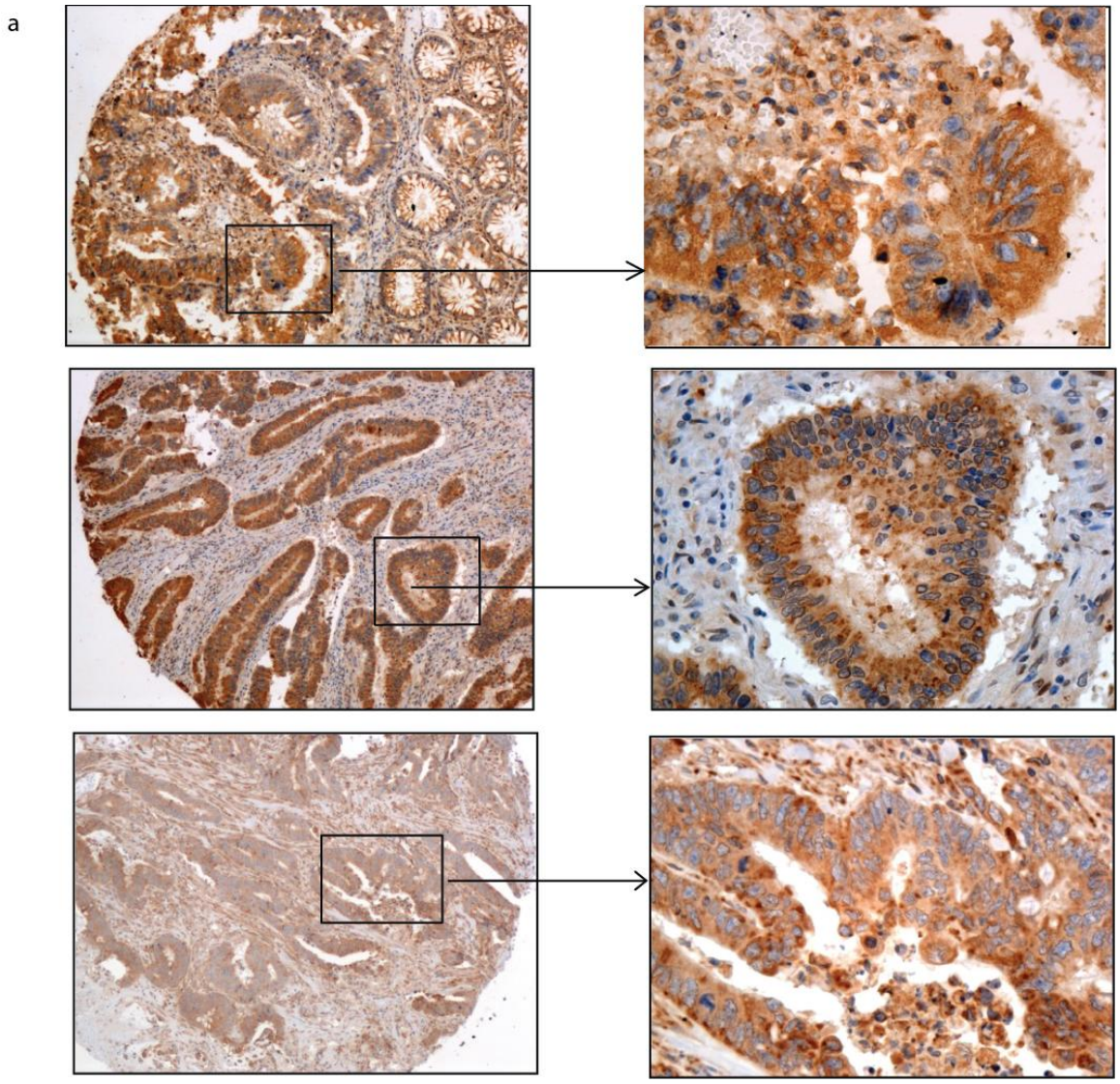
7.4.2 LC3 expression

The number of deaths and recurrences as well as overall and disease free survival of the patients whose samples were stained for LC3 was similar when compared to the total patient population (table 7.5).

Table 7.5 Survival characteristics for VICTOR participants (LC3). Details provided of all patients and those who did and did not provide samples for research and those with evaluable samples for LC3 immunostaining

	VICTOR Patients (N=2434)	Patients without samples (N=1428)	Patients with samples (N=1006)	Patients with LC3-stained samples
Deaths (N (%)	487 (20.0)	294 (20.59)	193 (19.18)	42 (20.39)
Recurrences/deaths (any cause)	704 (28.92)	427 (29.90)	277 (27.53)	59 (28.64)
Overall Survival (3-year % (95%CI))	87.3 (85.8, 88.6)	86.6 (84.7, 88.3)	88.1 (85.9, 90.0)	87.1 (81.6, 91.0)
Overall Survival (5-year % (95%CI))	78.2 (76.3, 78)	77.0 (74.5, 79.4)	79.7 (76.8, 82.2)	79.3 (72.4, 84.6)
Disease Free Survival (3-year % (95%CI))	74.6 (72.7, 76.3)	73.5 (71.0, 75.8)	76.1 (73.2, 78.7)	74.3 (67.5, 79.9)
Disease Free Survival (5-year % (95%CI))	66.5 (64.3, 68.7)	65.3 (62.4, 68.1)	68.2 (64.5, 71.5)	66.8 (58.2, 74.0)

There were populations of patients with positive and negative LC3 expression (figure 7.9). Just over 30% of patient samples were scored as positive (punctuate cytoplasmic staining) and the remainder were scored as negative (diffuse cytoplasmic staining, perinuclear staining). Patients were then divided into those who had developed a recurrence during the follow up period and those who had remained disease free.



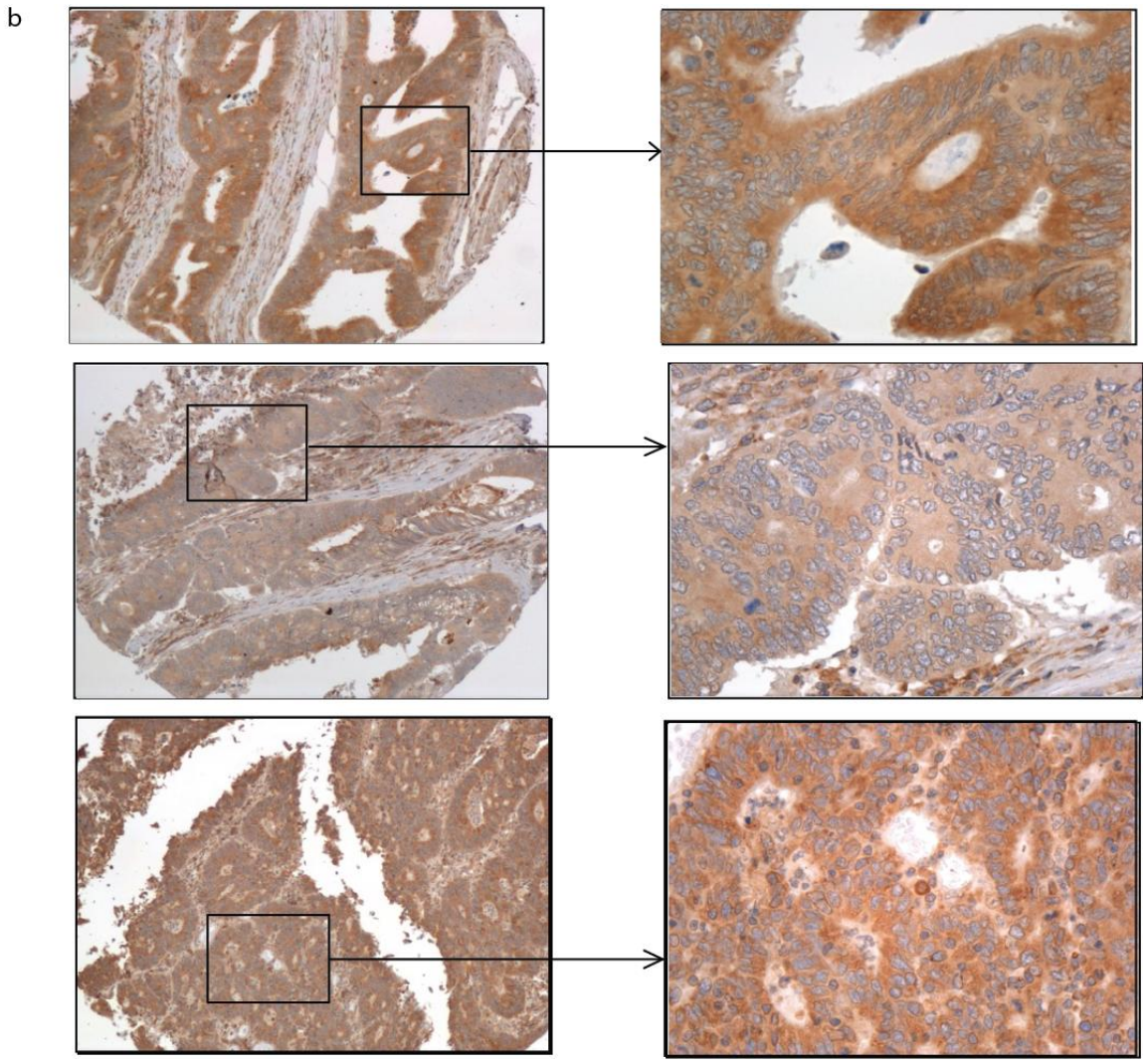


Figure 7.9

Examples of LC3 expression in colorectal cancer specimens from patients in VICTOR trial

TMAs of patient samples from the VICTOR trial were prepared and stained with anti-LC3. Punctate cytoplasmic staining was classified as positive and diffuse cytoplasmic staining and/or perinuclear staining was classified as negative. Examples of positive LC3 immunostaining are shown in (a) indicating high levels of autophagy and examples of negative LC3 immunostaining are shown in (b) indicating low or background levels of autophagy.

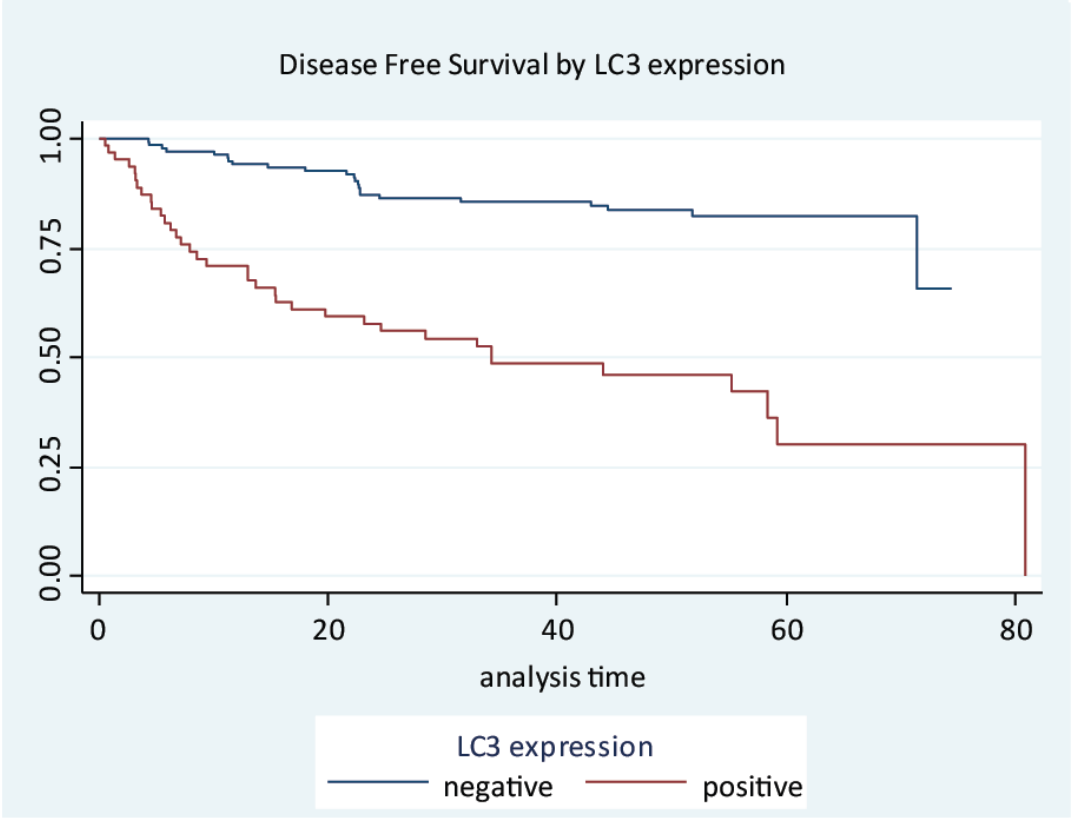
Tumours positive for LC3 expression had a worse DFS and OS compared to those with negative expression (table 7.6). Kaplan-Meier survival curves for both disease free and overall survival demonstrated this difference (figure 7.10). Cox models showed a significant difference between negative LC3 and positive LC3 expression for overall survival and disease free survival (table 7.7). Patients with positive LC3 expression had a worse survival and recurrence than patients with negative LC3 expression. These data suggest that presence of autophagocytic cells is a poor prognostic indicator.

Table 7.6: Overall and disease free survival stratified according to LC3 expression in VICTOR trial patients. 3 and 5 year DFS and OS in months with confidence intervals for patients scoring negative or positive for LC3.

LC3 score	3-year DFS (months) (95% CI)	5-year DFS (months) (95% CI)	3-year OS (months) (95% CI)	5-year OS (months) (95% CI)
Negative	85.7 (78.5, 90.6)	82.4 (74.2, 88.2)	94.9 (89.6, 97.6)	91.4 (84.8, 95.2)
Positive	48.6 (35.4, 60.7)	30.2 (14.5, 47.6)	69.9 (57.0, 80.0)	52.0 (37.5, 64.8)

Abbreviations: DFS, disease free survival, OS, overall survival, CI, confidence intervals

a


Disease Free Survival by LC3 expression
1.00
0.75
0.50
0.25
0.00
0
20
40
60
80
analysis time
LC3 expression
negative
positive

b

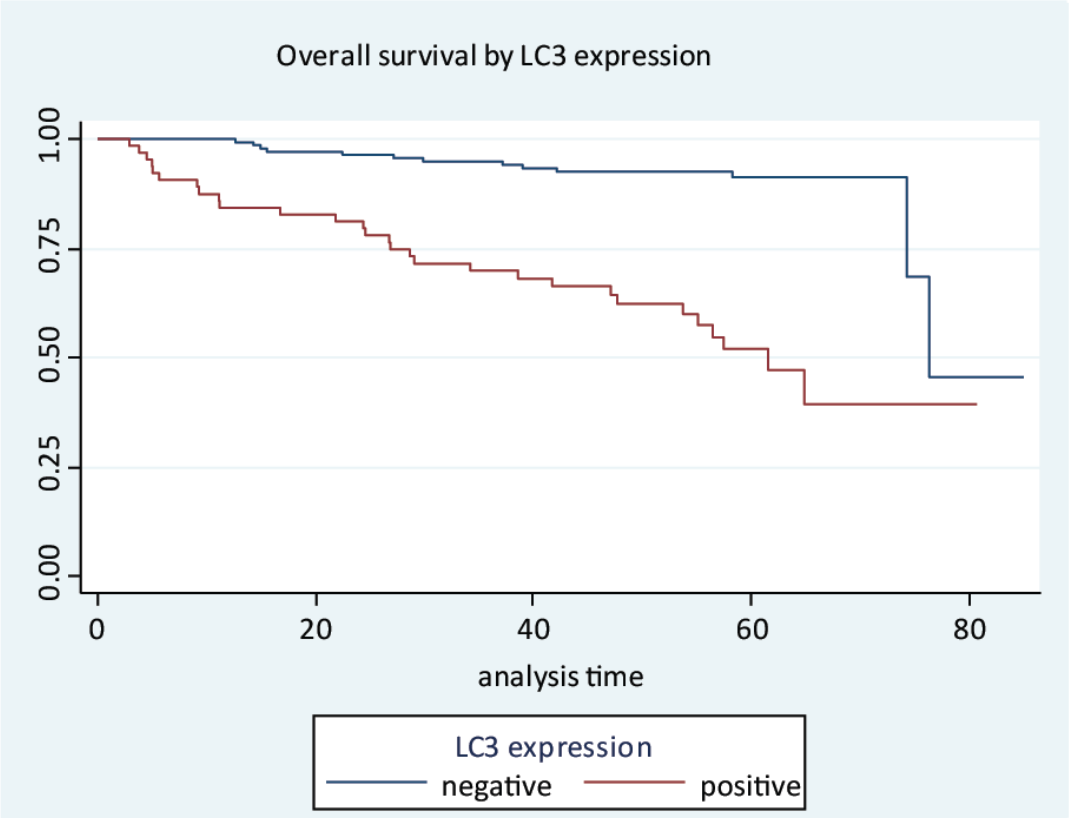

Overall survival by LC3 expression
1.00
0.75
0.50
0.25
0.00
0
20
40
60
80
analysis time
LC3 expression
negative
positive

Figure 7.10

Disease-free and overall survival in patients from VICTOR trial stratified according to LC3 expression

Cytoplasmic LC3 expression was determined according to presence of absence of punctate staining, diffuse cytoplasmic staining and peri-nuclear staining. Patients were thus stratified as negative or positive for LC3 expression.

(a) Kaplan –Meier plot of disease free survival stratified by expression of LC3 over time (months). Log-rank test $p<0.001$.

(b) Kaplan-Meier plot of overall survival stratified by expression of LC3 over time (months). Log-rank test $p<0.001$.

Table 7.7: Results of three separate univariate Cox models estimating effect of LC3 on disease free and overall survival. Hazard ratios are in comparison to a negative (0) score.

LC3	Explanatory variable	Univariate analysis		Multivariate analysis*	
		Hazard ratio (95% CI)	p-value	Hazard ratio (95% CI)	p-value
DFS	Positive vs. negative	4.74 (2.79, 8.05)	<0.001	4.77 (2.76, 8.23)	<0.001
OS	Positive vs. negative	6.24 (3.23, 12.06)	<0.001	7.27 (3.67, 14.41)	<0.001

Abbreviations: DFS, disease free survival, OS, overall survival

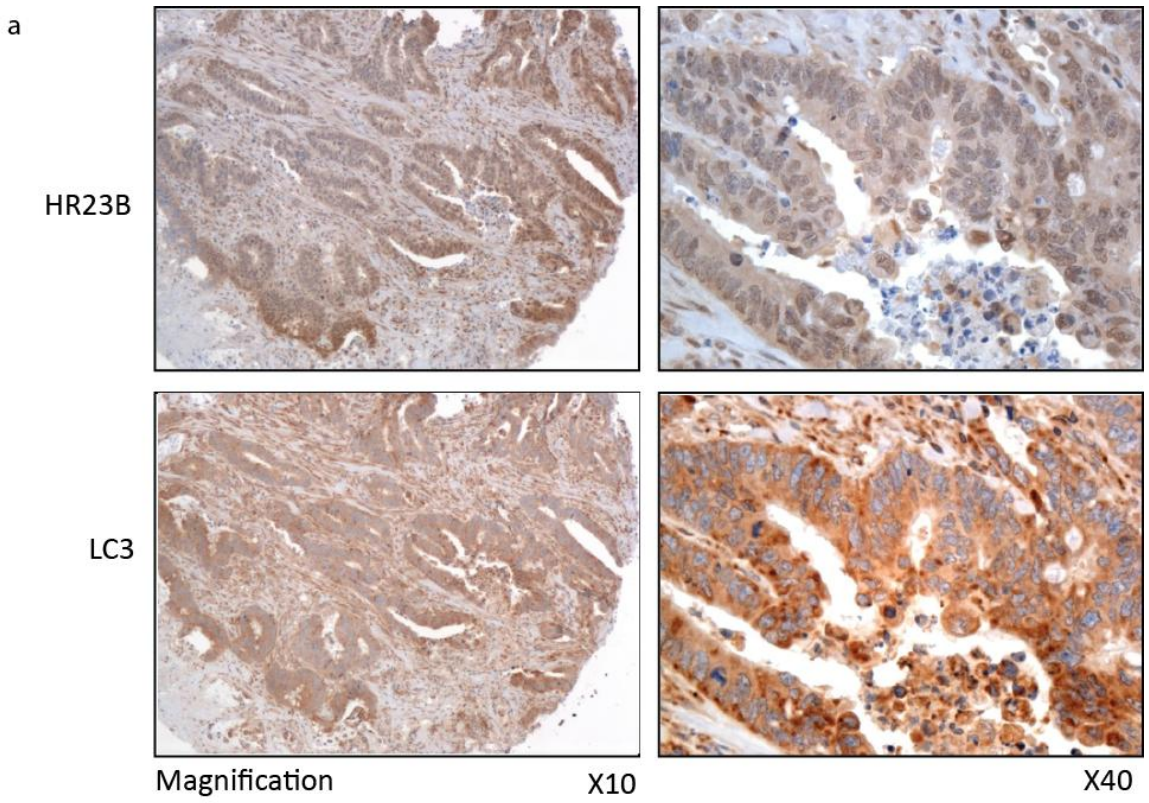
*age at randomisation, gender, chemotherapy, radiotherapy, treatment, disease site and stage were also included in the multivariate analysis.

7.4.3 Assessment of HR23B and LC3 expression

Patients with positive HR23B and negative LC3 were compared with patients with negative HR23B and positive LC3. Around 13% of the patients in this analysis were negative for HR23B and positive for LC3 (27 patients) and 52% of patients were negative for LC3 and positive for HR23B (107 patients) (table 7.8). Examples of these can be seen in figure 7.11.

Table 7.8: HR23B and LC3 score frequencies in VICTOR trial cohort

	Negative HR23B	Positive HR23B	Total
Negative LC3	34	107	141
Positive LC3	27	36	63
Total	61	143	204


a
HR23B
LC3
Magnification
X10
X40

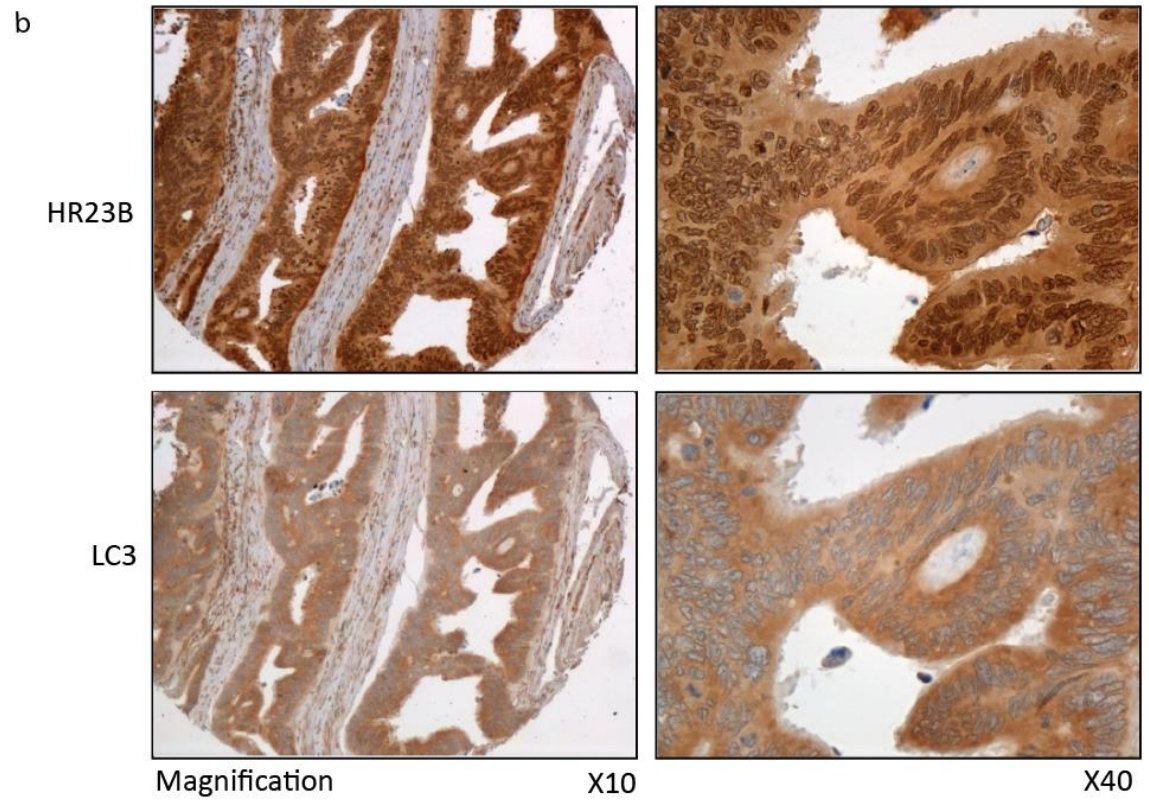

b
HR23B
LC3
Magnification
X10
X40

Figure 7.11

Examples of HR23B expression and LC3 expression in the same patients (colorectal cancer patients from the VICTOR trial).

Nuclear HR23B expression was determined according to frequency and intensity and patients and a total staining score (TSS) was derived. Patients were thus stratified as negative or positive for LC3 expression Cytoplasmic LC3 expression was determined according to presence of absence of punctate staining, diffuse cytoplasmic staining and peri-nuclear staining. Patients were thus stratified as negative or positive for LC3 expression.

(a) Examples of neoplastic colorectal cells showing positive LC3 immunostaining and negativeHR23B immunostaining

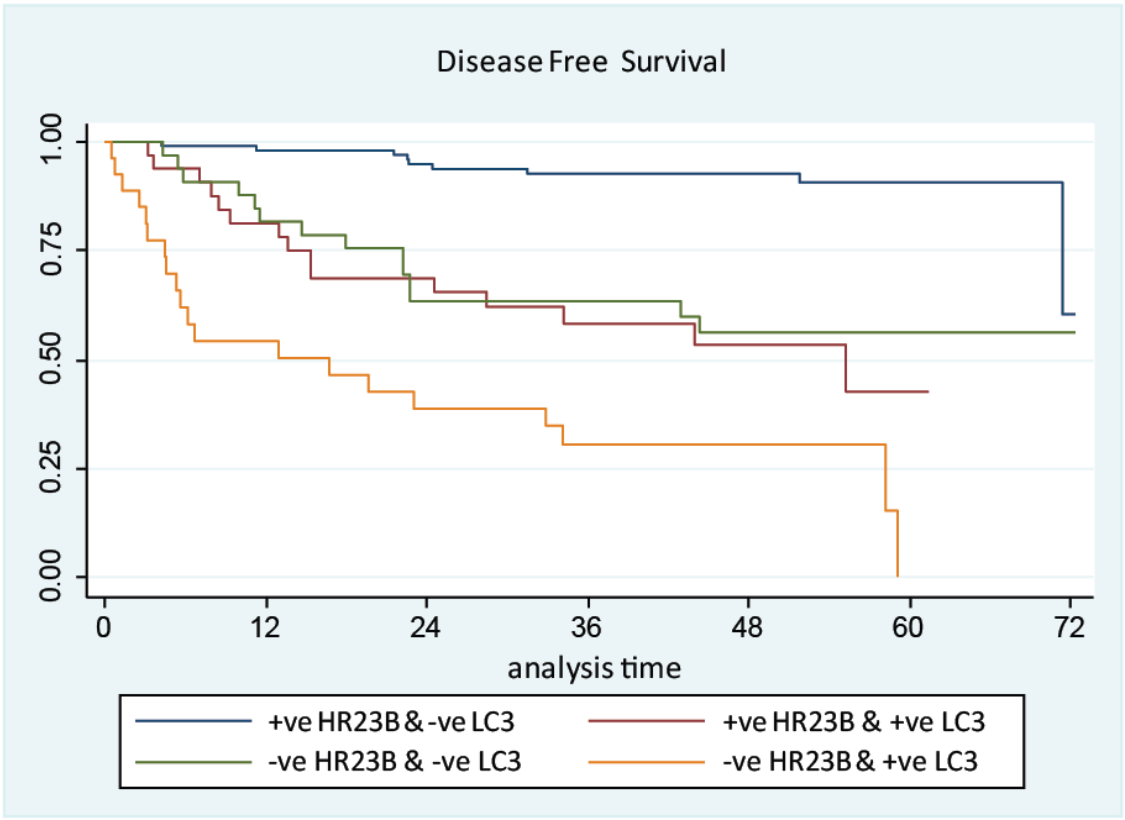
(b) Examples of neoplastic colorectal cells showing negative LC3 immunostaining and positive HR23B immunostaining.

When both data sets were combined, the difference between DFS and OS in positive HR23B/negative LC3 and negative HR23B/positive LC3 was even greater (table 7.9). Kaplan-Meier survival curves for both disease free and overall survival demonstrated this difference (figure 7.12). Cox models showed a significant difference between positive HR23B/negative LC3 and negative HR23B/positive LC3 for overall survival and disease free survival (table 7.10). By analogy with the results derived from the cell line studies, the correlation between positive HR23B immunostaining and improved DFS and OS most likely reflects the propensity of tumour cells for apoptosis. Conversely, in tumours negative for HR23B immunostaining coinciding with positive LC3 immunostaining, poor prognosis may reflect disease where autophagocytic mechanisms promote tumour cell survival. These results suggest that in CRC, the expression of HR23B and LC3 provide important prognostic information.

Table 7.9: Overall and disease free survival stratified according to HR2B and LC3 expression in VICTOR trial patients**.** 3 and 5 year DFS and OS in months with confidence intervals for patients scoring subdivided according to positive or negative HR23B and LC3 expression.

	3-year DFS (months) (95% CI)	5-year DFS (months) (95% CI)	3-year OS (months) (95% CI)	5-year OS (months) (95% CI)
Positive HR23B Negative LC3	92.7 (85.3, 96.5)	90.7 (81.8, 95.4)	98.0 (92.4, 99.5)	98.0 (92.4, 99.5)
Positive HR23B Negative LC3	61.0 (42.2, 75.3)	48.5 (26.8, 67.2)	80.2 (62.8, 90.0)	64.1 (43.2, 79.0)
Negative HR23B Negative LC3	64.7 (46.3, 78.2)	57.9 (39.3, 72.6)	85.3 (68.2, 93.6)	72.4 (53.4, 84.6)
Negative HR23B Positive LC3	30.5 (14.3, 48.5)	-	54.9 (34.4, 71.4)	34.9 (16.3, 54.2)

a


Disease Free Survival
1.00
0.75
0.50
0.25
0.00
0
12
24
36
48
60
72
analysis time
+ve HR23B & -ve LC3
+ve HR23B & +ve LC3
-ve HR23B & -ve LC3
-ve HR23B & +ve LC3

b

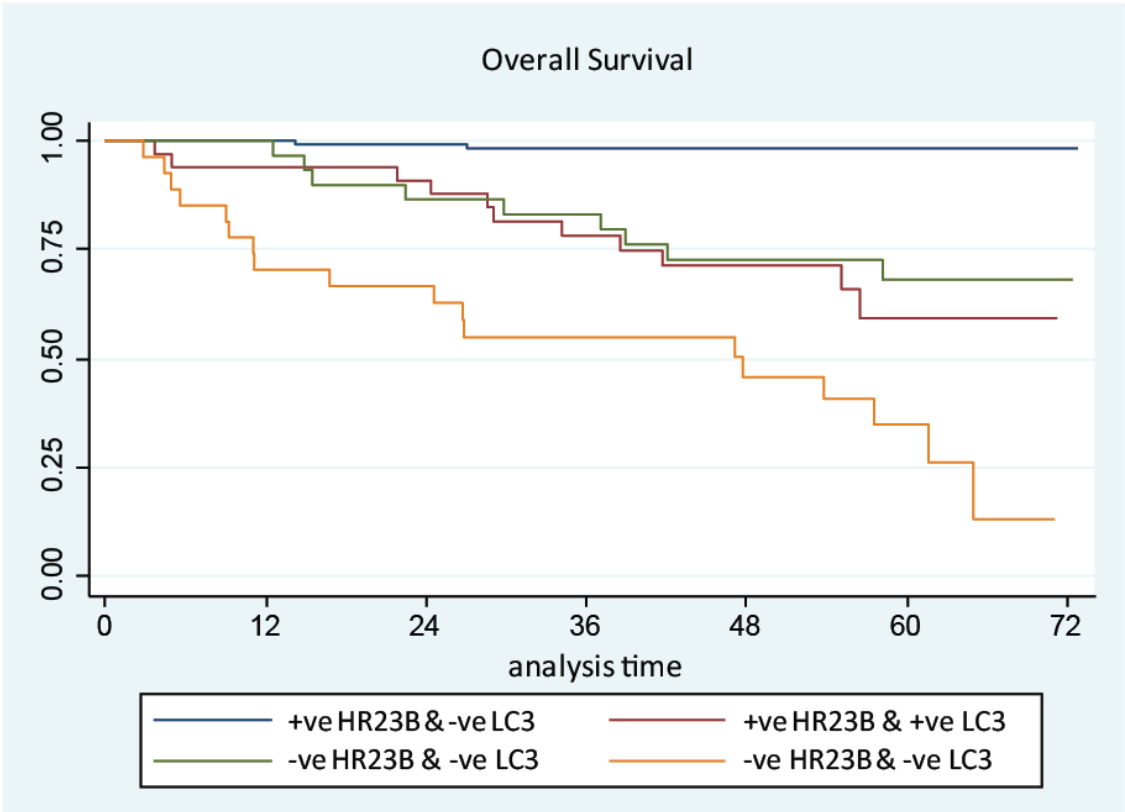

Overall Survival
1.00
0.75
0.50
0.25
0.00
0
12
24
36
48
60
72
analysis time
+ve HR23B & -ve LC3
+ve HR23B & +ve LC3
-ve HR23B & -ve LC3
-ve HR23B & -ve LC3

Figure 7.12

Disease-free and overall survival in patients from VICTOR trial stratified according to HR23B and LC3 expression

Nuclear HR23B expression was determined according to frequency and intensity and patients and a total staining score (TSS) was derived. Patients were thus stratified as negative or positive for HR23B expression. Cytoplasmic LC3 expression was determined according to presence of absence of punctate staining, diffuse cytoplasmic staining and peri-nuclear staining. Patients were thus stratified as negative or positive for LC3 expression. Patients were further stratified according to both HR23B and LC3 expression.

(a) Kaplan –Meier plot of disease free survival stratified by expression of HR23B and LC3 over time (months). Log-rank test $p<0.001$.

(b) Kaplan-Meier plot of overall survival stratified by expression of HR23B and LC3 over time (months). Log-rank test $p<0.001$.

Table 7.10: Results of three separate univariate Cox models estimating effect of HR23B and LC3 combined on disease free and overall survival. Hazard ratios are in comparison to a negative (0) score.

	Explanatory variable	Univariate analysis		Multivariate analysis*	
		Hazard ratio (95% CI)	p-value	Hazard ratio (95% CI)	p-value
DFS	–ve HR23B/ +ve LC3 vs. +ve HR23B/-ve LC3	17.02 (7.71, 37.59)	<0.001	15.70 (6.92, 35.60)	<0.001
OS	–ve HR23B/ +ve LC3 vs. +ve HR23B/-ve LC3	37.31 (10.96, 126.9)	<0.001	34.99 (9.97, 122.73)	<0.001

Abbreviations: DFS, disease free survival, OS, overall survival. –ve, negative, +ve, positive

*age at randomisation, gender, chemotherapy, radiotherapy, treatment, disease site and stage were also included in the multivariate analysis.

7.5. Conclusion.

There was a degree of heterogeneity of expression of HR23B in tumour samples from different types of tumours. Nonetheless, in colorectal cancer and melanoma, sub-groups positive for HR23B and negative for LC3 and the reverse expression pattern were identified. In a pilot clinical study of valproic acid administered to melanoma patients pre-operatively, there was one patient in whom significant changes in the gross pathology and immunostaining pattern post-treatment were observed when compared to pre-treatment biopsies. Negative HR23B expression

frequently occurred with negative LC3 expression and vice versa. In another patient where HR23B expression remained positive before and after HDAC inhibitor treatment, LC3 expression was also negative. Two further patients demonstrated the reverse pattern but pre-treatment biopsies were unavailable in these patients. This supports the observations *in vitro* where there appears to be a dose-dependent reciprocal relationship between HR23B and LC3 expression after HDAC inhibitor therapy although the fact that there is only one example of this in the pilot study limits the strength of this observation. Furthermore, in colorectal cancer and melanoma, positive HR23B expression correlated with improved clinical outcome compared to negative HR23B expression and conversely, positive LC3 expression conferred a worse prognosis. Therefore, based on the relationship between HR23B and autophagy, there may be an autophagocytic survival mechanism that confers a poor prognosis.

CHAPTER 8

DISCUSSION AND FUTURE PERSPECTIVES

8.1. Cell lines from different tumour types demonstrate differences in sensitivity to HDAC inhibitors with alterations in HR23B levels having similar effects on induction of apoptosis

The validation of HR23B has relied upon studies in cell culture and the aim of this project has been to assess its clinical utility as a predictive biomarker. Since vorinostat and romidepsin have gained regulatory approval (as Zolinza and Istodax respectively) for late stage refractory CTCL (Campas-Moya, 2009; Duvic and Vu, 2007) evaluating HR23B in CTCL cell lines, followed by an analysis of its expression and properties in the clinical setting could provide useful information about the longer term clinical potential of these HDAC inhibitors. Additionally, it was important to study solid tumours. Melanoma was selected as a tumour type for which there were, until recently, very few therapeutic options in cases of advanced disease. Colorectal cancer cell lines were used as a common solid tumour type for comparison.

The results suggest that CTCL cells are generally more sensitive to induction of apoptosis by HDAC inhibitors compared to melanoma cells with colorectal cancer demonstrating intermediate sensitivity. Although the number of cell lines utilised was relatively small, this suggests that CTCL may be more sensitive to the apoptotic effects of HDAC inhibitors; this is also seen clinically where response rates in melanoma and colorectal cancer for single agent HDAC inhibitor therapy remain disappointingly low (Khan and La Thangue, 2012c). Despite this, in CTCL and melanoma cell lines, HR23B influences sensitivity to HDAC inhibitor-induced apoptosis. Specifically, manipulating HR23B levels in CTCL and melanoma cells resulted in altered sensitivity to the effects of HDAC inhibitors, which, the results suggest, is partly mediated through the proteasome.

8.2 Patterns of HR23B expression after HDAC inhibitor treatment

Although the observation that HR23B protein expression increases with HDAC inhibitor treatment is interesting, its functional relevance is not clear. Although HR23B has been shown to be acetylated, acetylation levels were not increased after SAHA treatment despite the fact that there are a number of potential acetylation sites on HR23B (Fotheringham et al., 2009). HR23B levels may increase through a post-transcriptional mechanism in HDAC inhibitor treated cells; however this may involve other modifications or signals which are as yet unidentified. HDAC activity may have an impact on the ubiquitination of proteins which bind to HR23B or have an effect on HR23B activity itself, i.e. not cause but consequence.

Further investigation of proteins that HR23B targets to the proteasome would be of great interest and may enhance understanding of how its function can be modulated and provide further detail in illuminating its mechanism of action.

The loss-of-function screen used a shRNA library targeting human genes involved in cancer and genes were identified that influenced sensitivity of U2OS cells to HDAC inhibitors. Most importantly, silencing genes required for HDAC inhibitor-induced apoptosis allowed cells to survive in the presence of SAHA and these surviving cells were isolated and the relevant genes identified. HR23B was considered to be the most functionally relevant gene and was thereafter validated in functional assays as a determinant of HDAC inhibitor sensitivity. Pre-treatment

levels of HR23B are considered to be functionally relevant as the predictive biomarker because expression was silenced in the screen before drug treatment.

The role of HR23B as a biomarker of sensitivity to HDAC inhibitors was further explored in CTCL biopsies taken from one of the key phase II clinical trials that led to FDA approval of SAHA (Duvic et al., 2007). There was a frequent coincidence between HR23B and clinical response to HDAC inhibitor therapy, supporting the idea that HR23B may be a clinically useful biomarker. When the expression of HR23B was assessed in different cell lines pre-treated with HDAC inhibitors and correlated with sensitivity there was some coincidence although the data was not reliably reproducible and it was difficult to make a comparison with only a few cell lines for each tumour type.

The decreases seen in HR23B levels seen at the highest drug concentrations of both HDAC and proteasome inhibitors both as single agent as well as in combination are interesting. However, the regulation of HR23B in HDAC-inhibitor treated cells is a compelling but complicated question to address. Most of the data presented demonstrates HR23B expression after 48h of drug treatment. At this time point, at the highest concentrations of drug treatment, the majority of cells are in the sub-G1 phase and are likely to be apoptotic. It is possible that HR23B levels in these cells are low because these cells are no longer viable and that the loss of HR23B is simply a consequence of apoptosis induction and caspase activation. HR23B may simply be insoluble in these conditions. Further experiments that might elucidate this could involve blocking apoptosis using caspase inhibitors and monitoring the effects of HR23B expression following HDAC inhibitor treatment.

It is also possible that HR23B levels are low at the highest drug concentrations because only the resistant cells remain. These cells may have low or absent HR23B expression, which would be consistent with the hypothesis that HR23B is a biomarker of sensitivity to HDAC inhibitors. However HR23B levels in adherent cells after SAHA treatment are higher than in cells that have detached and are probably no longer viable. Furthermore, cells in the sub-G1 phase of the cell cycle appeared to be derived predominantly from detached cells. In this study, the longest duration that cell lines were treated with HDAC inhibitor was 72 hours. Although certain cell lines did demonstrate relative resistance to HDAC inhibitor therapy, no truly resistant cell lines were used and selection of resistance cells by exposure to HDAC inhibitor for longer periods was not attempted. Selection of truly resistant cells and measuring HR23B levels compared to sensitive cells from the same cell could shed further light on this question.

8.3. Extrapolating results from the shRNA screen to other cell lines and tumour types

HR23B has been shown to be a sensitivity determinant to SAHA and other HDAC inhibitors in CTCL and melanoma cell lines. Furthermore, in CTCL, the retrospective analysis of tumour biopsies demonstrated that HR23B is a sensitivity determinant for SAHA as well as other HDAC inhibitors. Ideally, to fully validate HR23B as a predictive biomarker for HDAC inhibitor therapy, the shRNA screen should be repeated in U2OS and other cell lines, particularly CTCL cell lines with SAHA as well as other HDAC inhibitors. This would be technically challenging especially with suspension cells as well as time-consuming.

8.4. The importance of the ubiquitin-proteasome pathway in the cellular response to HDAC inhibitors

The importance of the proteasome in the cellular response to HDAC inhibitors was confirmed in a number of different ways. Rescue from apoptosis after HR23B depletion with increased apoptosis upon HR23B induction was observed. The proteasome was also shown to be inhibited by HDAC inhibitors in functional and surrogate assays which could be modified by altering levels of HR23B. The fact that depleting HR23B also had an impact on the induction of apoptosis by proteasome inhibitors demonstrated that there might be some convergence in the proteolytic response of both groups of drugs and that these two very different classes of drugs may kill cells through a common pathway with HR23B as a component that integrates the two pathways. Moreover, additive effects or synergy between these compounds and the possible importance of corresponding HR23B levels gives further strength to this observation.

8.5. HR23B and resistance to HDAC inhibitor therapy via autophagy

The observation that autophagy is induced upon HDAC inhibitor therapy in a dose dependent fashion across a variety of cell lines is well-established. There is a coincidental decrease in HR23B protein levels when autophagy markers are at their highest. Selection of cells that are truly resistant to HDAC inhibitor therapy and comparing HR23B expression and expression of autophagy markers may provide clarification of this phenomenon.

Pre-treatment HR23B levels may once again be more relevant as lower levels of LC3 cleavage and fewer autophagocytic cells are seen when HR23B levels are induced. Decreasing autophagy using chloroquine as an inhibitor of autophagy when combining with HDAC inhibitor therapy resulted in enhanced apoptosis supporting the hypothesis that drug resistance of cells to HDAC inhibitors is mediated by autophagy induction. The fact that this effect is abrogated when HR23B levels are depleted pre-treatment with the combination suggests that the effect on reducing apoptosis induction overcomes the reversal of resistance. These observations could be further explored by using siRNA against autophagy proteins to assess if similar results are seen as with autophagy inhibition and with the use of other autophagy inhibitors such as bafilomycin A1 and 3-methyladenine.

Longer term colony assays would also be useful in determining the ultimate fate of cells treated with HDAC inhibitors. The effects of overexpressing or depleting HR23B as well as inhibiting autophagy on clonogenic capacity should provide more detailed information about what the impact of HR23B levels and autophagy is on cell fate.

It is important to bear in mind that the role of autophagy in cancer is complex and paradoxical as it is an adaptive process that is responsive to changes in the cellular microenvironment. Thus, autophagy can either suppress or support the growth of tumour cells depending on the cellular context.

8.6. HR23B and HDAC6

The observation that HDAC6 levels in HDAC inhibitor treated cells were at their highest when HR23B levels are at their lowest and also coincided with high levels of autophagy markers suggests a relationship between these two proteins. This was demonstrated further in experiments using a cell line in which HDAC6 was stably depleted. Ideally, a cell line that stably expressed a control shRNA should be used as a control but this was not available and therefore wild-type A549 cells were used. However, when HDAC6 was depleted in other cell lines including A549 cells and compared to cells treated with control siRNA, similar effects on HR23B levels as well as apoptosis and autophagy were observed.

The domains responsible for the interaction between HR23B and HDAC6 have been recently investigated using a series of mutants derived from each protein (New et al., 2013). The HDAC6 BUZ domain has been found to be responsible for the interaction with HR23B and the UbL domain in HR23B was found to be needed in the interaction with HDAC6. Furthermore, the BUZ domain was required to down-regulate HR23B suggesting that the catalytic activity of HDAC6 is not essential for the down-regulation of HR23B.

Further mechanistic insight into the HR23B/HDAC6 interaction has been recently provided by using a proteomic approach which has demonstrated that a series of protein networks exist that interact with HDAC6 involving tubulins, the chaperone HSP90 and proteins connected with DNA repair and cell metabolism (New et al., 2013). Interestingly, when HSP90 chaperone

activity was inhibited, HDAC6 failed to down-regulate HR23B providing evidence of HSP90 involvement in this interaction.

8.7. Immunohistochemistry and the expression of HR23B

There has been no known extensive examination of the expression of HR23B using immunohistochemistry and therefore there are no guidelines on interpretation of expression. Based on the results from this project, HR23B expression is both nuclear and cytoplasmic with little variability seen in cytoplasmic expression. Using immunofluorescence, there appeared to be an increase in cytoplasmic expression upon HDAC inhibitor treatment which might suggest that the function of HR23B is altered upon SAHA treatment where it plays more of a role in proteolysis and not in NER. However, visible changes in expression may not necessarily reflect change in function.

There was also significant inter- and intra-tumour variability of expression particularly in nuclear expression. From relatively small numbers analysed, there does appear to be an increase in expression in malignant cells compared to normal or non-malignant tissues although this conclusion would require strengthening by a more extensive analysis of non-malignant compared to malignant tissues from a wider range of tumour tissues. Intriguingly, in colorectal cancer, there appears to be a loss of nuclear HR23B staining with more advanced disease. While it is not possible to make any definitive conclusions based on this observation from a relatively small number of tumour specimens, one possible explanation for this might be that more advanced disease represents tumours that are more resistant to therapy with HDAC inhibitors. Prospective

trials assessing expression of HR23B and response to therapy would be needed to confirm or refute this.

Analysis of HR23B levels in a collection of CTCL biopsies taken from a phase II trial of SAHA, suggested that HR23B showed considerable promise as an informative biomarker. Specifically, an analysis of HR23B in 65 CTCL biopsies and relating expression levels to clinical response gave a PPV of 71.7%. The number of biopsies surveyed was limited but this still represented about two thirds of the cases enrolled in the phase II trial and this was one of the two trials on which regulatory approval of SAHA for CTCL was based. The results also suggest that baseline HR23B levels are important in determining outcome of HDAC inhibitor treatment. As the NPV of HR23B in this analysis was only 60%, the specificity of HR23B as a predictive biomarker for HDAC inhibitor response is lower than its sensitivity. The numbers in the NPV analysis were even smaller so need to be interpreted with caution.

8.8. Apoptosis, autophagy and prognosis

Although the total number of tumour specimens was small, sub-groups of tumours were identified where high levels of HR23B and low LC3 levels were detected as well as the reverse pattern. In a pilot clinical study of valproic acid administered to melanoma patients pre-operatively, there appeared to be some evidence of a reciprocal relationship between HR23B and LC3 expression which supported the observations *in vitro*. Although this is an interesting observation, the number of patients was very small and no definitive conclusions were possible.

When colorectal samples were analysed for HR23B and LC3 expression from a group of patients treated on the VICTOR trial, levels of HR23B correlated with improved clinical outcome compared to low HR23B levels and conversely, high LC3 levels conferred a worse prognosis. Once again, the number of samples available was relatively small and although the results were statistically very significant, further larger studies are needed to corroborate these findings. There are also confounding factors as some patients had chemotherapy and radiotherapy and further studies would ideally be performed in treatment naive patients. It would also be useful to investigate any differences seen in across different stages of colorectal cancer. Additionally, a similar analysis in CTCL biopsies would be invaluable although expression of the cytoplasmic marker LC3 might be difficult to interpret in malignant T cells that have a very scanty cytoplasm.

Measuring the cleaved form of LC3 is an established method both using IHC and immunoblotting even though it has limitations (chapter 1.7.9). Several proteins such as p62, hypoxia-upregulated protein 1 and keratins accumulate in cells with defective autophagy. A protein signature of autophagy could therefore be devised that informs on function (Janku et al., 2011c). While newer techniques such as PCR arrays that can measure multiple gene expression are promising for the future, a combination of the techniques in chapter 1.7.9 remains the standard methods of assessing autophagy. While it is clear that measurement of the number of autophagosomes is not a direct measure of autophagic flux, this measurement is an indication of the balance between their generation and their conversion to autolysosomes. Therefore, the accumulation of autophagosomes may represent induction, or inhibition of the autophagy process downstream of autophagosome production.

The prognostic data for LC3 from colorectal cancer patients corroborates findings from previous studies. In two of these studies (Giatromanolaki et al., 2010c; Sivridis et al., 2010), a so-called SLS (stone-like structure) pattern of LC3 expression was described and this was considered to represent an abnormal or excessive autophagic response which was also correlated with distant metastatic disease and a poorer prognosis. Perinuclear and diffuse cytoplasmic staining patterns were also described which were considered to be markers of better prognosis and believed to represent the basal rate functional autophagic machinery essential for cell survival.

In the analysis of colorectal samples from the VICTOR trial, no SLS pattern of LC3 expression was noted. However, similar to other studies, a punctate pattern was seen. This is an established and validated expression pattern for LC3-II (Mizushima et al., 2010b). Diffuse cytoplasmic and perinuclear staining patterns were demonstrated and interestingly, these patterns were present in almost all matched normal colon specimens with none of the normal colon displaying the punctate pattern seen in some tumours. This further strengthens the argument that in some tumours, there is a predominance of cells undergoing autophagy.

The fact that positive HR23B confers a much improved prognosis and negative HR23B a worse prognosis is interesting and mechanistically might be explained by the fact that cells that are positive for HR23B have a "sensitive" proteasome and might be more prone to apoptotic cell death even in the absence of therapy with the reverse being true for cells that are negative for HR23B expression. The data from combining patients with negative HR23B and positive LC3 staining and assessing their survival shows that these patients have a remarkably poor prognosis.

The patient numbers are very small and so repeating the analysis with much larger number of patients is essential.

Keeping in mind the fact that HR23B is considered as a possible biomarker for response to HDAC inhibitors, one fascinating possibility is that patients with negative HR23B expression are not only relatively resistant to HDAC inhibitor therapy but to any therapy. If LC3 expression is taken into consideration, then these patients might also be resistant to therapy due to their propensity for autophagy and consequently this implies that HR23B might have a predictive and prognostic role as a biomarker. Conversely, patients with tumours positive for HR23B and negative for LC3, appear to have a particularly good prognosis so the benefits of HDAC inhibitor therapy or indeed any therapy in the adjuvant setting (in colorectal cancer at least) might be quite small.

8.9. Clinical perspectives

It is evident that response rates to HDAC inhibitors in unselected patients have been disappointing in solid tumours and with the exception of CTCL and PTCL, there are few tumour types where HDAC inhibitors alone have demonstrated significant clinical efficacy. However, even in so-called negative studies, there are occasional patients who demonstrate good clinical responses to HDAC inhibitor therapy suggesting the existence of sub-groups of "susceptible" patients. Although numerous hypotheses have been proposed (Duvic and Zhang, 2006; Richon, 2006; Xu et al., 2007), the mechanism or mechanisms through which HDAC inhibitors exert anti-tumour activity in CTCL are not known. Accordingly, it remains uncertain whether CTCL is

the sole malignancy that is unusually sensitive to HDAC inhibitors or alternatively represents one of many malignancies yet to be proven sensitive. As phase 2 proof-of-concept clinical studies of HDAC inhibitors in CTCL and other tumour types become available, it should be possible to evaluate this important question. It can be challenging to predict tumour response to the therapy under investigation without an informative biomarker.

HR23B has been shown to potentially be a predictive biomarker for HDAC inhibitor therapy. Analysing HR23B's predictive value in retrospective cohorts is unrealistic due to pre-analytical heterogeneity as well as the variable nature of immunohistochemical analysis. Access to archival tissue may give false results and quality of archival tissue is unpredictable which may further skew HR23B analysis. Prospective analysis and incorporation in new and ongoing studies will be more fruitful.

HR23B status in patients with hepatocellular carcinoma treated with belinostat was investigated in a phase I/II study and HR23B expression was assessed in pre-treatment biopsies and correlated with outcome (Yeo et al., 2012). Although numbers of patient with biopsies were small (38), almost 60% of patients who had disease stabilisation has high HR23B expression with only 14% of patients with low expression demonstrating disease stabilisation. This difference was considered to be statistically significant and warrants further investigation. This study was also an example of a "randomise-all" design with retrospective analysis of the biomarker.

Clinical trials investigating HR23B should be designed so that the biomarker can be validated and its efficacy assessed simultaneously. An example of this type of trial design is the "adaptive parallel" design where two-stage trials are conducted in parallel in the biomarker positive and the biomarker negative group. After the first stage, the trials could continue in either one or both groups based upon early outcome analysis. Other designs include a two-step design where there is a learning stage to identify the biomarkers and an adaptive stage during which these biomarkers are used for adaptive randomization (Bayesian adaptive randomisation).

Biopsies of tumour tissue for pharmacodynamic assays that include HR23B expression would need to be performed pre-treatment and at regular intervals during the trial. It would also be useful to investigate surrogate biomarkers for HR23B and an investigation into its expression in peripheral blood mononuclear cells (PBMCs) would be useful. The key question when analysing PBMCs is to what extent changes there reflect what is happening in tumour cells and therefore, an investigation of HR23B expression in circulating tumour cells would also be beneficial.

A phase 1 trial of a novel HDAC inhibitor, CXD-101, is planned and once safety and maximum tolerated dose are determined, the next stage of the study would be to stratify patients according to HR23B expression assessed using immunohistochemistry incorporating an adaptive randomisation approach.

There is increasing evidence to support a synergistic interaction between HDAC and proteasome inhibitors in a wide array of tumour types (Carew et al., 2008). One mechanism through which this synergy occurs is likely to be due to aberrant proteasome activity and furthermore, if patients

can be selected based upon HR23B expression, it might be possible to select patients more likely to respond to such a combination and clinical trials investigating this possibility should be considered.

Finally, combination clinical trials of HDAC inhibitors and autophagy inhibitors are needed and once again, measuring HR23B and LC3 before treatment might provide valuable information about patients who might respond.

8.9. Conclusions

A genome-wide loss of function screen identified HR23B as a gene that impacts on the sensitivity of tumour cells to HDAC inhibitors. The ability of HR23B to engage in proteasomal shuttling highlights its role as a sensitivity determinant of HDAC inhibitor treatment and that aberrant proteasome activity occurs in tumour cells treated with HDAC inhibitors. This is likely to be an important mechanism in inducing apoptosis. CTCL cells are generally more sensitive to induction of apoptosis by HDAC inhibitors compared to melanoma cells. In CTCL and melanoma cell lines, HR23B influences sensitivity to HDAC inhibitor-induced apoptosis. Specifically, manipulating HR23B levels in CTCL and melanoma cells resulted in altered sensitivity to the effects of HDAC inhibitors, which, the results suggest, is partly mediated through the proteasome.

From the clinical perspective, the efficacy of HDAC inhibitors alone has been disappointing particularly in solid tumours however there is enough activity to suggest that a biomarker

selected approach is worth investigating. HDAC inhibitors have been studied in combination with an increasing array of anti-cancer agents (Khan and La Thangue 2008, Richon et al 2009), and clinical studies in which HDAC inhibitors were combined with proteasome inhibitors yielded results that suggest additive effects (Badros et al 2009, Siegel et al 2009, Stimson et al 2009). Based on the results described here, one may hypothesize that the improved clinical profile reflects the additive inhibition of the proteasome, resulting in greater levels of associated tumour cell death. It is possible that tumours positive for HR23B might undergo a particularly favourable response to such a combination treatment. Future studies in which HR23B levels are assessed in a combined therapy clinical trial would allow this interesting possibility to be assessed.

Clinical evaluation of HR23B as a predictive biomarker has been evaluated using a retrospective analysis of its expression in biopsies taken from patients treated with HDAC inhibitors and there was a good coincidence between HR23B expression and therapeutic response to treatment. This now needs to be evaluated further in prospective clinical trials that simultaneously validate HR23B as a predictive biomarker and assess efficacy of HDAC inhibitor therapy. However, it is likely to be some time before the results of any such trials become available even though mechanistic insights suggest how we might design trials to elucidate the predictive nature of the biomarker.

HDAC inhibitors cause apoptosis in cells positive for HR23B as determined by immunohistochemistry and in cells that are negative; HDAC inhibitor treatment is frequently associated with autophagy. Given the potential importance of apoptosis and autophagy in cancer

and the outcome of disease progression, it remains possible that HR23B, perhaps in conjunction with HDAC6 and HSP90, is a biomarker signature which has the ability to differentiate between tumours that have the propensity to enter apoptosis verses autophagy.

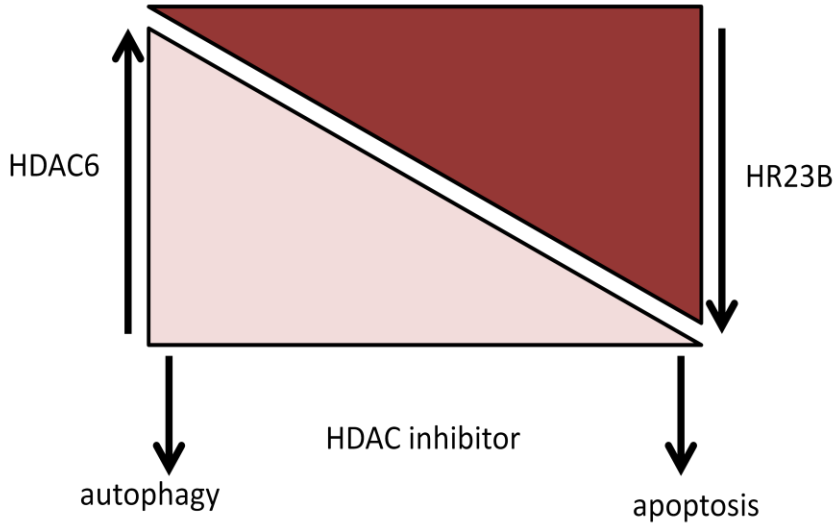


Figure 8.1: **A model for the interplay between HR23B and HDAC6 in regulating the cellular response to HDAC inhibitor therapy.** The levels of HR23B and HDAC6 impact on the response to HDAC inhibitors as reflected by apoptotic or autophagocytic outcomes of drug treatment.

Finally, a retrospective analysis of colorectal cancer specimens suggested that levels of HR23B and LC3 may provide prognostic information and this needs to be validated in prospective clinical trials.

Reference List

(Biomarkers and surrogate endpoints: preferred definitions and conceptual framework. Clin Pharmacol Ther 69:89-95.2001).

Amaravadi RK, Yu D, Lum JJ, Bui T, Christophorou MA, Evan GI, Thomas-Tikhonenko A, Thompson CB (Autophagy inhibition enhances therapy-induced apoptosis in a Myc-induced model of lymphoma. J Clin Invest 117:326-336.2007).

Bali P, Pranpat M, Bradner J, Balasis M, Fiskus W, Guo F, Rocha K, Kumaraswamy S, Boyapalle S, Atadja P, Seto E, Bhalla K (Inhibition of histone deacetylase 6 acetylates and disrupts the chaperone function of heat shock protein 90: a novel basis for antileukemia activity of histone deacetylase inhibitors. J Biol Chem 280:26729-26734.2005).

Bedford L, Lowe J, Dick LR, Mayer RJ, Brownell JE (Ubiquitin-like protein conjugation and the ubiquitin-proteasome system as drug targets. Nat Rev Drug Discov 10:29-46.2011).

Bellodi C, Lidonnici MR, Hamilton A, Helgason GV, Soliera AR, Ronchetti M, Galavotti S, Young KW, Selmi T, Yacobi R, Van Etten RA, Donato N, Hunter A, Dinsdale D, Tirro E, Vigneri P, Nicotera P, Dyer MJ, Holyoake T, Salomoni P, Calabretta B (Targeting autophagy potentiates tyrosine kinase inhibitor-induced cell death in Philadelphia chromosome-positive cells, including primary CML stem cells. J Clin Invest 119:1109-1123.2009).

Bence NF, Sampat RM, Kopito RR (Impairment of the ubiquitin-proteasome system by protein aggregation. Science 292:1552-1555.2001).

Bentley GA, Finch JT, Lewit-Bentley A, Roth M (The crystal structure of the nucleosome core particle by contrast variation. Basic Life Sci 27:105-117.1984).

Bhaskara S, Chyla BJ, Amann JM, Knutson SK, Cortez D, Sun ZW, Hiebert SW (Deletion of histone deacetylase 3 reveals critical roles in S phase progression and DNA damage control. Mol Cell 30:61-72.2008).

Boumber Y, Younes A, Garcia-Manero G (Mocetinostat (MGCD0103): a review of an isotype-specific histone deacetylase inhibitor. Expert Opin Investig Drugs 20:823-829.2011).

Boyault C, Sadoul K, Pabion M, Khochbin S (HDAC6, at the crossroads between cytoskeleton and cell signaling by acetylation and ubiquitination. Oncogene 26:5468-5476.2007).

Bruzzese F, Leone A, Rocco M, Carbone C, Piro G, Caraglia M, Di GE, Budillon A (HDAC inhibitor vorinostat enhances the antitumor effect of gefitinib in squamous cell carcinoma of head and neck by modulating ErbB receptor expression and reverting EMT. J Cell Physiol 226:2378-2390.2011).

Buchberger A (From UBA to UBX: new words in the ubiquitin vocabulary. Trends Cell Biol 12:216-221.2002).

Buglio D, Khaskhely NM, Voo KS, Martinez-Valdez H, Liu YJ, Younes A (HDAC11 plays an essential role in regulating OX40 ligand expression in Hodgkin lymphoma. Blood 117:2910-2917.2011).

Bukau B, Weissman J, Horwich A (Molecular chaperones and protein quality control. Cell 125:443-451.2006).

Buyse M, Michiels S, Sargent DJ, Grothey A, Matheson A, de GA (Integrating biomarkers in clinical trials. Expert Rev Mol Diagn 11:171-182.2011).

Campas-Moya C (Romidepsin for the treatment of cutaneous T-cell lymphoma. Drugs Today (Barc) 45:787-795.2009).

Carew JS, Espitia CM, Esquivel JA, Mahalingam D, Kelly KR, Reddy G, Giles FJ, Nawrocki ST (Lucanthone is a novel inhibitor of autophagy that induces cathepsin D-mediated apoptosis. J Biol Chem 286:6602-6613.2011).

Carew JS, Giles FJ, Nawrocki ST (Histone deacetylase inhibitors: mechanisms of cell death and promise in combination cancer therapy. Cancer Lett 269:7-17.2008).

Carew JS, Medina EC, Esquivel JA, Mahalingam D, Swords R, Kelly K, Zhang H, Huang P, Mita AC, Mita MM, Giles FJ, Nawrocki ST (Autophagy inhibition enhances vorinostat-induced apoptosis via ubiquitinated protein accumulation. J Cell Mol Med 14:2448-2459.2010).

Carey N, La Thangue NB (Histone deacetylase inhibitors: gathering pace. Curr Opin Pharmacol 6:369-375.2006).

Cashen A, Juckett M, Jumonville A, Litzow M, Flynn PJ, Eckardt J, LaPlant B, Laumann K, Erlichman C, DiPersio J (Phase II study of the histone deacetylase inhibitor belinostat (PXD101) for the treatment of myelodysplastic syndrome (MDS). Ann Hematol 91:33-38.2012).

Chan HM, Krstic-Demonacos M, Smith L, Demonacos C, La Thangue NB (Acetylation control of the retinoblastoma tumour-suppressor protein. Nat Cell Biol 3:667-674.2001).

Chen L, Madura K (Rad23 promotes the targeting of proteolytic substrates to the proteasome. Mol Cell Biol 22:4902-4913.2002).

Chen L, Shinde U, Ortolan TG, Madura K (Ubiquitin-associated (UBA) domains in Rad23 bind ubiquitin and promote inhibition of multi-ubiquitin chain assembly. EMBO Rep 2:933-938.2001).

Chen Y, Lu Y, Lu C, Zhang L (Beclin-1 expression is a predictor of clinical outcome in patients with esophageal squamous cell carcinoma and correlated to hypoxia-inducible factor (HIF)-1alpha expression. Pathol Oncol Res 15:487-493.2009).

Chinnaiyan P, Vallabhaneni G, Armstrong E, Huang SM, Harari PM (Modulation of radiation response by histone deacetylase inhibition. Int J Radiat Oncol Biol Phys 62:223-229.2005).

Ciechanover A (The ubiquitin-proteasome proteolytic pathway. Cell 79:13-21.1994).

Ciechanover A (Proteolysis: from the lysosome to ubiquitin and the proteasome. Nat Rev Mol Cell Biol 6:79-87.2005).

Ciechanover A, Ben-Saadon R (N-terminal ubiquitination: more protein substrates join in. Trends Cell Biol 14:103-106.2004).

Dai C, Whitesell L, Rogers AB, Lindquist S (Heat shock factor 1 is a powerful multifaceted modifier of carcinogenesis. Cell 130:1005-1018.2007).

Dantuma NP, Heinen C, Hoogstraten D (The ubiquitin receptor Rad23: at the crossroads of nucleotide excision repair and proteasomal degradation. DNA Repair (Amst) 8:449-460.2009).

de Ruijter AJ, van Gennip AH, Caron HN, Kemp S, van Kuilenburg AB (Histone deacetylases (HDACs): characterization of the classical HDAC family. Biochem J 370:737-749.2003a).

de Ruijter AJ, van Gennip AH, Caron HN, Kemp S, van Kuilenburg AB (Histone deacetylases (HDACs): characterization of the classical HDAC family. Biochem J 370:737-749.2003b).

De SH, Kimpe M, Isebaert S, Nuyts S (A systematic assessment of radiation dose enhancement by 5-Aza-2'-deoxycytidine and histone deacetylase inhibitors in head-and-neck squamous cell carcinoma. Int J Radiat Oncol Biol Phys 73:904-912.2009).

Degenhardt K, Mathew R, Beaudoin B, Bray K, Anderson D, Chen G, Mukherjee C, Shi Y, Gelinas C, Fan Y, Nelson DA, Jin S, White E (Autophagy promotes tumor cell survival and restricts necrosis, inflammation, and tumorigenesis. Cancer Cell 10:51-64.2006).

Dequiedt F, Kasler H, Fischle W, Kiermer V, Weinstein M, Herndier BG, Verdin E (HDAC7, a thymus-specific class II histone deacetylase, regulates Nur77 transcription and TCR-mediated apoptosis. Immunity 18:687-698.2003).

Dickinson M, Ritchie D, DeAngelo DJ, Spencer A, Ottmann OG, Fischer T, Bhalla KN, Liu A, Parker K, Scott JW, Bishton M, Prince HM (Preliminary evidence of disease response to the pan deacetylase inhibitor panobinostat (LBH589) in refractory Hodgkin Lymphoma. Br J Haematol 147:97-101.2009).

Ding ZB, Shi YH, Zhou J, Qiu SJ, Xu Y, Dai Z, Shi GM, Wang XY, Ke AW, Wu B, Fan J (Association of autophagy defect with a malignant phenotype and poor prognosis of hepatocellular carcinoma. Cancer Res 68:9167-9175.2008).

Driscoll JJ, Chowdhury RD (Molecular crosstalk between the proteasome, aggresomes and autophagy: translational potential and clinical implications. Cancer Lett 325:147-154.2012).

Duffy MJ (Predictive markers in breast and other cancers: a review. Clin Chem 51:494-503.2005).

Duvic M, Talpur R, Ni X, Zhang C, Hazarika P, Kelly C, Chiao JH, Reilly JF, Ricker JL, Richon VM, Frankel SR (Phase 2 trial of oral vorinostat (suberoylanilide hydroxamic acid, SAHA) for refractory cutaneous T-cell lymphoma (CTCL). Blood 109:31-39.2007).

Duvic M, Vu J (Vorinostat in cutaneous T-cell lymphoma. Drugs Today (Barc) 43:585-599.2007).

Elsasser S, Gali RR, Schwickart M, Larsen CN, Leggett DS, Muller B, Feng MT, Tubing F, Dittmar GA, Finley D (Proteasome subunit Rpn1 binds ubiquitin-like protein domains. Nat Cell Biol 4:725-730.2002).

Eyupoglu IY, Hahnen E, Trankle C, Savaskan NE, Siebzehnrubl FA, Buslei R, Lemke D, Wick W, Fahlbusch R, Blumcke I (Experimental therapy of malignant gliomas using the inhibitor of histone deacetylase MS-275. Mol Cancer Ther 5:1248-1255.2006).

Finnin MS, Donigian JR, Cohen A, Richon VM, Rifkind RA, Marks PA, Breslow R, Pavletich NP (Structures of a histone deacetylase homologue bound to the TSA and SAHA inhibitors. Nature 401:188-193.1999).

Fischer DD, Cai R, Bhatia U, Asselbergs FA, Song C, Terry R, Trogani N, Widmer R, Atadja P, Cohen D (Isolation and characterization of a novel class II histone deacetylase, HDAC10. J Biol Chem 277:6656-6666.2002).

Fotheringham S, Epping MT, Stimson L, Khan O, Wood V, Pezzella F, Bernards R, La Thangue NB (Genome-wide loss-of-function screen reveals an important role for the proteasome in HDAC inhibitor-induced apoptosis. Cancer Cell 15:57-66.2009a).

Fotheringham S, Epping MT, Stimson L, Khan O, Wood V, Pezzella F, Bernards R, La Thangue NB (Genome-wide loss-of-function screen reveals an important role for the proteasome in HDAC inhibitor-induced apoptosis. Cancer Cell 15:57-66.2009b).

Frankland-Searby S, Bhaumik SR (The 26S proteasome complex: an attractive target for cancer therapy. Biochim Biophys Acta 1825:64-76.2012).

Fu H, Reis N, Lee Y, Glickman MH, Vierstra RD (Subunit interaction maps for the regulatory particle of the 26S proteasome and the COP9 signalosome. EMBO J 20:7096-7107.2001).

Galli M, Salmoiraghi S, Golay J, Gozzini A, Crippa C, Pescosta N, Rambaldi A (A phase II multiple dose clinical trial of histone deacetylase inhibitor ITF2357 in patients with relapsed or progressive multiple myeloma. Ann Hematol 89:185-190.2010).

Gammoh N, Lam D, Puente C, Ganley I, Marks PA, Jiang X (Role of autophagy in histone deacetylase inhibitor-induced apoptotic and nonapoptotic cell death. Proc Natl Acad Sci U S A 109:6561-6565.2012).

Ghaboosi N, Deshaies RJ (A conditional yeast E1 mutant blocks the ubiquitin-proteasome pathway and reveals a role for ubiquitin conjugates in targeting Rad23 to the proteasome. Mol Biol Cell 18:1953-1963.2007).

Giaccone G, Rajan A, Berman A, Kelly RJ, Szabo E, Lopez-Chavez A, Trepel J, Lee MJ, Cao L, Espinoza-Delgado I, Spittler J, Loehrer PJ, Sr. (Phase II study of belinostat in patients with recurrent or refractory advanced thymic epithelial tumors. J Clin Oncol 29:2052-2059.2011).

Giatromanolaki A, Koukourakis MI, Harris AL, Polychronidis A, Gatter KC, Sivridis E (Prognostic relevance of light chain 3 (LC3A) autophagy patterns in colorectal adenocarcinomas. J Clin Pathol 63:867-872.2010a).

Giatromanolaki A, Koukourakis MI, Harris AL, Polychronidis A, Gatter KC, Sivridis E (Prognostic relevance of light chain 3 (LC3A) autophagy patterns in colorectal adenocarcinomas. J Clin Pathol 63:867-872.2010b).

Giatromanolaki A, Koukourakis MI, Harris AL, Polychronidis A, Gatter KC, Sivridis E (Prognostic relevance of light chain 3 (LC3A) autophagy patterns in colorectal adenocarcinomas. J Clin Pathol 63:867-872.2010c).

Gilon T, Chomsky O, Kulka RG (Degradation signals for ubiquitin system proteolysis in Saccharomyces cerevisiae. EMBO J 17:2759-2766.1998).

Glaser KB, Staver MJ, Waring JF, Stender J, Ulrich RG, Davidsen SK (Gene expression profiling of multiple histone deacetylase (HDAC) inhibitors: defining a common gene set produced by HDAC inhibition in T24 and MDA carcinoma cell lines. Mol Cancer Ther 2:151-163.2003).

Glickman MH, Rubin DM, Fried VA, Finley D (The regulatory particle of the Saccharomyces cerevisiae proteasome. Mol Cell Biol 18:3149-3162.1998).

Goh AM, Walters KJ, Elsasser S, Verma R, Deshaies RJ, Finley D, Howley PM (Components of the ubiquitin-proteasome pathway compete for surfaces on Rad23 family proteins. BMC Biochem 9:4.2008).

Goldstein G, Scheid M, Hammerling U, Schlesinger DH, Niall HD, Boyse EA (Isolation of a polypeptide that has lymphocyte-differentiating properties and is probably represented universally in living cells. Proc Natl Acad Sci U S A 72:11-15.1975).

Gregoretti IV, Lee YM, Goodson HV (Molecular evolution of the histone deacetylase family: functional implications of phylogenetic analysis. J Mol Biol 338:17-31.2004).

Groll M, Bajorek M, Kohler A, Moroder L, Rubin DM, Huber R, Glickman MH, Finley D (A gated channel into the proteasome core particle. Nat Struct Biol 7:1062-1067.2000).

Groll M, Berkers CR, Ploegh HL, Ovaa H (Crystal structure of the boronic acid-based proteasome inhibitor bortezomib in complex with the yeast 20S proteasome. Structure 14:451-456.2006).

Groll M, Ditzel L, Lowe J, Stock D, Bochtler M, Bartunik HD, Huber R (Structure of 20S proteasome from yeast at 2.4 A resolution. Nature 386:463-471.1997).

Groll M, Heinemeyer W, Jager S, Ullrich T, Bochtler M, Wolf DH, Huber R (The catalytic sites of 20S proteasomes and their role in subunit maturation: a mutational and crystallographic study. Proc Natl Acad Sci U S A 96:10976-10983.1999).

Guerrant W, Patil V, Canzoneri JC, Oyelere AK (Dual targeting of histone deacetylase and topoisomerase II with novel bifunctional inhibitors. J Med Chem 55:1465-1477.2012).

Haberland M, Montgomery RL, Olson EN (The many roles of histone deacetylases in development and physiology: implications for disease and therapy. Nat Rev Genet 10:32-42.2009).

Hainsworth JD, Infante JR, Spigel DR, Arrowsmith ER, Boccia RV, Burris HA (A phase II trial of panobinostat, a histone deacetylase inhibitor, in the treatment of patients with refractory metastatic renal cell carcinoma. Cancer Invest 29:451-455.2011).

Hauschild A, Trefzer U, Garbe C, Kaehler KC, Ugurel S, Kiecker F, Eigentler T, Krissel H, Schott A, Schadendorf D (Multicenter phase II trial of the histone deacetylase inhibitor pyridylmethyl-N-{4-[(2-aminophenyl)-carbamoyl]-benzyl}-carbamate in pretreated metastatic melanoma. Melanoma Res 18:274-278.2008).

Heessen S, Masucci MG, Dantuma NP (The UBA2 domain functions as an intrinsic stabilization signal that protects Rad23 from proteasomal degradation. Mol Cell 18:225-235.2005).

Heinemeyer W, Fischer M, Krimmer T, Stachon U, Wolf DH (The active sites of the eukaryotic 20 S proteasome and their involvement in subunit precursor processing. J Biol Chem 272:25200-25209.1997).

Heinen C, Acs K, Hoogstraten D, Dantuma NP (C-terminal UBA domains protect ubiquitin receptors by preventing initiation of protein degradation. Nat Commun 2:191.2011).

Hideshima T, Richardson PG, Anderson KC (Mechanism of action of proteasome inhibitors and deacetylase inhibitors and the biological basis of synergy in multiple myeloma. Mol Cancer Ther 10:2034-2042.2011).

Hofmann K, Falquet L (A ubiquitin-interacting motif conserved in components of the proteasomal and lysosomal protein degradation systems. Trends Biochem Sci 26:347-350.2001).

Holt SV, Wyspianska B, Randall KJ, James D, Foster JR, Wilkinson RW (The development of an immunohistochemical method to detect the autophagy-associated protein LC3-II in human tumor xenografts. Toxicol Pathol 39:516-523.2011).

Huang X, Wang S, Lee CK, Yang X, Liu B (HDAC inhibitor SNDX-275 enhances efficacy of trastuzumab in erbB2-overexpressing breast cancer cells and exhibits potential to overcome trastuzumab resistance. Cancer Lett 307:72-79.2011).

Imai S, Johnson FB, Marciniak RA, McVey M, Park PU, Guarente L (Sir2: an NAD-dependent histone deacetylase that connects chromatin silencing, metabolism, and aging. Cold Spring Harb Symp Quant Biol 65:297-302.2000).

Inche AG, La Thangue NB (Chromatin control and cancer-drug discovery: realizing the promise. Drug Discov Today 11:97-109.2006).

Janku F, McConkey DJ, Hong DS, Kurzrock R (Autophagy as a target for anticancer therapy. Nat Rev Clin Oncol 8:528-539.2011a).

Janku F, McConkey DJ, Hong DS, Kurzrock R (Autophagy as a target for anticancer therapy. Nat Rev Clin Oncol 8:528-539.2011b).

Janku F, McConkey DJ, Hong DS, Kurzrock R (Autophagy as a target for anticancer therapy. Nat Rev Clin Oncol 8:528-539.2011c).

Jenuwein T, Allis CD (Translating the histone code. Science 293:1074-1080.2001).

Jin S, DiPaola RS, Mathew R, White E (Metabolic catastrophe as a means to cancer cell death. J Cell Sci 120:379-383.2007).

Jin S, White E (Tumor suppression by autophagy through the management of metabolic stress. Autophagy 4:563-566.2008).

Johnston JA, Ward CL, Kopito RR (Aggresomes: a cellular response to misfolded proteins. J Cell Biol 143:1883-1898.1998).

Kabeya Y, Mizushima N, Ueno T, Yamamoto A, Kirisako T, Noda T, Kominami E, Ohsumi Y, Yoshimori T (LC3, a mammalian homologue of yeast Apg8p, is localized in autophagosome membranes after processing. EMBO J 19:5720-5728.2000).

Kalac M, Scotto L, Marchi E, Amengual J, Seshan VE, Bhagat G, Ulahannan N, Leshchenko VV, Temkin AM, Parekh S, Tycko B, O'Connor OA (HDAC inhibitors and decitabine are highly synergistic and associated with unique gene-expression and epigenetic profiles in models of DLBCL. Blood 118:5506-5516.2011).

Kane RC, Dagher R, Farrell A, Ko CW, Sridhara R, Justice R, Pazdur R (Bortezomib for the treatment of mantle cell lymphoma. Clin Cancer Res 13:5291-5294.2007).

Kane RC, Farrell AT, Sridhara R, Pazdur R (United States Food and Drug Administration approval summary: bortezomib for the treatment of progressive multiple myeloma after one prior therapy. Clin Cancer Res 12:2955-2960.2006).

Kao HY, Lee CH, Komarov A, Han CC, Evans RM (Isolation and characterization of mammalian HDAC10, a novel histone deacetylase. J Biol Chem 277:187-193.2002).

Karantza-Wadsworth V, Patel S, Kravchuk O, Chen G, Mathew R, Jin S, White E (Autophagy mitigates metabolic stress and genome damage in mammary tumorigenesis. Genes Dev 21:1621-1635.2007).

Karapetis CS, Khambata-Ford S, Jonker DJ, O'Callaghan CJ, Tu D, Tebbutt NC, Simes RJ, Chalchal H, Shapiro JD, Robitaille S, Price TJ, Shepherd L, Au HJ, Langer C, Moore MJ, Zalcberg JR (K-ras mutations and benefit from cetuximab in advanced colorectal cancer. N Engl J Med 359:1757-1765.2008).

Kawaguchi Y, Kovacs JJ, McLaurin A, Vance JM, Ito A, Yao TP (The deacetylase HDAC6 regulates aggresome formation and cell viability in response to misfolded protein stress. Cell 115:727-738.2003a).

Kawaguchi Y, Kovacs JJ, McLaurin A, Vance JM, Ito A, Yao TP (The deacetylase HDAC6 regulates aggresome formation and cell viability in response to misfolded protein stress. Cell 115:727-738.2003b).

Khan O, Fotheringham S, Wood V, Stimson L, Zhang C, Pezzella F, Duvic M, Kerr DJ, La Thangue NB (HR23B is a biomarker for tumor sensitivity to HDAC inhibitor-based therapy. Proc Natl Acad Sci U S A 107:6532-6537.2010).

Khan O, La Thangue NB (Drug Insight: histone deacetylase inhibitor-based therapies for cutaneous T-cell lymphomas. Nat Clin Pract Oncol 5:714-726.2008).

Khan O, La Thangue NB (HDAC inhibitors in cancer biology: emerging mechanisms and clinical applications. Immunol Cell Biol 90:85-94.2012a).

Khan O, La Thangue NB (HDAC inhibitors in cancer biology: emerging mechanisms and clinical applications. Immunol Cell Biol 90:85-94.2012b).

Khan O, La Thangue NB (HDAC inhibitors in cancer biology: emerging mechanisms and clinical applications. Immunol Cell Biol 90:85-94.2012c).

Kim EJ, Hess S, Richardson SK, Newton S, Showe LC, Benoit BM, Ubriani R, Vittorio CC, Junkins-Hopkins JM, Wysocka M, Rook AH (Immunopathogenesis and therapy of cutaneous T cell lymphoma. J Clin Invest 115:798-812.2005).

Kimura T, Takabatake Y, Takahashi A, Isaka Y (Chloroquine in cancer therapy: a double-edged sword of autophagy. Cancer Res 73:3-7.2013).

Kirsh O, Seeler JS, Pichler A, Gast A, Muller S, Miska E, Mathieu M, Harel-Bellan A, Kouzarides T, Melchior F, Dejean A (The SUMO E3 ligase RanBP2 promotes modification of the HDAC4 deacetylase. EMBO J 21:2682-2691.2002).

Kisselev AF, Goldberg AL (Proteasome inhibitors: from research tools to drug candidates. Chem Biol 8:739-758.2001).

Klionsky DJ, Abeliovich H, Agostinis P, Agrawal DK, Aliev G, Askew DS, Baba M, Baehrecke EH, Bahr BA, Ballabio A, Bamber BA, Bassham DC, Bergamini E, Bi X, Biard-Piechaczyk M, Blum JS, Bredesen DE, Brodsky JL, Brumell JH, Brunk UT, Bursch W, Camougrand N, Cebollero E, Cecconi F, Chen Y, Chin LS, Choi A, Chu CT, Chung J, Clarke PG, Clark RS, Clarke SG, Clave C, Cleveland JL, Codogno P, Colombo MI, Coto-Montes A, Cregg JM, Cuervo AM, Debnath J, Demarchi F, Dennis PB, Dennis PA, Deretic V, Devenish RJ, Di SF, Dice JF, Difiglia M, Dinesh-Kumar S, Distelhorst CW, Djavaheri-Mergny M, Dorsey FC, Droge W, Dron M, Dunn WA, Jr., Duszenko M, Eissa NT, Elazar Z, Esclatine A, Eskelinen EL, Fesus L, Finley KD, Fuentes JM, Fueyo J, Fujisaki K, Galliot B, Gao FB, Gewirtz DA, Gibson SB, Gohla A, Goldberg AL, Gonzalez R, Gonzalez-Estevez C, Gorski S, Gottlieb RA, Haussinger D, He YW, Heidenreich K, Hill JA, Hoyer-Hansen M, Hu X, Huang WP, Iwasaki A, Jaattela M, Jackson WT, Jiang X, Jin S, Johansen T, Jung JU, Kadowaki M, Kang C, Kelekar A, Kessel DH, Kiel JA, Kim HP, Kimchi A, Kinsella TJ, Kiselyov K, Kitamoto K, Knecht E, Komatsu M, Kominami E, Kondo S, Kovacs AL, Kroemer G, Kuan CY, Kumar R, Kundu M, Landry J, Laporte M, Le W, Lei HY, Lenardo MJ, Levine B, Lieberman A, Lim KL, Lin FC, Liou W, Liu LF, Lopez-Berestein G, Lopez-Otin C, Lu B, Macleod KF, Malorni W, Martinet W, Matsuoka K, Mautner J, Meijer AJ, Melendez A, Michels P, Miotto G, Mistiaen WP, Mizushima N, Mograbi B, Monastyrska I, Moore MN, Moreira PI, Moriyasu Y, Motyl T, Munz C, Murphy LO, Naqvi NI, Neufeld TP, Nishino I, Nixon RA, Noda T, Nurnberg B, Ogawa M, Oleinick NL, Olsen LJ, Ozpolat B, Paglin S, Palmer GE, Papassideri I, Parkes M, Perlmutter DH, Perry G, Piacentini M, Pinkas-Kramarski R, Prescott M, Proikas-Cezanne T, Raben N, Rami A, Reggiori F, Rohrer B, Rubinsztein DC, Ryan KM, Sadoshima J, Sakagami H, Sakai Y, Sandri M, Sasakawa C, Sass M, Schneider C, Seglen PO, Seleverstov O, Settleman J, Shacka JJ, Shapiro IM, Sibirny A, Silva-Zacarin EC, Simon HU, Simone C, Simonsen A, Smith MA, Spanel-Borowski K, Srinivas V, Steeves M, Stenmark H, Stromhaug PE, Subauste CS, Sugimoto S, Sulzer D, Suzuki T, Swanson MS, Tabas I, Takeshita F, Talbot NJ, Talloczy Z, Tanaka K, Tanaka K, Tanida I, Taylor GS, Taylor JP, Terman A, Tettamanti G, Thompson CB, Thumm M, Tolkovsky AM, Tooze SA, Truant R, Tumanovska LV, Uchiyama Y, Ueno T, Uzcategui NL, van dK, I, Vaquero EC, Vellai T, Vogel MW, Wang HG, Webster P, Wiley JW, Xi Z, Xiao G, Yahalom J, Yang JM, Yap G, Yin XM, Yoshimori T, Yu L, Yue Z, Yuzaki M, Zabirnyk O, Zheng X, Zhu X, Deter RL (Guidelines for the use and interpretation of assays for monitoring autophagy in higher eukaryotes. Autophagy 4:151-175.2008).

Klionsky DJ, Cregg JM, Dunn WA, Jr., Emr SD, Sakai Y, Sandoval IV, Sibirny A, Subramani S, Thumm M, Veenhuis M, Ohsumi Y (A unified nomenclature for yeast autophagy-related genes. Dev Cell 5:539-545.2003).

Kopito RR (Aggresomes, inclusion bodies and protein aggregation. Trends Cell Biol 10:524-530.2000).

Kotian S, Liyanarachchi S, Zelent A, Parvin JD (Histone deacetylases 9 and 10 are required for homologous recombination. J Biol Chem 286:7722-7726.2011).

Koukourakis MI, Giatromanolaki A, Sivridis E, Pitiakoudis M, Gatter KC, Harris AL (Beclin 1 over- and underexpression in colorectal cancer: distinct patterns relate to prognosis and tumour hypoxia. Br J Cancer 103:1209-1214.2010).

Kouzarides T (Chromatin modifications and their function. Cell 128:693-705.2007).

Kovacs JJ, Murphy PJ, Gaillard S, Zhao X, Wu JT, Nicchitta CV, Yoshida M, Toft DO, Pratt WB, Yao TP (HDAC6 regulates Hsp90 acetylation and chaperone-dependent activation of glucocorticoid receptor. Mol Cell 18:601-607.2005).

Krejsgaard T, Odum N, Geisler C, Wasik MA, Woetmann A (Regulatory T cells and immunodeficiency in mycosis fungoides and Sezary syndrome. Leukemia 26:424-432.2012).

Krug LM, Kindler H, Calvert H, Manegold C, Tsao AS, Fennell D, Lubiniecki GM, Sun X, Smith M, Baas P (VANTAGE 014: Vorinostat (V) in Patients With Advanced Malignant Pleural Mesothelioma (MPM) who Have Failed Prior Pemetrexed and Either Cisplatin or Carboplatin Therapy: A Phase III, Randomized, Double-Blind, Placebo-Controlled Trial. European Journal of Cancer 47, Supplement 2:2-3.2011).

La Thangue NB, Kerr DJ (Predictive biomarkers: a paradigm shift towards personalized cancer medicine. Nat Rev Clin Oncol 8:587-596.2011).

Ladoire S, Chaba K, Martins I, Sukkurwala AQ, Adjemian S, Michaud M, Poirier-Colame V, Andreiuolo F, Galluzzi L, White E, Rosenfeldt M, Ryan KM, Zitvogel L, Kroemer G (Immunohistochemical detection of cytoplasmic LC3 puncta in human cancer specimens. Autophagy 8:1175-1184.2012).

Lambertson D, Chen L, Madura K (Investigating the importance of proteasome-interaction for Rad23 function. Curr Genet 42:199-208.2003).

Lazova R, Klump V, Pawelek J (Autophagy in cutaneous malignant melanoma. J Cutan Pathol 37:256-268.2010).

Lee H, Rezai-Zadeh N, Seto E (Negative regulation of histone deacetylase 8 activity by cyclic AMP-dependent protein kinase A. Mol Cell Biol 24:765-773.2004).

Li BX, Li CY, Peng RQ, Wu XJ, Wang HY, Wan DS, Zhu XF, Zhang XS (The expression of beclin 1 is associated with favorable prognosis in stage IIIB colon cancers. Autophagy 5:303-306.2009).

Li X, Song S, Liu Y, Ko SH, Kao HY (Phosphorylation of the histone deacetylase 7 modulates its stability and association with 14-3-3 proteins. J Biol Chem 279:34201-34208.2004).

Li Y, Kao GD, Garcia BA, Shabanowitz J, Hunt DF, Qin J, Phelan C, Lazar MA (A novel histone deacetylase pathway regulates mitosis by modulating Aurora B kinase activity. Genes Dev 20:2566-2579.2006).

Lian ZR, Xu YF, Wang XB, Gong JP, Liu ZJ (Suppression of histone deacetylase 11 promotes expression of IL-10 in Kupffer cells and induces tolerance following orthotopic liver transplantation in rats. J Surg Res 174:359-368.2012).

Lopez G, Torres K, Lev D (Autophagy blockade enhances HDAC inhibitors' pro-apoptotic effects: potential implications for the treatment of a therapeutic-resistant malignancy. Autophagy 7:440-441.2011).

Luger K, Mader AW, Richmond RK, Sargent DF, Richmond TJ (Crystal structure of the nucleosome core particle at 2.8 A resolution. Nature 389:251-260.1997).

Luo M, Kelley MR (Inhibition of the human apurinic/apyrimidinic endonuclease (APE1) repair activity and sensitization of breast cancer cells to DNA alkylating agents with lucanthone. Anticancer Res 24:2127-2134.2004).

Mackay HJ, Hirte H, Colgan T, Covens A, MacAlpine K, Grenci P, Wang L, Mason J, Pham PA, Tsao MS, Pan J, Zwiebel J, Oza AM (Phase II trial of the histone deacetylase inhibitor belinostat in women with platinum resistant epithelial ovarian cancer and micropapillary (LMP) ovarian tumours. Eur J Cancer 46:1573-1579.2010).

Madura K (Rad23 and Rpn10: perennial wallflowers join the melee. Trends Biochem Sci 29:637-640.2004).

Marchion DC, Bicaku E, Turner JG, Schmitt ML, Morelli DR, Munster PN (HDAC2 regulates chromatin plasticity and enhances DNA vulnerability. Mol Cancer Ther 8:794-801.2009).

Marks PA (The clinical development of histone deacetylase inhibitors as targeted anticancer drugs. Expert Opin Investig Drugs 19:1049-1066.2010a).

Marks PA (The clinical development of histone deacetylase inhibitors as targeted anticancer drugs. Expert Opin Investig Drugs 19:1049-1066.2010b).

Marks PA, Xu WS (Histone deacetylase inhibitors: Potential in cancer therapy. J Cell Biochem 107:600-608.2009).

Martin AP, Mitchell C, Rahmani M, Nephew KP, Grant S, Dent P (Inhibition of MCL-1 enhances lapatinib toxicity and overcomes lapatinib resistance via BAK-dependent autophagy. Cancer Biol Ther 8:2084-2096.2009).

Masutani C, Sugasawa K, Yanagisawa J, Sonoyama T, Ui M, Enomoto T, Takio K, Tanaka K, van der Spek PJ, Bootsma D, . (Purification and cloning of a nucleotide excision repair complex involving the xeroderma pigmentosum group C protein and a human homologue of yeast RAD23. EMBO J 13:1831-1843.1994).

Mateos MV, Richardson PG, Schlag R, Khuageva NK, Dimopoulos MA, Shpilberg O, Kropff M, Spicka I, Petrucci MT, Palumbo A, Samoilova OS, Dmoszynska A, Abdulkadyrov KM, Schots R, Jiang B, Esseltine DL, Liu K, Cakana A, Van D, V, San Miguel JF (Bortezomib plus melphalan and prednisone compared with melphalan and prednisone in previously untreated multiple myeloma: updated follow-up and impact of subsequent therapy in the phase III VISTA trial. J Clin Oncol 28:2259-2266.2010).

Mathew R, Karp CM, Beaudoin B, Vuong N, Chen G, Chen HY, Bray K, Reddy A, Bhanot G, Gelinas C, DiPaola RS, Karantza-Wadsworth V, White E (Autophagy suppresses tumorigenesis through elimination of p62. Cell 137:1062-1075.2009).

Matsuyama A, Shimazu T, Sumida Y, Saito A, Yoshimatsu Y, Seigneurin-Berny D, Osada H, Komatsu Y, Nishino N, Khochbin S, Horinouchi S, Yoshida M (In vivo destabilization of dynamic microtubules by HDAC6-mediated deacetylation. EMBO J 21:6820-6831.2002).

Meng L, Mohan R, Kwok BH, Elofsson M, Sin N, Crews CM (Epoxomicin, a potent and selective proteasome inhibitor, exhibits in vivo antiinflammatory activity. Proc Natl Acad Sci U S A 96:10403-10408.1999).

Meusser B, Hirsch C, Jarosch E, Sommer T (ERAD: the long road to destruction. Nat Cell Biol 7:766-772.2005).

Midgley RS, McConkey CC, Johnstone EC, Dunn JA, Smith JL, Grumett SA, Julier P, Iveson C, Yanagisawa Y, Warren B, Langman MJ, Kerr DJ (Phase III randomized trial assessing rofecoxib in the adjuvant setting of colorectal cancer: final results of the VICTOR trial. J Clin Oncol 28:4575-4580.2010).

Miller KM, Tjeertes JV, Coates J, Legube G, Polo SE, Britton S, Jackson SP (Human HDAC1 and HDAC2 function in the DNA-damage response to promote DNA nonhomologous end-joining. Nat Struct Mol Biol 17:1144-1151.2010).

Miracco C, Cevenini G, Franchi A, Luzi P, Cosci E, Mourmouras V, Monciatti I, Mannucci S, Biagioli M, Toscano M, Moretti D, Lio R, Massi D (Beclin 1 and LC3 autophagic gene expression in cutaneous melanocytic lesions. Hum Pathol 41:503-512.2010a).

Miracco C, Cevenini G, Franchi A, Luzi P, Cosci E, Mourmouras V, Monciatti I, Mannucci S, Biagioli M, Toscano M, Moretti D, Lio R, Massi D (Beclin 1 and LC3 autophagic gene expression in cutaneous melanocytic lesions. Hum Pathol 41:503-512.2010b).

Mitsiades CS, Mitsiades NS, McMullan CJ, Poulaki V, Shringarpure R, Hideshima T, Akiyama M, Chauhan D, Munshi N, Gu X, Bailey C, Joseph M, Libermann TA, Richon VM, Marks PA, Anderson KC (Transcriptional

signature of histone deacetylase inhibition in multiple myeloma: biological and clinical implications. Proc Natl Acad Sci U S A 101:540-545.2004a).

Mitsiades CS, Mitsiades NS, McMullan CJ, Poulaki V, Shringarpure R, Hideshima T, Akiyama M, Chauhan D, Munshi N, Gu X, Bailey C, Joseph M, Libermann TA, Richon VM, Marks PA, Anderson KC (Transcriptional signature of histone deacetylase inhibition in multiple myeloma: biological and clinical implications. Proc Natl Acad Sci U S A 101:540-545.2004b).

Mizushima N (The pleiotropic role of autophagy: from protein metabolism to bactericide. Cell Death Differ 12 Suppl 2:1535-1541.2005).

Mizushima N, Levine B, Cuervo AM, Klionsky DJ (Autophagy fights disease through cellular self-digestion. Nature 451:1069-1075.2008).

Mizushima N, Yoshimori T, Levine B (Methods in mammalian autophagy research. Cell 140:313-326.2010a).

Mizushima N, Yoshimori T, Levine B (Methods in mammalian autophagy research. Cell 140:313-326.2010b).

Montgomery RL, Davis CA, Potthoff MJ, Haberland M, Fielitz J, Qi X, Hill JA, Richardson JA, Olson EN (Histone deacetylases 1 and 2 redundantly regulate cardiac morphogenesis, growth, and contractility. Genes Dev 21:1790-1802.2007).

Mullenders J, Bernards R (Loss-of-function genetic screens as a tool to improve the diagnosis and treatment of cancer. Oncogene 28:4409-4420.2009).

Munster P, Marchion D, Bicaku E, Lacevic M, Kim J, Centeno B, Daud A, Neuger A, Minton S, Sullivan D (Clinical and biological effects of valproic acid as a histone deacetylase inhibitor on tumor and surrogate tissues: phase I/II trial of valproic acid and epirubicin/FEC. Clin Cancer Res 15:2488-2496.2009).

Munster PN, Daud AI (Preclinical and clinical activity of the topoisomerase I inhibitor, karenitecin, in melanoma. Expert Opin Investig Drugs 20:1565-1574.2011).

Munster PN, Thurn KT, Thomas S, Raha P, Lacevic M, Miller A, Melisko M, Ismail-Khan R, Rugo H, Moasser M, Minton SE (A phase II study of the histone deacetylase inhibitor vorinostat combined with tamoxifen for the treatment of patients with hormone therapy-resistant breast cancer. Br J Cancer 104:1828-1835.2011).

New M, Olzscha H, La Thangue NB (HDAC inhibitor-based therapies: Can we interpret the code? Mol Oncol 6:637-656.2012).

New M, Olzscha H, Liu G, Khan O, Stimson L, McGouran J, Kerr D, Coutts A, Kessler B, Middleton M, La Thangue NB (A regulatory circuit that involves HR23B and HDAC6 governs the biological response to HDAC inhibitors. Cell Death Differ 20:1306-1316.2013).

Nguyen T, Dai Y, Attkisson E, Kramer L, Jordan N, Nguyen N, Kolluri N, Muschen M, Grant S (HDAC inhibitors potentiate the activity of the BCR/ABL kinase inhibitor KW-2449 in imatinib-sensitive or -resistant BCR/ABL+ leukemia cells in vitro and in vivo. Clin Cancer Res 17:3219-3232.2011).

Niesvizky R, Ely S, Mark T, Aggarwal S, Gabrilove JL, Wright JJ, Chen-Kiang S, Sparano JA (Phase 2 trial of the histone deacetylase inhibitor romidepsin for the treatment of refractory multiple myeloma. Cancer 117:336-342.2011).

Ocio EM, Vilanova D, Atadja P, Maiso P, Crusoe E, Fernandez-Lazaro D, Garayoa M, San-Segundo L, Hernandez-Iglesias T, de AE, Shao W, Yao YM, Pandiella A, San-Miguel JF (In vitro and in vivo rationale for the triple combination of panobinostat (LBH589) and dexamethasone with either bortezomib or lenalidomide in multiple myeloma. Haematologica 95:794-803.2010).

Ohkuma S, Poole B (Cytoplasmic vacuolation of mouse peritoneal macrophages and the uptake into lysosomes of weakly basic substances. J Cell Biol 90:656-664.1981).

Ortolan TG, Chen L, Tongaonkar P, Madura K (Rad23 stabilizes Rad4 from degradation by the Ub/proteasome pathway. Nucleic Acids Res 32:6490-6500.2004).

Pandey UB, Batlevi Y, Baehrecke EH, Taylor JP (HDAC6 at the intersection of autophagy, the ubiquitin-proteasome system and neurodegeneration. Autophagy 3:643-645.2007a).

Pandey UB, Nie Z, Batlevi Y, McCray BA, Ritson GP, Nedelsky NB, Schwartz SL, DiProspero NA, Knight MA, Schuldiner O, Padmanabhan R, Hild M, Berry DL, Garza D, Hubbert CC, Yao TP, Baehrecke EH, Taylor JP (HDAC6 rescues neurodegeneration and provides an essential link between autophagy and the UPS. Nature 447:859-863.2007b).

Peart MJ, Smyth GK, van Laar RK, Bowtell DD, Richon VM, Marks PA, Holloway AJ, Johnstone RW (Identification and functional significance of genes regulated by structurally different histone deacetylase inhibitors. Proc Natl Acad Sci U S A 102:3697-3702.2005).

Pickart CM (Mechanisms underlying ubiquitination. Annu Rev Biochem 70:503-533.2001).

Piekarz RL, Frye R, Prince HM, Kirschbaum MH, Zain J, Allen SL, Jaffe ES, Ling A, Turner M, Peer CJ, Figg WD, Steinberg SM, Smith S, Joske D, Lewis I, Hutchins L, Craig M, Fojo AT, Wright JJ, Bates SE (Phase 2 trial of romidepsin in patients with peripheral T-cell lymphoma. Blood 117:5827-5834.2011).

Pirtoli L, Cevenini G, Tini P, Vannini M, Oliveri G, Marsili S, Mourmouras V, Rubino G, Miracco C (The prognostic role of Beclin 1 protein expression in high-grade gliomas. Autophagy 5:930-936.2009).

Poole B, Ohkuma S (Effect of weak bases on the intralysosomal pH in mouse peritoneal macrophages. J Cell Biol 90:665-669.1981).

Prince HM, Dickinson M (Romidepsin for cutaneous T-cell lymphoma. Clin Cancer Res 18:3509-3515.2012).

Qu X, Yu J, Bhagat G, Furuya N, Hibshoosh H, Troxel A, Rosen J, Eskelinen EL, Mizushima N, Ohsumi Y, Cattoretti G, Levine B (Promotion of tumorigenesis by heterozygous disruption of the beclin 1 autophagy gene. J Clin Invest 112:1809-1820.2003).

Raasi S, Varadan R, Fushman D, Pickart CM (Diverse polyubiquitin interaction properties of ubiquitin-associated domains. Nat Struct Mol Biol 12:708-714.2005).

Ramalingam SS, Belani CP, Ruel C, Frankel P, Gitlitz B, Koczywas M, Espinoza-Delgado I, Gandara D (Phase II study of belinostat (PXD101), a histone deacetylase inhibitor, for second line therapy of advanced malignant pleural mesothelioma. J Thorac Oncol 4:97-101.2009).

Ramalingam SS, Maitland ML, Frankel P, Argiris AE, Koczywas M, Gitlitz B, Thomas S, Espinoza-Delgado I, Vokes EE, Gandara DR, Belani CP (Carboplatin and Paclitaxel in combination with either vorinostat or placebo for first-line therapy of advanced non-small-cell lung cancer. J Clin Oncol 28:56-62.2010).

Rao R, Balusu R, Fiskus W, Mudunuru U, Venkannagari S, Chauhan L, Smith JE, Hembruff SL, Ha K, Atadja P, Bhalla KN (Combination of pan-histone deacetylase inhibitor and autophagy inhibitor exerts superior efficacy against triple-negative human breast cancer cells. Mol Cancer Ther 11:973-983.2012).

Rao R, Fiskus W, Yang Y, Lee P, Joshi R, Fernandez P, Mandawat A, Atadja P, Bradner JE, Bhalla K (HDAC6 inhibition enhances 17-AAG--mediated abrogation of hsp90 chaperone function in human leukemia cells. Blood 112:1886-1893.2008).

Ravid T, Hochstrasser M (Diversity of degradation signals in the ubiquitin-proteasome system. Nat Rev Mol Cell Biol 9:679-690.2008).

Repnik U, Stoka V, Turk V, Turk B (Lysosomes and lysosomal cathepsins in cell death. Biochim Biophys Acta 1824:22-33.2012).

Richardson PG, Barlogie B, Berenson J, Singhal S, Jagannath S, Irwin D, Rajkumar SV, Srkalovic G, Alsina M, Alexanian R, Siegel D, Orlowski RZ, Kuter D, Limentani SA, Lee S, Hideshima T, Esseltine DL, Kauffman M, Adams J, Schenkein DP, Anderson KC (A phase 2 study of bortezomib in relapsed, refractory myeloma. N Engl J Med 348:2609-2617.2003).

Richardson PG, Sonneveld P, Schuster MW, Irwin D, Stadtmauer EA, Facon T, Harousseau JL, Ben-Yehuda D, Lonial S, Goldschmidt H, Reece D, San-Miguel JF, Blade J, Boccadoro M, Cavenagh J, Dalton WS, Boral AL, Esseltine DL, Porter JB, Schenkein D, Anderson KC (Bortezomib or high-dose dexamethasone for relapsed multiple myeloma. N Engl J Med 352:2487-2498.2005).

Richly H, Rape M, Braun S, Rumpf S, Hoege C, Jentsch S (A series of ubiquitin binding factors connects CDC48/p97 to substrate multiubiquitylation and proteasomal targeting. Cell 120:73-84.2005).

Rocca A, Minucci S, Tosti G, Croci D, Contegno F, Ballarini M, Nole F, Munzone E, Salmaggi A, Goldhirsch A, Pelicci PG, Testori A (A phase I-II study of the histone deacetylase inhibitor valproic acid plus chemoimmunotherapy in patients with advanced melanoma. Br J Cancer 100:28-36.2009).

Ropero S, Fraga MF, Ballestar E, Hamelin R, Yamamoto H, Boix-Chornet M, Caballero R, Alaminos M, Setien F, Paz MF, Herranz M, Palacios J, Arango D, Orntoft TF, Aaltonen LA, Schwartz S Jr, Esteller M (A truncating mutation of HDAC2 in human cancers confers resistance to histone deacetylase inhibition. Nat Genet 38:566-569.2006).

Rubinsztein DC (The roles of intracellular protein-degradation pathways in neurodegeneration. Nature 443:780-786.2006).

Saeki Y, Sone T, Toh-e A, Yokosawa H (Identification of ubiquitin-like protein-binding subunits of the 26S proteasome. Biochem Biophys Res Commun 296:813-819.2002).

Scagliotti G (Proteasome inhibitors in lung cancer. Crit Rev Oncol Hematol 58:177-189.2006).

Schilsky RL (Personalized medicine in oncology: the future is now. Nat Rev Drug Discov 9:363-366.2010).

Schlesinger DH, Goldstein G, Niall HD (The complete amino acid sequence of ubiquitin, an adenylate cyclase stimulating polypeptide probably universal in living cells. Biochemistry 14:2214-2218.1975).

Shao W, Growney JD, Feng Y, O'Connor G, Pu M, Zhu W, Yao YM, Kwon P, Fawell S, Atadja P (Activity of deacetylase inhibitor panobinostat (LBH589) in cutaneous T-cell lymphoma models: Defining molecular mechanisms of resistance. Int J Cancer 127:2199-2208.2010).

Simonini MV, Camargo LM, Dong E, Maloku E, Veldic M, Costa E, Guidotti A (The benzamide MS-275 is a potent, long-lasting brain region-selective inhibitor of histone deacetylases. Proc Natl Acad Sci U S A 103:1587-1592.2006).

Singh R, Cuervo AM (Autophagy in the cellular energetic balance. Cell Metab 13:495-504.2011).

Sivridis E, Koukourakis MI, Zois CE, Ledaki I, Ferguson DJ, Harris AL, Gatter KC, Giatromanolaki A (LC3A-positive light microscopy detected patterns of autophagy and prognosis in operable breast carcinomas. Am J Pathol 176:2477-2489.2010).

Sjoblom T, Jones S, Wood LD, Parsons DW, Lin J, Barber TD, Mandelker D, Leary RJ, Ptak J, Silliman N, Szabo S, Buckhaults P, Farrell C, Meeh P, Markowitz SD, Willis J, Dawson D, Willson JK, Gazdar AF, Hartigan J, Wu L, Liu C, Parmigiani G, Park BH, Bachman KE, Papadopoulos N, Vogelstein B, Kinzler KW, Velculescu VE (The consensus coding sequences of human breast and colorectal cancers. Science 314:268-274.2006).

Soldani C, Scovassi AI (Poly(ADP-ribose) polymerase-1 cleavage during apoptosis: an update. Apoptosis 7:321-328.2002).

Solomon VR, Lee H (Chloroquine and its analogs: a new promise of an old drug for effective and safe cancer therapies. Eur J Pharmacol 625:220-233.2009).

Sridhar S, Botbol Y, Macian F, Cuervo AM (Autophagy and disease: always two sides to a problem. J Pathol 226:255-273.2012).

Steele NL, Plumb JA, Vidal L, Tjornelund J, Knoblauch P, Rasmussen A, Ooi CE, Buhl-Jensen P, Brown R, Evans TR, DeBono JS (A phase 1 pharmacokinetic and pharmacodynamic study of the histone deacetylase inhibitor belinostat in patients with advanced solid tumors. Clin Cancer Res 14:804-810.2008).

Stimson L, La Thangue NB (Biomarkers for predicting clinical responses to HDAC inhibitors. Cancer Lett 280:177-183.2009a).

Stimson L, La Thangue NB (Biomarkers for predicting clinical responses to HDAC inhibitors. Cancer Lett 280:177-183.2009b).

Stimson L, Wood V, Khan O, Fotheringham S, La Thangue NB (HDAC inhibitor-based therapies and haematological malignancy. Ann Oncol 20:1293-1302.2009).

Sun X, Wei L, Chen Q, Terek RM (HDAC4 represses vascular endothelial growth factor expression in chondrosarcoma by modulating RUNX2 activity. J Biol Chem 284:21881-21890.2009).

Takami Y, Nakayama T (N-terminal region, C-terminal region, nuclear export signal, and deacetylation activity of histone deacetylase-3 are essential for the viability of the DT40 chicken B cell line. J Biol Chem 275:16191-16201.2000).

Takamura A, Komatsu M, Hara T, Sakamoto A, Kishi C, Waguri S, Eishi Y, Hino O, Tanaka K, Mizushima N (Autophagy-deficient mice develop multiple liver tumors. Genes Dev 25:795-800.2011).

Thomas S, Thurn KT, Bicaku E, Marchion DC, Munster PN (Addition of a histone deacetylase inhibitor redirects tamoxifen-treated breast cancer cells into apoptosis, which is opposed by the induction of autophagy. Breast Cancer Res Treat 130:437-447.2011).

Ting AH, McGarvey KM, Baylin SB (The cancer epigenome--components and functional correlates. Genes Dev 20:3215-3231.2006).

Urbich C, Rossig L, Kaluza D, Potente M, Boeckel JN, Knau A, Diehl F, Geng JG, Hofmann WK, Zeiher AM, Dimmeler S (HDAC5 is a repressor of angiogenesis and determines the angiogenic gene expression pattern of endothelial cells. Blood 113:5669-5679.2009).

Varadan R, Assfalg M, Raasi S, Pickart C, Fushman D (Structural determinants for selective recognition of a Lys48-linked polyubiquitin chain by a UBA domain. Mol Cell 18:687-698.2005).

Vega RB, Matsuda K, Oh J, Barbosa AC, Yang X, Meadows E, McAnally J, Pomajzl C, Shelton JM, Richardson JA, Karsenty G, Olson EN (Histone deacetylase 4 controls chondrocyte hypertrophy during skeletogenesis. Cell 119:555-566.2004).

Verdin E, Dequiedt F, Kasler HG (Class II histone deacetylases: versatile regulators. Trends Genet 19:286-293.2003).

Verma R, Oania R, Graumann J, Deshaies RJ (Multiubiquitin chain receptors define a layer of substrate selectivity in the ubiquitin-proteasome system. Cell 118:99-110.2004).

Wan XB, Fan XJ, Chen MY, Xiang J, Huang PY, Guo L, Wu XY, Xu J, Long ZJ, Zhao Y, Zhou WH, Mai HQ, Liu Q, Hong MH (Elevated Beclin 1 expression is correlated with HIF-1alpha in predicting poor prognosis of nasopharyngeal carcinoma. Autophagy 6:395-404.2010).

Watkins JF, Sung P, Prakash L, Prakash S (The Saccharomyces cerevisiae DNA repair gene RAD23 encodes a nuclear protein containing a ubiquitin-like domain required for biological function. Mol Cell Biol 13:7757-7765.1993).

Welchman RL, Gordon C, Mayer RJ (Ubiquitin and ubiquitin-like proteins as multifunctional signals. Nat Rev Mol Cell Biol 6:599-609.2005).

Whittaker SJ, Demierre MF, Kim EJ, Rook AH, Lerner A, Duvic M, Scarisbrick J, Reddy S, Robak T, Becker JC, Samtsov A, McCulloch W, Kim YH (Final results from a multicenter, international, pivotal study of romidepsin in refractory cutaneous T-cell lymphoma. J Clin Oncol 28:4485-4491.2010).

Wilkinson CR, Seeger M, Hartmann-Petersen R, Stone M, Wallace M, Semple C, Gordon C (Proteins containing the UBA domain are able to bind to multi-ubiquitin chains. Nat Cell Biol 3:939-943.2001).

Witt O, Deubzer HE, Milde T, Oehme I (HDAC family: What are the cancer relevant targets? Cancer Lett 277:8-21.2009).

Wu WK, Cho CH, Lee CW, Wu K, Fan D, Yu J, Sung JJ (Proteasome inhibition: a new therapeutic strategy to cancer treatment. Cancer Lett 293:15-22.2010).

Xie Z, Klionsky DJ (Autophagosome formation: core machinery and adaptations. Nat Cell Biol 9:1102-1109.2007).

Yang XJ, Seto E (The Rpd3/Hda1 family of lysine deacetylases: from bacteria and yeast to mice and men. Nat Rev Mol Cell Biol 9:206-218.2008).

Yang ZJ, Chee CE, Huang S, Sinicrope FA (The role of autophagy in cancer: therapeutic implications. Mol Cancer Ther 10:1533-1541.2011).

Yeo W, Chung HC, Chan SL, Wang LZ, Lim R, Picus J, Boyer M, Mo FK, Koh J, Rha SY, Hui EP, Jeung HC, Roh JK, Yu SC, To KF, Tao Q, Ma BB, Chan AW, Tong JH, Erlichman C, Chan AT, Goh BC (Epigenetic therapy using belinostat for patients with unresectable hepatocellular carcinoma: a multicenter phase I/II study with biomarker and pharmacokinetic analysis of tumors from patients in the Mayo Phase II Consortium and the Cancer Therapeutics Research Group. J Clin Oncol 30:3361-3367.2012).

Yoshioka A, Miyata H, Doki Y, Yamasaki M, Sohma I, Gotoh K, Takiguchi S, Fujiwara Y, Uchiyama Y, Monden M (LC3, an autophagosome marker, is highly expressed in gastrointestinal cancers. Int J Oncol 33:461-468.2008).

Young P, Deveraux Q, Beal RE, Pickart CM, Rechsteiner M (Characterization of two polyubiquitin binding sites in the 26 S protease subunit 5a. J Biol Chem 273:5461-5467.1998).

Yu W, Wang J, Jin J, Qian W, Qian J, Cheng Y, Wang L (Heat shock protein 90 inhibition results in altered downstream signaling of mutant KIT and exerts synergistic effects on Kasumi-1 cells when combining with histone deacetylase inhibitor. Leuk Res 35:1212-1218.2011).

Yue Z, Jin S, Yang C, Levine AJ, Heintz N (Beclin 1, an autophagy gene essential for early embryonic development, is a haploinsufficient tumor suppressor. Proc Natl Acad Sci U S A 100:15077-15082.2003).

Zauderer MG, Krug LM (Novel therapies in phase II and III trials for malignant pleural mesothelioma. J Natl Compr Canc Netw 10:42-47.2012).

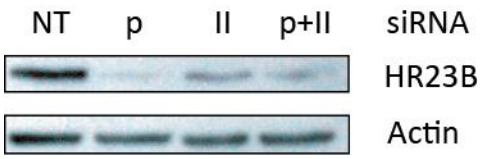
Zhang CL, McKinsey TA, Chang S, Antos CL, Hill JA, Olson EN (Class II histone deacetylases act as signal-responsive repressors of cardiac hypertrophy. Cell 110:479-488.2002a).

Zhang CL, McKinsey TA, Olson EN (Association of class II histone deacetylases with heterochromatin protein 1: potential role for histone methylation in control of muscle differentiation. Mol Cell Biol 22:7302-7312.2002b).

Zhang X, Ozawa Y, Lee H, Wen YD, Tan TH, Wadzinski BE, Seto E (Histone deacetylase 3 (HDAC3) activity is regulated by interaction with protein serine/threonine phosphatase 4. Genes Dev 19:827-839.2005).

Zhou X, Marks PA, Rifkind RA, Richon VM (Cloning and characterization of a histone deacetylase, HDAC9. Proc Natl Acad Sci U S A 98:10572-10577.2001).

APPENDICES

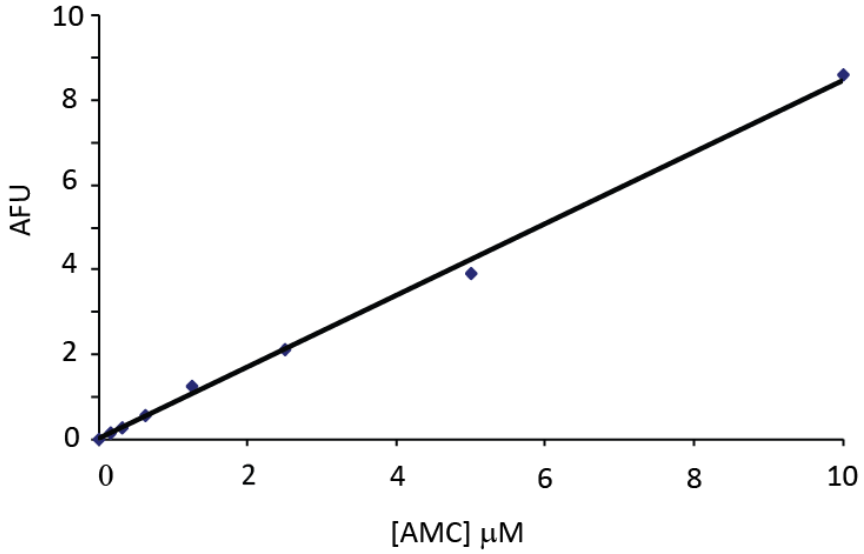


Appendix I

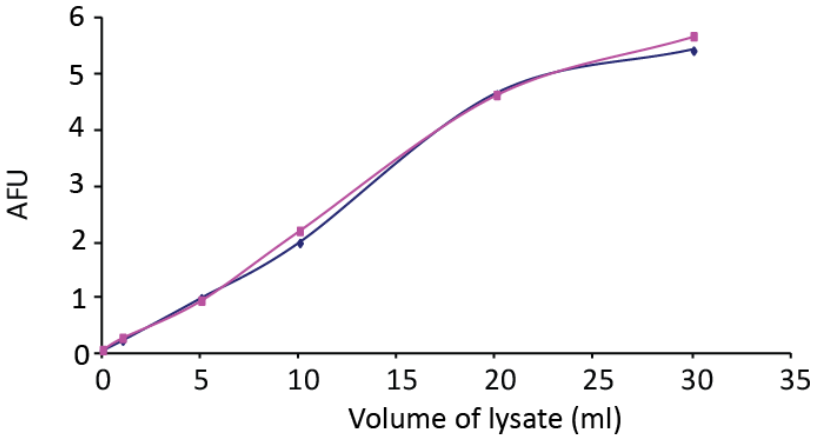
siRNA optimisation

Immunoblot showing protein levels of HR23B after 96h treatment with HR23B siRNA (p and II) or a combination of both or with control siRNA (NT) siRNA or 2 different HR23B siRNAs (nominated p and II) . Actin levels are shown as loading controls.

a

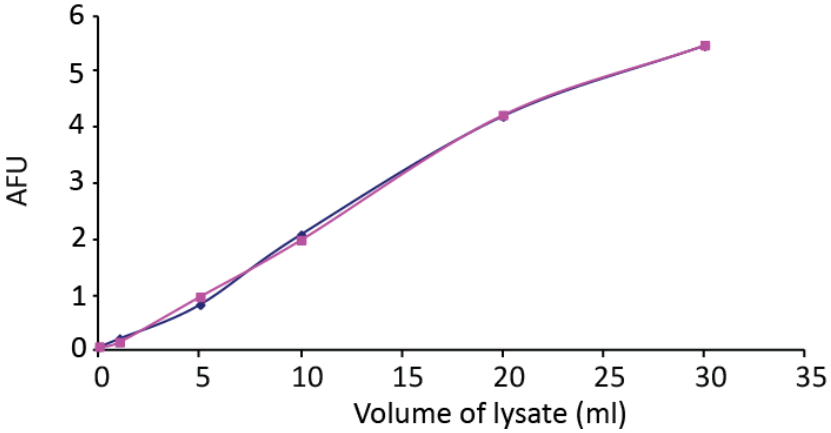


b



MYLA

c



A2058

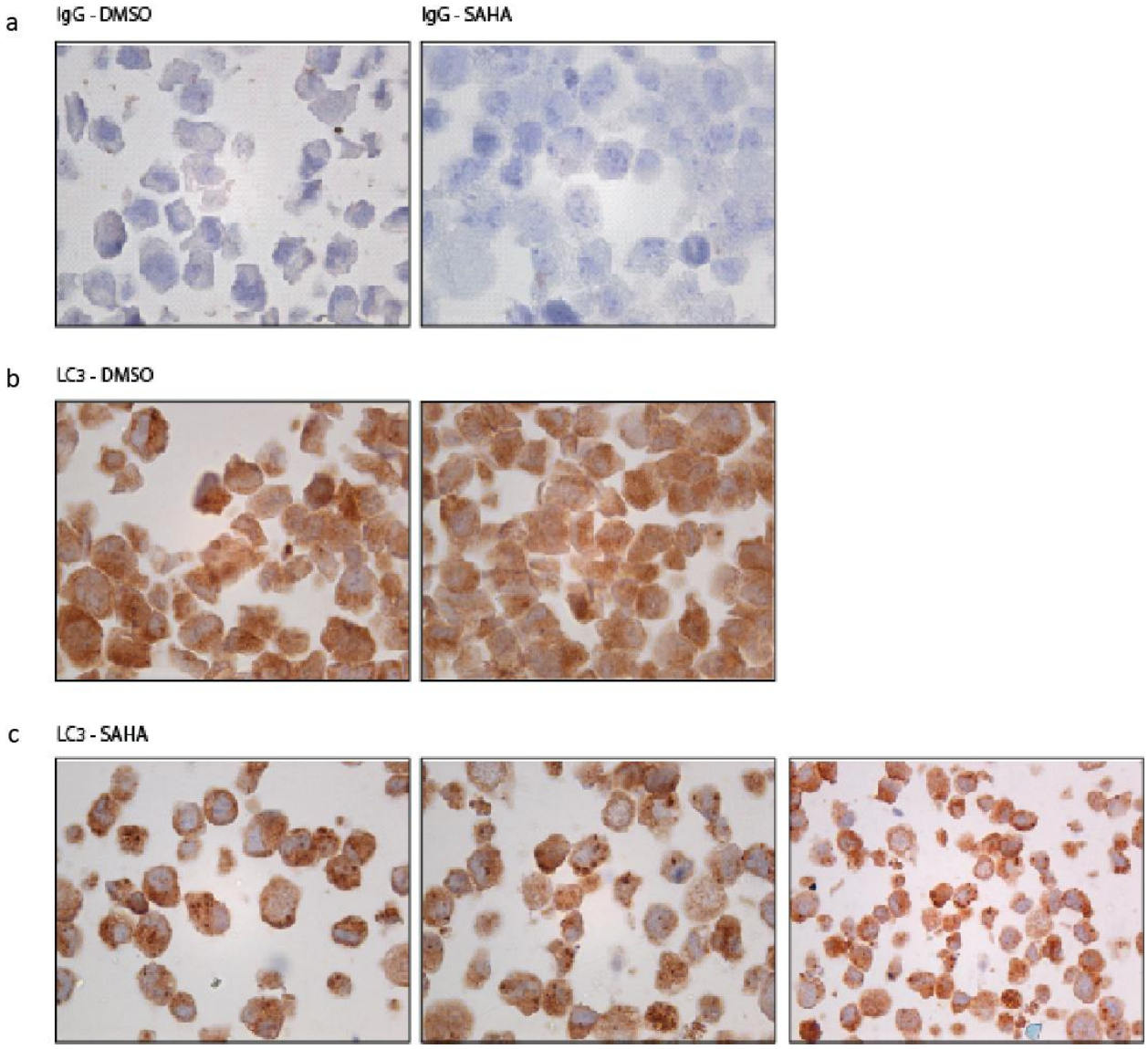
Appendix II

Proteasome assay optimisation

(a) MYLA cells were plated out and harvested after 24h growth, prepared for proteasome assay as described and incubated with varying concentrations of 7-Amino-4-methylcoumarin (AMC) as indicated. Cleaved substrate (as arbitrary fluorescence units; AFU) representative of active proteasome was measured after 60 minutes and plotted against concentration of AMC.

(b) MYLA cells were plated out and harvested after 24h growth, prepared for proteasome assay as described and cleaved substrate activity (as arbitrary fluorescence units; AFU) was measured after 60 minutes incubation of different volumes of lysate. AFU was plotted against concentration and the experiment was performed in duplicate.

(c) A2058 cells were plated out and harvested after 24h growth, prepared for proteasome assay as described and cleaved substrate activity (as arbitrary fluorescence units; AFU) was measured after 60 minutes incubation of different volumes of lysate. AFU was plotted against concentration and the experiment was performed in duplicate.



Appendix III

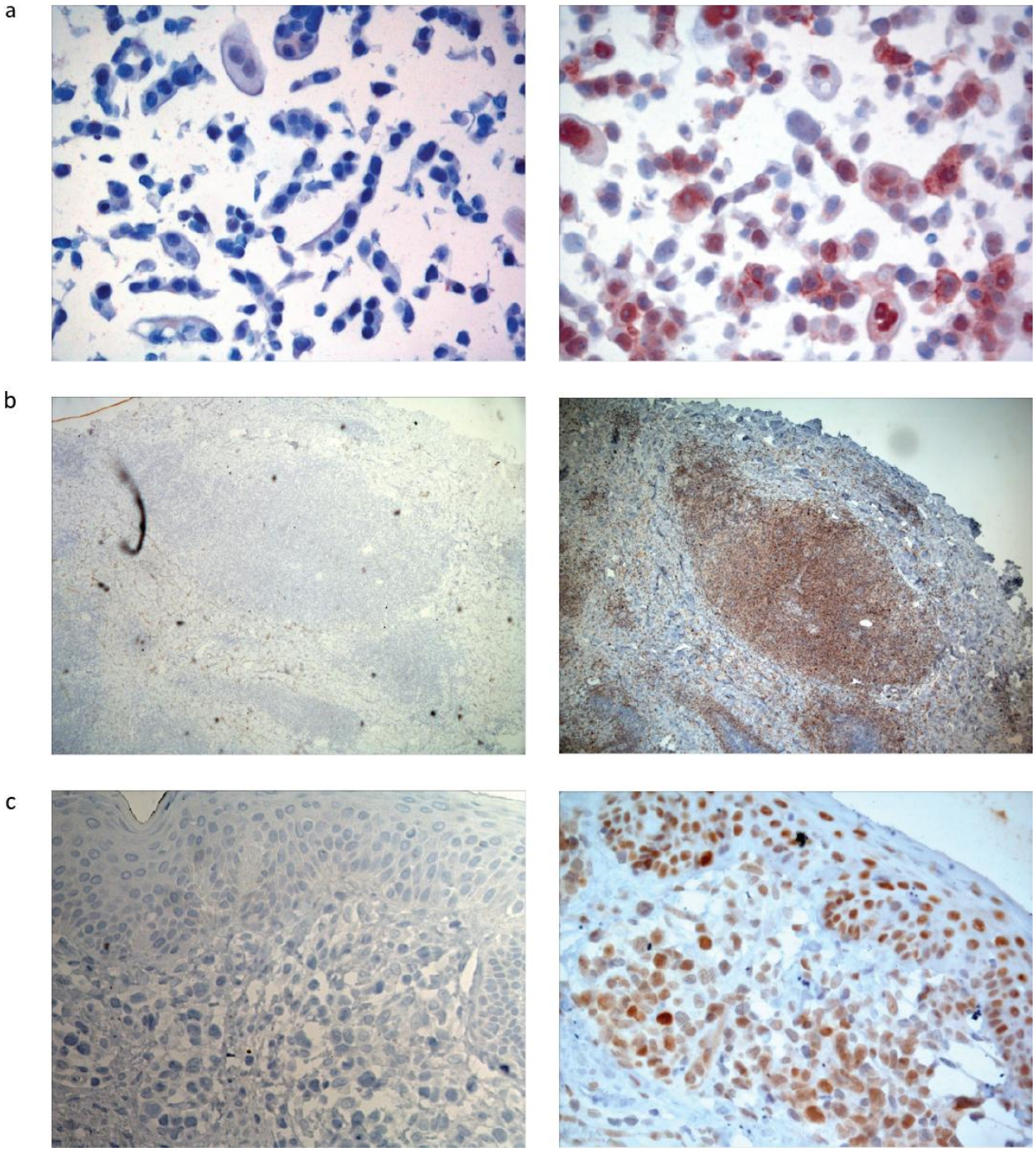
LC3 antibody optimisation

U2OS cells were plated and grown for 24h followed by treatment with DMSO or SAHA at 5 µM for 24 hours. Cells were then harvested, spun down and cell pellets were fixed in formalin and embedded in paraffin. Sections (5µm) were then placed on glass slides and staining was performed with anti-LC3.

(a) U2OS cells were treated with DMSO and SAHA as indicated and incubated with mouse IgG overnight at 4ºC for immunostaining.

(b) U2OS cells were treated with DMSO and incubated with LC3 (1:100 dilution) overnight at for immunostaining (two examples are shown)

(c) U2OS cells were treated with SAHA (5mM) and incubated with LC3 (1:100) dilution overnight at 4ºC for immunostaining. A punctate pattern of LC3 immunostaining was evident after SAHA treatment (three examples are shown).



Appendix IV

Immunohistochemistry controls

(a) MCF7 cells, (b) cutaneous CD30+ lymphoproliferative disorder (histology number 13), (c) mycosis fungoides (histology number 7) immunostained with and without HR23B antibody showing no brown immunostaining when primary antibody absent.

Appendix 5

a

Value of κ	Strength of agreement
< 0.20	Poor
0.21 - 0.40	Fair
0.41 - 0.60	Moderate
0.61 - 0.80	Good
0.81 - 1.00	Very good

b CTCL - HDAC inhibitor treated specimens (HR23B)

Score		
Observer 1	Observer 2	Number of cases
Positive	Positive	69
Negative	Positive	2
Postive	Negative	4
Negative	Negative	13

Kappa score: 0.771

Appendix 5

c Melanoma TMA (HR23B)

Nuclear			Cytoplasm		
Score			Score		
Observer 1	Observer 2	Number of cases	Observer 1	Observer 2	Number of cases
Positive	Positive	90	Positive	Positive	101
Negative	Positive	8	Negative	Positive	4
Postive	Negative	8	Postive	Negative	4
Negative	Negative	16	Negative	Negative	10
Kappa score: 0.644			Kappa score: 0.676		

d Selected samples from VICTOR trial TMAs

Score			
Observer 1	Observer 2	HR23B	LC3
Positive	Positive	57	20
Negative	Positive	15	3
Positive	Negative	3	2
Negative	Negative	25	75
Kappa score		0.605	0.857

Appendix V

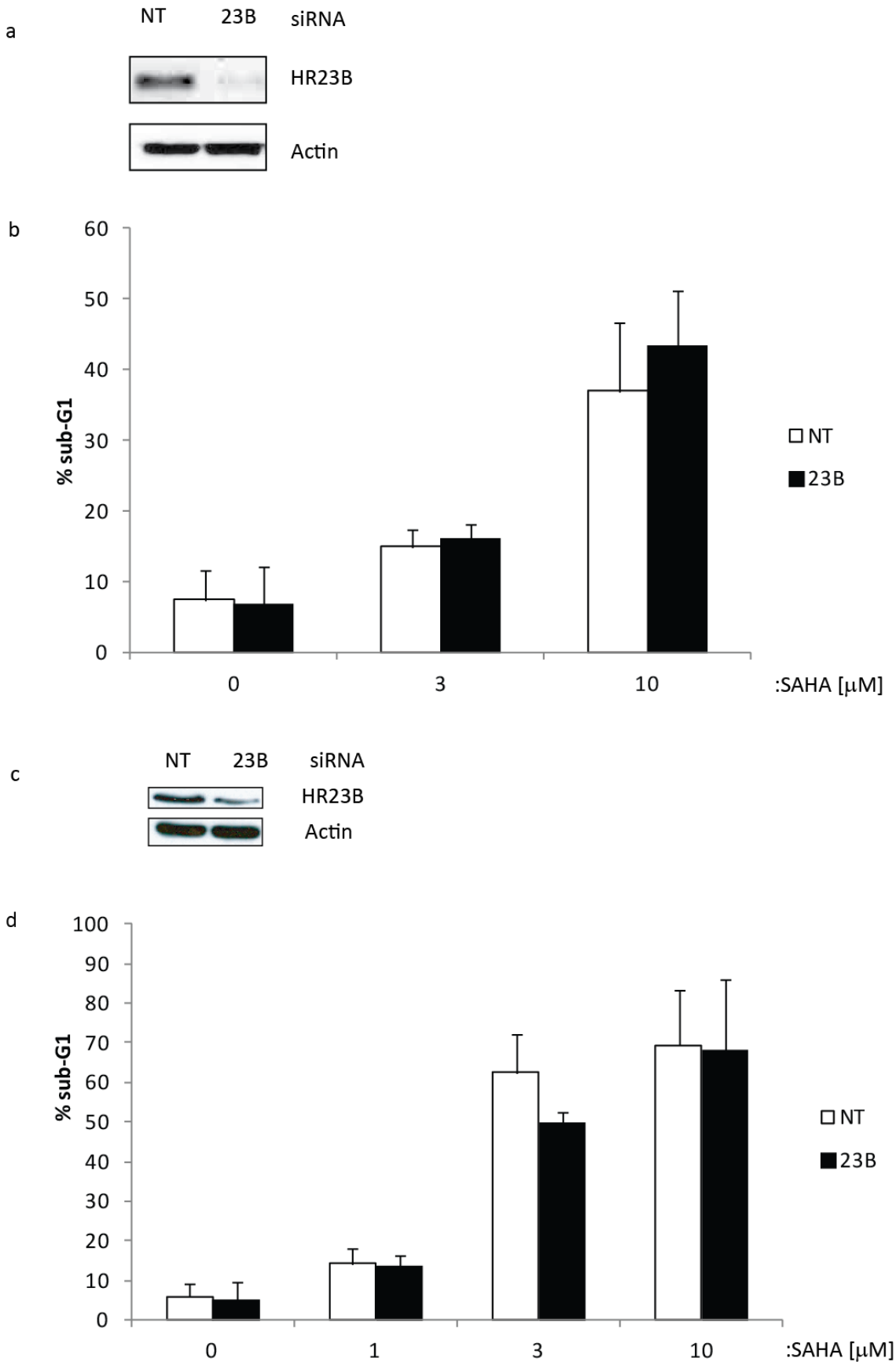
Inter-observer agreement using the Kappa statistic of immunohistochemistry scoring

(a) Table showing the values of the kappa statistic and corresponding strength of agreement

(b) Graph showing the scoring by two independent observers of HR23B immunostaining of CTCL specimens from retrospective analysis of HDAC inhibitor treated patients along with kappa statistic.

(c) Graph showing the scoring by two independent observers of HR23B immunostaining of melanoma TMA along with kappa statistic.

(d) Graph showing the scoring by two independent observers of HR23B (nuclear) and LC3 immunostaining of a random selection of colorectal specimens from VICTOR trial patients along with kappa statistic.


a
NT
23B
siRNA
HR23B
Actin
b
% sub-G1
60
50
40
30
20
10
0
0
3
10
:SAHA [μM]
NT
23B
c
NT
23B
siRNA
HR23B
Actin
d
% sub-G1
100
90
80
70
60
50
40
30
20
10
0
0
1
3
10
:SAHA [μM]
NT
23B

Appendix VI

Effect of depleting HR23B using siRNA in colorectal and melanoma cells upon HDAC inhibitor-induced apoptosis

HCT116 cells (a) and A375 (c) cells were treated with HR23B or non-targeting control (NT) siRNA for 48h, followed by immunoblotting. Actin served as the loading control. The levels of sub-G1 HCT116 cells (b) and A375 cells (d) determined by FACS after treatment with HR23B siRNA or non-targeting control (NT) siRNA for 48h followed by treatment with DMSO control or increasing concentrations of SAHA (μM) as indicated for 48h.